# Development of functional immune readouts for the confirmation of Mendelian Susceptibility to Mycobacterial Disease and related Primary Immunodeficiencies

**Ansia van Coller**

Thesis presented in fulfilment of the requirements for the degree of Master of Science in the Faculty of Medicine and Health Sciences at Stellenbosch University




Supervisor: Dr Richard Glashoff

Co-supervisor: Prof. Monika Esser

Department of Pathology. Division of Medical Microbiology. Unit of Immunology

April 2019

# Declaration

By submitting this thesis electronically, I declare that the entirety of the work contained therein is my own, original work, that I am the sole author thereof (save to the extent explicitly otherwise stated), that reproduction and publication thereof by Stellenbosch University will not infringe any third-party rights and that I have not previously in its entirety or in part submitted it for obtaining any qualification.

April 2019

# Abstract

**Background:** Mendelian Susceptibility to Mycobacterial Disease (MSMD) is a primary immunodeficiency (PID) characterised by a predisposition to infection by weakly-pathogenic mycobacteria. In countries with a high prevalence of tuberculosis, individuals with MSMD are also prone to severe, persistent, unusual or recurrent infections by pathogenic *Mycobacterium tuberculosis*. Several MSMD-associated genes have been described, including *IFNGR1*, *IFNGR2*, *IL12RB1*, *IL12B*, *STAT1*, *NEMO*, *ISG15*, *IRF8*, *TYK2*, and *CYBB*, many resulting in a disruption of IL-12 and IFN-γ cytokine axis, which is essential for control of mycobacterial infections. This genetic heterogeneity results in many distinct disorders, which vary in their mode of inheritance and clinical presentation. An accurate molecular diagnosis, confirmed by immune functional studies, is essential to ensure that the patient receives optimal treatment and prophylaxis for infections. The aim of this study was to implement and optimise a set of immune phenotyping and functional validation tests for the key pathway, the IFN-γ and IL-12 cytokine axis, involved in MSMD, and to use these assays to assess immune function in a cohort of suspected MSMD patients.

**Methodology:** Blood was collected from 17 participants with MSMD-like clinical phenotypes. DNA was extracted and PBMCs were isolated from the patients' blood. Whole exome sequencing (WES) was performed and the resulting data was processed using an in-house bioinformatics pipeline, TAPER™. A set of flow cytometry and ELISA-based functional assays were implemented and optimised to assess the integrity of the IL-12-IFN-γ pathway. IFN-γR1 and IL-12Rβ1 expression were assessed by means of standard surface flow cytometry, and IFN-γ and IL-12 signalling was assessed by the detection of pSTAT1 and pSTAT4 respectively through intracellular phospho-specific flow cytometry. IFN-γ-induced IL-12 production as well as IL-12-induced IFN-γ production was also assessed by ELISA after 48-hour *in vitro* stimulation. The functional and genetic data were then reconciled in order to confirm the extent of functional impairment associated with each genetic variant.

**Results:** Plausible disease-causing variants were identified through genetic investigations for 11 of the 17 participants. Variants in MSMD-associated genes were found in 8 of these patients, although only one of the identified variants, *IFNGR1* (c.818del4), has been described before. Variants in genes not previously associated with MSMD were also found, including variants in *IKZF1*, *NOD2*, *IRAK1*, *IKBKB*, and *NFKB2*. All the functional assays were optimised and the combination of the three assays for the assessment of the integrity of the IL-12-IFN-γ pathway was successful in identifying immune deficits in essentially all of the participants included in this study.

**Conclusions:** The current study led to the implementation of functional immune readouts that allowed for the evaluation of the functional impact of both novel and previously described genetic variants on the IL-12-IFN-γ pathway. The results generated from the functional assays were highly variable and often defects within the same gene lead to different phenotypes, which emphasises the importance of *in vitro* functional confirmation of all PIDs. Hence it would be beneficial to apply these assays routinely for patients with suspected PID relating to mycobacterial susceptibility. A molecular diagnosis with confirmed functional impairment paves the way for targeted treatment and improved disease management options for these patients.

# Opsomming

**Agtergrond**: Mendeliese vatbaarheid vir mikobakteriële siektes (MSMD) is ‘n primêre immuundefek (PID) wat deur vatbaarheid tot infeksie deur minder-patogeniese mikobakterieë gekenmerk word. In lande met ‘n hoë voorkoms van tuberkulose, het hierdie individue ‘n hoër waarskynlikheid om ernstige, ongewone, aanhoudende of herhalende infeksies met die patogeniese *Mycobacterium tuberculosis* te kry. Verskeie gene wat met MSMD geassosieer word is reeds beskryf, onder andere *IFNGR1*, *IFNGR2*, *IL12RB1*, *IL12B*, *STAT1*, *NEMO*, *ISG15*, *IRF8*, *TYK2* en *CYBB*. Hierdie gene lei almal tot die ontwrigting van die IL-12-IFN-γ sitokien padweë wat noodsaaklik is vir die beheer van mikobakteriële infeksies. Hierdie genetiese diversiteit lei tot verskeie unieke versteurings wat verskil in die manier van oorerflikheid en kliniese voorkoms. ‘n Akkurate molekulêre diagnose, wat bevestig is deur funksionele studies, is daarom belangrik om te verseker dat die pasiënt optimale behandeling en profilakse vir infeksies ontvang. Die doel van hierdie studie was om ‘n stel immuun-fenotipering en funksionele validering toetse te implementeer en optimaliseer vir die MSMD kenmerkende sitokien padweë van IL-12 en IFN-γ.

**Metodes:** Bloedmonsters van 17 pasiënte met ‘n kenmerkende MSMD kliniese fenotipe is vir DNS ekstraksie en PBMC isolasie geneem. Volledige-eksoom-volgordebepaling (WES) is op pasiënt DNS uitgevoer en die data is deur ‘n binne-huis bioinformatika pyplyn, TAPER™, verwerk. ‘n Stel vloeisitometrie en ELISA-gebaseerde funksionele toetse was geïmplementeer en geöptimaliseer om the integriteit van die IL-12 en IFN-γ padweë te ondersoek. IFN-γR1 en IL-12Rβ1 uitdrukking is deur middel van standard vloeisitometrie bepaal, en IFN-γ en IL-12 sein-oordrag is bepaal deur ondersoek van pSTAT1 en pSTAT4 deur middel van fosfo-spesifieke vloeisitometrie. IFN-γ-geïnduseerde-IL-12-produksie, asook IL-12-geïnduseerde-IFN-γ-produksie, is deur ELISA bepaal na 48 uur *in vitro* stimulasie met die onderskeie sitokiene. Funksionele en genetiese data was versoen om MSMD te bevestig of uit te sluit as die betrokke PID.

**Resultate:** Moontlike patogeniese genetiese variante is geïdentifiseer in 11 van die 17 pasiënte. Variante in MSMD-veroorsakende gene is in 8 van hierdie pasiënte gevind, maar slegs een van hierde variante, *IFNGR1* (c.818del4), is al voorheen beskryf. Variante is ook in gene gevind wat nog nie voorheen met MSMD geassosieer is nie, insluitend *IKZF1*, *NOD2*, *IRAK1*, *IKBKB* en *NFKB2*. Die funksionele toetse was suksesvol geöptimaliseer en die kombinasie van hierdie toetse vir die integriteit van die IL-12 en IFN-γ padweë het immuundefekte in die meerderheid van die pasiënte geïdentifiseer.

**Gevolgtrekkings:** Hierdie studie het gelei tot die implementering van funksionele immuunassesseringstoetse wat dit moonlik maak om die impak van beide nuwe en vooraf-beskryfde genetiese variante op die IL-12 en IFN-γ padweë te bepaal. Die resultate van die funksionele toetse het gewissel en dikwels het variante in dieselfde geen tot verskillende fenotipes gelei. Dít beklemtoon die noodsaaklikheid van *in vitro* funksionele bevestiging van alle PIDs. Dit sal voordelig wees om hierdie toetse op ‘n roetine wyse aan te wend vir pasiënte wat vermoedelik ‘n PID het wat verwant is aan tuberkulose-vatbaarheid. ‘n Molekulêre diagnose sal lei tot beter behandelingopsies vir hierdie pasiënte, omdat die molekulêre meganisme van die individu se siekte toegelig is.

# Acknowledgements

Several individuals contributed significantly to the completion of this thesis and I extend my gratitude to you all.

Firstly, I would like to acknowledge my supervisors, Dr Richard Glashoff and Prof. Monika Esser, for their ongoing support and willingness to help me in whichever way I needed. Thank you for always providing me with insightful guidance when I needed it. The enthusiasm you show for my research motivated me to keep going and to keep aiming higher. I am grateful for all the opportunities that arose due to this research and I look forward to working with you in the future.

Dr Andrea Gutschmidt, for assistance with setting up the flow panels and always being around whenever things went wrong with the flow cytometer. Dr Tongai Maponga and Ms Shalena Naidoo, for always lending a helping hand and an eager ear. Without you around it would have taken me three times longer to figure everything out by myself.

Our PIDDGEN collaborators at the Department of Molecular Biology and Human Genetics, for their assistance with the genetic analysis and recruitment of laboratory volunteers. A special thanks to Dr Brigitte Glanzmann for always going out of her way to help me with anything I needed, no matter how big or small the task.

Dr Adre Lourens, Dr Helena Cornelissen, the C3A nursing staff, and other doctors and registrars that aided in patient blood collection and delivery.

I also want to thank my colleagues and peers for creating an environment that encourages learning and self-discovery. I am very blessed to have such a friendly work environment. And, of course, thank you Paulina for always keeping my seat (and desk) warm for me whenever I leave the office.

I thank my family and friends for their support and encouragement.

Lastly, I would like to acknowledge the funders, without whom none of this research would be possible.

Project funders:

National Health Laboratory Science (NHLS) Research Trust
Harry Crossley Foundation

Personal funders:

National Research Foundation (NRF) Innovation Scholarship
Stellenbosch University, Merit Bursary

# Publications & Presentations

**Poster presentation** at LISA Summer Academy in Immunology, 15 August 2017. Hannover, Germany:

> *Ansia van Coller, Brigitte Glanzmann, Marlo Möller, Michael Urban, Nikola Schlechter, Craig Kinnear, Monika Esser, Richard Glashoff.* Identification of variants associated with the Primary Immunodeficiency Mendelian Susceptibility to Mycobacterial Disease (MSMD) in South Africa.

**Oral and Poster presentation** at South African Immunology Society (SAIS) Conference, 4 September 2017. Gordon's bay, South Africa:

> *Ansia van Coller, Brigitte Glanzmann, Marlo Möller, Michael Urban, Nikola Schlechter, Craig Kinnear, Monika Esser, Richard Glashoff.* Identification of variants associated with the Primary Immunodeficiency Mendelian Susceptibility to Mycobacterial Disease (MSMD) in South Africa.

**Oral presentation** at the Annual Academic Day of the Faculty of Medicine and Health Sciences. 29 August 2018. Tygerberg Campus, Stellenbosch University

> *Ansia van Coller, Brigitte Glanzmann, Marlo Möller, Craig Kinnear, Caitlin Uren, Michael Urban, Mardelle Schoeman, Monika Esser, Richard Glashoff.* Variable Clinical and Molecular Phenotypes of *IFNGR1* Mutations in Mendelian Susceptibility to Mycobacterial Disease in South Africa.

**Poster presentation** at the 18th Biennial meeting for the European Society for Immunodeficiencies, 24-27 October 2018. Lisbon, Portugal:

> *Ansia van Coller, Brigitte Glanzmann, Marlo Möller, Craig Kinnear, Caitlin Uren, Michael Urban, Mardelle Schoeman, Monika Esser, Richard Glashoff.* Variable Clinical and Molecular Phenotypes of *IFNGR1* Mutations in Mendelian Susceptibility to Mycobacterial Disease in South Africa.

**Co-authored publication in peer-reviewed journal.**

> *Brigitte Glanzmann, Caitlin Uren, Nikola de Villiers, Ansia van Coller, Richard Glashoff, Michael Urban, Eileen G. Hoal, Monika M. Esser, Marlo Möller, Craig Kinnear.* (2018) Primary immunodeficiency diseases in a tuberculosis endemic region - challenges and opportunities. Genes and Immunity.

# Table of Contents

# List of Tables

# List of Figures

# List of Abbreviations

| | |
|---|---|
| .fcs | Flow Cytometry Standard File |
| .vcf | Variant Called Format File |
| ACMG | American College of Medical Genetics and Genomics |
| AEC | Airway epithelial cells |
| AFB | Acid-fast bacteria |
| AMs | Alveolar macrophages |
| APC | Allophycocyanin |
| APCs | Antigen presenting cells |
| ASL | Airway surface liquid |
| BB700 | Brilliant Blue 700 |
| BCG | Bacillus Calmette–Guérin |
| BCGosis | Disseminated disease caused by BCG |
| BP | Band-pass filter |
| BV421 | Brilliant Violet 421 |
| BV510 | Brilliant Violet 510 |
| CADD | Combined Annotation Dependant Depletion |
| CAF | Central Analytic Facility |
| CD | Cluster of differentiation |
| CD119 | CD marker for IFN-γR1 |
| CD212 | CD marker for IL-12Rβ1 |
| CDC | Centers for Disease Control and Prevention |
| CFP-10 | Culture filtrate proteins -10 |
| CGD | Chronic granulomatous disease |
| $CO_2$ | Carbon dioxide |
| CS&T | Cytometer Setup and Tracking |
| CVID | Common Variable Immunodeficiency |
| DCs | Dendritic cells |
| DMSO | Dimethyl sulfoxide |
| DNA | Deoxyribonucleic acid |
| EDTA | Ethylenediaminetetraacetic acid |
| ELISA | Enzyme-linked immunosorbent assay |

| | |
|---|---|
| ELIspot | Enzyme-linked immunospot assay |
| ERK | Extracellular signal-regulated kinases |
| ESAT-6 | Early secrete antigenic target-6 |
| FAS | First Apoptosis Signal |
| FATHMM | Functional Analysis Through Hidden Markov Models |
| FBS | Foetal Bovine Serum |
| FcγR | Fc gamma Receptor |
| FcγRIIB | Inhibitor of FcγR |
| FITC | Fluorescein isothiocyanate |
| FMO | Fluorescence Minus One |
| FSC | Forward Scatter |
| FVS | Fixable Viability Stain |
| GAF | Gamma-activating factor |
| GERP | Genomic Evolutionary Rate Prediction |
| HIV | Human Immunodeficiency Virus |
| HREC | Human Research Ethics Committee |
| HSCT | Hematopoietic stem cell transplantation |
| IFN | Interferon |
| Ig | Immunoglobulin |
| IGRAs | Interferon-gamma release assays |
| IL | Interleukin |
| IPEX | Immune deficiency associated with faulty regulatory T cell development |
| IQR | Interquartile range |
| IRAK | Interleukin-1 receptor-associated kinase |
| IRF | Interferon Regulatory Factor |
| ISG | Interferon-Stimulated gene |
| ISGF | Interferon-Stimulated gene Factor |
| IU | International units |
| IUIS | International Union of Immunological Sciences |
| JAK | Janus Kinase |
| JMF | Jeffrey Modell Foundation |
| LP | Long-pass filter |
| *M.avium* | *Mycobacterium avium* |

| | |
|---|---|
| *M.bovis* | *Mycobacterium bovis* |
| *M.tb* | *Mycobacterium tuberculosis* |
| mAb | Monoclonal Antibody |
| MAIT | Mucosal associated invariant T cell |
| MDR | Multi-drug resistant |
| MFI | Median Fluorescence Intensity |
| MSMD | Mendelian Susceptibility to Mycobacterial Disease |
| MTBC | *Mycobacterium tuberculosis* complex |
| MyD88 | Myeloid differentiation primary response 88 |
| NEMO | NF-κB essential modulator protein, also known as IKK-γ |
| NF-κB | Nuclear factor kappa B |
| NHLS | National Health Laboratory Service |
| NIL | Negative control |
| NK | Natural Killer |
| OD | Optical Density |
| p | Probability value |
| PAMPs | Pathogen associated molecular patterns |
| PBMCs | Peripheral blood mononuclear cells |
| PBS | Phosphate Buffered Saline |
| PCR | Polymerase chain reaction |
| PE | Phycoerythrin |
| PE-Cy5 | Phycoerythrin-Cyanin5 |
| PE-Cy7 | Phycoerythrin-Cyanin7 |
| PerCP-Cy5.5 | Peridinin-chlorophyll protein-Cyanin5.5 |
| PHA | Phytohaemagglutinin |
| Phosflow | Phospho-specific flow cytometry |
| PID | Primary Immunodeficiency |
| PIDDGEN | Primary Immunodeficiencies Diseases Genetics Research Group |
| pSTAT | Phosphorylated STAT molecule |
| PMT | Photomultiplier tubes |
| QFT | QuantiFERON |
| q-PCR | Real-time polymerase chain reaction |
| r | Spearman correlation coefficient |

| | |
|---|---|
| RCF | Relative Centrifugal Force |
| ROS | Reactive Oxygen Species |
| RPMI | Roswell Park Memorial Institute medium |
| rSD | Robust standard deviation |
| $rSD_{EN}$ | Robust standard deviation of electronic noise |
| SCID | Severe Combined Immunodeficiency |
| SD | Standard deviation |
| SIFT | Sorting intolerant from tolerant |
| SSC | Side Scatter |
| STAT | Signal transducer and activator of transcription |
| TAPER | Tool for Automated selection and Prioritisation for Efficient Retrieval of sequence variants |
| TB | Tuberculosis |
| TBH | Tygerberg Academic Hospital |
| TBM | Tuberculous meningitis |
| $T_H1$ | T lymphocyte helper subset 1 |
| $T_H2$ | T lymphocyte helper subset 2 |
| TLR | Toll-like Receptor |
| TMA | Torrent mapping alignment |
| TNF | Tumour Necrosis Factor |
| TST | Tuberculin skin test |
| TYK | Tyrosine kinase |
| USA | United States of America |
| WAS | Wiskott-Aldrich Syndrome |
| WES | Whole Exome Sequencing |
| WHO | World Health Organisation |

# Chapter 1 Introduction

Primary immunodeficiencies (PIDs) are genetically inherited disorders caused by defects in one or more elements of the immune system. There is very little reporting of PIDs in Africa and it is suspected that they may be a lot more common than previously thought (Modell et al. 2016). The under-reporting of PIDs from socially and economically disadvantaged communities is of special concern and increased awareness is needed in order to diagnose, treat and prevent devastating childhood infections due to immune deficits in these communities (Eley and Esser 2014).

South Africa is among the countries with the highest burden of tuberculosis (TB) (WHO 2016) and PIDs that relate specifically to susceptibility to mycobacterial infection, such as Mendelian Susceptibility to Mycobacterial Disease (MSMD) is of particular importance. Being an area of high endemicity, children with MSMD are at further increased risk for acquiring severe, recurrent, unusual and persistent TB infections (Esser et al. 2016).

In countries with high TB burden, it is essential to identify individuals with MSMD early since they are at risk for developing potentially devastating TB infections, including early BCG (Bacillus Calmette–Guérin)-dissemination if they are not diagnosed timeously. It is possible that MSMD and other PIDs relating to TB susceptibility are more common in South Africa than previously believed due to these PIDs being overshadowed by the massive Human Immunodeficiency Virus (HIV)-TB co-epidemics. It is therefore important to find a more rational immunological approach for the screening and diagnosis of MSMD.

Currently, the most reliable way to diagnose MSMD and other PIDs relating to TB susceptibility is through Whole Exome Sequencing (WES). After a plausible disease-causing variant has been identified through WES, patient immune cells should be studied *in vitro* in order to confirm the functional manifestation of the identified variant (Gallo et al. 2016; Casanova et al. 2013).

In this study, a set of functional immune screening tests relating to the Interleukin-12-Interferon-gamma (IL-12-IFN-γ) pathway, which is essential for the control of mycobacteria, were implemented and optimised to aid in the diagnosis of MSMD and related PIDs in our setting. These assays were then used to assess the integrity of the IL-12-IFN-γ pathway in 17 suspected MSMD patients.

A validated functional screen for MSMD would allow for confirmation of functional manifestations of known and novel genetic signatures of this condition. Effective and accurate diagnosis of this condition is important in the broader context of PIDs in general in that these assays could provide a resource for screening for PIDs that overlap, especially at the level of cytokine gene function and related immunological signalling cascades.

Reliable functional screening tests to aid in the diagnosis of PIDs relating to TB are essential to ensure that the affected individuals receive the correct treatment and long-term care.

# Chapter 2 Literature Review

## 2.1. Primary Immunodeficiencies

PIDs are genetically inherited, non-communicable heterogeneous disorders caused by defects in different elements of the immune system. PIDs are generally characterised by severe, persistent, unusual and/or recurrent infections usually presenting in infancy and early childhood. These infections often involve microorganisms that rarely cause disease in healthy people. PIDs consist of a group of more than 350 genetically determined mono-genetic conditions that have an identified molecular basis (Picard et al. 2018). The pattern, frequency and severity of infections depend on the underlying immunological defect as well as geographical and social determinants (Modell et al. 2016; Eley and Esser 2014).

PIDs can present in many different ways, apart from unusual infections. Particular organ problems (e.g. diseases involving the skin, heart, facial development and skeletal system) may be present in certain conditions. Others may predispose to the development of tumours or autoimmune disease, where the immune system reacts to the body's own tissues. The type of infections, as well as the additional features can provide clues as to the exact nature of the immune defect (Al-Mousa and Al-Saud 2017; Bonilla et al. 2015; Routes et al. 2014; Arkwright and Gennery 2011). A summary of general warning signs for PID are listed in Table 2.1.

In most countries, PID screening is not routinely performed on individuals at birth (or any other stage of life), therefore PIDs are usually only detected after the affected individual has experienced severe or recurrent infections. A study from Bousfiha et al. (2013) has revealed that PIDs are a lot more common than previously estimated and that about 1-2% of the population worldwide are affected by some form of PID.

Awareness of PIDs among healthcare professionals, patients and the general public remains a challenge and there is a pressing need to improve awareness in order to ensure early diagnosis, treatment and management of these conditions and ultimately reduce the associated morbidity and mortality (Picard et al. 2018; Chapel et al. 2014).

**Table 2.1**: **Summary of PID warning signs**. Adapted from de Vries et al. (2012) & van den Berg et al. (2017).

| **Findings Suggestive of Immunodeficiency** |
|---|
| Persistent lymphopaenia |
| Severe, Persistent, Unusual and Recurrent (SPUR) infections<br>• Eight ear infections, two sinus infections per year, two episodes of pneumonia within one year or chronic suppurative chest infection/lesion<br>• Rare or unusual complications, for example, complicated varicella or vaccination complication<br>• Infections caused by unexpected or opportunistic microorganisms |
| Dependence on or refractory to antibiotic therapy<br>• Need for intravenous antibiotics to clear infection<br>• Two or more deep-seated infections (e.g. sepsis, meningitis, pneumonia) |
| Organisms<br>• Less virulent or opportunistic causative agent<br>• Persistent oral thrush or cutaneous candidiasis (especially in children older than four months)<br>• *Neisseria meningitidis* meningitis. |
| Constitutional symptoms<br>• Failure to thrive<br>• Persistent, extensive, atypical dermatitis or erythroderma<br>• Chronic diarrhoea |
| Clinical examination<br>• Lymph nodes and tonsils may be absent in severe PID<br>• Evidence of chronic ear infection; Evidence of bronchiectasis |
| Family History<br>• Diagnosed PID in the family or familial occurrence of similar symptoms; Unexplained sudden death in infancy<br>• Consanguinity<br>• Autoimmunity or malignancy in several family members |
| Age and Gender<br>• Severe Combined Immunodeficiency (SCID) presents in early infancy<br>• Profound antibody deficiency usually presents in first year of life<br>• Severe immunodeficiencies more commonly affect boys |
| Unexplained fever or autoimmunity |

## 2.1.1. Types of Primary Immunodeficiencies

The International Union of Immunological Sciences (IUIS) PID expert committee has proposed a PID classification system, which facilitates clinical research and comparative studies worldwide. It is updated every other year to include new disorders or disease-causing genes (Picard et al. 2018; Bousfiha et al. 2015; Ochs and Hagin 2014). Table 2.2 shows the global prevalence of the different types of PID, as reported by physicians in 2016 (Modell et al. 2016).

**Table 2.2: Physician reported prevalence of primary immunodeficiencies globally**. Adapted from Modell et al. (2016)

| Type of Primary Immunodeficiency | n | % |
|---|---|---|
| Combined immunodeficiency | 4 762 | 5.3 |
| Well-Defined Syndromes with Combined Immunodeficiency | 11 597 | 12.9 |
| Predominantly Antibody Deficiencies | 47 548 | 53.0 |
| Diseases of Immune Dysregulation | 2 633 | 2.9 |
| Congenital Defects of Phagocyte number, function or both | 4 654 | 5.2 |
| Defects in Innate Immunity | 954 | 1.1 |
| Autoinflammatory Disorders | 6 402 | 7.1 |
| Complement Deficiencies | 4 948 | 5.5 |
| Unspecified or Other Deficiencies (Phenocopies of PID) | 6 136 | 6.8 |
| **Total** | **89 634** | **100** |

Primary immunodeficiencies are broadly characterised into nine distinct groups (Picard et al. 2018; Al-Herz et al. 2015; Ochs and Hagin 2014; Routes et al. 2014):

(1) **Combined immunodeficiency**, which includes severe combined immunodeficiency (SCID) and other combined immunodeficiencies with less profound effects. This mainly includes defects in signalling pathways, abnormal development of T and B cells and insufficient DNA repair;

(2) **Combined immunodeficiency with associated/syndromic features**, which refers to disorders of combined immunodeficiency associated with characteristic features that may present prior to immune defects for instance Wiskott-Aldrich (WAS), DiGeorge, hyper Immunoglobulin (Ig) E syndromes, etc.;

(3) **Antibody deficiency**, which results in reduction in one or more serum immunoglobulin isotypes and a profound decrease in B cell numbers, for example common variable immunodeficiency (CVID) and CD40/CD40L deficiency;

(4) **Immune dysregulation**, which includes a wide range of disorders such as immune deficiency associated with faulty regulatory T cell development (e.g. Immune deficiency associated with faulty regulatory T cell development [IPEX] syndrome) or other defects affecting lymphocyte proliferation or the cytotoxic or apoptotic functions of lymphocytes;

(5) **Defects of phagocyte number and/or function**, which includes defects that lead to abnormal differentiation of myeloid cells, decreased neutrophil mobility due to abnormal adherence to endothelium, defects in respiratory oxidative burst, and defects in macrophage and lymphocyte signalling pathways;

(6) **Defects in innate immunity**, which is due to defects in pathways involved with germline encoded receptors [e.g. Toll-like receptors (TLRs)], this usually results in lack of cytokine production and overall lack of response in innate immune cells, examples include defects in Interleukin-1 receptor-associated kinase 4 (IRAK4) and Myeloid differentiation primary response 88 (MyD88) which impairs TLR3 signalling;

(7) **Autoinflammatory disorders**, which are associated with recurring fevers and other inflammation-associated features. These disorders can be due to inflammasome defects (e.g. overproduction of pro-inflammatory cytokine such as IL-1β) or non-inflammasome related defects (e.g. deficiency of IL-1 receptor antagonist);

(8) **Complement deficiency**, which refers to defects in the classic, alternative and/or lectin complement regulatory pathways. This results in a broad range of clinical phenotypes, which ranges from susceptibility to encapsulated bacteria to autoimmunity;

(9) **Phenocopies of primary immunodeficiency disease**, which includes conditions that resemble PID but lack causative germline mutations, for instance autoantibody production against various cytokines.

## 2.1.2. Diagnosis of Primary Immunodeficiencies

Underdiagnoses and diagnostic delay contribute to mortality and morbidity associated with PIDs. Identification of the cause of the PID at the molecular level as well as the associated disease mechanisms could enable earlier protective interventions and targeted treatment. Identifying defects as early as possible is also essential in order to minimise administration of certain treatments and procedures, for instance an X-ray will exacerbate the condition of patients with PIDs associated with 'unstable DNA (Stray-Pedersen et al. 2017; Routes et al. 2014). Precise diagnosis is necessary, not only to ensure that the patient receives defect-specific treatment and care, but also so that the affected family members can receive genetic counselling and/or pre-natal screening for future children (Chapel et al. 2014).

While recurrent, persistent and unusual infections are the most common presentation of PID, other clinical and laboratory findings can be equally informative for diagnosis. The first step toward a PID diagnosis involves a thorough analysis of a suspected patient's medical history. Birth route, vaccination and infection history, response to antibiotic therapy, etc. are all to be considered when investigating a PID (Ochs and Hagin 2014; Madkaikar et al. 2013). Complete physical examination, with attention to dysmorphic features, evaluation of lymphoid tissue, rashes, warts, and thrush should also be performed. The medical history and physical examinations should direct further investigations, such as screening of different components of the immune system by means of laboratory testing (Ochs and Hagin 2014).

Several laboratory tests can be performed if a patient is suspected of having a PID. These may include, but are not limited to, full blood count, differential leukocyte subset counts (enumeration of granulocytes, lymphocytes, monocytes), lymphocyte subset count (enumeration of T cells [total CD3+, CD4+ and CD8+ subsets], B cells and Natural Killer [NK] cells), neutrophil burst assay, immunoglobulin isotypes/subclasses, and total complement assessment. These initial laboratory tests can give an indication as to which type of immune defect, based on the World

Health Organisation (WHO)/IUIS classification format, the patient might have (Picard et al. 2018; Al-Herz et al. 2015; Bonilla et al. 2015; Madkaikar et al. 2013). Sometimes, however, the baseline laboratory tests do not reveal an obvious immune defect. In such cases molecular testing, such as sequencing of specific genes, WES and chromosomal microarrays, can provide valuable information. Molecular testing is discussed further in section 2.3.2**.** More detailed information on the routine laboratory methods used for the evaluation of immunodeficiencies of both adaptive and innate immunity can be found in Table 2.3 (Chapel et al. 2014; Ochs and Hagin 2014).

**Table 2.3: Evaluation of Immunodeficiencies of Adaptive and Innate Immunity**. Adapted from Ochs and Hagin (2014).

| System | Quantitative evaluation | Qualitative evaluation |
|---|---|---|
| **Adaptive Immunity** | | |
| B cells and antibody production | ○ Flow cytometry to enumerate and characterise B cells.<br>○ Serum Immunoglobulin isotype levels (IgG, IgA, IgM, IgE).<br>○ Specific Antibody levels (to vaccines). | ○ B cell flow-based immunophenotyping to evaluate B cell development and maturation.<br>○ Antibody responses to booster immunisation.<br>○ Antibody responses to neoantigens. |
| T cells | ○ Flow cytometry to enumerate and characterise T cell subsets. | ○ T cell flow-based immunophenotyping to evaluate T cell development and maturation.<br>○ Mitogen and antigen proliferation assays.<br>○ Anti-CD3 proliferation assay. |
| **Innate Immunity** | | |
| Complement system | ○ Levels of individual complement component (usually ordered after abnormal pathway activity). | ○ $CD_{50}$ (classical pathway activity).<br>○ $AH_{50}$ (alternative pathway activity).<br>○ Lectin pathway activity.<br>○ Function of individual complement. |
| Phagocytic system | ○ Blood cell count and differential.<br>○ Examination of stained blood smear.<br>○ Flow cytometry for adhesion molecules.<br>○ Bone marrow biopsy. | ○ Measurement of oxidase function (nitroblue tetrazolium test or equivalent). |
| NK cells | ○ Flow cytometry to enumerate NK cells. | ○ Target cell lysis. |
| TLRs | | ○ Expression of degranulation surface marker.<br>○ Cytokine production in response to different TLR antagonists. |

Abbreviations: Ig, Immunoglobulin; $AH_{50}$, complement, alternative pathway; $CD_{50}$, total haemolytic complement assay; NK, natural killer; TLR, Toll-like receptor.

## 2.1.3. Treatment of Primary Immunodeficiencies

Most PIDs are lifelong conditions and there is a great need to detect these defects as early as possible in order to refer individuals to specialised care centres or to initiate therapies that can be continued in an open-ended fashion. Early diagnosis and therapy is the best approach to prevent significant disease-associated morbidity. (Oliveira and Fleisher 2010; Immune Deficiency Foundation 2009).

Different PIDs present with varying degrees of susceptibility to pathogenic organisms, depending on the specific disorder as well as other environmental factors. Many PIDs have defining characteristics which can guide the diagnostic and treatment approach. Where PIDs are associated with decreased immunoglobulin isotypes (Ig), such as IgA deficiency or IgG subclass deficiency, immunoglobulin replacement therapy is a preferred treatment option (Bonilla et al. 2015; Chapel et al. 2014). PIDs associated with SCID or severe immune dysregulation, including lymphoproliferation and syndromes with autoimmunity, aggressive chemotherapy followed by hematopoietic stem cell transplantation (HSCT) is recommended as soon as possible in order to prevent demise of the patient (Eley and Esser 2014; Routes et al. 2014). Phagocytic defects are often treatable with IFN-γ and antimicrobials, although in some cases HSCT has been performed successfully. Prophylactic anti-microbials and anti-fungal agents are often prescribed for PID patients in order to prevent future infection, and often this is the only way to manage PIDs for which no other treatment is available or effective (Bonilla et al. 2015; Chapel et al. 2014; Immune Deficiency Foundation 2009).

More recently, gene therapy, which ‘edits’ the patient’s DNA and replaces a faulty gene with a functional one, is being assessed for use in children for which HSCT is not available (generally due a lack of a matched donor for HSCT). Gene therapy is not currently used as a routine treatment approach, although it has been performed successfully, in clinical trials, on several patients mostly SCID, chronic granulomatous disease (CGD) and WAS patients, and they generally no longer require therapy or prophylaxis. A small number of patients who have received gene therapy developed leukaemia-like disorders as a result of random mutations introduced into the host due to the viral vector used for gene therapy. To minimise this mutagenic effect of the vectors, new improved self-inactivating viral vectors have been developed and are currently being used in clinical trials and have thus far proven much safer than the original vectors (Ghosh and Gaspar 2017; Modell et al. 2016; Chapel et al. 2014; Immune Deficiency Foundation 2009). Gene therapy holds great promise for the future treatment of PIDs with defined molecular diagnoses.

The role of vaccination in PID has been greatly debated. Vaccines, specifically inactivated vaccines rather than live vaccines in most cases, are beneficial in some PIDs (e.g. neutrophil defects, complement deficiency, other antibody failure PIDs) and will contribute to prevention of

severe infections. On the other hand, vaccination can also be detrimental in certain PIDs (e.g. SCID, CGD, T-cell defects). BCG dissemination, also referred to as BCGosis, due to vaccination can compromise HSCT in these patients. It is recommended that vaccination be delayed in all children with suspected PID until the nature of their condition has been elucidated (Principi and Esposito 2014).

Specialist PID care is often unavailable in less developed regions of the world, even once a diagnosis is made. Governments in such countries often do not fund life-long immunoglobulin replacement or HSCT. Management of PID patients is a financial and technical challenge for developing countries (Chapel et al. 2014).

## 2.1.4. Prevalence of Primary Immunodeficiency in South Africa

There is very little reporting of PIDs in Africa. In the 2016 Jeffrey Modell Foundation (JMF) global survey, 1 237 patients with PIDs out of a global total of 83 743 were from Africa (Table 2.4) (Modell et al. 2016). This low under-reported prevalence of 1.5% contrasts with Africa's contribution of approximately 15% to the total global population. Speculation based on population size and world-wide prevalence data, suggests that from 58 000 to as many as 902 000 PID cases should be reported from Africa (Bousfiha et al. 2013). In South Africa, assuming the prevalence of PID is similar to that in well-resourced settings, the total number of people with PIDs should range between 3 000 and 46 000. However, in total fewer than 400 PID cases have been reported in South Africa (Esser et al. 2016; Naidoo et al. 2010). The patients in the South African National PID Registry reflect similar deficiencies to those in European and USA data, with the majority being antibody deficiencies. The under-reporting of PIDs from disadvantaged communities is of special concern. As infections are common in childhood in such communities, an increased level of awareness is needed to investigate those infections that may be caused by an immune deficit (Eley and Esser 2014).

**Table 2.4: The number of patients followed, diagnosed and referred with primary immunodeficiency globally compared to in Africa in 2015.** Adapted from Modell et al. (2016)

| | **Globally (2015)** | **Africa (2015)** |
|---|---|---|
| **Patients evaluated and followed** | 157 454 | 1 627 |
| **Patients diagnosed with Primary immunodeficiencies** | 83 743 | 1 237 |
| **Patients referred** | 81 339 | 2 260 |

## 2.2. Tuberculosis

In 1882, Robert Koch discovered and described *Mycobacterium tuberculosis* (*M.tb*), the causative agent of TB. *M.tb* is an obligate intracellular pathogenic bacterium that primarily infects the lungs or other parts of the respiratory system (Keshavjee and Farmer 2012). It has been theorised that the *M.tb* complex, which consists of a group of closely related Mycobacterium species, originated in Africa and co-evolved, migrated and expanded with their human hosts. This theory of the co-expansion of *M.tb* and modern humans is supported by the similarities in geographical locations of branching and divergence events that were found after comparing *M.tb* phylogeny and human mitochondrial genomes (Comas et al. 2013; Blouin et al. 2012; Hershberg et al. 2008; Wirth et al. 2008).

Currently, TB is the worldwide leading cause of death due to a single infectious agent (Fogel 2015; Tiruviluamala and Reichman 2002). It is estimated that approximately one third of the global population is infected with TB. In 2016, there was an estimated 1.3 million deaths globally due to TB and an additional 374 000 deaths due to HIV-TB co-infection. The WHO reported an estimated TB incidence of 10.4 million cases worldwide in 2016. South Africa is one of 14 countries listed by the WHO with the highest burden of TB, HIV-TB co-infections and also multi-drug resistant (MDR)-TB cases. Figure 2.1 illustrates the estimated global incidence of TB, as recorded in 2016. South Africa has a TB incidence of 258 000 cases per year and an additional 19 000 incidence cases of MDR-TB. The high TB incidence is also associated with high rates of mortality in both TB mono- and HIV-TB co-infection (CIA World Factbook 2018; World Health Organization 2017).

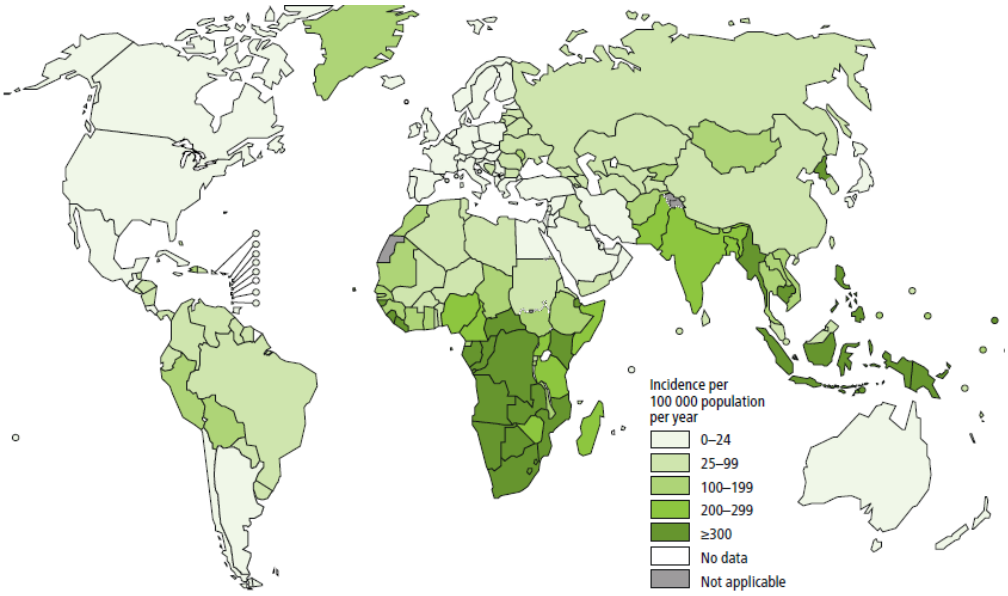


**Figure 2.1: Estimated TB incidence worldwide in 2016 (World Health Organization 2017).** South Africa, with a TB incidence of 258 000 cases a year, is one of the 14 countries in the world with the highest TB incidence.

## 2.2.1. Host Immune Response to Mycobacterial Infection

*M.tb* enters the host via the respiratory tract through the inhalation of contaminated droplets. The preferred target cell is the alveolar macrophage. Once the organism has infected alveolar macrophages there are 4 potential outcomes: (1) The initial host immune response is effective in killing the organism, which means that there is no chance that the individual will develop TB; (2) The bacterium can multiply effectively in the lung macrophages, which will lead to clinical disease known as pulmonary or primary TB; (3) The bacterium becomes dormant and does not cause any clinical disease, this is known as latent TB infection; (4) Dormant or latent *M.tb* can start to multiply again to cause clinical disease similar to (2), this is often referred to as 'reactivation' of TB (O'Garra et al. 2013; Schluger and Rom 1998).

Generally, the *M.tb* bacterium can be controlled by the immune response in healthy people. An effective immune response consists of both the innate and adaptive immune components. The innate immune response refers to the initial immune response carried out by host immune cells upon first contact with the pathogen. The adaptive immune response, on the other hand, is dependent on prior contact with the pathogen's antigens or immunogenic components and is initiated after the initial innate responses. The adaptive immune response is more specifically directed against the particular invading pathogen, due to the antigen-epitope specificity of adaptive immune cells. The antigen specificity allows for more effective control and/or elimination of the pathogen from the host than innate immunity, which operates on a broader pathogen pattern recognition principle (Jasenosky et al. 2015; Lerner et al. 2015; O'Garra et al. 2013; Vankayalapati and Barnes 2009). Figure 2.2 summarises the general innate and adaptive immune responses to pathogens. Figure 2.3 illustrates the cellular immune response to TB.

### Innate Immunity

Two out of three people that are exposed to TB, do not develop active TB disease, suggesting that the innate immune responses of most healthy individuals is capable of preventing *M.tb* infection without the need for an adaptive, T or B cell mediated response (Lerner et al. 2015; Gupta et al. 2012; Vankayalapati and Barnes 2009). A short summary of the effector mechanisms of the major innate immune cells is summarised in Table 2.5.

**Table 2.5: Effector mechanisms of the major innate immune cells.** Adapted from Gupta et al. (2012)

| | **Effector mechanism(s)** |
|---|---|
| **Neutrophils** | Degranulation<br>Production of reactive oxygen species |
| **Macrophages** | Phagocytosis<br>Production of reactive nitrogen intermediates and nitic oxide |
| **NK cells** | Cytolysis of infected cells/intracellular bacteria<br>Activation of macrophages via IFN-γ |
| **Complement system** | Membrane attack complex, opsonisation and phagocytosis by macrophages |

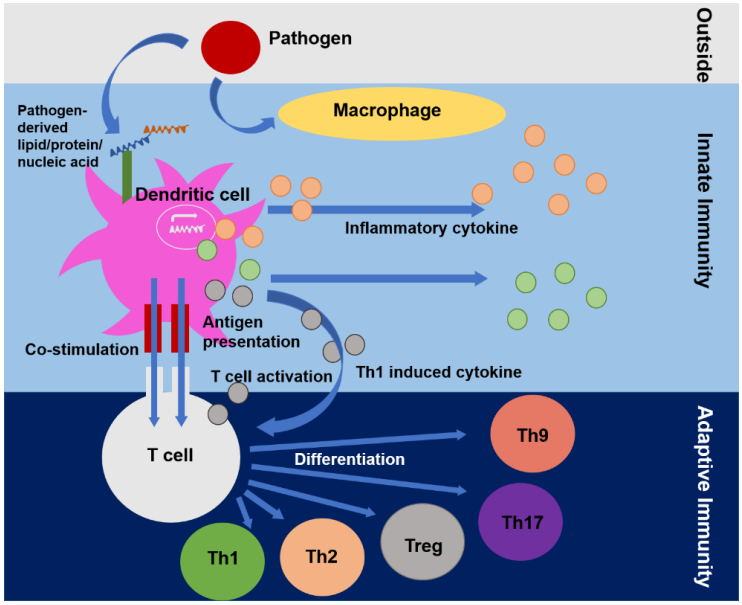


**Figure 2.2: The innate and adaptive immune response to a pathogen.** Innate immune responses are initiated on first contact with a pathogen and leads to a general inflammatory response through the production of various mediators. The innate immune cells play an important role in activating adaptive immune responses, which are more specific and is mediated by various adaptive immune cell subsets.

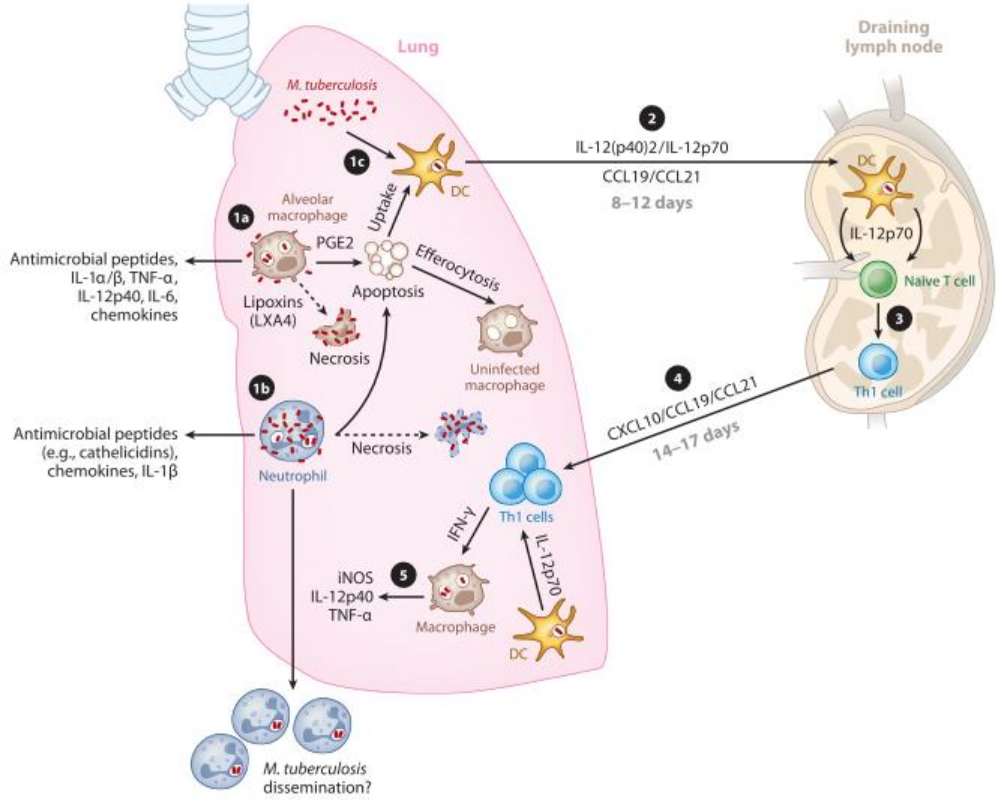


**Figure 2.3. The cellular immune response to *M. tb* (O'Garra et al. 2013)**. (1) After initial infection with *M.tb*, (1a) alveolar macrophages, (1b) neutrophils and (1c) dendritic cells (DCs) can become infected, which leads to production of antimicrobial peptides and cytokines and subsequent apoptosis or necrosis. Infected cells can also be taken up by DCs, which then (2) migrate to the lymph nodes under the influence of IL-12 and various chemokines to initiate differentiation of naïve T cells into $T_H1$ cells. (3) $T_H1$ cells migrate back to the site of infection and produce IFN-γ which leads to (4) macrophage activation, cytokine/chemokine production as well as the induction of (5) microbicidal factors to enhance bacterial control.

When *M.tb* is inhaled, it passes along the respiratory mucosa of the airway, which forms the first line of defence against *M.tb*. The respiratory mucosa consists of a layer of epithelial cells that forms a barrier against invasion. Below the epithelial cells is a layer of connective tissues and immune cells such as lymphocytes and macrophages. Airway epithelial cells (AECs) can recognise pathogen associated molecular patterns (PAMPs) present on the surfaces of *M.tb*. After exposure to *M.tb* AECs can present antigens to mucosal associated invariant T cells (MAITs) and stimulate them to produce IFN-γ, tumour necrosis factor (TNF)-α and granzyme, which all contribute to the clearance of *M.tb*. MAITs respond very rapidly to infection and activate macrophages (Lerner et al. 2015; Harriff et al. 2012; Gold et al. 2010). AECs also influence the composition of the airway surface liquid (ASL), which contains mucus, immunoglobulin A and other innate immune factors such as anti-microbial peptides (Lerner et al. 2015; Harriff et al. 2012; Li et al. 2012; Middleton et al. 2003) that aid in the defence against pathogens.

*M.tb* that manages to pass through the upper airways are delivered to the alveoli, which consist of a lining of epithelial cells as well as other immune cells such as neutrophils, dendritic cells (DCs) and alveolar macrophages (AMs) (Lerner et al. 2015). Similar to AECs, alveolar epithelia can also produce anti-microbial molecules (Rivas-Santiago et al. 2005) as well as pulmonary surfactant, which cause agglutination (Ferguson et al. 1999) and enhanced phagocytosis (Gaynor et al. 1995) by macrophages upon binding to *M.tb*.

AMs are the primary tissue resident phagocytic cells involved in the initial immune response to *M.tb. M.tb* infected AMs can elicit signals that lead to the killing of the infected cells through the induction of apoptotic responses. Unfortunately, *M.tb* has developed ways to circumvent the apoptotic-driven immune responses of AMs and can often survive and proliferate in AMs (Lavalett et al. 2017; Queval et al. 2017; Srivastava et al. 2014).

DCs, also among the first cell types to encounter *M.tb*, have various receptors on their surfaces to detect PAMPs and they are very efficient phagocytes. After the uptake of *M.tb* into the cell, DCs in the alveoli will mature and migrate to the draining lymph nodes to present antigens to T cells; therefore, DCs are an important link between the innate and adaptive immune systems (Lerner et al. 2015; Marino et al. 2004).

In individuals with active TB, *M.tb* often infects neutrophils in the airways (O'Garra et al. 2013; Eum et al. 2010). Neutrophils are professional phagocytes and have been described to play conflicting roles in the pathology of TB, dependent on the host factors, pathogen virulence factors and the stage of the disease. It has been observed that neutrophils can both favour (Denis 1991) or restrict (Brown et al. 1987) the growth of *M.tb*. *M.tb* infected neutrophils can be phagocytosed by macrophages, leading to improved killing of the bacterium. Another major role of neutrophils, apart from phagocytosis, is the production of chemokines and pro-inflammatory cytokines which

lead to the activation and recruitment of other immune cells (Lerner et al. 2015; Riedel and Kaufmann 1997).

NK cells are the primary mediators for the innate immune response against TB, and mediate the production of effector molecules and cytokines that will aid in an effective immune response (Lerner et al. 2015; Li et al. 2012). NK cells are recruited to the site of infection early on and are very effective at eliciting an immune response against *M.tb*. NK cells can lyse macrophages (Vankayalapati and Barnes 2009) that are infected and also produce IFN-γ to further activate macrophages and expand T cell populations for the adaptive immune response (Lerner et al. 2015).

There is evidence that *M.tb* activates all three pathways of the complement system (classical, lectin and alternative), which enhances the inflammatory response and increases phagocytic uptake of the bacteria by AMs (Lerner et al. 2015; Gupta et al. 2012).

The innate response to TB requires a wide range of cell types to protect the host and the natural physical barriers and anti-microbial substances are just as important as the immune cells for defending the host against infection (Lerner et al. 2015; O'Garra et al. 2013). If the innate immune response is ineffective at killing *M.tb*, it will likely disseminate, and the host's adaptive immune response will become essential for control of the infection.

## Adaptive Immunity

The adaptive immune response is mediated mainly by lymphocytes. Adaptive immunity can be divided into two distinct categories, namely the humoral response, which is mediated mainly by B cells, and the cell-mediated response, which is mediated by T cells (Gupta et al. 2012; Vankayalapati and Barnes 2009). Regarding the adaptive response to TB, T cell-mediated immunity has been described to play the most vital role in the elimination of *M.tb* (Vankayalapati and Barnes 2009), however, more recent studies have shown that the humoral immune response (B cells) also play an important role in TB infection (Kozakiewicz et al. 2013; O'Garra et al. 2013). The effector mechanisms of the adaptive immune system are summarised in Table 2.6.

**Table 2.6: Effector mechanisms of the major adaptive immune cells**. Adapted from Gupta et al. (2012)

| | **Effector mechanism(s)** |
|---|---|
| **CD4+ T cells** | Cytolysis of infected cells/intracellular bacteria<br>Activation of macrophages through IFN-γ and TNF-α |
| **CD8+ T cells** | Cytolysis of infected cells/intracellular bacteria<br>Activation of macrophages through IFN-γ |
| **B cells** | Opsonisation and phagocytosis by macrophages<br>Modulation of T cell responses |

***Cell-mediated immunity***

DCs and macrophages, which can act as both phagocytes and antigen presenting cells (APCs), produce IL-12 and IL-23 during the innate immune response which drives the inflammatory response and the initiation of the cell-mediated adaptive immunity (Cooper et al. 2007; Losana et al. 2002). APCs (primarily DCs) migrate to the draining lymph nodes where they can induce the activation of naïve T cells by providing antigen-specific stimulus as well as additional signals required for the development of effector T cells (Cooper 2009). IL-12, produced during the innate immune response, has been shown to promote the migration of DCs to the lymph nodes (Khader et al. 2006; Demangel et al. 2002).

APCs (primarily DCs in the initial induction of effector T cells) induce the proliferation and differentiation of predominantly T lymphocyte helper subset 1 ($T_H1$) type effector cells. Mature *M.tb*-specific $T_H1$ (CD4+) cells then migrate to the primary site of infection to mediate the immune response to *M.tb* (Jasenosky et al. 2015; Cooper 2009). CD4+ T cell effector subtypes produce a range of essential cytokines, including IL-2, IFN-γ, and TNF-α, which play roles in activation of phagocytes (Darrah et al. 2007). IFN-γ is the main cytokine involved in the activation of macrophages and monocytes, which allows them to control infection by phagocytosis or by secreting products that can directly kill *M.tb*.

For IFN-γ production by CD4+ cells, the crucial need for IL-12 and IL-23, produced by mainly by DCs and macrophages, has been demonstrated extensively (O'Garra et al. 2013; Cooper et al. 2007; van de Vosse and Ottenhoff 2006; Khader et al. 2005; Losana et al. 2002). Decreased CD4+T cells, for instance in lymphopaenic HIV patients, has been linked to increased susceptibility to TB (Cooper 2009; North and Jung 2004; Orme et al. 1993). CD8+ T cells also contribute to immunity against *M.tb* by secreting IFN-γ, however CD8+ cells are unable to fully compensate for a lack of CD4+ cells (North and Jung 2004; Flynn and Chan 2001).

The IL-12 and IFN-γ cytokine pathways and their importance in immunity against *M.tb* is discussed in more detail in section 2.3.

In an attempt to contain the infection, granulomas, consisting of AMs, T cells and DCs are often formed to surround the bacterium to prevent further spread of the pathogen. Additional T and B lymphocytes are recruited if necessary to surround these structures in order to contain the bacteria and damaged tissues. Granuloma formation is considered to be a hallmark of TB and it signifies both infection by *M.tb* as well as an induction of a host immune response against the pathogen (Martinot 2017; Lerner et al. 2015; O'Garra et al. 2013; Gupta et al. 2012; Volkman et al. 2010). Granuloma-mediated immune cells function similarly to other immune cells and produce various cytokines, including IL-12 and IFN-γ, which aids in containment of the infection. Macrophage effector functions, including phagolysosome fusion and the deployment of reactive

oxygen/nitrogen species, all apply pressure on *M.tb* to engage in rigorous responses that arrest bacterial growth (Martinot 2017).

***Humoral immunity***

Upon exposure to pathogens, it known that CD4+ T cells can shape B cell responses, including expansion, class switching, somatic hypermutation, affinity maturation of antibodies, the development of memory B cells and antibody-producing plasma cells, as well as cytokine production (Chan et al. 2014; Vinuesa et al. 2005). B cell activity is often dependent on T cell responses; however, B cells can also modulate T cell immunity due to their ability to present antigens to naïve T cells in the lymph nodes (Lund and Randall 2010; Gray et al. 2007). This capability of B cells to present antigens to T cells have been demonstrated in a model system lacking other APCs (Liu et al. 1995; Kurt-Jones et al. 1988).

B cells can also modulate the activity of T cells through the production of a wide range of cytokines, which are either constitutively expressed or induced upon interaction with antigens or T cells (Harris et al. 2000; Mosmann 2000). In a $T_H1$ environment, B cells are primed to produce IFN-γ, IL-12, TNF, IL-10 and IL-6, which in turn promotes T cell driven immunity (Mauri and Bosma 2012; Lund and Randall 2010; Harris et al. 2005; Mosmann 2000).

Antibodies, produced by specialised B cells, can bind to *M.tb* antigens to form immune complexes, which can bind to Fcγ receptor (FcγR) to enhance the priming of T cells (Chan et al. 2014; Nimmerjahn and Ravetch 2008). Studies have shown that in mice that lack FcγRIIB, an inhibitor of FcγR, higher frequencies of IFN-γ producing CD4+ T cells were observed (Chan et al. 2014; Maglione et al. 2008).

## BCG vaccination and tuberculosis

BCG is an attenuated live strain of *M.bovis* that was initially developed to prevent the development of TB disease. Vaccination with BCG has been shown to be highly effective at preventing TB-meningitis (TBM) and disseminated extra-pulmonary TB; however, the efficacy thereof for preventing pulmonary TB varies greatly between children, youth, adults and the elderly. Some studies have reported 80% efficacy of BCG, whereas others have reported 0% efficacy (Kaufmann et al. 2010; Colditz et al. 1994). Regardless of its variable efficacy, BCG is one of the most widely administered vaccines around the world (Moliva et al. 2017; Trunz et al. 2006).

BCG mediates immunity by inducing the development of antigen-specific memory T cells which allows a quick immune response following subsequent infection with *M.tb* (Henao-Tamayo et al. 2014; Shen et al. 2002). This is most likely the reason that BCG is able to protect against disseminated TB and TBM, however, it is not entirely clear why this mechanism fails to prevent

the development of pulmonary TB, although it is speculated that the pulmonary immune response is driven by innate rather than T cell mediated immunity (Moliva et al. 2017; Connor et al. 2010).

### 2.2.2. Diagnosis of TB

Due to the non-specific classical clinical phenotype of TB, which overlaps with other diseases such as lung cancer, pneumonia, and sarcoidosis, laboratory tests are essential for the diagnosis of active TB disease (O'Garra et al. 2013).

The classical workflow for the laboratory detection of TB infection generally starts with assessment of the presence of acid-fast mycobacteria through microscopic examination of patient sputum, i.e. the smear test. The smear test, however, cannot distinguish between *M.tb* and other mycobacteria and is also known to have variable sensitivity. Due to the difficulty of obtaining sputum samples from paediatric patients, and the lower sensitivity of the smear test in these patients, bacterial culture is the preferred method for diagnosis of mycobacterial infections for all patients, paediatric and adult (Brent et al. 2017; O'Garra et al. 2013).

Culturing of patient samples for the identification of *M.tb* can take up to six weeks. Invasive procedures, such as bronchoscopy or biopsy, are often necessary (in 30-50% of cases) for successful culture of *M.tb*. Positive bacterial cultures are then identified as either *M.tb* complex (MTBC) or non-MTBC by means of commercial identification kits. After identification of MTBC or non-MTBC, the bacteria undergo further drug-susceptibility testing such as the Hain Genotype® line probe assay, which can detect resistance to the most common first-line anti-TB drugs isoniazid and rifampicin (Brent et al. 2017; O'Garra et al. 2013).

Due to the long turn-over time of microbial cultures, the WHO endorses the Xpert MTB/RIF automated molecular polymerase chain reaction (PCR) based test, which can rapidly detect the presence of *M.tb* and rifampicin resistance genes. Rifampicin is the most common first-line TB drug. The Xpert MTB/RIF assay has decreased sensitivity compared to the culture 'gold standard' and it is therefore recommended that both are performed (Brent et al. 2017).

More recently, assays that detect TB infection based on *in vitro* evaluation of T cell immunity have been developed. These IFN-γ release assays (IGRAs) detect IFN-γ secretion by leukocytes in response to TB antigens, most commonly early secrete antigenic target-6 (ESAT-6) and culture filtrate protein 10 (CFP-10). Commercially available IGRAs include the T-SPOT® TB test (Oxford Immunotec, Oxford, UK), with an enzyme-linked immunospot (ELISpot) assay used to detect individual IFN-γ-producing T cells, and the QuantiFERON®-TB (QFT) test (Cellestis, Ltd, Australia) with an enzyme-linked immunoassay (ELISA) that measures IFN-γ concentration in blood plasma (El Azbaoui et al. 2016; Kobashi et al. 2009).

Although the QFT test was developed to be used as a TB test for adults, the utility of this test has been tested previously in children by El Azbaoui et al. (2016), Ge et al. (2014) and Howley et al.

(2015), and has been shown to be reliable. The QFT IGRA is not affected by BCG vaccination, unlike the tuberculin skin test (TST) which may give inaccurate results due to BCG-driven immune responses (Riazi et al. 2012).

### 2.2.3. Primary Immunodeficiencies relating to TB Susceptibility

South Africa has the second highest TB incidence in the world and contributes to about 80% of the total estimated new TB cases (World Health Organization 2017). Due to the high prevalence of TB in South Africa, the BCG vaccine is customarily administered at birth and although it is aimed at reducing the risk for severe or disseminated TB in childhood, it presents an early life threat for children with immune deficits. The dissemination of BCG in HIV negative infants is usually suggestive of an underlying genetic immune defect (Esser et al. 2016; Eley and Esser 2014).

Individuals with PID are, in general, susceptible to multiple infections although some PIDs have been found to confer specific predisposition to infections by mycobacteria. Examples of such PIDs, that have been documented in the South African PID Registry, include the prototypic TB susceptibility PID viz. Mendelian Susceptibility to Mycobacterial Disease (MSMD) as well as CGD, Hyper IgM syndrome, SCID and CVID (Esser et al. 2015, 2016; Haverkamp et al. 2014).

In high TB prevalence regions, individuals with PIDs are continuously exposed to TB and will most likely present with TB at some point in time if not already before any other particular PID-defining infection. Very little is known about the frequency, complications and recurrence of TB in PID patients in regions with high TB endemicity. Hence, there are no current guidelines for the prevention and management of TB in PID patients with excessive exposure to TB. There are also no reports in the literature on prevention, screening and individualised treatment of PID patients in TB endemic regions (Esser et al. 2016; Eley and Esser 2014).

## 2.3. Mendelian Susceptibility to Mycobacterial Disease

MSMD is the prototype PID relating to mycobacterial susceptibility. MSMD is characterised by selective predisposition to infection by weakly virulent mycobacteria, e.g. BCG vaccines and environmental mycobacteria. This MSMD designation however does not account for all the clinical features observed in patients, as affected individuals are also prone to infection by *Salmonella*, *Candida* and other intra-macrophagic bacteria, parasites and fungi. In regions with high prevalence of TB it has been reported that these patients can present with very severe, persistent, unusual or recurrent *M.tb* infection. The patients generally display no other major abnormalities as evidenced by normal haematological profiling (Apt et al. 2017; Esser et al. 2016; Naranbhai 2016; Boisson-dupuis et al. 2015; Bustamante et al. 2014; Merchant et al. 2013; Boisson-Dupuis et al. 2011; Cooke et al. 2006; Caragol and Casanova 2003).

To date, ten MSMD disease-causing genes have been described. Of these, eight are autosomal (*IFNGR1*, *IFNGR2*, *STAT1*, *IL12B*, *IL12RB1*, *TYK2, ISG15* and *IRF8*) and two are X-linked (*NEMO* and *CYBB*). These MSMD causing genes have all been associated with a disruption in IFN-γ and IL-12 immunity, which has been shown to be essential in the control of mycobacterial infections (Masserot et al. 2017; Naranbhai 2016; Boisson-dupuis et al. 2015; O'Garra et al. 2013; Caragol and Casanova 2003). The allelic heterogeneity of these ten genes results in at least 19 distinct genetic disorders, which vary in their mode of inheritance and clinical presentation. Although it has high levels of allelic heterogeneity, MSMD displays physiological homogeneity, since all associated defects ultimately impair IFN-γ immunity by either hindering the production of IFN-γ or by causing abnormal responses to IFN-γ signalling (Casanova 2015; Bustamante et al. 2011; Al-Muhsen and Casanova 2008). The IFN-γ-IL-12 pathway and the MSMD-associated mutations within this pathway are illustrated in Figure 2.4.

Mutations in *IL12B*, *IL12RB1*, *STAT1* and *IFNGR1* have been described in patients with multiple episodes of TB or disseminated TB (Chapgier et al. 2006; Ozbek et al. 2005; Caragol et al. 2003; Picard et al. 2002; Jouanguy et al. 1997).

MSMD was initially classified as a phagocyte defect (Al-Herz et al. 2015; Ramirez-Alejo and Santos-Argumedo 2014), but according to the 2018 IUIS Criteria, it is now classified as a defect in innate or intrinsic immunity (Picard et al. 2018).

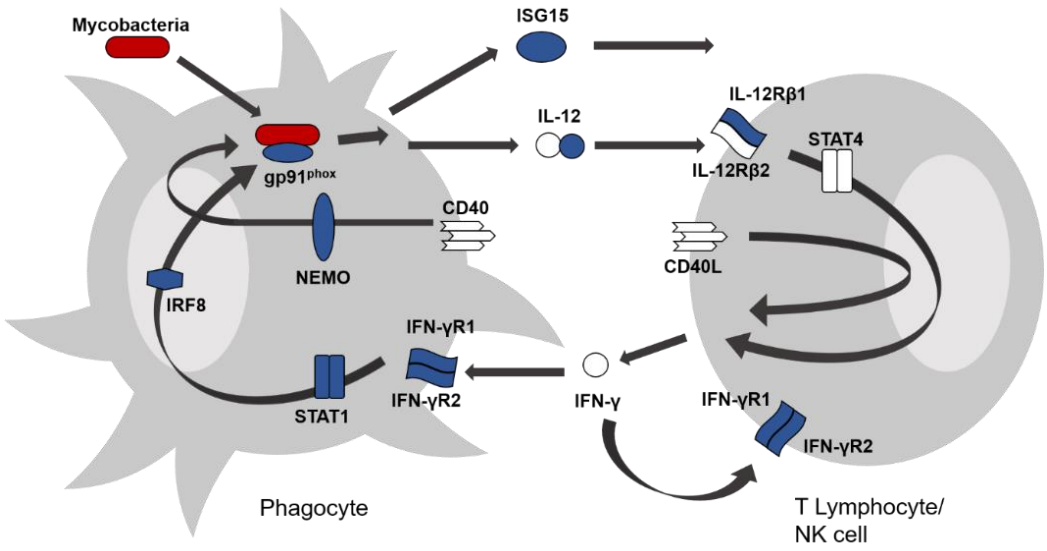


**Figure 2.4: Cells producing and responding to IFN-γ.** The IFN-γ-IL-12 pathway is involved in the host response to infection with mycobacteria and Salmonella. Macrophages and dendritic cells (DCs) secrete IL-12 (and IL-23) which bind to their receptors on T lymphocytes and NK cells, inducing the production of IFN-γ. IL-12 production is enhanced by a CD40-triggered, NEMO/NFκB-dependent pathway. Proteins for which mutations in the corresponding genes have been identified and associated with MSMD are indicated in blue. Mutations in IFNGR1, IFNGR2, CYBB, STAT1 and IRF8 impair the action of IFN-γ while mutations in IL12B, IL12RB1, ISG15, NEMO and IRF8 impair IFN-γ production (Adapted from Bustamante et al. 2014). TYK2 is not indicated in this figure but is involved in IL-12/23 signalling as it provides a docking site for STAT4 (See Figure 2.5).

## 2.3.1. Mutations associated with MSMD

Mutations associated with MSMD either impair the production of IFN-γ or the action thereof. Both IL-12 and IFN-γ and their associated signalling pathways are essential for an effective immune response to mycobacteria. A defect in any of the receptor components or in any of the downstream signalling components can result in impairment or collapse of the IFN-γ-IL-12 pathway, leading to an insufficient or total lack of an immune response against mycobacteria. Mutations in different parts of a gene will have different effects, for example a mutation in a receptor gene may lead to either increased or decreased receptor expression with variable functionality. An illustration of the IL-12 and IFN-γ receptors and the associated signalling components can be seen in Figure 2.5 (Haverkamp et al. 2014).

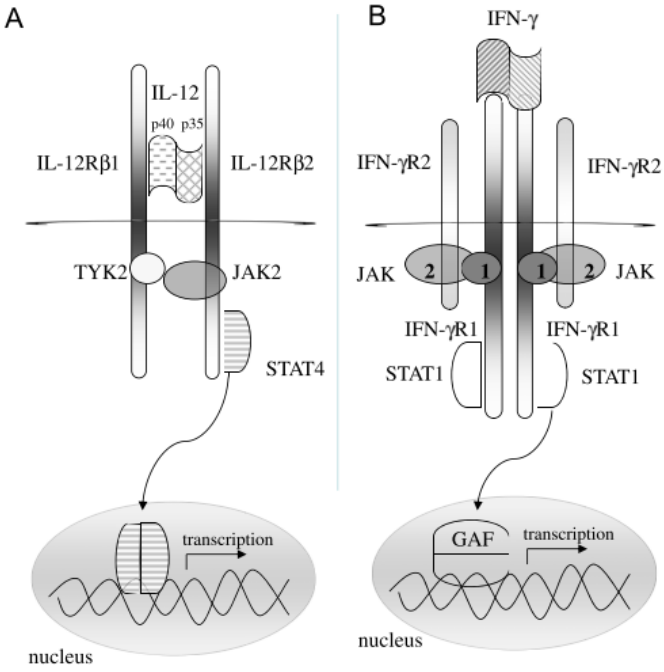


**Figure 2.5: IL-12 and IFN-γ signalling.** (A) The IL-12 receptor consists of two subunits, IL-12Rβ1 and IL-12Rβ2. Co-expression of both subunits are required to generate high affinity for IL-12. Signal transduction through IL-12R firstly induces phosphorylation of JAK2 and TYK2, which in turn activates and phosphorylates STAT4. STAT4 forms a homodimer, which translocates to the nucleus where it activates the transcription of IL-12 responsive genes, including IFN-γ. (B) The IFN-γR consists of the ligand binding subunit (IFN-γR1) and the signal transducing subunit (IFN-γR2). After IFN-γ binds to IFN-γR1, it associates with IFN-γR2. Receptor assembly leads to phosphorylation of JAK1 and JAK2, which leads to the recruitment and subsequent phosphorylation of STAT1 molecules. STAT1 homodimers (also known as GAF, gamma-activating factor) then translocate to the nucleus to activate a wide range of IFN-γ response genes. Adapted from Haverkamp et al. (2014).

### IFNGR1 and IFNGR2

Complete IFN-γ receptor ligand-binding chain (IFN-γR1) deficiency was the first described genetic aetiology of MSMD. Mutations in IFN-γ receptor signalling chain (IFN-γR2) were subsequently found to be associated with MSMD (Casanova and Abel 2002). Recessive mutations in either *IFNGR1* or *IFNGR2* can result in a complete lack of IFN-γ receptor (IFN-γR)

expression on cell surfaces, leading to a lack of cellular responses to IFN-γ. In all forms of complete IFN-γR deficiency, elevated levels of IFN-γ can be detected in circulating blood (Apt et al. 2017; Fraser et al. 2003; Casanova and Abel 2002).

Partial IFN-γR deficiencies have also been reported. This means that the IFN-γR is being expressed at lower than normal levels and has reduced affinity for IFN-γ or the signalling response to IFN-γ is impaired (Apt et al. 2017; Fraser et al. 2003; Casanova and Abel 2002). Partial dominant IFN-γR1 deficiencies occur where truncated IFN-γR is capable of binding IFN-γ but cannot transduce IFN-γ-triggered signals due to a lack of intracellular binding sites (Casanova and Abel 2002).

### STAT1 defects

Signal transducer and activator of transcription (STAT) 1 is an essential transducer of IFN-γ signals and mediates signalling either as STAT1 homodimers, designated as gamma-activating factor (GAF), or STAT1/STAT2/p48 trimers, also known as interferon-stimulated gamma factor 3 (ISGF3). Not all mutations in *STAT1* necessarily result in mycobacterial disease, although in some cases it can lead to loss of STAT1 function, resulting in clinical phenotypes that are very similar to IFN-γR deficiency (Apt et al. 2017; Ramirez-Alejo and Santos-Argumedo 2014; Sharfe et al. 2014).

### IL12B

The *IL12B* gene encodes for the p40 subunit of IL-12, which is a potent IFN-γ inducing cytokine that is secreted mainly by monocytes (or resident macrophages) and DCs. In the case of an *IL12B* mutation resulting in a complete deficiency of IL-12p40, neither monocytes nor DCs are capable of producing functional IL-12. In some cases, the impaired IFN-γ secretion can be compensated for by administering exogenous recombinant IL-12 to affected individuals (Casanova and Abel 2002; Picard et al. 2002).

### IL-12RB1

Autosomal recessive *IL12RB1* mutations, which result in lack of expression of the IL-12β1 receptor subunit on lymphocytes, are the most commonly reported aetiology of MSMD. T cells and NK cells from these patients do not respond effectively to IL-12 and as a result produce no to very low levels of IFN-γ. Individuals with this defect usually present early in life and generally display broad resistance to other infectious agents, apart from mycobacteria and *Salmonella*. A *IL12RB1* gene defect was the first of the MSMD-associated genes to be associated with TB (Altare et al. 2001). IL-12Rβ1 deficiencies also need to be considered in cases where salmonellosis, particularly cases of extra-intestinal non-typhoidal salmonellosis, is the only clinical presentation (Alinejad Dizaj et al. 2018; Boisson-Dupuis et al. 2011; de Beaucoudrey et al. 2011).

### NEMO

NEMO, also known as inhibitor of nuclear factor kappa-B kinase subunit gamma (IKK-γ), encoded by the *IKBKG* gene, forms an integral path of Nuclear factor kappa B (NFκB) signalling, which is crucial for the transmission of information between immune cells through CD40/CD40L. A defect in NEMO leads to impaired NK cell activity, hyper IgM as well as impaired IL-12 and IFN-γ production. The impaired IL-12 and IFN-γ production is due to a lack of cross-talk between monocytes and lymphocytes. Approximately 6% of all NEMO mutations are MSMD cases (Neehus et al. 2017; Braue et al. 2015; Haverkamp et al. 2014).

### CYBB

*CYBB*, which encodes for $gp91^{phox}$, is an IFN-γ inducible component of the oxidative burst that is a feature of all phagocytes. Patients with mutations in *CYBB* often lack a normal respiratory burst response. An effective respiratory burst, driven by Reactive Oxygen Species (ROS) is crucial for protective immunity against mycobacteria (Haverkamp et al. 2014; Bustamante et al. 2011; Al-Muhsen and Casanova 2008).

### TYK2

TYK2 is a tyrosine kinase that phosphorylates multiple cytokine receptors. It provides docking sites for STAT4 as part of the IL-12 and IL-23 signalling cascade. Mutations reported in *TYK2* lead to defects in IL-12/23 signalling causing an imbalance between the $T_H1$ and T lymphocyte helper subset 2 ($T_H2$) immune responses. Not all cases of TYK2 defects are associated with MSMD phenotypes (Haverkamp et al. 2014).

### IRF8

Interferon Regulatory Factor 8 (IRF8) is an IFN-α/β inducible transcription factor that regulates the differentiation of phagocytes and macrophages. It also plays important roles in the cross-talk between TLRs and IFN-γ signalling pathways, and in IFN-γ-induced production of IL-12 and TNF. Reported defects in IRF8 caused mild forms of MSMD, due to extremely low numbers of IL-12 producing DCs (Haverkamp et al. 2014; Lee et al. 2011).

### ISG15

*ISG15* is the most recent MSMD-associated gene to be described. Interferon-Stimulated gene (ISG) is an IFN-α/β inducible intracellular protein that is present in secretory granules of granulocytes. ISG15 tags intracellular proteins for degradation, similar to ubiquitin. Additionally, secreted ISG15 acts synergistically with IL-12 to induce IFN-γ production by NK and T cells. Reported defects in ISG15 resembled the phenotypes observed in *IL12B/IL12RB1* deficiency (Haverkamp et al. 2014).

## 2.3.2. Diagnosis of MSMD

It is important to diagnose MSMD patients based on their specific molecular defect as it has a major impact on their clinical outcomes and responses to anti-bacterial/TB therapy. It is estimated that about half of MSMD patients lack a defined genetic aetiology (Cottle 2011). Delayed diagnosis can hinder the proper treatment for the affected patients. It is recommended that patients with suspected MSMD should undergo molecular testing in order to accurately diagnose their particular immune deficit (Parvaneh et al. 2015; Wang et al. 2012).

Molecular investigations are generally only pursued after the initial laboratory screening, as discussed in section 2.1.2, i.e. full blood count, leukocyte differential count, lymphocyte subsets, oxidative burst screen, total complement screen and enumeration of antibody classes/isotypes.

Diagnosis at the molecular level is desirable in most cases of PID (including MSMD) in order to (i) establish a clear, definitive diagnosis, (ii) permit accurate genetic counselling, (iii) allow planning of future pregnancies or their potential outcomes, (iv) better define genotypic/phenotypic associations, and (v) identify candidate patients for gene-specific therapies (Bonilla et al. 2015).

### Genetic testing for PIDs

There are several target gene sequencing panels available for PIDs, which can assess several targeted genes of interest. However, there are no gene panels that are specific to MSMD available in South Africa, and shipping samples from suspected MSMD patients to countries that do offer such gene panels is only feasible in selected cases, for instance if the family can afford the tests and if it is possible to collect enough sample (sputum or blood) required for the tests. More generalised PID panels can be performed in certain private pathology laboratories, but at high cost and with the caveat that only well-described mutations will be screened. Targeted gene panels only sequence very specific regions of genes that have been implicated in a disease phenotype, therefore they are unable to detect novel, *de novo* mutations that could also result in the disease phenotype (Stray-Pedersen et al. 2017; van den Berg et al. 2017; Esser et al. 2016).

Currently, the most effective way of diagnosing rare genetic defects is by means of WES of patient DNA. With WES, only the exome or protein-coding regions of the genome is sequenced. Although the exome only makes up approximately 2% of the genome, it contains more that 85% of genetic alterations associated with human disease. Due to the feasibility and relative cost-effectiveness, WES has become the new first-line approach to identify disease-causing mutations in individuals with Mendelian disorders (Gallo et al. 2016; Naranbhai 2016; Casanova et al. 2013). WES-identified genetic variants are usually validated by traditional Sanger sequencing.

WES provides rapid molecular diagnosis and improves the diagnostic yield, which is particularly useful in a clinically and genetically heterogenous disorder such as MSMD (Stray-Pedersen et

al. 2017). Analysis of exome data, although very time-consuming and complex (Glanzmann et al. 2016), can identify probable disease causing genetic variants. However, the identification of a genetic variant does not necessarily imply dysfunctionality of the associated protein; it is therefore also important to do *in vitro* functional assessment to confirm any suspected disorder (Gallo et al. 2016).

## Functional Assessment in suspected PID cases

Functional assessment of the immune system is often more affordable than extensive genomic analysis, but in most cases, it is only used after a defect has been identified by molecular investigations, such that a particular pathway involving the candidate defective component can be assessed (Abraham and Aubert 2016; Gallo et al. 2016).

Functional assays are performed to ascertain the impact of variants identified by WES. Functional analysis may include: lymphocyte proliferation assays, assessment of NK cell mediated lysis of target cells, detection of expression of various cell proteins on cell surfaces (e.g. cytokine receptors or First Apoptosis Signal [FAS] death receptors), and measurement of cytokine production upon TLR stimulation. Assays to detect protein transcription or expression can be done through real-time PCR (qPCR), flow cytometry or Western blot (Gallo et al. 2016).

### *Flow cytometry in MSMD diagnosis*

Flow cytometry has many different applications in many different fields of research and can be used on almost all cellular sources (body fluid, tissue, bone marrow, blood), which makes it an ideal tool for screening, diagnosis or functional assessment of PIDs. Flow cytometry is the preferred method for many routine immune investigations, including immune cell subset enumeration, phenotyping and functional profiling. It is also the preferred method for investigating disease-specific immune defects (Abraham and Aubert 2016).

In patients with MSMD, flow cytometry has been used to assess the expression of IFN-γR and IL-12R subunits on the surfaces of immune cells (de Vor et al. 2016; Robinson 2015; Holland 2007; Caragol and Casanova 2003; Caragol et al. 2003). Additionally, flow cytometry is also used to detect intracellular production of IFN-γ and IL-12 (de Vor et al. 2016; Losana et al. 2002).

Assessment of signalling pathways, by detecting phosphorylation of signalling proteins, has been performed since 1980 by detection of radioisotope-labelled proteins and electrophoresis. Since the 1990s, Western blot has been the most popular tool for studying proteome-wide phosphorylation events. (Bonilla et al. 2008).

More recently, phospho-specific flow cytometry, more commonly referred to as phospho-flow or Phosflow, has been implemented to detect intracellular phosphorylated proteins. During Phosflow, blood-cells are stimulated with cytokines or antigens which will activate signalling pathways, resulting in phosphorylation of signalling proteins such STAT or Extracellular signal-

regulated kinases (ERK). After stimulation, cells are stained with fluorochrome-conjugated anti-phospho-protein (e.g. anti-pSTAT or anti-pERK) antibodies that bind to the phosphorylated protein of interest. Stained samples are then analysed by a flow cytometer. In contrast to Western blot, which indicates only the presence or absence of the phosphoprotein in the proteome (entire set of proteins expressed by all cells), Phosflow can quantify the degree of phosphorylation in single cells by comparing the fold-increase in phospho-protein detection in stimulated cells compared to unstimulated cells (Davies et al. 2016; Bonilla et al. 2008).

### 2.3.3. Treatment of MSMD

Treatment of MSMD patients need to be targeted to the specific disease-causing genetic defect and clinical presentation. Generally, established infections are treated with the appropriate antimicrobials and prophylactic antimicrobials are administered, even in periods of disease remission (Caragol and Casanova 2003).

MSMD patients with causative mutations identified in genes that result in insufficient IFN-γ production, which include *IL12B, IL12RB1,* NEMO/*IKBKG, IRF8, ISG15,* as well as partial IFN-γR defects, may benefit significantly from treatment with recombinant exogenous IFN-γ. Recombinant IFN-γ therapy has been shown to have less severe side effects than recombinant IL-12 therapy, which was previously used for patients with defects in *IL12B.* Long-term IFN-γ treatment has been deemed safe and well tolerated in both adult and paediatric patients (Haverkamp et al. 2014; Holland 2000).

For MSMD patients with defects in proteins that are essential for IFN-γ signalling, which impairs the action of IFN-γ, such as *IFNGR1, IFNGR2, STAT1, TYK2* and *CYBB*, HSCT is the only curative treatment option (Haverkamp et al. 2014; Caragol and Casanova 2003; Dorman and Holland 2000; Holland 2000).

Gene therapy is another potentially appropriate solution for MSMD patients, however this field is still in its early stages and is generally only recommended in severe cases of PID where HSCT is not available. Gene therapy has been successfully performed *in vitro*, where IL-12Rβ1 expression, together with IFN-γ production, was restored in cell-lines that had defects in *IL12RB1*. There are no known successful cases of *in vivo* gene therapy for MSMD, although research is ongoing (Haverkamp et al. 2014; Routes et al. 2014).

### 2.3.4. Towards a rational immunological approach to MSMD screening and diagnosis

In countries with high TB burden, it is essential to identify individuals with MSMD since they could acquire early potentially devastating TB infections if they are not diagnosed timeously. It is possible that MSMD and other PIDs relating to TB susceptibility are a lot more common in South Africa than previously believed due to these PIDs being overshadowed by the massive HIV-TB co-epidemics. It is therefore important to find a more rational immunological approach to screening/diagnosis of MSMD.

In suspected MSMD cases (either pre- or post-molecular investigation), IGRAs, such as the QFT test can be used as a broad initial screen to assess the integrity of the IFN-γ pathway. If the QFT test result is negative for a patient that has or ever had a culture positive TB result, it is a clear indication that the patient's immune cells cannot produce IFN-γ in response to TB antigens. An indeterminate QFT result, where the positive control failed to induce an IFN-γ response, can indicate an even more severe IFN-γ deficit due to lack of response to not only TB antigens but also to the mitogen.

The IGRAs can then be followed by flow cytometry-based techniques to assess IL-12R and IFN-γR expression. ELISA or Luminex can be used to measure basal plasma levels of IFN-γ, which is often higher in cases of IFN-γ-signalling defects, as well as induced IL-12 and IFN-γ production. Finally, flow cytometry or western blot can be used to measure downstream signalling molecules (e.g. STAT1 and STAT4) to assess the integrity of the IFN-γ and IL-12 signalling pathways.

## Study Rationale

South Africa is among the countries with the highest burden of TB and has the third highest incidence in the world. These incidence rates have increased by over 400% in the last 15 years (World Health Organization 2017). PIDs that relate specifically to susceptibility to mycobacterial infection, such as MSMD are of special importance in South Africa. It is estimated that about 15-20% of TB cases in high burden areas are observed among children (Esser et al. 2015). Being an area of high endemicity, children with MSMD are at risk for acquiring potentially devastating and recurrent TB infections and post-vaccination BCGosis.

In the Tygerberg Academic Hospital (TBH) setting (Located in Bellville, South Africa) between 10 and 20 unusual TB infections in children are flagged as potential MSMD each year. These children often present with severe, persistent, unusual and recurrent TB or acquire TB-like diseases from weakly virulent strains of Mycobacteria (for example the BCG vaccine or other environmental strains of mycobacteria).

Currently the most reliable diagnostic technique available for the diagnosis of MSMD and closely related PIDs is WES. Although WES is reliable, it is very time consuming to process and interpret the massive data sets that are generated (Glanzmann et al. 2016; Naranbhai 2016). Even after a candidate genetic variant suspected to be the involved in causing the disease phenotype has been identified by WES, functional validation tests still need to be done in order to confirm the manifestation of the genetic defect in the patients' immune cells. More affordable and rapid diagnostic tests are required for PIDs such as MSMD, especially in countries like South Africa with a high endemicity of TB.

The goal of this study was to implement and optimise a set of functional screening tests that will aid in the diagnosis of MSMD in South Africa, a high TB burden setting. These assays were then used to investigate immune functionality in 17 suspected MSMD cases. Having a validated functional screen for MSMD would allow for confirmation of functional manifestations of known genetic signatures of this condition. Effective and accurate diagnosis of this condition is important in the broader context of PIDs in general in that the development of such a testing algorithm could provide a resource for screening for other PIDs that overlap, especially at the level of cytokine gene function and related signalling cascades. Reliable functional screening tests aiding in the diagnosis of PIDs in children are essential in order to ensure that the affected individuals receive the correct treatment and care.

# Aims and Objectives

The aim of this study was to implement and optimise immune phenotyping and functional validation tests for the key genes/pathways involved in MSMD. This was primarily focussed on the IFN-γ and IL-12 cytokine axis pathways.

The objectives of the study included:

I. Implementation and optimisation of flow cytometry-based assays to:
   a. Evaluate surface expression of key cytokine receptors (IFN-γR1 and IL-12Rβ1) on the surfaces of lymphocytes, monocytes and NK cells (Standard surface flow cytometry).
   b. Evaluate IFN-γ and IL-12 signalling by measuring intracellular phosphorylated STAT proteins, STAT1 and STAT4, in lymphocytes, monocytes and NK cells upon stimulation with IFN-γ or IL-12 respectively (Phosflow).

II. Implementation and optimisation of a secreted cytokine assay to determine the levels of *in vitro* IFN-γ-induced IL-12 production and IL-12-induced IFN-γ production after 48-hours. Assay readout was through IFN-γ and IL-12 ELISAs.

III. Comparing the functional and genetic (WES) data for 17 suspected MSMD patients to ascertain the impact of the genetic defect on the IFN-γ and IL-12 pathways.

# Chapter 3 Methodology

## 3.1. Participant recruitment and initial investigations

The research documented in this thesis formed part of a larger genetic study by the collaborative **P**rimary **I**mmuno**d**eficiency **D**iseases **Gen**etics (PIDDGEN) Research group, within the Departments of Molecular Biology and Human Genetics and Pathology at Stellenbosch University. PIDDGEN aims to identify genes and gene variants contributing to susceptibility to TB in individuals with suspected PIDs. This study was approved by the Health Research Ethics Committee (HREC), Faculty of Medicine and Health Sciences at Stellenbosch University (N13/05/075; PI: Dr Craig Kinnear).

The study was based at the TBH Paediatric immunology clinic and National Health Laboratory Service (NHLS) Immunology Unit. The patients came from all over the Western Cape as they are often referred to TBH by physicians from other hospitals. Patients were recruited over a period of 24 months spanning the period June 2016 to June 2018.

Immunology consultant and NHLS Immunology Unit head, Prof. Monika Esser, aided in the identification of children with suspected PID with mycobacterial associations. Reported suspect cases were reviewed based on standard clinical examination criteria and routine laboratory results, and either excluded or included into the study. All patients were assessed by a paediatrician in consultation with the Immunology Unit; relevant family histories were recorded and PID diagnosis was evaluated according to internationally recognised warning signs and PID category diagnosis was made according to the 2017 IUIS criteria (Picard et al. 2018).

Patients and their parents or guardians were required to give comprehensive informed consent in order to be included in the study (Appendix A). All patients and their families received pre-test genetic counselling, as well as further genetic counselling depending on outcome of genetic analyses.

### Routine Laboratory Tests

All suspected PID patients (including those in this study) undergo standard clinical examination and a set of routine laboratory tests at TBH or at their referral medical facility. These routine laboratory tests include: conventional TB testing by means of GeneXpert® and/or bacterial culture followed by acid fast bacteria (AFB) identification and further drug susceptibility testing (e.g. Hain test); full blood counts (FBC) and differentials (neutrophil, lymphocyte, monocyte and eosinophil subset enumeration); lymphocyte subset enumeration (T and B lymphocytes and NK cells); and levels of specific-immunoglobulin classes (total IgG, IgM, IgA).

### Inclusion/Exclusion Criteria

Patients showing clinical and/or immunological evidence for a mycobacterial-associated PID during routine immunology assessment, including possible disseminated BCG infection or infection with other atypical mycobacteria or Salmonella, as well as patients presenting with recurrent, persistent and unusual TB were included in the study. Patients that were positive for HIV infection or had other acquired causes for immunodeficiency, such as immunosuppressive therapy, were excluded from the study.

Patients that form part of the larger PIDDGEN study cohort, that were flagged as potential MSMD cases before the start of this study were also included, although only if the patient was able to return for a follow-up visit to TBH for blood collection and additional routine tests (if not already performed during a previous visit).

## 3.1.1. Sample collection and processing

Following consent, approximately 15 to 20 mL of blood was collected by venepuncture into Ethylenediaminetetraacetic acid (EDTA) BD Vacutainer tubes (BD Vacutainer, CA, USA) as well as 1 mL into each of the four QuantiFERON TB Gold Plus® Tubes (Qiagen, Hilden, Germany) for each patient. Samples were also collected from consenting family members where appropriate, i.e. where a family member has the same clinical presentation or family history of PID. Blood samples were collected in the Paediatric Immunology clinic (ward C3A, TBH) or, in certain cases, in the other wards where patients were hospitalised (TBH or another nearby hospital). In cases where it was not possible to collect sufficient blood at a single visit, additional blood was collected at a follow-up visit.

Blood was also collected from 10 self-reported healthy adult laboratory volunteers (age range: 22 - 45) to serve as non-PID controls for this study. Participants signed informed consent forms (Appendix B) and the collection of blood from volunteers was ethically approved by the HREC, Faculty of Medicine and Health Sciences at Stellenbosch University (N10/08/249; PI: Prof Eileen Hoal). Control blood was only used for PBMC isolation and not for DNA extraction or subsequent genetic analysis.

### PBMC Isolation and Cryopreservation

Peripheral blood mononuclear cells (PBMCs) were isolated from patient and control whole blood within 4 hours of collection by means of the Ficoll-gradient method, adapted from Boyum (1976). Patient whole blood was centrifuged at 2000 relative centrifugal force (RCF) for 10 minutes using the Rotanta 46R (Hettich Zentrifugen, Tuttlingen, Germany) centrifuge, thereafter the top plasma layer was collected and stored in 1 mL aliquots at -80°C. An equal amount of complete Roswell Park Memorial Institute medium (RPMI-1640 with AQmedia™, with L-alanyl-glutamine, sodium

bicarbonate, 1% Penicillin-Streptomycin; Sigma-Aldrich®, MO, USA) was then added to the remaining volume of whole blood and mixed thoroughly. The diluted blood was then layered carefully onto a 10 mL layer of Ficoll Histopaque-1077 (Sigma-Aldrich®, MO, USA) and centrifuged at 1500 RCF, with the lowest settings for acceleration and brakes, for 30 minutes. The PBMC interface was then carefully pipetted into a new tube containing 10 mL complete RPMI. The PBMC-RPMI solution was centrifuged at 1200 RCF for 12 minutes, also with the lowest settings for acceleration and brakes, and the resulting supernatant was discarded in one swift movement and the pellet was dislodged by flicking the tube. The PBMCs were resuspended in complete RPMI containing 10% heat-inactivated Foetal Bovine Serum (FBS; Sigma-Aldrich®, MO, USA) and a cell count was performed using a 1:1 dilution of cell suspension to Trypan blue on a TC20™ cell counter (Bio-Rad Laboratories, CA, USA) to determine cell concentration and viability. The cell-suspension was then centrifuged at 1000 RCF for 10 minutes, acceleration and brake settings at maximum, and the resulting supernatant was discarded, and pellet dislodged. Freezing medium [made up from 40% complete RPMI, 10% Dimethyl sulfoxide (DMSO; Sigma-Aldrich®, MO, USA) and 50% FBS] was added in a dropwise manner whilst gently shaking the tube, on ice, so that the final cell concentration was 1-3 million cells per mL. The PBMCs in freezing medium were aliquoted into 1 mL cryovials, which were placed in a Mr Frosty (Thermo Fisher Scientific™, California, USA) at -80°C overnight. The PBMCs were transferred to liquid nitrogen for longer-term storage within 2 days.

### DNA Extraction

DNA was extracted from 5-10 mL of blood, depending on availability. DNA extractions were performed by collaborators at the Department of Molecular Biology and Human Genetics, Stellenbosch University, within 48 hours of blood collection. DNA was extracted using the Nucleon BACC3 kit (Amersham Biosciences, Buckinghamshire, UK) according to manufacturers' instructions.

## 3.1.2. Genetic Analyses

WES, Sanger Sequencing as well as sequence analysis and annotations was performed by collaborators Drs Brigitte Glanzmann, Marlo Möller, and Craig Kinnear at the Department of Molecular Biology and Human Genetics at Stellenbosch University, Tygerberg Medical Campus.

### Whole exome capture and sequencing

Library preparation for sequencing was carried out using the Ion AmpliSeq™ Exome RDY and the Ion Xpress™ Barcode Adaptors 1-16 Kit (Life Technologies, CA, USA). The DNA template for sequencing was prepared on the Ion Chef system using the Ion PI™ Hi-Q™ Chef Kit and the Ion™ Chip Kit v3. Sequencing was performed on an Ion Proton™ (Thermo Fisher Scientific™,

CA, USA) at the Central Analytical Facility (CAF) at Stellenbosch University, Stellenbosch, South Africa.

## Read mapping, variant detection and annotation

Sequences were aligned to the human reference genome, hg19 using Torrent mapping alignment (TMA; version 5.2.1) in the ion-analysis workflow on the Torrent Suite (version 5.2.1) (Thermo Fisher Scientific™, California, USA). Base quality score recalibration, indel realignment and variant calling were performed using the variantCaller (version 5.2.1.1) plugin on the Torrent Suite and variant annotation was performed. Variant prioritisation was performed using TAPER™ (Tool for Automated selection and Prioritisation for Efficient Retrieval of sequence variants), a custom-designed in-house method, and variants in a homozygous recessive state or compound heterozygous state were prioritised as potential candidate variants (Glanzmann et al. 2016). In brief, TAPER™ 1) submits variant called format (.vcf) files to an online variant caller, 2) removes all synonymous and non-frameshift variants, 3) removes all variants with a frequency of greater than 1%, if present in the 1000 Genomes Project or Exome Sequencing Project 6500, 4) removes all variants with negative Genomic Evolutionary Rate Prediction (GERP) +++ scores, 5) removes all variants with Functional Analysis Through Hidden Markov Models (FATHMM) scores greater than 0.1, 6 and lastly 6) identifies associated disorders for prioritised genes.

Various *in-silico* prediction tools were used to estimate the likelihood of pathogenicity of the identified variants. Sorting intolerant from tolerant (SIFT) (Kumar et al. 2009), PolyPhen (Adzhubei et al. 2010), MutationTaster (Schwarz et al. 2014) and Combined Annotation Dependant Depletion (CADD) Scores (Kircher et al. 2014) were all used. Thereafter The American College of Medical Genetics and Genomics (ACMG) criteria (Green et al. 2013) and the newer Sherloc criteria, which is a refined version of the ACMG criteria, (Nykamp et al. 2017) were used to make a final call on the pathogenicity of each variant. A brief description of each of the *in-silico* tools used can be found in Appendix C, which also illustrates the various combinations of variables used to determine the pathogenicity, as suggested by the ACMG/Sherloc criteria.

## Sanger Sequencing

A fragment containing each of the candidate variants was PCR-amplified from genomic DNA from the patient and the relevant family members. Each amplicon was bi-directionally sequenced using the BigDye® Terminator v3.1 Cycle Sequencing Kit (Perkin-Elmer, Applied Biosystems Inc., CA, USA.), followed by electrophoresis on an ABI 3130XL Genetic Analyzer (Perkin-Elmer, Applied Biosystems Inc., CA, USA). All automated DNA sequencing reactions were performed at CAF at Stellenbosch University, Stellenbosch, South Africa. The Primers used for PCR/Sanger sequencing can be found in Appendix D.

### 3.1.3. QuantiFERON TB Gold Plus® Test

The QFT Gold Plus® test is an IGRA available as a commercialised TB diagnostic test, but it is not yet routinely used in South Africa. The test involves the collection of patient blood into four specialised tubes labelled NIL, TB1, TB2 and Mitogen. This test is used to establish responsiveness of patient cells to *M.tb* antigens (Kobashi et al. 2009; Mazurek et al. 2005).

The TB1 and TB2 tubes contain *M.tb*-specific antigens, ESAT-6 and CFP-10, that elicits a cell-mediated immune response in CD4+ helper T lymphocytes (TB1) and CD8+ cytotoxic T lymphocytes (TB2), respectively. Patient T lymphocytes respond to the TB antigens and produce IFN-γ. The NIL tube contains no antigen and detects the background or baseline IFN-γ production. The mitogen tube serves as a positive control (El Azbaoui et al. 2016; Kobashi et al. 2009).

QFT-plus was only performed on a subset of 8 patients due to the others patients not being able to return to the clinic solely for the QFT-plus test. In-house QFT-plus was performed on 5 of the 8 patients. In-house QFT-plus could only be performed when there was sufficient reagents and expertise available on the day. For the other 3 patients, samples were collected in QFT-plus tubes and then outsourced to a private pathology laboratory, PathCare, for incubation and analysis.

#### Sample collection and incubation

Blood was collected and incubated according to manufacturer's instructions. After blood collection, the tubes were inverted several times to ensure that the inner surface of the tubes are coated with blood so that the antigens dissolved into the blood. Tubes were then incubated upright for 16-24 hours at 37˚C (no $CO_2$ required). Following incubation, tubes were centrifuged for 15 minutes at 2000 RCF and the resulting plasma was harvested with a pipette and aliquoted into 1.5 mL tubes for storage at -20˚C.

#### QuantiFERON TB Gold Plus® ELISA

The QFT-plus IFN-γ ELISA was performed according to the manufacturers' recommended protocol (Qiagen® 2015). In brief, 50 µL of test plasma samples as well as 50 µL of each of the IFN-γ ELISA standards (4.0 international units [IU]/mL, 1.0 IU/mL, 0.25 IU/mL, and 0.0 IU/mL; where 1 IU = 0.5 ng) were added to respective wells containing 50 µL IFN-γ ELISA conjugate and incubated at room temperature for 2 hours. Thereafter the wells were washed 6 times with at least 400 µL of wash buffer using the ImmunoWash™ 1575 microplate washer (Bio-Rad Laboratories, CA, USA). Enzyme substrate (100 µL) solution was then added to each well and after 30 minutes incubation at room temperature 50 µL of enzyme stopping solution was added. The optical density (OD) of each well was measured, using the iMark™ microplate reader (Bio-Rad Laboratories, CA, USA), at 450nm with a 650nm reference filter. The OD results were

analysed manually, with MS Excel 365, to determine the IFN-γ concentration in each well as well as to calculate the overall test results.

***Interpretation of Test***

QFT-plus ELISA test results were judged based on Centers for Disease Control and Prevention (CDC) guidelines (Kobashi et al. 2009; Mazurek et al. 2005). The test result was considered positive if the IFN-γ level in the sample (minus the background IFN-γ level in the NIL tube), after stimulation with the TB antigens, was ≥0.35 IU/mL, regardless the result for the positive control well. The test was considered negative if the IFN-γ level in the sample (minus the background IFN-γ level in the NIL tube) was either <0.35 IU/mL, regardless of and the positive control well, or ≥0.35 IU/mL, if the positive control well had an IFN-γ level of ≥0.5 IU/mL. The test result was recorded as indeterminate if the IFN-γ was <0.5 IU/mL in the positive control well. Figure 3.1 shows a simplified QFT-plus interpretation flowchart.

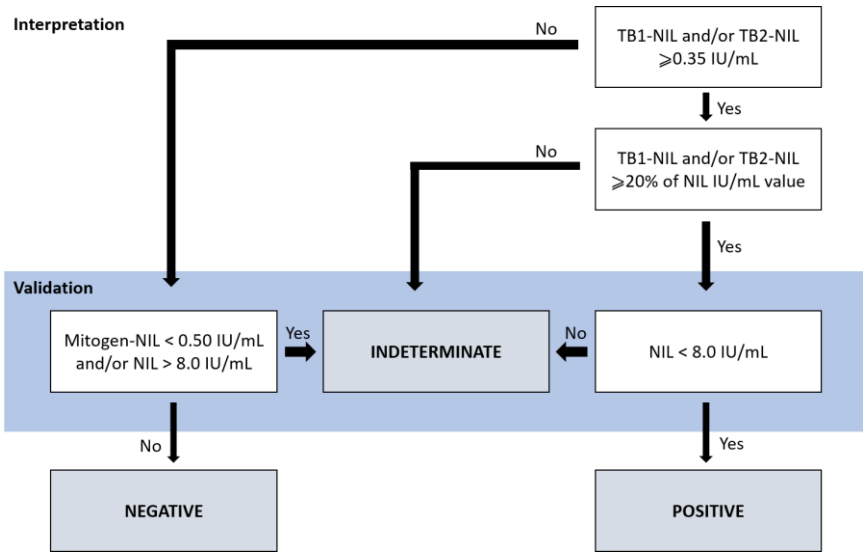


**Figure 3.1: Interpretation of the QuantiFERON TB Gold Plus® test.** Adapted from QFT-plus product insert (Qiagen® 2015).

The QFT-plus test is intended for use as a TB diagnostic test and therefore a positive result would imply that TB infection is very likely, and a negative result implies that TB infection is unlikely in a patient. If a QFT-plus result is reported as indeterminate, it is usually due to either a high background in the NIL tube or a low response in the positive control, Mitogen, tube.

Indeterminate results, which are generally due to technical factors resulting from incorrect sample handling and processing, may provide information on the immune status of the individual, especially in cases where the patient currently had or previously had culture or GeneXpert® confirmed TB. A defective IFN-γ production pathway could produce an indeterminate result due to lack of induction of IFN-γ following mitogenic Phytohaemagglutinin (PHA) stimulation

## 3.2. Evaluation of the IL-12–IFN-γ pathway by flow cytometry

Two separate flow cytometry-based assays were implemented and optimised for this study. The expression of cytokine receptors on cell surfaces was assessed by means of standard surface marker flow cytometry and the cytokine signalling, which is mediated through these cytokine receptors, was assessed by means of an intracellular Phosflow assay.

***Surface flow cytometry – Cytokine receptor detection***

Surface expression of IFN-γR1 (CD119) and IL-12Rβ1 (CD212) on lymphocyte subsets, NK cells and monocytes was evaluated by standard surface flow cytometry, whereby cells were stained with fluorochrome-conjugated antibodies and the fluorescence data acquired by a flow cytometer**.** Detection of IFN-γR1 and IL-12Rβ1 has previously been used to confirm several cases of MSMD (Esteve-Solé et al. 2018; Neehus et al. 2017; Kong et al. 2013; de Beaucoudrey et al. 2011; Fieschi 2004).

***Phosflow – Assessment of cytokine signalling***

IFN-γ and IL-12 signalling was assessed by measuring the intracellular phosphorylation of the respective cytokine receptor-associated signal transducer molecules STAT1 and STAT4. This was achieved by an intracellular flow cytometric-based phosphorylation assay – Phosflow – where, after PBMC stimulation with either IFN-γ or IL-12, levels of phosphorylated STAT1 and STAT4 (pSTAT1 and pSTAT4) were measured intracellularly by detecting the bound phospho-specific fluorochrome-conjugated antibodies. The Phosflow protocol differs significantly from standard surface flow cytometry and involves brief stimulation of the cells, followed by fixation and permeabilisation prior to staining and acquisition of fluorescent data on a flow cytometer**.** Detection of pSTAT1 and pSTAT4 has also previously been used to assess IFN-γ and IL-12 signalling in several MSMD cases (Esteve-Solé et al. 2018; Kong et al. 2013; van de Vosse et al. 2009).

### 3.2.1. Panel Design

Two nine-colour staining panels were designed, designated as the Receptor Panel and the Signalling/Phosflow Panel, for each of the two flow cytometric assays. The two panels shared the following fluorochrome-conjugated antibodies: Fixable viability stain 575V (FVS575V), which is a fixable amine-reactive viability marker; CD3-Fluorescein isothiocyanate (FITC); CD4-Allophycocyanin (APC); CD8-Phycoerythrin-Cyanin5 (PE-Cy5); CD14-Phycoerythrin-Cyanin7 (PE-Cy7) and; CD56-Brilliant Violet 510 (BV510). The Receptor Panel also contained: CD19-Brilliant Blue 700 (BB700); CD119-Phycoerythrin (PE) and; CD212-Brilliant Violet 421 (BV421). The Signalling Panel contained: CD20(Intracellular)-Peridinin-chlorophyll protein-Cyanin5.5 (PerCP-Cy5.5); pSTAT1-BV421; and pSTAT4-PE. All antibodies used in this study were

procured from BD (BD Biosciences, CA, USA). Table 3.1 shows a summary of the clone, isotype and reactivity information of the monoclonal antibodies (mAbs) that were used in this study.

**Table 3.1: Clone, isotype and reactivity information on the monoclonal antibodies used to in this study.** For the monoclonal antibodies shared across both panels, specific clones known to be compatible with the Phosflow protocol were chosen.

| | Target | mAb | Fluorochrome | Clone | Isotype | Reactivity | BD Catalogue number |
|---|---|---|---|---|---|---|---|
| Used in both the Receptor and Signalling Panels | Dead cells | FVS575V (a dye, not a mAb) | Intracellular amine reactive dye with emission detectable in 605/40BP filter | N/A | N/A | Mammalian | 565694 |
| | T cells | CD3 | FITC | UCHT1 | Mouse IgG1, κ | Human | 561806 |
| | T helper cells | CD4 | APC | SK3 | Mouse IgG1, κ | Human | 565994 |
| | T cytotoxic cells | CD8 | PE-Cy5 | HIT8a | Mouse IgG1, κ | Human | 561946 |
| | Monocytes | CD14 | PE-Cy7 | M5E2 | Mouse IgG2, κ | Human | 560919 |
| | NK cells | CD56 | BV510 | R19-760 | Mouse IgG1, κ | Human | 744218 |
| Exclusive to Receptor Panel | B cells | CD19 | BB700 | HIB19 | Mouse IgG1, κ | Human | 566397 |
| | IFN-γR1 | CD119 | PE | GIR-208 | Mouse IgG1, κ | Human | 558934 |
| | IL-12Rβ1 | CD212 | BV421 | 2.4E6 (2-4E6) | Mouse IgG1, κ | Human | 744202 |
| Exclusive to Signalling Panel | B cells | CD20 (I/C)* | PerCP-Cy5.5 | H1 (FB1) | Mouse IgG2a, κ | Human | 560907 |
| | Phosphorylated STAT1 | pSTAT1 | BV421 | 4a | Mouse IgG2a, κ | Human | 566238 |
| | Phosphorylated STAT4 | pSTAT4 | PE | 38/p-Stat4 | Mouse IgG2a, κ | Human | 558249 |

N/A – Not Applicable
* CD20(I/C) is an intracellular B cell marker. This is used instead of CD19 in the Signalling panel, due to most commercially available CD19 clones being incompatible with the Phosflow protocol.
mAb: Monoclonal antibody

## 3.2.2. Implementation of flow cytometry panels

### Sample preparation

Cryopreserved PBMCs were thawed rapidly to preserve the viability of the cells (Hønge et al. 2017). For the thawing process, cryovials containing PBMCs were transferred, on dry ice, from liquid nitrogen storage to a 37˚C bead bath. The cells were left in the bead bath for 1-2 minutes or until vial contents had liquefied. Complete RPMI medium containing 10% FBS (pre-warmed to 37˚C) was added in a dropwise manner into the cryovial so that the final volume is double that of the cell suspension. The PBMCs were transferred to a 50-mL BD FALCON® tube (Corning Science, NY, USA) and the cryovial was rinsed twice with the pre-warmed complete RPMI (10% FBS). The cell suspension was then centrifuged at 1200 RCF for 10 minutes. The supernatant

was discarded, and pellet dislodged by gently flicking the tube. The PBMC pellet was washed twice, each time by adding 10 mL complete RPMI with 10% FBS followed by centrifugation at 1200 RCF, and the resulting supernatant was discarded. The PBMC pellet was then resuspended with desired volume of complete RPMI with 10% FBS. The number of cells and their viability was determined using a 1:1 dilution of the cell suspension and trypan blue and the TC20™ cell counter.

For immediate staining of PBMCs, a total of between $5x10^5$ and $1x10^6$ cells, depending on availability, were transferred to 5-mL BD Falcon™ polystyrene round-bottom tubes (BD Biosciences, MA, USA), where they were once again centrifuged, and the supernatant discarded. The PBMCs were then 'washed' with staining media (Phosphate buffered saline [PBS; Sigma-Aldrich®, MO, USA] with 2% FBS), i.e. 10 mL staining media was added, followed by another 10-minute centrifugation and discarding of the resultant supernatant. The PBMCs were then stained with the appropriate volumes of antibody.

For processing of PBMCs for the signalling panel, an overnight (approximately 18 hours) resting period was required after thawing in order for cells to be able to respond optimally to the short-term cytokine stimulation of the Phosflow protocol. Resting of PBMCs also reduce the basal levels of phosphorylation (Uzel et al. 2001). Therefore, after thawing and washing, PBMCs were resuspended in complete RMPI with 10% FBS and then transferred to 5-mL BD FALCON® polypropylene round-bottom tubes (Corning Science, NY, USA) and placed in an incubator with 5% $CO_2$ to rest overnight.

Polypropylene tubes, instead of the conventional polystyrene tubes were required for overnight incubation to prevent attachment of monocytes to tube walls. Although EDTA or other specialised solutions can be used to detach the cells from the tube walls, it was discovered during the optimisation experiments that these solutions impaired the ability of the cells to optimally respond to stimuli.

### Instrument set-up

Flow cytometric data acquisition was performed on a BD LSRII (BD Biosciences, CA, USA) using BD FACSDiva™ software at the BD Flow Cytometry training centre-CAF at Stellenbosch University, Tygerberg Medical Campus. This flow cytometer is equipped with Blue (488 nm), Violet (405 nm) and Red (633 nm) lasers and emission filters for PE-Cy7 (Long-pass filter [LP]: 735, Band-pass filter [BP]: 780/60), PerCP-Cy5.5/BB700 (LP: 685, BP 695/40), PE-Cy-5 (LP: 635, BP 670/14), PE (LP: 550, BP 575/26), FITC (LP: 505, BP 530/30), BV605 (LP: 505, BP 605/40), BV510 (LP: 505, BP 525/50), BV421 (LP: -, BP 440/40), APC (LP: -, BP 660/20), and others (which are not relevant for this study).

The cytometer was calibrated with BD cytometer setup and tracking (CS&T) beads (BD Biosciences, CA, USA) on each day that an experiment was performed in order to verify that the fluidics and optics systems of the instrument were performing optimally.

***Voltage set-up***

For the Receptor panel, a cryopreserved, unstained PBMC sample was used to adjust the instrument's voltages to standardise the light scatter [forward scatter (FSC) and side scatter (SSC)]. The unstained PBMC sample was also used to adjust the robust standard deviation (rSD) of each fluorescent parameter so that it was equivalent to 2.5 or more times the rSD of the electronic noise ($rSD_{EN}$).

Similarly, a cryopreserved, rested, unstained PBMC sample that had undergone fixation and permeabilisation was used to set the voltages for the Signalling/Phosflow panel.

***Monoclonal antibody titrations***

Antibody titrations were performed to determine the optimal antibody volumes to be used that would provide optimal discrimination between positive and negative populations**.** The signal-to-noise ratio, calculated by dividing the median fluorescence intensity (MFI) of the positive population by that of the negative population, was used to determine the ability to distinguish between positive and negative populations (Figure 3.2). To be able to make accurate measurements of fluorescence, it is important to maximise the signal while reducing the noise. Some noise is unavoidable which comes from the cells (autofluorescence), and the inherent noise in the system. Titration helps minimise noise due to non-specific binding of the antibodies to low-affinity targets (Cossarizza et al. 2017).

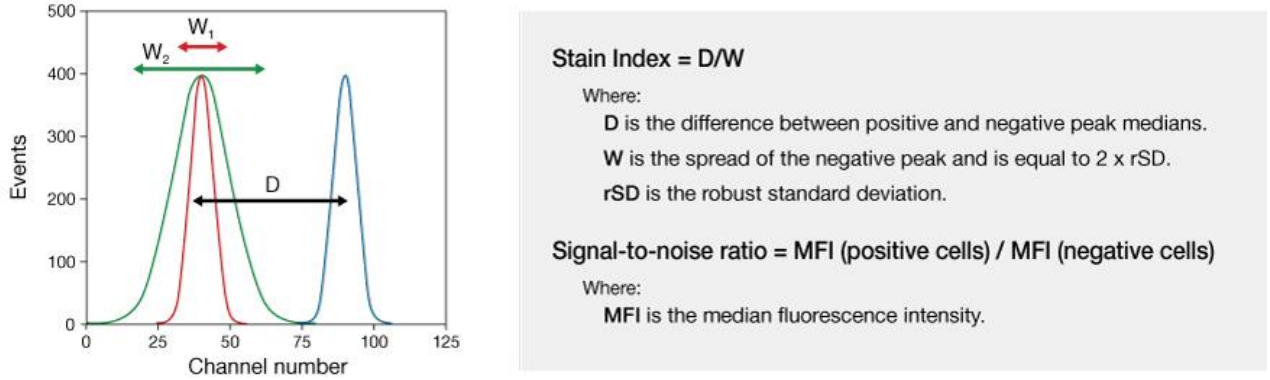


**Figure 3.2: Signal-to-noise ratio calculation**. The Signal-to-noise ratio is calculated by dividing the MFI of the positive cells with the MFI of the negative cells. The higher the signal-to-noise ratio, the easier it is to discriminate between positive and negative populations. The stain index, also shown in the figure, refers to the relative 'brightness' of a particular fluorochrome compared to a negative (unstained) control.

When an antibody is titrated, it needs to be done under the same conditions in which it will be used during the experiment. For this study PBMCs were cryopreserved, thawed and stained in the exact same way for titrations and experiments. Only the antibodies from the Receptor panel,

which includes the antibodies that are shared between the two panels, were titrated under standard surface staining conditions. The antibodies that are exclusive to the Signalling panel were not titrated and were used at manufacturer recommended concentrations throughout.

For the antibody titration experiments, cryopreserved PBMCs were thawed and then stained with decreasing concentrations of fluorochrome-conjugated antibodies. Where the manufacturers' recommended staining dilution was 1:20, cells were stained with a doubling dilution series of 1:10, 1:20, 1:40, 1:80 and 1:160. Likewise, where the recommended staining dilution was 1:5, cells were stained with a dilution series of 1:2.5, 1:5, 1:10, 1:20 and 1:40. The cells were stained with 50 µL of the appropriate dilution for 30 minutes, away from direct light. After staining, the cells were washed twice by adding 1mL staining buffer, which consists of PBS (Sigma-Aldrich®, MO, USA) and 2% FBS, and centrifuging for 10 minutes at 1200 RCF. The supernatant was discarded after each wash and the pellet was resuspended in 200 µL for acquisition on the flow cytometer. For titration of CD212 (IL-12Rβ1), cells were first incubated with 5µg/ mL PHA (Sigma-Aldrich®, MO, USA) for 24 hours at 37°C with 5% $CO_2$ to upregulate CD212 expression (de Beaucoudrey et al. 2011; Fieschi 2004). Table 3.2 shows the optimal titrated staining dilutions for the antibodies, as determined by the titration experiments.

**Table 3.2: Optimal titrated staining dilutions for each of the antibodies in this study, as determined by the titration experiments.**

| Monoclonal Antibody | Fluorochrome | Manufacturer recommended staining dilution factor | Titrated staining dilution factor |
|---|---|---|---|
| FVS575V | Intracellular amine reactive dye with emission detectable in 605/40BP filter | 1:1000 | 1:2000 |
| CD3 | FITC | 1:5 | 1:20 |
| CD4 | APC | 1:20 | 1:160 |
| CD8 | PE-Cy5 | 1:5 | 1:40 |
| CD14 | PE-Cy7 | 1:20 | 1:40 |
| CD56 | BV510 | N/A** | 1:20 |
| CD19 | BB700 | 1:20 | 1:160 |
| CD119 | PE | 1:20 | 1:20 |
| CD212 | BV421 | N/A** | 1:20 |
| CD20 (I/C)* | PerCP-Cy5.5 | 1:10 | - |
| pSTAT1 | BV421 | 1:20 | - |
| pSTAT4 | PE | 1:5 | - |

*CD20(I/C) is an intracellular B cell marker. This is used instead of CD19 in the Signalling panel, due to CD19 being incompatible with the Phosflow protocol

**CD56-BV510 and CD212-BV421 are BD Optibuild reagents and do not have specified recommended staining dilutions

### *Compensation for spectral overlap*

Spectral overlap occurs when the fluorescence of one fluorochrome 'spills' into an adjacent detector, for example the fluorescence emitted by the fluorochrome PE is often detected in the FITC detector. In order to compensate for spectral overlap between fluorochromes, the

Photomultiplier tubes' (PMT) voltage settings of the cytometer are adjusted for each detector to ensure that all fluorescence detected in each of the detectors belongs only to the fluorochrome of its designated detector (Cossarizza et al. 2017; Roederer 2001).

A representation of the spectral overlap that occurs for the fluorochromes used in for the Receptor flow cytometry panel can be seen in Figure 3.3. These images were generated using the BD Fluorescence Spectrum Viewer online tool (BD Biosciences 2018 http://www.bdbiosciences.com /us/s/spectrumviewer).

Anti-mouse Ig, kappa (κ) chain and Negative Control Compensation Particles (BD CompBeads; BD Biosciences, CA, USA) were used for setting up the compensation for each panel. For each fluorochrome in a panel, one drop of BD CompBeads anti-mouse Ig and one drop of the BD CompBeads negative control were added to 100 µL staining buffer.

For the Receptor panel, the optimal staining concentration, determined by the titration experiment, for each fluorochrome-conjugated antibody was added to the compensation beads and then incubated for 30 minutes at room temperature away from direct light. After staining, the beads were washed with staining buffer and resuspended in 500 µL staining buffer for acquisition. FVS575V is an amine-reactive viability dye and does not bind to BD CompBeads, therefore thawed PBMCs, with between 50% and 80% viability, as determined by the TC20™ cell counter, were used for FVS575V compensation set-up.

For the Signalling panel, the BD CompBeads and the negative control beads were incubated with the BD Cytofix™ (BD Biosciences, CA, USA) buffer for 10 minutes at 37˚C, and thereafter permeablised with the permeabilisation buffer. The beads were then stained for 60 minutes at room temperature away from direct light. After staining the beads were washed with staining buffer and resuspended in 500 µL staining buffer for acquisition. FVS575V was compensated for in the same way as mentioned above for the Receptor panel.

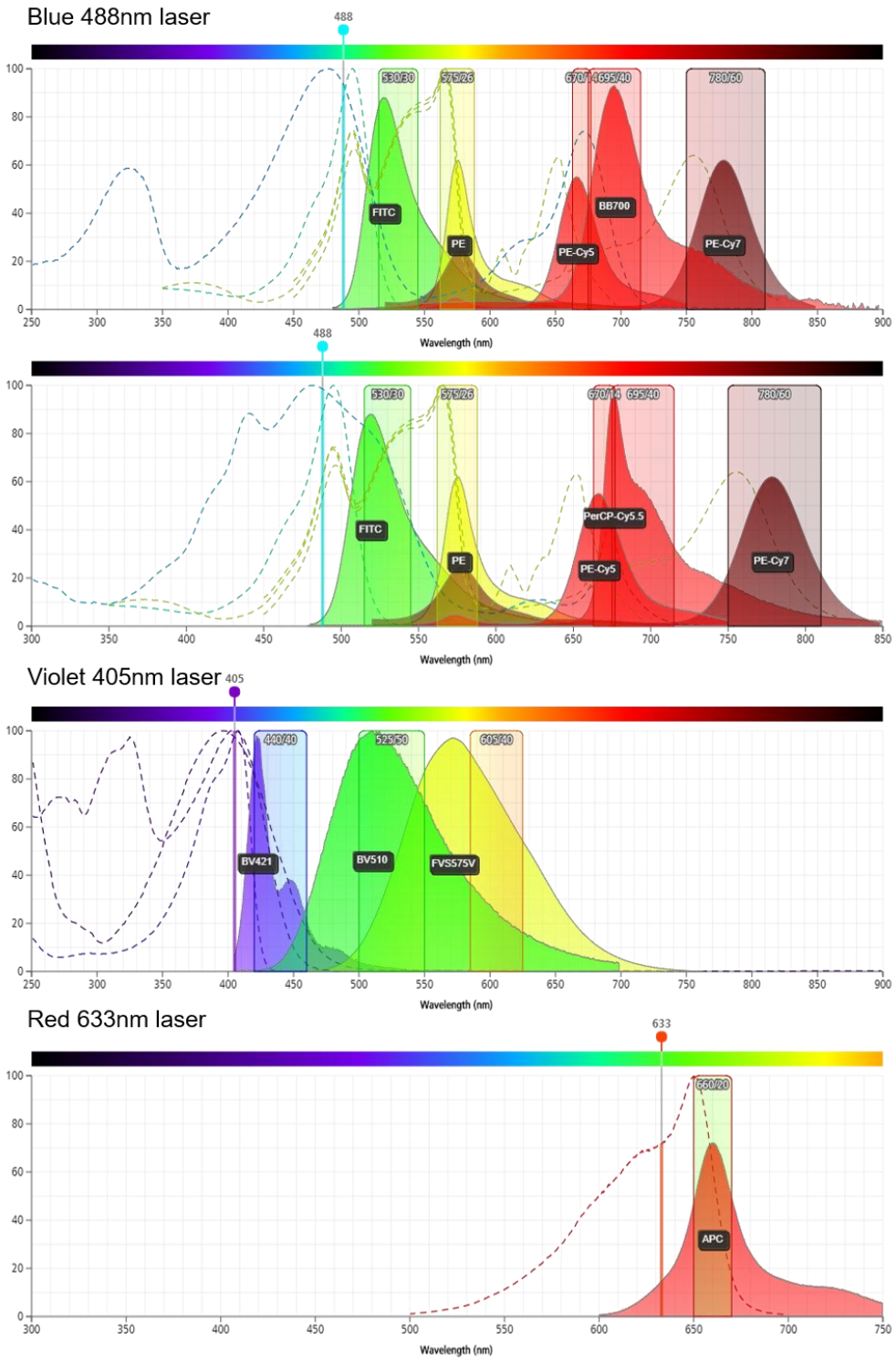


**Figure 3.3: Spectral overlap between fluorochromes used in this study**. The absorption (dotted lines) and emission spectrum (solid lines with coloured graphs) for each of the fluorochromes in this study are shown for the blue 488nm, violet 405nm and red 633nm lasers. The rectangles on each of the spectra represent the band-pass filters of the flow cytometer that determine which parts of the spectrum can be detected in each of the filters. It is evident that there is significant overlap of some fluorochromes into the detectors of adjacent fluorochromes. The observed spill-over needs to be compensated for before multi-colour staining experiments can be performed.

## Fluorescence Minus One Controls for gating

Fluorescence minus one (FMO) analyses was performed in order to establish accurate discrimination between positive and negative (background) marker expression. For the FMO controls, PBMCs from a healthy volunteer were stained with all of the fluorochrome-conjugated antibodies in the panel minus the one fluorochrome-conjugated antibody of interest.

Designated population gates, defining populations with specific scatter or fluorescence characteristics, were created in order to identify and examine the various cell sub-populations based on the expression of various surface markers. FMO controls were then used to place or adjust positive vs. negative discriminator regions. The full gating strategy is described in the next section. FMOs were only performed for the 2 cytokine receptors, CD119-PE, CD212-BV421. The use of unstained control samples was sufficient for setting up accurate gates and regions for the other fluorochrome-conjugated antibodies in this study, due to them having well-described and very distinct positive and negative populations. An example of the FMO controls for CD119 on monocytes and CD212 on lymphocytes are shown in Figure 3.4.

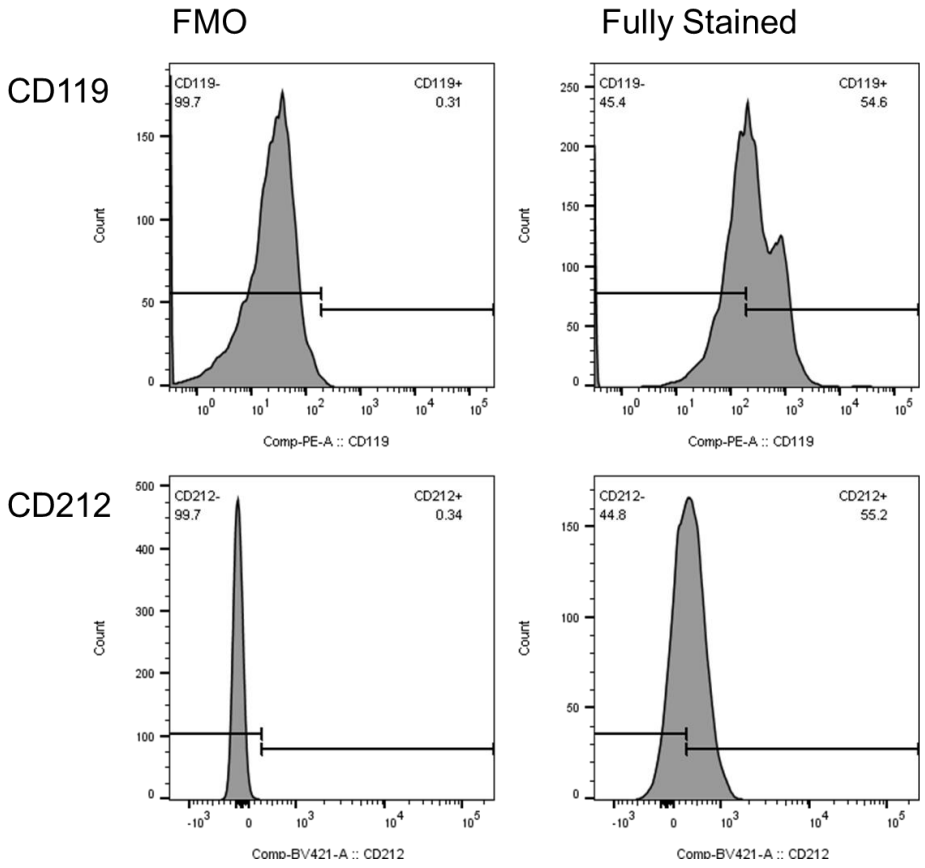


**Figure 3.4: Fluorescence Minus One (FMO) gating control for CD119 and CD212.** Histograms showing the fluorescence intensity for CD119 (on FSC vs. SSC monocytes) and CD212 (on FSC vs. SSC lymphocytes) for PBMCs stained without either CD119 or CD212 (i.e. FMO controls) compared to fully stained samples. FMO controls allow for the establishment of gates that allow accurate discrimination between positive and negative populations.

## 3.2.3. Acquisition and gating

After the cytometer had been set up optimally for each of the two respective panels, antibody cocktails containing the optimal titrated volumes of each antibody in a panel were prepared and then used to stain the thawed PBMC samples.

### Acquisition parameters

Samples were acquired on the BD LSR II using a medium flow rate. BD FACSDiva™ software was used for acquisition. There was no defined gating strategy for acquisition, apart from the FSC vs. SSC lymphocyte-defined gate. The FSC vs SSC lymphocyte gate was used as an acquisition "stopping gate" i.e. once there was a specified number of events recorded within the gate, no further data was acquired. All events, not just the ones within the stopping gate, were stored in Flow Cytometry Standard data files (.fcs) for further analysis. A total of 50 000 events, within the FSC vs. SSC lymphocyte gate, were acquired for the Receptor panel. For the Signalling panel, a total of 100 000 events, also within the FSC vs. SSC lymphocyte gate were acquired.

### Gating strategy

FlowJo® software was used for post-acquisition gating and analysis. The gating strategy for the Receptor and the Signalling panel were overall very similar. A 'Time' gate, with SSC vs. Time, was created first in order to confirm that data acquisition was stable over time. The live cells were then gated (i.e. the FVS575V negative population) thereafter an FSC vs. SSC dot-plot was used to distinguish between the overall lymphocyte and monocyte subsets. The FSC vs. SSC dot-plots generated by the Receptor and Signalling panel differ significantly due to the effect that the harsh Phosflow protocol has on the cells.

From the FSC vs. SSC lymphocyte population, doublets were excluded by using an SSC-Area vs. SSC-Height gate. Various lymphocyte sub-populations were then identified based on the expression of CD56 (NK cells), CD3 (T lymphocytes) or CD19/CD20 (B lymphocytes). The CD3+ T lymphocytes were then further characterised by the expression of CD4 (T helper cells) or CD8 (Cytotoxic T cells). From the FSC vs. SSC monocyte population, CD14+ cells were gated using an SSC-Height vs. CD14 dot-plot. Doublet exclusion was not performed for the monocyte populations due to their larger size and propensity to adhere to one another.

For the Receptor panel, CD119 expression was assessed for the FSC vs. SSC monocyte population as well as the CD14+ monocyte population. CD212 expression was assessed for all of the lymphocyte sub-populations. CD119-, CD119+, CD212- and CD212+ regions were created for each of the abovementioned cell subpopulations by means of FMO controls. Similarly, for the Signalling panel, pSTAT1 was assessed for the FSC vs. SSC monocyte population and the CD14+ populations, while pSTAT4 was assessed for all lymphocyte sub-populations.

The gating strategy was slightly adjusted in PHA stimulated samples due to the induced changes in lymphocyte morphology. The lymphocyte gates were therefore adjusted to include activated lymphocytes that have increased size and granularity compared to cells that were not stimulated with PHA.

A graphical example of the gating strategy for the Receptor panel and the Signalling panel is shown in Figures 3.5 and 3.6 respectively.

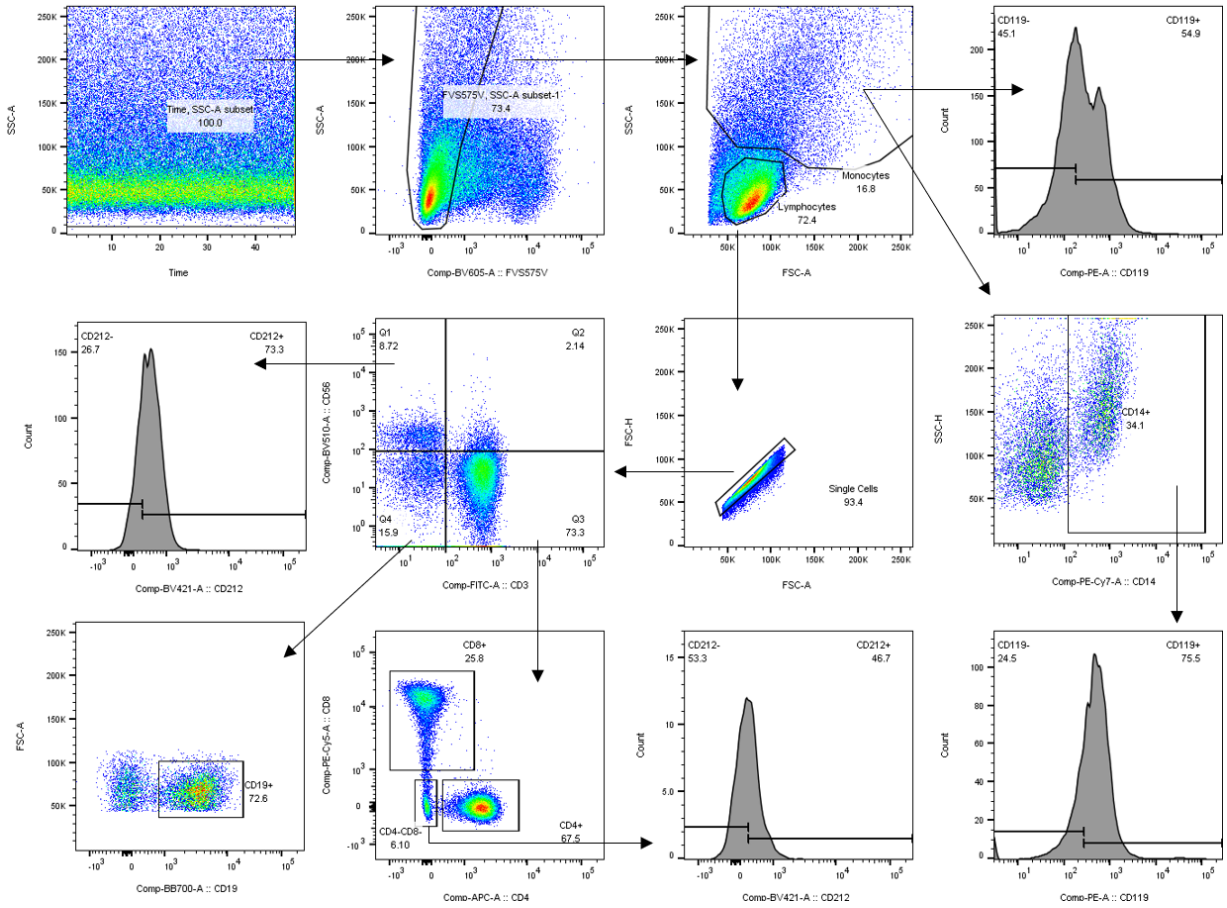


**Figure 3.5: Gating Strategy for Receptor panel**. CD119 expression is measured for all lymphocyte and monocyte subsets. CD119 expression in FSC vs. SSC monocytes as well as in CD14+ monocyte populations are shown in the figure as examples. CD212 expression is assessed for all lymphocyte and monocyte subsets. CD212 expression in CD56+ and CD3+CD4-CD8- subsets are shown in the figure as an example. Bisector gates for CD119 and CD212 were created according to FMO controls.

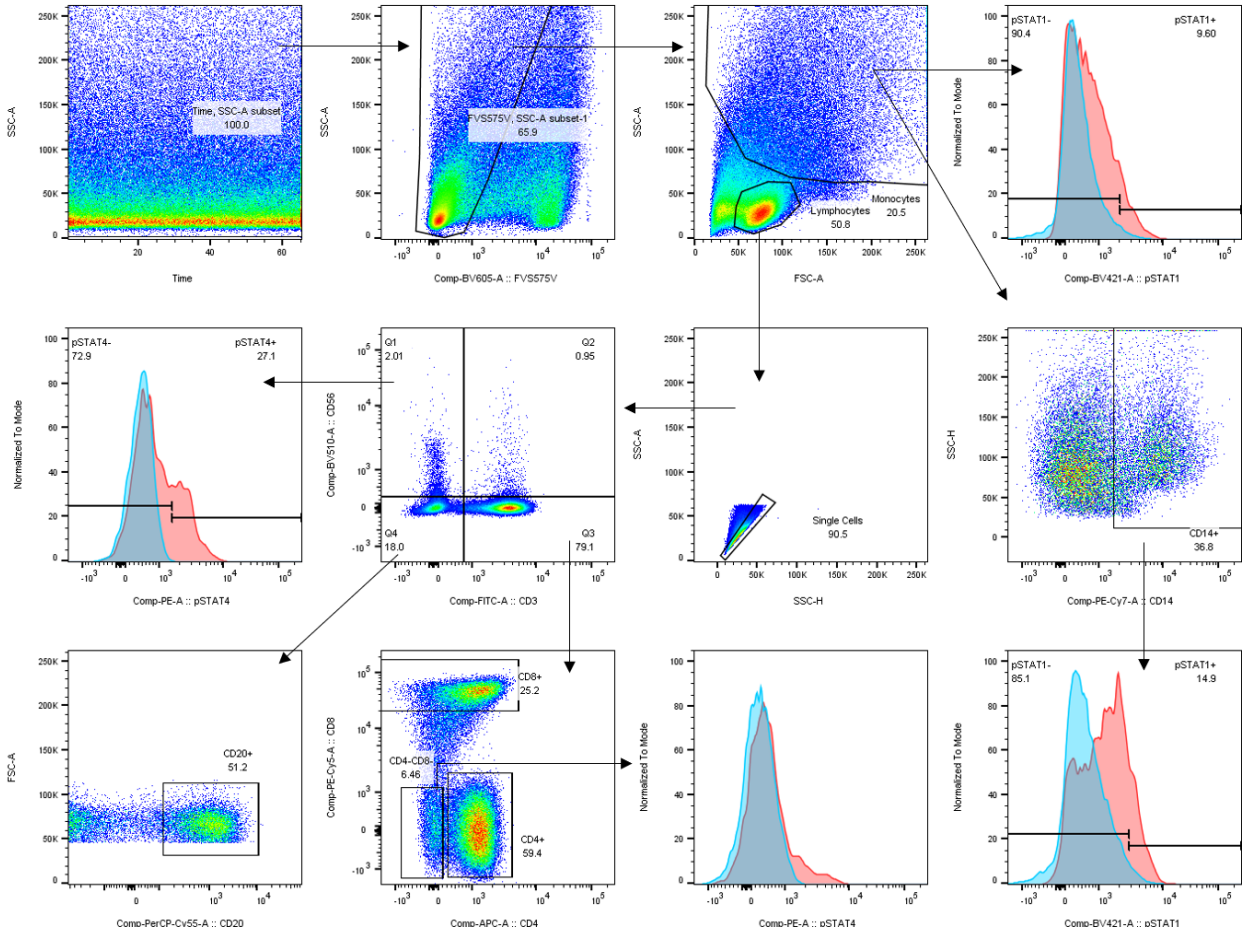


**Figure 3.6: Gating Strategy for the Signalling panel**. Gating strategy for the Signalling panel differs from the Receptor panel due to the effect of the Phosflow protocol on the cells. In the figure, detection of pSTAT1 in FSC vs. SSC monocytes and in CD14+ monocytes are shown for IFN-γ stimulated (blue) and unstimulated (red) samples. Detection of pSTAT4 in CD56+ and CD3+CD4-CD8- subsets are shown for IL-12 stimulated (blue) and unstimulated (red) samples.

## 3.2.4. Optimisation of flow cytometry panels

Several optimisation steps were required to set up both the Receptor and Signalling panels. The optimisation findings are described in Chapter 4; however, the fully optimised protocols are described below in section 3.2.5.

### Receptor

#### *PHA stimulation and its effect on CD212 and CD119 expression*

According to de Beaucoudrey et al. (2011) and Fieschi et al. (2004), PBMCs should be stimulated with PHA for 72 hours and co-cultured with IL-2 for optimal upregulation of CD212 expression on the surfaces of lymphocytes. In order to simplify the workflow for this study, patient PBMCs were not incubated for extended periods and no co-culture with IL-2 was performed. The simplified assays were compared to the abovementioned previously published assays to determine whether the simplification of the assays significantly impact on the results.

Stimulation of cells with PHA alone is known to upregulate the expression of CD212 on lymphocytes, however, the effect of PHA on CD119 expression has not been reported. In order to determine the effect of PHA on the expression of CD119 and CD212 on lymphocytes in our setting, thawed PBMCs were incubated with PHA (5 µg/mL) for 0, 24 and 48 hours at 37˚C and 5% $CO_2$ and then stained with an antibody cocktail from the Receptor panel for 30 minutes.

The fold change in CD212 expression ($\Delta CD212 = \frac{CD212\ MFI\ fully\ stained\ sample}{CD212\ MFI\ unstained\ sample}$) was calculated for both the PHA stimulated and unstimulated samples and used to determine the effect of PHA on CD212. The percentage of CD119 expression on FSC vs. SSC monocytes and CD14+ monocytes were assessed for the PHA stimulated and unstimulated samples to determine the effect of PHA on CD119.

## Phosflow

### *Permeabilisation buffers*

Two separate permeabilisation buffers namely BD Phosflow™ Perm Buffer III and BD Phosflow™ Perm Buffer IV (BD Biosciences, CA, USA) were evaluated to determine which would provide the best detection of pSTAT1 and pSTAT4 whilst resulting in minimal destruction of surface epitopes.

To test the effect of each permeabilisation buffer on each of the surface markers, thawed PBMCs were fixed with BD Cytofix™ buffer (BD Biosciences, CA, USA) and then permeablised with either Perm III (30 minutes on ice) or Perm IV (1X) (20 minutes at room temperature) prior to staining with each of the respective surface marker fluorochrome-conjugated antibodies. Perm IV (1X) is prepared by diluting the Perm IV (10X) stock solution with PBS.

To determine which permeabilisation buffer allowed optimal detection of pSTAT1 and pSTAT4, thawed PBMCs were either stimulated for 15 minutes with IFN-γ (100 ng/mL) and IL-12 (100 ng/mL) or left unstimulated. The cells were then fixed with BD Cytofix™ and permeablised with Perm III and Perm IV (1X) respectively. The cells were then stained with both pSTAT1-BV421 and pSTAT4-PE. The fold change ($\frac{MFI\ stimulated\ sample}{MFI\ unstimulated\ sample}$) in pSTAT1 and pSTAT4 was calculated to determine which buffer was best suited.

### *PHA stimulation and pSTAT4 detection*

Uzel et al. (2001), one of the first groups to describe pSTAT4 detection by means of Phosflow, activated PBMCs with PHA and IL-2 prior to IL-12 stimulation. In this study, however, PBMCs were stimulated with 5 µg/mL PHA, without IL-2, for 24 hours in order to assess the impact of PHA on pSTAT4 detection.

***Cytokine dosage effect of pSTAT detection***

To determine the optimal concentrations of cytokines to be used for stimulation, the Phosflow protocol was performed using varying concentrations of IFN-γ and IL-12. Stimulation with IFN-γ or IL-12 at concentrations of 10, 50, 100, 150 and 200 ng/mL was assessed.

The effect of stimulation time was not investigated in this study, since several sources have reported that 15 minute cytokine stimulation is optimal for both pSTAT1 and pSTAT4 detection (Esteve-Solé et al. 2018; Depner et al. 2016; Pertovaara et al. 2016; Uzel et al. 2001; Yao et al. 1999).

## 3.2.5. Optimised protocols

### Receptor Panel

Cryopreserved PBMCs were thawed and washed with RPMI with 10% FBS, as described in section 3.2.2, and then split into two separate 5 mL round-bottom polypropylene tubes with each then containing at least 2.5 x $10^5$ cells. One of the tubes was left unstimulated, for CD119 detection, and 5 µg/mL PHA was added to the other, for upregulation of CD212. Both tubes were placed into a 37˚C, 5% $CO_2$ incubator for 24 hours. After the incubation period, the PBMCs were washed twice, first with complete RPMI with 10% FBS and then with staining buffer.

Cells were then stained with the viability marker, FVS575V, for 10 minutes at room temperature and then washed with staining buffer. Thereafter each tube was stained for 30 minutes at room temperature with 50 µL of an antibody cocktail containing all antibodies from the Receptor Panel, as listed in Table 3.1, with the optimal staining dilution for each antibody as listed in Table 3.2.

After staining, the cells were washed with staining buffer and then resuspended in 200 µL staining buffer. The tubes were thoroughly vortexed before the sample was acquired immediately within 2 hours on the BD LSR II at the BD CAF Flow Cytometry Centre.

### Signalling Panel

Similar to the Receptor Panel, cryopreserved PBMCs were thawed and washed with RPMI with 10% FBS, as described in section 3.2.2, and then split into three separate 5-mL round-bottom polypropylene tubes, labelled unstimulated, IFN-γ stimulated, and IL-12 stimulated, with each containing at least 5 x $10^5$ cells. PHA (5 µg/mL) was added to only one of the tubes – IL-12 stimulated – to upregulate CD212 expression, allowing for optimal pSTAT4 detection. All three tubes were then placed into a 37˚C, 5% $CO_2$ incubator overnight (approximately 18 hours). After the incubation period, the PBMCs were washed with complete RPMI with 10% FBS.

After the overnight incubation, the cells were stained with the fixable viability marker, FVS575V, for 10 minutes at room temperature and then washed with complete RPMI with 10% FBS. Tubes

were then stimulated with 500 µL of either complete RPMI with 10% FBS (unstimulated), 100 ng/mL human recombinant IFN-γ (IFN-γ stimulated) or 100 ng/mL human recombinant IL-12 (PHA pre-stimulated IL-12 stimulated tube) for 15 minutes at 37˚C, 5% $CO_2$.

Immediately after stimulation, an equal volume of BD Cytofix™ was added, and the cells were placed in a 37˚C bead-bath for 10 minutes in order to fix the cells. The cells were then centrifuged for 10 minutes at 2300 RCF, and the supernatant discarded. The tubes were then vortexed vigorously to resuspend the cells completely. To permeablise the cells, 1 mL Perm IV (1X), made from a 1:10 dilution of Perm IV (10X) in PBS, was added and incubated for 20 minutes at room temperature. After permeabilisation, cells were washed twice by adding at least 2 mL staining buffer and then centrifuging for 10 minutes at 2300 RCF.

Thereafter, each tube was stained for 60 minutes at room temperature with 50 µL of an antibody cocktail containing all antibodies from the Signalling Panel, as listed in table 3.1, with the optimal staining dilution for each antibody as listed in Table 3.2. After staining, the cells were washed with staining buffer and then resuspended in 200 µL staining buffer. The tubes were thoroughly vortexed before being acquired on the BD LSR II at the BD CAF Flow Cytometry Centre.

## 3.2.6. Processing of control and patient PBMCs and analysis of flow cytometry data

### Using control PBMCs to establish a baseline

For each panel, 10 controls, which were all assumed healthy, non-PID adult laboratory volunteers, were processed using the optimal protocol described above in 3.2.5 to establish a ‘normal’ baseline range that patient samples could be compared to. For the Receptor panel, the frequency (%) of CD119 and CD212 expression for each of the parent populations were measured as well as the density (MFI) of expression on each cell subset. For the Signalling panel, the fold change in pSTAT detection between the cytokine stimulated and unstimulated samples for each patient was determined for both pSTAT1 and pSTAT4.

Data acquired from the LSR II using the BD FACSDiva™ software was exported as .fcs files and further analysed in FlowJo®. Raw cytometry data generated using FlowJo® was exported into MS Excel format and then GraphPad Prism (version 7) was used for further analysis of percentage expression and fold change in MFI data. Descriptive statistics of receptor expression, for both CD119 and CD212, and fold change in pSTAT detection were generated for each of the various cell subtypes. Non-parametric spearman correlation tests were performed to determine whether receptor expression correlated with fold change in pSTAT detection. The data for all cell subsets were combined for the correlation analyses.

### Processing of patient samples

Patient PBMCs were processed, similarly to the controls, using the optimised protocol for each of the respective flow cytometric assays. Functional work was also performed on family members' PBMCs for comparison in cases where the family member had or was suspected of having the same variant as the patient.

Data acquired from the LSR II using the BD FACSDiva™ software was exported as .fcs files and further analysed in FlowJo®. Percentage and MFI data was exported from FlowJo® to MS Excel format. Thereafter, patient data was compared to a 90% reference interval obtained from controls' data, i.e. for each patient, it was assessed whether the patient data falls within the 5$^{th}$ to 95$^{th}$ percentile of the control, or reference, data.

## 3.3. Detection of Induced Cytokine Production

## 3.3.1. Cytokine stimulation

The levels of IL-12-induced IFN-γ production and IFN-γ-induced IL-12 production was measured *in vitro* after 48-hour stimulation of PBMCs. This assay was derived from the 'gold standard' method, developed by Feinberg et al. (2004) for the study of the integrity of the IFN-γ pathway. The Feinberg et al. method involved the measurement of IL-12p40, IL12p70 and IFN-γ after stimulation of whole blood or PBMCs with BCG with or without recombinant IL-12p70 or IFN-γ. Dorman and Holland (1998) used a similar method where they stimulated PBMCs with PHA, rather than BCG, and IL-12 to describe a defect in the IFN-γ signal-transducing chain in a patient with a mutation in IFN-γR2.

For this assay, cryopreserved PBMCs were activated with 5 µg/mL PHA, similar to Dorman and Holland (1998), with or without recombinant human IFN-γ or IL-12p70 (BD Biosciences, CA, USA), in order to assess the integrity of the IFN-γ-IL-12 pathway as proposed by Feinberg et al. (2004).

Cryopreserved PBMCs were rapidly thawed, washed with complete RPMI containing 10% FBS and a cell count was performed and recorded as described in 3.3.2. Four wells in a 24-well cell culture plate (Corning Incorporated, NY, USA) were prepared for each patient or control PBMC sample: (i) no activation, (ii) PHA activation (5 µg/mL), (iii) PHA activation and IL-12 stimulation (20 ng/mL), and (iv) PHA activation and IFN-γ stimulation (50 ng/mL). Between 150 000 and 500 000 cells were added per well, depending on availability of input material. The exact number of cells added into each was recorded in order to adjust cytokine concentrations to represent cytokine production per $10^5$ cells (as indicated in ELISA analysis section 3.3.2). The components of each well are also listed in Table 3.3. The plate was then incubated for 48 hours at 37°C in an incubator with 5% $CO_2$. After the incubation period, the total contents of each well were

transferred to a 1.5 mL tube and centrifuged at 2500 RCF for 10 minutes. The supernatants were then transferred to 1.5 mL safe-lock tubes for storage at -80°C until ELISA analysis.

**Table 3.3: Composition of the four wells prepared for each sample in the cytokine-induced cytokine production assay**. The first well contained only cells and media, this serves as a negative control; The second well contained cells, media and PHA, this serves as a second control, for PHA stimulation; The third well contained cells, media, PHA and IL-12; The fourth well contained cells, media, PHA and IFN-γ.

| Well number/name | 1 | 2 | 3 | 4 |
|---|---|---|---|---|
| | **No activation** | **PHA** | **PHA + IL-12** | **PHA + IFN-γ** |
| **Cells** (PBMC in suspension) | **+** | **+** | **+** | **+** |
| **PHA** (5ug/ml final concentration) | - | **+** | **+** | **+** |
| **IL-12** (20ng/ml final concentration) | - | - | **+** | - |
| **IFN-γ** (50ng/ml final concentration) | - | - | - | **+** |
| **Media** | **+** | **+** | **+** | **+** |
| Total volume | 1 mL | 1 mL | 1 mL | 1 mL |

Ten healthy control PBMCs, the exact same controls used for the flow cytometry assays, were processed and the results were recorded in order to establish a 'normal' baseline that could be used for comparison to patients. Thereafter the cytokine-induced cytokine production assay was performed on PBMCs for all patients as well as for their family members' where appropriate.

## 3.3.2. Cytokine detection

### ELISAs

A human IFN-γ Quantikine® ELISA kit as well as a high-sensitivity human IL-12p70 Quantikine® HS ELISA kit (R&D Systems, MN, USA) were used to measure the levels of IFN-γ and IL-12p70 for each patient in each of the 4 wells from the abovementioned activation and cytokine stimulation assay. In addition to the cell culture supernatants from the 48-hour activation and cytokine stimulation assay, IFN-γ levels, but not IL-12p70 levels, present in plasma samples harvested from whole blood during PBMC isolation (3.1.1) will also be analysed by means of ELISA.

The manufacturers' recommended protocol for each assay was followed. Before analysis by ELISA, samples were thawed to room temperature and centrifuged at 13 000 RCF for 15 minutes to remove particulate material from the cell culture supernatants or plasma. Briefly, sample cell-culture supernatant or standard was added to a well in a 96-well plate containing assay diluent and incubated for 2 (IFN-γ) or 3 (IL-12) hours at room temperature. The standards for the IFN-γ ELISA were 1000 pg/mL, 500 pg/mL, 250 pg/mL, 125 pg/mL, 62.5 pg/mL, 31.3 pg/mL and 15.6 pg/mL. The standards for the IL-12p70 ELISA were 40 pg/mL, 20 pg/mL, 10 pg/mL, 5 pg/mL, 2.5 pg/mL, 1.25 pg/mL and 0.625 pg/mL. After the incubation, each well was washed thoroughly, using the Bio-Rad ImmunoWash™ 1575 microplate washer, with the respective wash buffer and then the human IFN-γ or IL-12p70 conjugate was added to each well and incubated for 2 hours,

followed by another washing step. Substrate solution was then added to each well and after an incubation period of 30 minutes (IFN-γ) or 1 hour (IFN-γ) the stop solution was added – prior to adding the stopping solution for the IL-12p70 ELISA, an amplifier solution, which allows the detection low concentrations of IL-12p70, is added and allowed to incubate for another hour.

The optical density (OD) of each well was determined within 30 minutes of adding the stop solution. OD was measured using the Bio-Rad iMark™ Microplate Reader at 450 nm (570 nm correction wavelength) for the IFN-γ ELISA and at 490 nm (670 correction wavelength) for the IL-12p70 HS ELISA.

## ELISA Analysis

Duplicate OD readings were averaged for each standard, control or sample, and the average OD of the zero/blank standard was subtracted. A standard curve was generated by plotting the mean absorbance for each standard on the y-axis against the concentration on the x-axis. Examples of the standard curves generated for the IFN-γ and HS IL-12p70 ELISAs are illustrated in Figures 3.7 and 3.8, respectively. Quantification of cytokine levels requires comparison with the standard curve that was generated, for each ELISA assay, from a non-linear regression model generated in MS Excel 365 (Microsoft, USA).

Concentrations of each cytokine were expressed as pg/mL cytokine produced by the equivalent of $10^5$ PBMCs:

$$[cytokine\ produced\ per\ 10^5\ cells\ (pg/mL) = \frac{total\ cytokine\ concentration\ (pg/mL)\ measured\ by\ ELISA}{number\ of\ cells\ per\ well} \times 10^5]$$

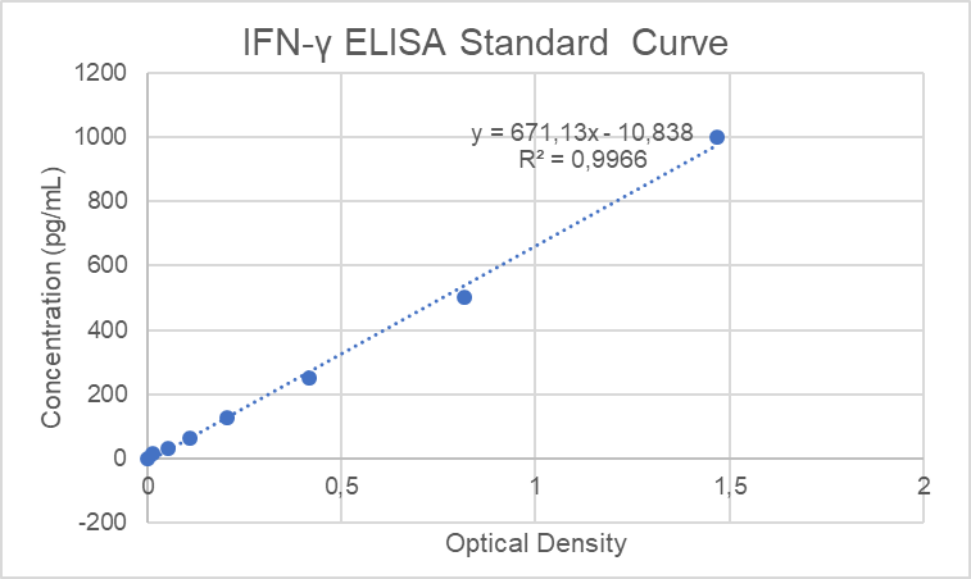


**Figure 3.7: Example of standard curve generated for the IFN-γ ELISA using MS Excel 365**.

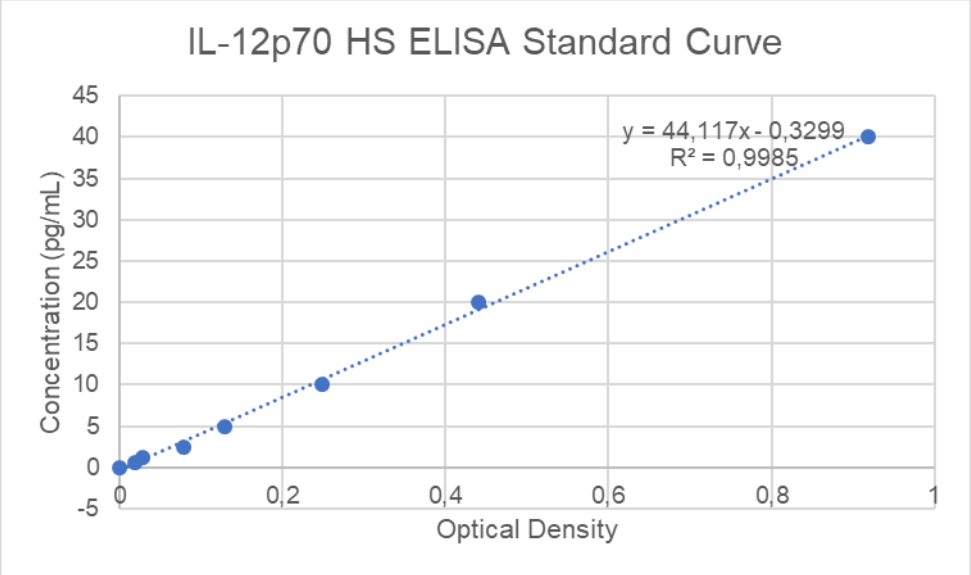


**Figure 3.8: Example of standard curve generated for the IL-12p70 HS ELISA using MS Excel 365.**

## 3.4. Statistical Analysis

Data was exported from FlowJo® into Microsoft Excel files and statistical analysis was performed using the GraphPad Prism Software for Windows (Version 7.0, GraphPad, CA USA). Normality of the data was determined through the D'Agostino-Pearson test. Non-parametric data was not normalised. Medians and Interquartile ranges (IQRs) were used to describe the non-parametric data. Kruskal Wallis 1-way ANOVA was used, followed by Dunn's multiple comparison post-test to compare the patient and control data for each cell subtype in each assay. Results were considered significant when the p-value was less than 0.05 ($p<0.05$). Spearman's rank correlation analysis was performed to determine whether there are significant correlations between cytokine receptor expression and cytokine receptor-related signalling.

# Chapter 4 Results

This chapter consists of three sections. The first section (4.1) describes the participants and their associated genetic findings. The second section (4.2) describes the optimisation of the flow cytometry-based assays. The last section (4.3) describes the results obtained from the flow cytometry-based assays as well as the ELISA-based cytokine assays for both the healthy control samples and the suspected MSMD patients.

## 4.1. Participants

Sixteen patients with suspected PID with mycobacterial associations were included in this study. One additional TB unexposed patient with recurrent Salmonella infections, an infection which has previously been described in MSMD patients, was also included in this study. The patients were assigned random identifiers (PID01 to PID17).

### 4.1.1. Case Reports and Routine Laboratory findings

Of the 17 patients included in this study, 10 (59%) patients had multiple TB episodes, and 12 (71%) had disseminated or extrapulmonary TB. Non-tuberculous mycobacterial infections were confirmed in only 1 case, PID01 (*M.avium*), although suspected in PID09 as well. All participants received BCG vaccination as infants, although only 1 (PID09) presented with suspected BCGosis. None of the participants were HIV exposed. All of the participants were HIV negative and none had a family history of PID diagnoses. One of the patients, PID08, had a sibling with a similar clinical presentation who had died in infancy. Another patient, PID16, had a history of severe TB on the paternal side of the family. Some of the participants had household TB contacts from an early age, although most had no known TB contacts in their home environment.

There was no predominant gender bias amongst the participants, 9 (53%) were male and 8 (47%) were female. The participants were ethnically diverse, with 14 patients self-identifying as mixed-race, and the other 3 were white. Most of the patients had similar socio-economic backgrounds. Only 2 of the participants, PID04 and PID09 were referred to TBH Immunology clinic from private health care facilities, while the others were all in the public healthcare system.

QFT-plus was performed for 8 (47%) of the total patients of which 4 (50%) had a negative result (PID03, PID08, PID09, and PID12). Three of the 4 patients that had negative QFT-plus results have had at least one culture confirmed TB episode, which contradicted the QFT-plus results (TB was not successfully cultured for the fourth patient, PID09, who has suspected disseminated BCG infection).

The clinical presentation and relevant routine laboratory results for all the patients are summarised in Table 4.1.

## 4.1.2. Genetic Findings

Plausible disease-causing variants were identified for 11 of the total 17 patients (65%). This equates to 11 of the 12 patients (92%) who were sequenced (either WES plus Sanger or Sanger alone). WES identified mutations in 9 patients, whereas Sanger sequencing alone identified mutations in 2 patients. Targeted Sanger sequencing alone was only used in cases where a variant in a specific gene was highly suspected prior to genetic analysis, such as the *IFNGR1* variant in PID01 and the *CYBB* variant in PID09, due to it being more cost-effective than WES. All variants identified by WES were in turn confirmed by Sanger sequencing. There was one patient, PID12, that underwent WES and for whom no plausible disease-causing variant could be identified. At the time of conclusion of this study, WES had not yet been performed on 5 of the original 17 patients due to funding constraints.

Variants in known MSMD-associated genes were found in 8 of the 12 sequenced participants (67%). This includes variants in *IFNGR1*, identified for 3 patients (c.G1009A, c.C864G, and c.818del4), *IL12RB1*, in 2 patients (c.G684C and c.G863C), *IL12B*, in 2 patients (c.A320G and c.G863C), and *CYBB* (c.A302G) in 1 patient. Only 1 of these variants, IFNGR1 c.818del4, has been previously described (Al-Muhsen and Casanova 2008; Dorman and Holland 2000), the others represent novel variants. The genetic findings and clinical presentation of PID01 (*IFNGR1* c.818del4) has been published (Glanzmann et al. 2018a), although none of the functional immune assays in this study have previously been performed.

Other genetic variants, which are currently not known or described as associated with MSMD but could still potentially explain the phenotype, were detected in the other participants. These include *IKZF1* (c.G1009A), *NOD2* (c.C374T), *IRAK1* (c.C1939T), *IKBKB* (c.G2257A), and *NFKB2* (c.C2042T).

The genetic findings of each patient are detailed in Table 4.2.

Functional work was also performed on 2, clinically unaffected, closely related family members. One of these was the child of patient PID01, the other was the father of PID02. Both of these individuals shared the genetic variant identified in the respective patient to whom they are related.

.

**Table 4.1: Clinical information for participants**

| Patient | Sex | Clinical Presentation | QFT-plus result | Age at first presentation | Family History? | Routine Lab results (Igs, Compl, Nburst, FBCs & Diff) |
|---|---|---|---|---|---|---|
| PID01 | F | Concurrent pulmonary TB, TB lymphadenitis and recurrent disseminated *M.avium* infection | Not performed | 6 months | No relevant PID history | Routine Immunological workup normal |
| PID02 | F | Diagnosed with pulmonary TB and TBM (Stage III) at age 9. | Not performed | 9 years | TB exposed (mom). Younger sib also developed TBM. | Routine Immunological workup not done in full. All investigations done were normal. |
| PID03 | F | Recurrent pulmonary TB (3 episodes), including MDR TB, as well as TB lymphadenitis | Not performed | 5 years | No relevant PID history. Household TB contacts (mom) | High IgA and High IgM (raised less than 2 SD) |
| PID04 | M | Chronic mucoid diarrhoea since 3 weeks of age. Recurrent Salmonella type C infections. | Not performed | 3 weeks | No relevant PID history. No known household TB contacts. | Autoimmune investigation normal, and no identifiable atopy/food intolerance. All routine lab investigations normal. |
| PID05 | M | Recurrent pulmonary TB - 4 culture confirmed cases, each more than 1 year apart. Previously diagnosed with Goldberg-Shprintzen Syndrome. | Positive | 9 months | No relevant PID history | Routine Immunological workup not done in full. All investigations done were normal. |
| PID06 | M | Unusual extrapulmonary TB with spine and liver involvement. | Not performed | 11 years | No relevant PID history. Household TB contacts. | Anaemia, raised IgG and IgA, raised CD19 cells, normal neutrophil burst |
| PID07 | M | Recurrent TB lymphadenitis requiring prolonged duration of treatment. | Positive | 3 years | No relevant PID history | Routine Immunological workup not done in full. All investigations done were normal. |
| PID08 | F | Miliary TB and TB lymphadenitis. | Negative | 1 year | Sibling died early in childhood, with similar clinical presentation | Anaemia. Routine Immunological workup not done in full. All investigations done were normal. |
| PID09 | M | Disseminated Mycobacterium complex disease, suspected to be BCG. | Negative | 6 months | No relevant PID history | Non-responsive neutrophil burst, compatible with CGD diagnosis. *CYBB* gene Sanger Sequenced. All other routine immunological workup normal. |
| PID10 | F | Recurrent TB of the liver (6+ episodes). Shortly after end of treatment, TB reactivates, and patient needs to restart treatment. The most recent TB episode was MDR TB. | Not performed | 1 year | No relevant PID history. MDR TB household contact. | Routine Immunological workup normal |
| PID11 | M | Recurrent TB. First episode was miliary TB and 6 months after end of treatment presented with TBM. Second TBM episode (Stage II) 8 months after completion of TB treatment for previous episode. | Not performed | 3 months | No relevant PID history | Routine Immunological workup normal |
| PID12 | F | This patient had a new-born that was diagnosed with TB. Upon investigation it was revealed that she (the mother) has had 6 suspected, although 4 confirmed, and treated episodes of pulmonary TB. | Negative | 15 years | No relevant PID history | Routine Immunological workup normal |
| PID13 | M | Recurrent TB abscess of anterior chest wall | Positive | 2 years | No relevant PID history. Household TB contacts | Routine Immunological workup normal |
| PID14 | M | Septic arthritis and miliary TB, which progressed to TBM and eventual MDR TB regime | Not performed | 11 months | No relevant PID history | Anaemia. Routine Immunological workup normal |
| PID15 | F | Unusual TBM diagnosis in 9-year-old | Not performed | 9 years | No relevant PID history | Routine Immunological workup normal |
| PID16 | F | Recurrent TB, with hip involvement, and MDR TB. | Positive | unknown | No relevant PID history | Routine Immunological workup normal |
| PID17 | M | Recurrent TB (4 episodes), including MDR TB. | Positive | 6 months | History of severe& recurrent TB on paternal side | Routine Immunological workup normal |

**Table 4.2: Genetic results for suspected MSMD patients.**

| Patient | WES performed? | WES Result- Gene(s) & Variant(s) | Zygosity | Sanger Confirmed/ Sanger Only? | *In silico* predicted effect of identified variant |
|---|---|---|---|---|---|
| PID01 | No | *IFNGR1* (c.818del4) | Heterozygous | Sanger only | Pathogenic |
| PID02 | Yes | *IFNGR1* (c.C864G p.I288M) | Heterozygous | Sanger confirmed | Pathogenic |
| | | *NOD2* (c.C374T p.P125L) | Heterozygous | Sanger confirmed | Pathogenic |
| PID03 | Yes | *IKZF1* (c.G1009A p.G337S) | Homozygous | Sanger confirmed | Pathogenic |
| | | *IFNGR1* (c.698C>T p.G233A) | Heterozygous | Sanger confirmed | Pathogenic |
| PID04 | Yes | *IL12RB1* (c.G684C p.R213Q) | Homozygous | Sanger confirmed | Pathogenic |
| PID05 | Yes | *IL12RB1* (c.C139T p.P47S) | Homozygous | Sanger confirmed | Likely pathogenic |
| PID06 | Yes | *IL12B* (c.A320G p.K107R) | Heterozygous | Sanger confirmed | Pathogenic |
| | | *NFKB2* (c.C2042T p.P681L) | Heterozygous | Sanger confirmed | Likely pathogenic |
| PID07 | Yes | *IL12B* (c.G863C p.R288T) | Homozygous | Sanger confirmed | Pathogenic |
| PID08 | Yes | *IFNGR2* (c.A708T p.E236D) | Homozygous | Sanger confirmed | Pathogenic |
| PID09 | No | *CYBB* (c. A302G p.H101R) | Hemizygous | Sanger only | Pathogenic |
| PID10 | Yes | *IKBKB* (c.G2257A p.A753T) | Homozygous | Sanger confirmed | Likely pathogenic |
| | | *NFKB2* (c.C2042T p.P681L) | Heterozygous | Sanger confirmed | Likely pathogenic |
| PID11 | Yes | *IRAK1* (c.C1939T p.L647P) | Homozygous | Sanger confirmed | Pathogenic |
| PID12 | Yes | No result | N/A | N/A | N/A |
| PID13 | No | N/A | N/A | N/A | N/A |
| PID14 | No | N/A | N/A | N/A | N/A |
| PID15 | No | N/A | N/A | N/A | N/A |
| PID16 | No | N/A | N/A | N/A | N/A |
| PID17 | No | N/A | N/A | N/A | N/A |

## 4.2. Optimisation of the flow cytometry assays

### 4.2.1. Receptor Panel

#### PHA stimulation and its effect on CD212 (IL-12Rβ2) and CD119 (IFN-γR1) expression

PHA (5 µg/mL) stimulation for 24 hours prior to staining, increased CD212 receptor expression on the surfaces of all lymphocyte subsets (Figure 4.1). Longer, 48-hour PHA stimulation only minimally further increased CD212 expression compared to 24-hour stimulation. CD119 expression on monocytes, on the other hand, decreased after 24 and 48-hour PHA stimulation prior to staining. A substantial reduction in CD119 detection was observed in 24-hour PHA stimulation, which moderated slightly after 48-hour stimulation. Therefore, in subsequent experiments, PBMCs were pre-stimulated for 24 hours with 5 µg/mL PHA prior to assessment of CD212 expression while CD119 expression was only assessed on unstimulated PBMCs.

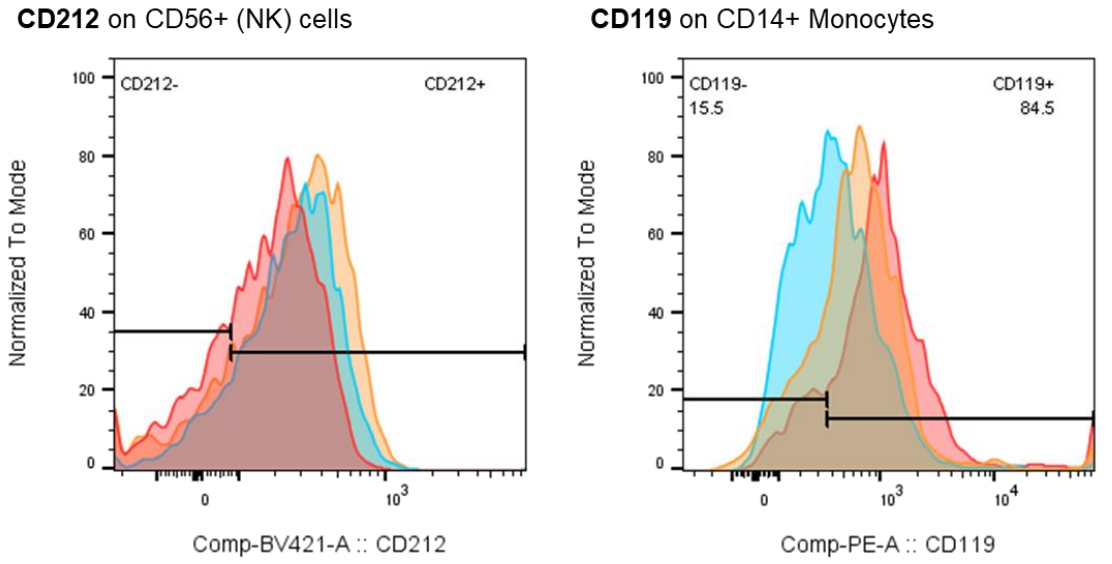


| | Sample | CD212 MFI | %CD212+ cells |
|---|---|---|---|
| | No PHA stimulation | 192 | 74,7 |
| | 24h PHA stimulation | 275 | 86,2 |
| | 48h PHA stimulation | 295 | 83,5 |

| | Sample | CD119 MFI | %CD119+ cells |
|---|---|---|---|
| | No PHA stimulation | 941 | 84,5 |
| | 24h PHA stimulation | 399 | 54,3 |
| | 48h PHA stimulation | 634 | 75,7 |

**Figure 4.1: The effect of PHA stimulation on CD212 and CD119 expression**. Expression of CD212 is upregulated with PHA (5 µg/mL) stimulation. 48-hour PHA stimulation does not appear to significantly enhance CD212 expression compared to 24-hour stimulation. CD119 detection is greater in unstimulated samples compared to 24 and 48-hour PHA stimulation. CD212 expression on CD56+ (NK) cells show a 1.43-fold increase in expression (MFIstim / MFIunstim) with 24-hour PHA stimulation (with other lymphocyte subsets showing similar trends), whilst CD119 expression on CD14+ monocytes showed a 2.36-fold decrease in expression with 24-hour PHA stimulation.

## 4.2.2. Phosflow Panel

### Permeabilisation buffers

Both BD Biosciences Perm III and Perm IV (1X) reduced the signal-to-noise ratio for each of the surface antibodies compared to a regular staining procedure without fixation or permeabilisation steps. Histogram overlays in Figure 4.2 illustrate the loss-of-signal effect that the permeabilisation buffers had on the detection of surface markers compared to regular staining. Overall, Perm III resulted in a greater loss of signal than Perm IV.

**CD3 - FITC**

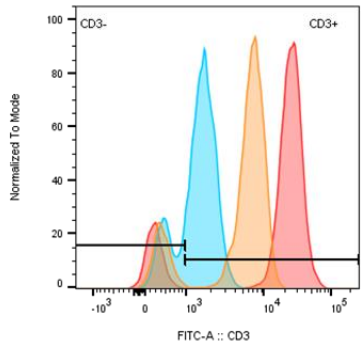


| | Sample | CD3 MFI | %CD3+ |
|---|---|---|---|
| | No Fix/Perm, surface stain | 22237 | 82,5 |
| | Perm III Buffer | 1515 | 79,2 |
| | Perm IV (1X) Buffer | 6308 | 82,9 |

**CD4 - APC**

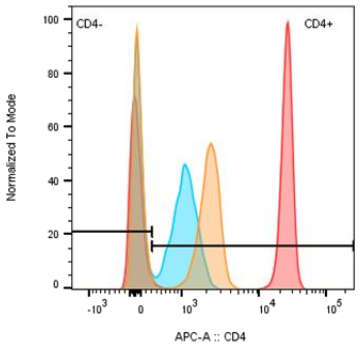


| | Sample | CD4 MFI | %CD4+ |
|---|---|---|---|
| | No Fix/Perm, surface stain | 19484 | 57,3 |
| | Perm III Buffer | 649 | 55,3 |
| | Perm IV (1X) Buffer | 1432 | 54,6 |

**CD8 - PE-Cy5**

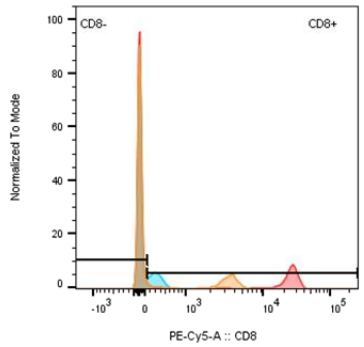


| | Sample | CD8 MFI | %CD8+ |
|---|---|---|---|
| | No Fix/Perm, surface stain | 24,4 | 30,4 |
| | Perm III Buffer | 21,8 | 19,6 |
| | Perm IV (1X) Buffer | 24,4 | 25,7 |

**CD14 - PE-Cy7**

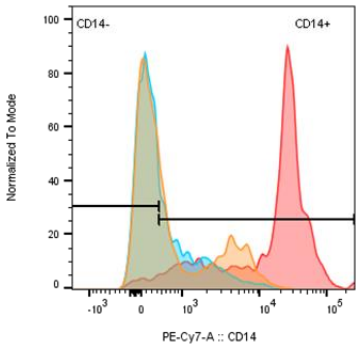


| | Sample | CD14 MFI | %CD14+ |
|---|---|---|---|
| | No Fix/Perm, surface stain | 22395 | 96,3 |
| | Perm III Buffer | 317 | 38,0 |
| | Perm IV (1X) Buffer | 373 | 44,5 |

**Figure 4.2: Effect of permeabilisation buffers on the detection of surface markers**. Both Perm III and Perm IV resulted in decreased detection of surface markers compared to regular surface staining without fixation or permeabilisation. Only CD3-FITC, CD4-APC, CD8-PE, and CD14-PE-Cy7 are shown here, although the same trend was observed in other cell subsets. Perm IV resulted in a less dramatic loss-of-signal for all the surface markers.

In PBMCs stimulated with 100ng/mL of IL-12 and IFN-γ, the fold change in pSTAT detection ($\frac{\text{MFI of stimulated sample}}{\text{MFI of unstimulated sample}}$) was similar overall for both permeabilisation buffers, although Perm IV had a slightly higher pSTAT fold change than Perm III (Figure 4.3). pSTAT1 detection was slightly better with Perm IV than Perm III. With Perm IV, there was better shift in pSTAT1 detection in the cytokine-stimulated sample from the unstimulated sample compared to Perm III (i.e. fold change in pSTAT1 was higher for Perm IV). Fold change in pSTAT4 was also higher with Perm IV as compared to Perm III.

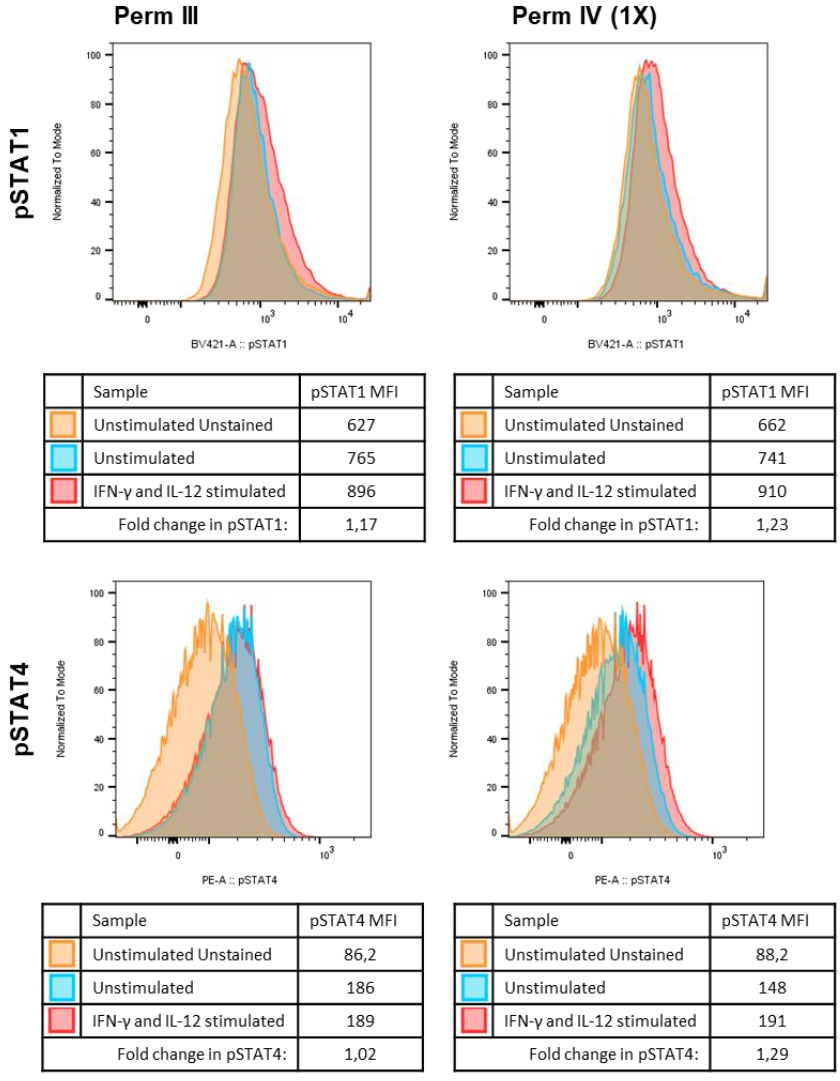


| | Sample | pSTAT1 MFI |
|---|---|---|
| | Unstimulated Unstained | 627 |
| | Unstimulated | 765 |
| | IFN-γ and IL-12 stimulated | 896 |
| | Fold change in pSTAT1: | 1,17 |

| | Sample | pSTAT1 MFI |
|---|---|---|
| | Unstimulated Unstained | 662 |
| | Unstimulated | 741 |
| | IFN-γ and IL-12 stimulated | 910 |
| | Fold change in pSTAT1: | 1,23 |

| | Sample | pSTAT4 MFI |
|---|---|---|
| | Unstimulated Unstained | 86,2 |
| | Unstimulated | 186 |
| | IFN-γ and IL-12 stimulated | 189 |
| | Fold change in pSTAT4: | 1,02 |

| | Sample | pSTAT4 MFI |
|---|---|---|
| | Unstimulated Unstained | 88,2 |
| | Unstimulated | 148 |
| | IFN-γ and IL-12 stimulated | 191 |
| | Fold change in pSTAT4: | 1,29 |

**Figure 4.3: Effect of permeabilisation buffers on pSTAT detection.** Both pSTAT1 and pSTAT4 fold changes were higher for Perm IV (1X) than Perm III, indicating that Perm IV was the superior buffer for the detection of pSTATs. Fold change in pSTAT = $\frac{MFI\ of\ stimulated\ sample}{MFI\ of\ unstimulated\ sample}$.

Perm IV, rather than Perm III, was used as permeabilisation buffer for all subsequent experiments due to the less dramatic impact on surface marker fluorescence and superior detection of pSTATs.

## Cytokine dosage effect of pSTAT detection

There was not much variation in pSTAT1 and pSTAT4 fold changes for the varying concentrations of cytokine stimuli used (Figure 4.4).

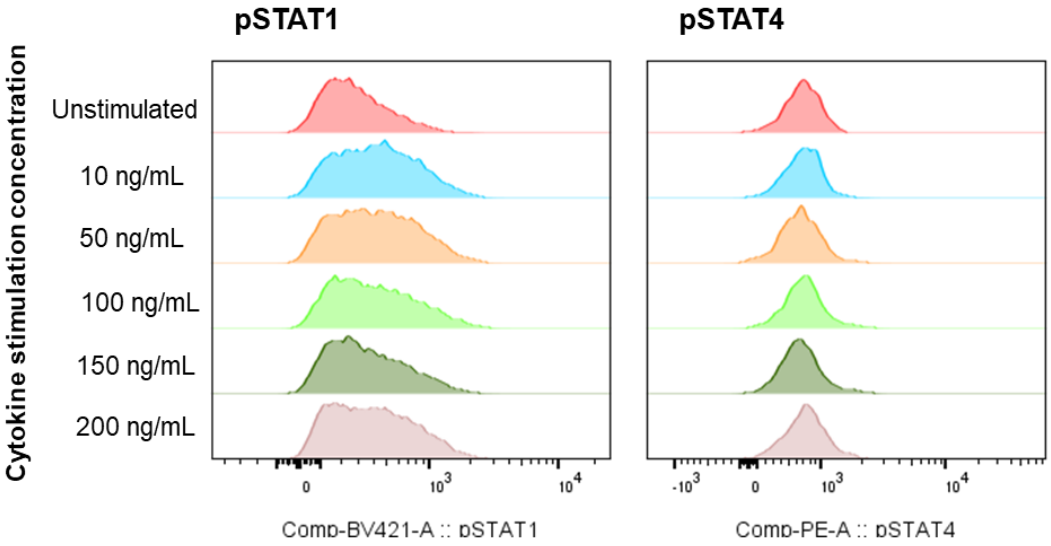


| | Sample | pSTAT1 MFI | pSTAT1 fold change |
|---|---|---|---|
| | Unstimulated | 255 | N/A |
| | 10 ng/mL IFN-γ | 413 | 1,62 |
| | 50 ng/mL IFN-γ | 397 | 1,56 |
| | 100 ng/mL IFN-γ | 370 | 1,45 |
| | 150 ng/mL IFN-γ | 316 | 1,24 |
| | 200 ng/mL IFN-γ | 370 | 1,45 |

| | Sample | pSTAT4 MFI | pSTAT4 fold change |
|---|---|---|---|
| | Unstimulated | 692 | N/A |
| | 10 ng/mL IL-12 | 708 | 1,02 |
| | 50 ng/mL IL-12 | 658 | 0,95 |
| | 100 ng/mL IL-12 | 705 | 1,02 |
| | 150 ng/mL IL-12 | 653 | 0,94 |
| | 200 ng/mL IL-12 | 739 | 1,07 |

**Figure 4.4: Cytokine dosage effect on pSTAT detection**. PBMC were stimulated with either 10, 50, 100, 150, and 200 ng/mL IFN-γ for pSTAT1 detection in lymphocytes or with 10, 50, 100, 150, and 200 ng/mL IL-12 for the detection of pSTAT4 in lymphocytes. Data shown for CD14+ monocytes (pSTAT1) and CD56+ (NK) cells (pSTAT4); Similar effects were observed in other cell subsets.
Fold change in pSTAT = $\frac{MFI\ of\ stimulated\ sample}{MFI\ of\ unstimulated\ sample}$ (pSTAT1 stimulus = IFN-γ, pSTAT4 stimulus = IL-12).

Due to there not being any significant differences in pSTAT detection with the varying concentrations used for stimulation, the intermediate concentration (100 ng/mL) was used for both IL-12 and IFN-γ stimulation in subsequent experiments.

## PHA stimulation and pSTAT4 detection

Stimulation of PBMCs with PHA (5 µg/mL) for 24 hours prior to the Phosflow protocol increased pSTAT4 detection in lymphocytes after IL-12 stimulation compared to PBMCs that were not pre-stimulated with PHA. There was little to no pSTAT4 signal in the cells that were not pre-stimulated with PHA and there was a more prominent shift in pSTAT4 signal for PHA pre-stimulated PBMCs as can be seen in Figure 4.5. This experiment was only performed using Perm IV as the permeabilisation buffer, due to it being the 'better' buffer for pSTAT detection, with minimal loss of surface marker detection, as determined in the previous experiments.

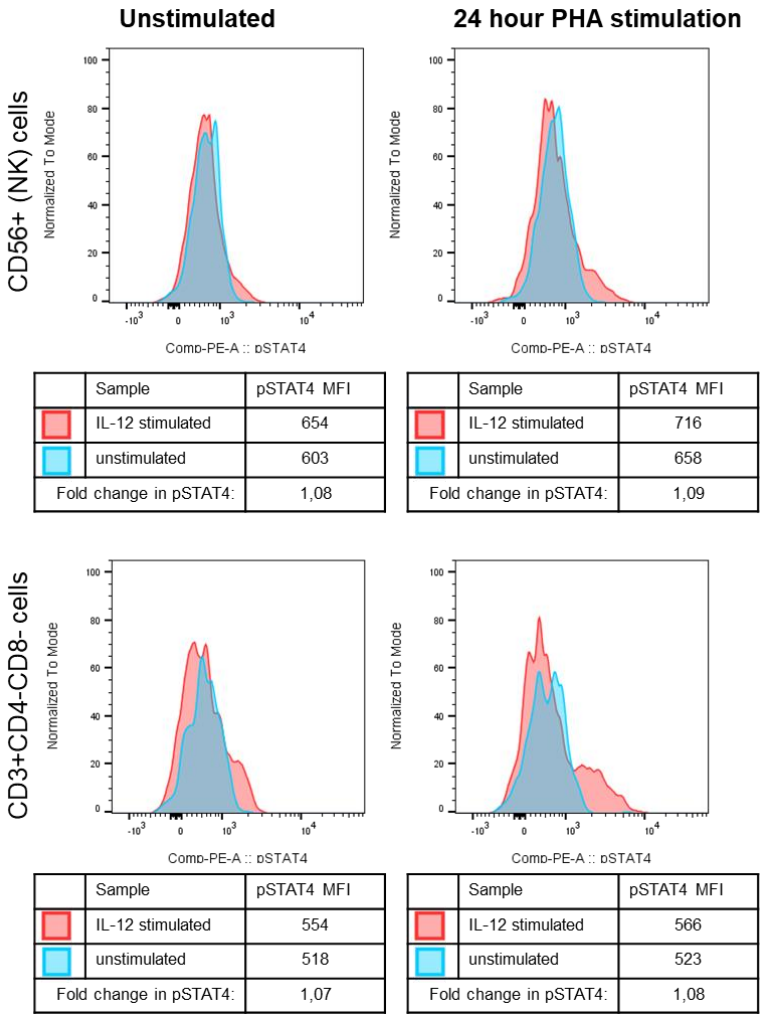


| | Sample | pSTAT4 MFI |
|---|---|---|
| | IL-12 stimulated | 654 |
| | unstimulated | 603 |
| Fold change in pSTAT4: | | 1,08 |

| | Sample | pSTAT4 MFI |
|---|---|---|
| | IL-12 stimulated | 716 |
| | unstimulated | 658 |
| Fold change in pSTAT4: | | 1,09 |

| | Sample | pSTAT4 MFI |
|---|---|---|
| | IL-12 stimulated | 554 |
| | unstimulated | 518 |
| Fold change in pSTAT4: | | 1,07 |

| | Sample | pSTAT4 MFI |
|---|---|---|
| | IL-12 stimulated | 566 |
| | unstimulated | 523 |
| Fold change in pSTAT4: | | 1,08 |

**Figure 4.5: pSTAT4 detection without vs. with PHA pre-stimulation.** pSTAT4 detection was enhanced in lymphocytes [CD56+ (NK) cells and CD4-CD8- T cells (γδ T cells) cells shown here, although the same trend was observed in other subsets] that were pre-stimulated with PHA for 24 hours. There is a second, distinctly positive peak for pSTAT4 in the IL-12 (100 ng/mL) stimulated sample for the PHA stimulated cells. Fold change in pSTAT = $\frac{MFI\ of\ stimulated\ sample}{MFI\ of\ unstimulated\ sample}$ (pSTAT1 stimulus = IFN-γ, pSTAT4 stimulus = IL-12).

## 4.3. Implementation of the assays

### 4.3.1. Establishment of normal expression range in control non-PID donor samples

PBMCs for 10, reportedly healthy, non-PID adult laboratory volunteers were used for each of the assays.

For all subsequent data, CD212 (IL-12Rβ1) data is from PHA pre-stimulated PBMCs whereas CD119 (IFN-γR1) data is from unstimulated PBMCs.

## Receptor Panel

CD119 expression was highest on CD14+ monocytes and CD19+ (B) cells, with median percentage positive cells of 77.2% (IQR: 56.75-83.15%) and 76.75% (IQR: 68.23-80.83%) respectively. The IFNγR1 receptor density per cell, i.e. CD119 MFI, for CD14+ monocytes and CD19+ (B) lymphocytes had IQRs of 625-790 (median 723) and 98-130 (median 118), respectively. CD119 had overall lower percentage expression on non-B lymphocyte subsets, such as CD3+ (T) cells and CD56+ (NK) cells, with medians ranging between 20.30% and 45.75%. IFNγR1 receptor density (MFI) was lower on lymphocyte subsets compared to monocytes, for instance CD56+ (NK) cells and CD3+ CD4-CD8- (primarily γδ T cells; Bluestone et al. 1988) had CD119 MFI IQRs of 51-66 (median 58) and 59-98 (median 74) respectively. According to Dunn's multiple comparison, the percentage CD119 expression on both CD14+ monocytes and CD19+ B cells were significantly higher than T lymphocytes, i.e. Total CD3+ ($p<0.0001$), CD4+ ($p<0.0001$), CD8+ ($p<0.0001$), CD4-CD8- ($p<0.01$).

High CD212 expression was consistently observed across all lymphocyte subsets. CD56+ (NK), CD3+CD56+ (NKT), CD8+ T cells and CD4-CD8- (γδ) T cells had the highest percentage of CD212 positive cells with medians of 91.6% (IQR: 89.53-95.30%), 87.00% (IQR: 83.83-92.18%), 88.35% (IQR: 77.88-91.55%), and 86.10% (IQR: 82.13-91.15%), respectively. A lower percentage of monocytes (CD14+) were CD212 positive, as compared to the lymphocyte subsets (median: 51.90; IQR: 23.88-60.25%). As with CD119 expression on lymphocyte subsets, CD212 expression levels appear to be well-conserved in lymphocytes and they generally had a smaller range of variance than monocytes (as seen in standard deviations). Despite lower percentage expression, the IL12Rβ1 receptor density per cell was higher for CD14+ monocytes (IQR 1281-1763) compared to all lymphocyte subsets (CD56+ IQR: 595-786; CD3+CD56+ IQR: 465-661; CD8+ IQR: 284-474; CD4-CD8- IQR: 333-485). According to Dunn's multiple comparison, percentage CD212 expression, compared to CD14+ monocytes, was significantly higher for CD56+ NK ($p<0.0001$), CD3+CD56+ NKT ($p=0.0008$), CD8+ ($p=0.0029$) and CD4-CD8- cells ($p=0.0036$).

Descriptive statistics for CD119 and CD212 expression for controls on various cell subsets can be found in Table 4.3. Box-and-whiskers graphs in Figures 4.6 and 4.7 show the distribution of the receptor percentage expression data from the controls. CD119 expression was assessed on unstimulated cells, while CD212 expression was measured after 24 hours stimulation with PHA (5 µg/mL), as described in section 3.2.5.

**Table 4.3: Descriptive statistics for CD119 (IFNγR1) and CD212 (IL12Rβ1) percentage expression and receptor density (MFI) for controls on various cell subsets**. The IQR of the control data was used as the 'normal' range against which patient data could be compared.

| | **Percentage CD119 expression** Median (IQR) | **CD119 MFI** Median (IQR) | **Percentage CD212 expression** Median (IQR) | **CD212 MFI** Median (IQR) |
|---|---|---|---|---|
| **FSC/SSC Monocytes** | 47.80 (40.8 – 62.60) | 376 (310 – 474) | 40.20 (28.78 – 52.03) | 1465 (1281 – 1763) |
| **CD14+ Monocytes** | 77.20 (56.75 – 83.15) | 723 (625 – 790) | 51.90 (23.88 – 60.25) | 2153 (1446 – 2450) |
| **FSC/SSC Lymphocytes** | 29.90 (26.03 – 35.08) | 82 (71 – 87) | 83.30 (72.50 – 86.55) | 344 (239 – 427) |
| **CD56+ (NK) Cells** | 45.75 (39.33 – 49.90) | 58 (51 – 66) | 91.60 (89.53 – 95.30) | 669 (595 – 786) |
| **CD3+CD56+ (NKT) Cells** | 38.00 (30.98 – 47.18) | 112 (96 – 119) | 87.00 (83.83 – 92.18) | 560 (465 – 661) |
| **CD3+ (T) Cells** | 22.55 (24.25 – 27.13) | 84 (72 – 88) | 83.70 (70.53 – 86.28) | 324 (202 – 391) |
| **CD4+ T Cells (Helper T cells)** | 20.30 (19.23 – 24.58) | 75 (67 – 79) | 78.60 (62.70 – 81.53) | 277 (168 – 361) |
| **CD8+ T Cells (Cytotoxic T cells)** | 23.35 (20.78 – 27.73) | 109 (103 – 120) | 88.35 (77.88 – 91.55) | 424 (284 – 474) |
| **CD4-CD8- T Cells (primarily γδ T cells)** | 28.75 (24.50 – 41.98) | 74 (59 – 98) | 86.10 (82.13 – 91.15) | 417 (333 – 485) |
| **CD19+ (B) Cells** | 76.75 (68.23 – 80.83) | 118 (98 – 130) | 82.70 (72.58 – 86.98) | 273 (183 – 354) |

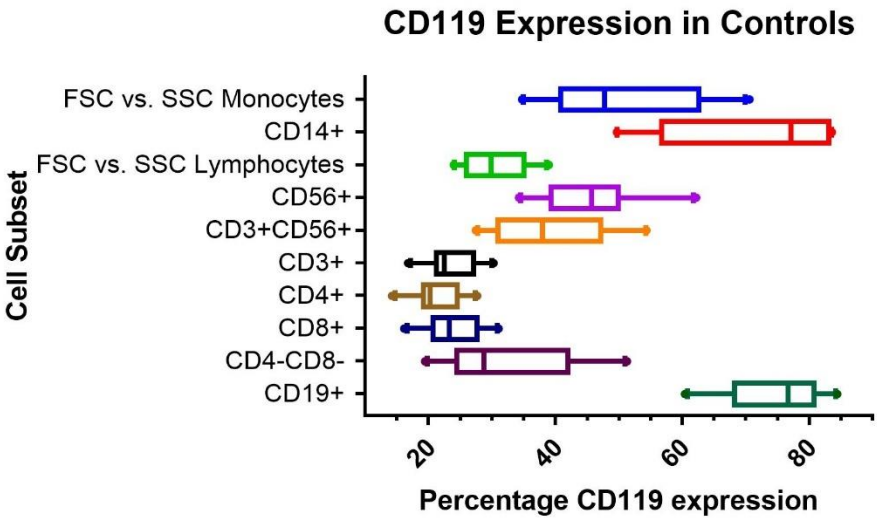


**Figure 4.6: Box-and-whisker plot showing the distribution of CD119 (IFNγR1) expression on various cell subsets for controls (n = 10)**. CD119 expression was highest on CD14+ monocytes and CD19+ (B) lymphocytes. CD119 expression was measured on unstimulated PBMCs. The box-and-whisker plot shows the 10$^{th}$ to 90$^{th}$ percentile of the data. The rectangular part of the box-plot represents the IQR of the data, with the line in the middle representing the median. Outliers are shown as dots.

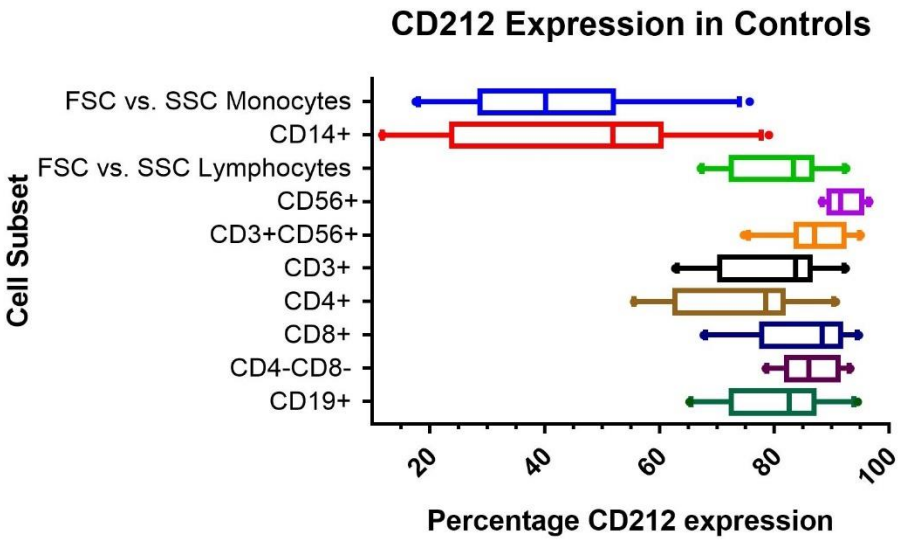


**Figure 4.7: Box-and-whiskers plot showing the distribution of CD212 (IL12Rβ1) expression on various cell subsets for controls (n=10)**. CD56+ (NK), CD3+CD56+ (NKT), CD8+ T cells and CD4-CD8- (γδ) T cells had the highest percentage of CD212 positive cells. Monocytes had much lower levels of expression compared to the lymphocyte subsets, which all had median CD212 expression levels of 78.60% or higher. CD212 expression was measured on PHA pre-stimulated PBMCs. The box-and-whisker plot shows the 10$^{th}$ to 90$^{th}$ percentile of the data. The rectangular part of the box-plot represents the IQR of the data, with the line in the middle representing the median. Outliers are shown as dots.

## Signalling Panel

The fold change in pSTAT1 (i.e. $\frac{pSTAT1\ MFI\ IFN{-}\gamma\ stimulated}{pSTAT1\ MFI\ unstimulated}$) was highest for CD14+ monocytes and CD20+ (B) cells, with medians of 1.60 (IQR: 1.39-2.05) and 1.63 (IQR: 1.28-1.81) respectively. The pSTAT1 fold change was lowest in CD56+ (NK) cells (1.16). CD56+ (NK) cells, CD8+ T cells, and CD4-CD8- (γδ) T cells had the highest fold change in pSTAT4 (i.e. $\frac{pSTAT4\ MFI\ IL{-}12\ stimulated}{pSTAT4\ MFI\ unstimulated}$), with medians of 2.31 (IQR: 2.04-2.75), 1.71 (IQR: 1.33-2.19) and 1.95 (IQR: 1.41-2.74) respectively. According to Dunn's multiple comparisons, fold changes in pSTAT1 did not differ significantly between the various cell subsets ($p>0.05$). Fold changes in pSTAT4 also showed no significant differences between the monocyte and lymphocyte subsets, although the fold change in CD56+ NK cells were significantly higher compared to CD4+ T cells ($p=0.0047$) and CD20+ B cells ($p=0.0011$).

Descriptive statistics for fold changes in pSTAT1 and pSTAT4 for controls in various cell subsets can be found in Table 4.4. Box-and-whisker plots in Figures 4.8 and 4.9 show the distribution of the receptor expression data from the controls for CD119 and CD212 respectively. PBMCs were stimulated with IFN-γ (100 ng/mL) prior to pSTAT1 detection. For the detection of pSTAT4, PBMCs were pre-stimulated for 16-18 hours with PHA (5 µg/mL), followed by stimulation with IL-12 (100 ng/mL), as described in section 3.2.5.

**Table 4.4: Descriptive statistics of fold changes in pSTAT1 (i.e. IFN-γ signalling) and pSTAT4 (i.e. IL-12 signalling) for controls on various cell subsets**. Fold change in pSTAT = $\frac{MFI\ cytokine\ stimulated}{MFI\ unstimulated}$. The IQR of the control data was used as the 'normal' range against which patient data could be compared.

| | **Fold change in pSTAT1** Median (IQR) | **Fold change in pSTAT4** Median (IQR) |
|---|---|---|
| **FSC vs. SSC Monocytes** | 1.29 (0.97 – 1.75) | 1.81 (1.53 – 2.07) |
| **CD14+ Monocytes** | 1.60 (1.39 – 2.05) | 1.94 (1.38 – 2.12) |
| **FSC vs. SSC Lymphocytes** | 1.58 (1.16 – 1.86) | 1.51 (1.19 – 1.58) |
| **CD56+ (NK) cells** | 1.16 (0.89 – 1.34) | 2.31 (2.04 – 2.75) |
| **CD3+CD56+ (NKT) cells** | 1.51 (1.17 – 1.83) | 1.52 (1.23 – 1.73) |
| **CD3 (T) Cells** | 1.60 (1.20 – 1.98) | 1.47 (1.20 – 1.65) |
| **CD4+ T cells (Helper T cells)** | 1.53 (1.23 – 2.10) | 1.36 (1.18 – 1.46) |
| **CD8+ T cells (Cytotoxic T cells)** | 1.55 (1.17 – 1.82) | 1.71 (1.33 – 2.19) |
| **CD4-CD8- T cells (primarily γδ T cells)** | 1.42 (0.96 – 2.33) | 1.95 (1.41 – 2.74) |
| **CD20+ (B) cells** | 1.63 (1.28 – 1.81) | 1.24 (0.98 – 1.53) |

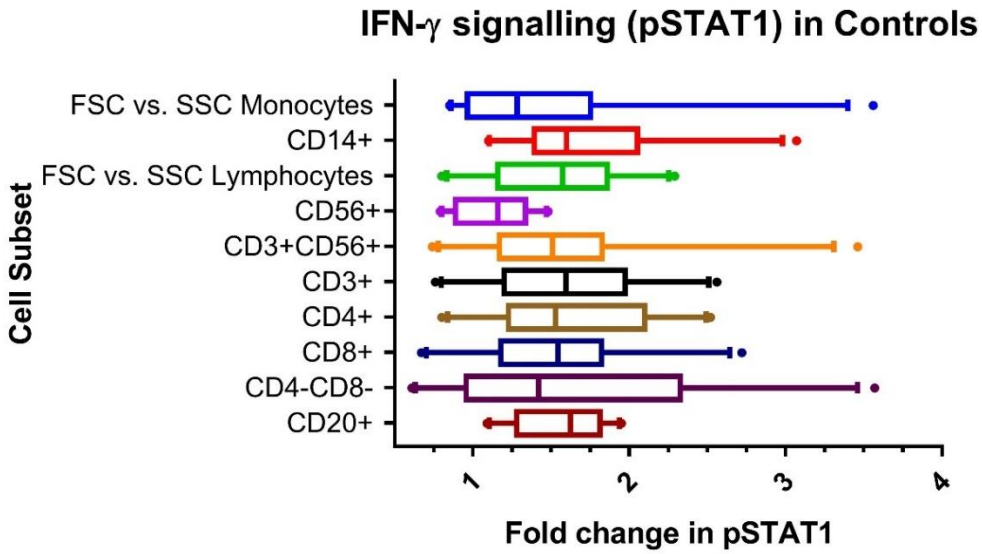


**Figure 4.8: Box-and-whiskers plot showing the distribution of fold changes in pSTAT1 (i.e. IFN-γ signalling) in various cell subsets for controls (n=10).** Fold change in pSTAT1 was highest for CD14+ monocytes and CD20+ (B) cells, although it was not much lower for other lymphocyte subsets. The box-and-whisker plot shows the 10$^{th}$ to 90$^{th}$ percentile of the data. The rectangular part of the box-plot represents the IQR of the data, with the line in the middle representing the median. Outliers are shown as dots.

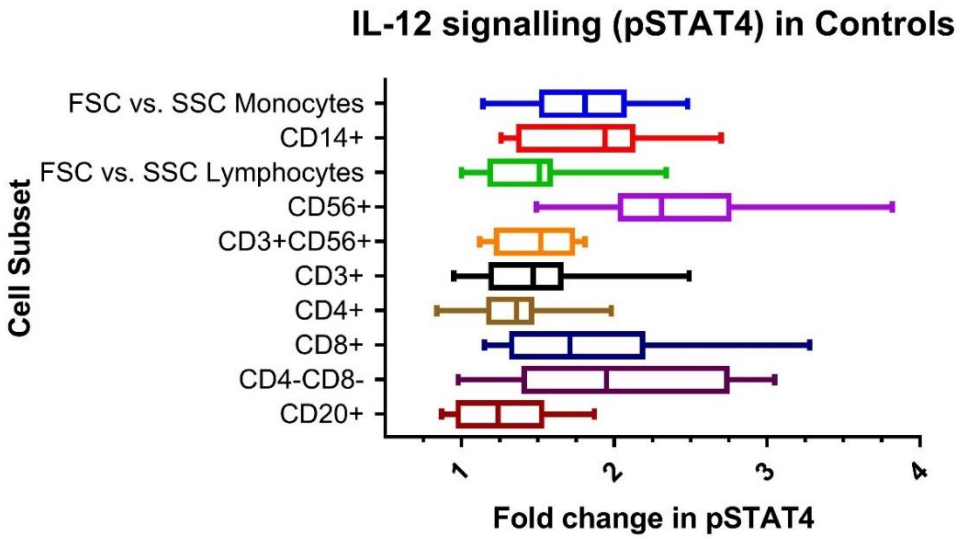


**Figure 4.9: Box-and-whiskers plot showing the distribution of fold changes in pSTAT4 (i.e. IL-12 signalling) in various cell subsets for controls (n=10)**. Fold change in pSTAT4 was highest in CD56+ (NK), CD8+ T cells and CD4-CD8- (γδ) T cells. The box-and-whisker plot shows the 10$^{th}$ to 90$^{th}$ percentile of the data. The rectangular part of the box-plot represents the IQR of the data, with the line in the middle representing the median. Outliers are shown as dots.

### Correlation between cytokine receptor expression and phosphorylation of the receptor-associated signalling molecule

There was a significant positive correlation between IL12Rβ1 expression and fold changes in pSTAT4 (p=0.0097; r = 0.3048). There was, however, no correlation between IFN-γR1 expression levels and fold changes in pSTAT1 (p=0.4; r=0.08108). Figure 4.10A and 4.10B show the correlation of receptor expression and signalling.

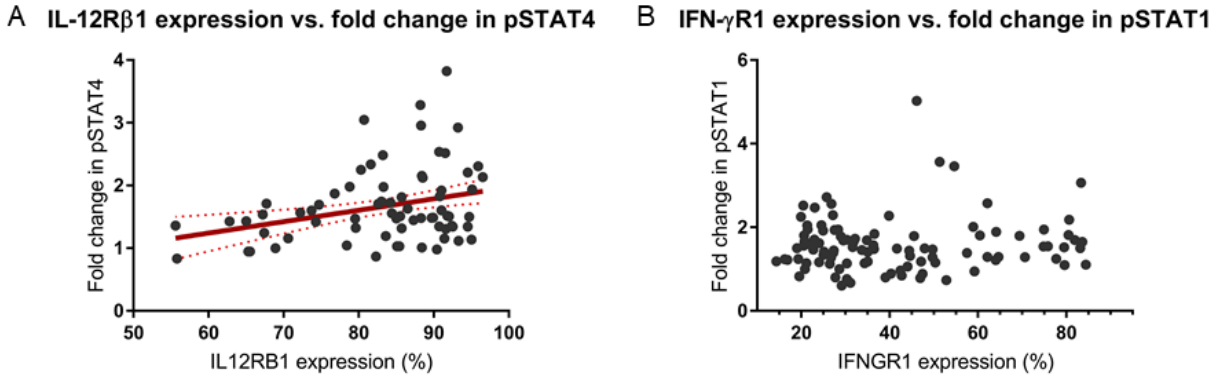


**Figure 4.10: Scatter plots showing correlations of receptor expression and fold change in pSTAT.** A. IL12Rβ1 expression levels correlated with fold changes in pSTAT4 detection (p=0.0079; r=0.3048). The red line through the plot is a linear regression line with error bars (dotted lines). B. There was no correlation between IFNGR1 expression and fold changes in pSTAT1 detection (p=0.4; r=0.8108).

## Cytokine Release Assay

### *Cytokine-induced cytokine production*

Stimulation of PBMCs with PHA only resulted in IFN-γ production (median: 167.50 pg/mL per $10^5$ cells; IQR: 57.03-658.20 pg/mL), with very little to no IL-12 production (median: 0.26 pg/mL per $10^5$

cells; IQR: 0.13-1.69 pg/mL). Co-stimulation with IL-12 resulted in significantly higher levels of IFN-γ production (median: 506.00 pg/mL per $10^5$ cells; IQR: 454.40-692.90 pg/mL; p=0.0004; Figure 4.11A) and similarly, co-stimulation with IFN-γ significantly enhanced IL-12 production (median: 17.79 pg/mL per $10^5$ cells; IQR: 11.22-19.42 pg/mL; p<0.0001; Figure 4.11B). Descriptive statistics for the induced-cytokine production assays can be found in Table 4.5.

**Table 4.5: Descriptive statistics for the cytokine-induced cytokine production assays for the controls**. The IQR of the control data was used as the 'normal' range against which patient data could be compared.

| **IFN-γ production assay:** | | **IL-12 production assay:** | |
|---|---|---|---|
| | **IFN-γ production (pg/mL)** Median (IQR) | | **IL-12 production (pg/mL)** Median (IQR) |
| PHA | 167.50 (57.03 – 658.20) | PHA | 0.26 (0.13 – 1.69) |
| PHA + IL-12 | 506.00 (454.40 – 692.90) | PHA + IFN-γ | 17.79 (11.22 – 19.42) |
| Net IL-12-induced IFN-γ production | 390.00 (176.10 – 443.60) | Net IFN-γ-induced IL-12 production | 17.06 (11.08 – 18.02) |

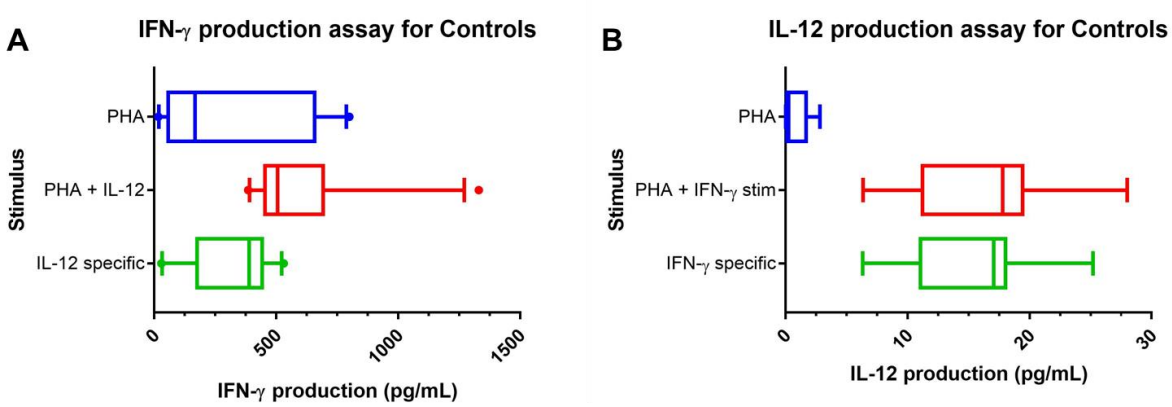


**Figure 4.11: Box-and-whisker plot showing the distribution of the data for the cytokine production assays for the controls (n=10).** A. IFN-γ production following stimulation with PHA or PHA and IL-12. IL-12 co-stimulation significantly increased IFN-γ production (p=0.0004); B.IL-12 production following stimulation with PHA or PHA and IFN-γ. IFN-γ significantly enhanced IL-12 production (p<0.0001). The box-and-whisker plot shows the 10th to 90th percentile of the data. The rectangular part of the box-plot represents the IQR of the data, with the line in the middle representing the median. Outliers are shown as dots.

### *Baseline IFN-γ levels*

The baseline IFN-γ levels present in the blood plasma of controls were all below the minimum detectable concentration of 15.6 pg/mL. Therefore, any detectable IFN-γ in plasma of patient samples could be considered abnormal.

## 4.3.2. Patient assay results

Although a wide range of plausible disease-causing variants were found in the patient group, all suspected MSMD patients' functional data was grouped and compared to the control group in order to determine whether any generalized differences could be observed.

When assessing the full cohort of suspected MSMD patients as a group (n = 19; 17 patients plus 2 family members) as compared to controls (n = 10), CD119 expression was essentially similar, however the patients had larger ranges of expression (Figure 4.12A). As with CD119, CD212 expression was similar overall for controls and patients, with patients again showing larger ranges for expression (Figure 4.12B). Dunn's multiple comparison tests revealed that there were no significant differences between patient and control receptor expression on any of the various cell subsets assessed (with $p \geq 0.5$ for most subsets). The difference in CD212 percentage expression between patients and controls on the CD4-CD8- (γδ) T lymphocyte subset was approaching significance ($p=0.0753$).

Fold changes in pSTATs were similar overall for patients and controls, although the patient group had much larger ranges. Dunn's multiple comparison tests revealed that there was no difference between the controls and patients for both pSTAT1 and pSTAT4 fold changes in any of the various cell subsets. Box-and-whiskers plots comparing the fold change in pSTAT in controls and patients can be found in Figure 4.13.

There were no significant differences in IL-12-induced IFN-γ production or IFN-γ-induced IL-12 production between controls and patients ($p = 0.7950$ and $p = 0.5087$ respectively). There are, however, several patients that fall outside of the 'normal' IQR of the controls, which can be clearly observed in Figure 4.14. There appears to be clustering of high and low IL-12 producing sub-groups in the patient cohort.

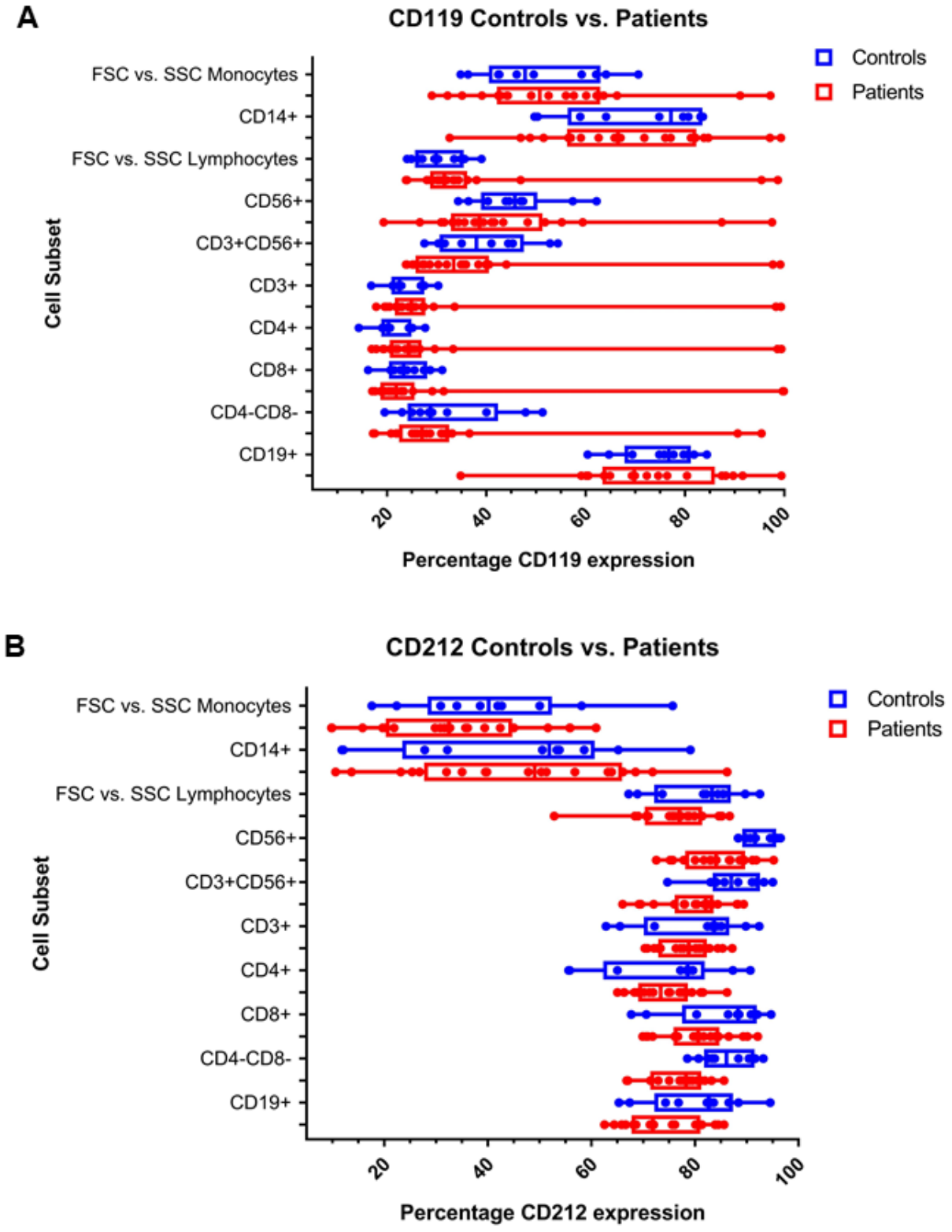


**Figure 4.12: Comparison of distribution of cytokine receptor expression levels for controls and patients**. A. CD119, i.e. IFN-γR1, percentage expression on unstimulated PBMCs for controls and patients on various cell subsets; B. CD212, i.e. IL-12Rβ1, percentage expression on PHA pre-stimulated PBMCs for controls and patients on various cell subsets. The box-and-whisker plot shows the 10$^{th}$ to 90$^{th}$ percentile of the data. The rectangular part of the box-plot represents the IQR of the data, with the line in the middle representing the median. Outliers are shown as dots.

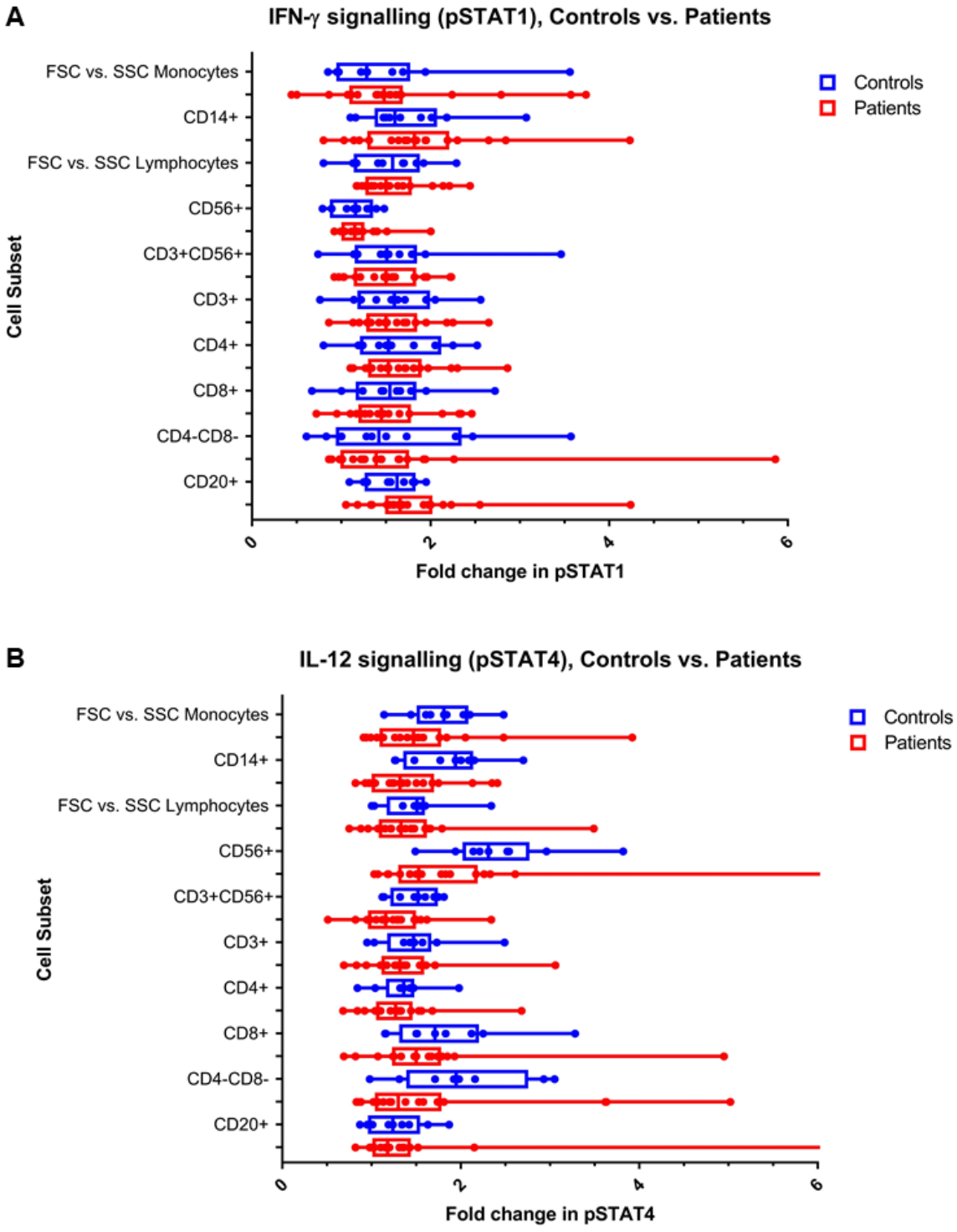


**Figure 4.13: Comparison of distribution of fold changes in pSTATs for controls and patients**. A. Fold change in pSTAT1, i.e. IFN-γ signalling, for controls and patients in various cell subsets. pSTAT1 was measured for both unstimulated and IFN-γ (100ng/mL) stimulated PBMCs; B. Fold change in pSTAT4, i.e. IL-12 signalling, for controls and patients in various cell subsets. pSTAT4 was measured on PHA pre-stimulated PBMCs that were then either left unstimulated or stimulated with IL-12 (100 ng/mL). The box-and-whisker plot shows the 10$^{th}$ to 90$^{th}$ percentile of the data. The rectangular part of the box-plot represents the IQR of the data, with the line in the middle representing the median. Outliers are shown as dots.

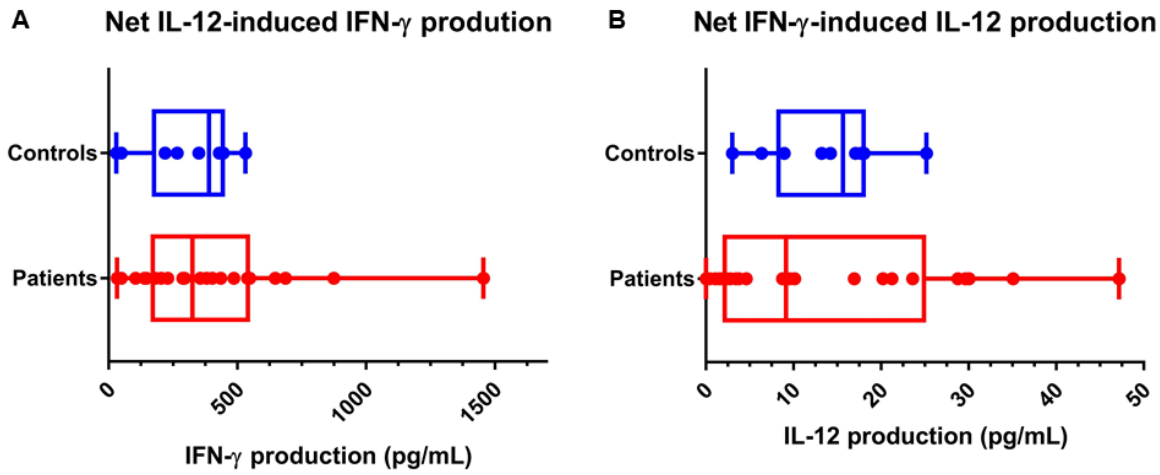


**Figure 4.14: Comparison of distribution of cytokine-induced cytokine production for controls and patients**. A. IL-12-induced IFN-γ production. The patient group has a larger range, with several patients falling outside the IQR of the control group; B. IFN-γ-induced IL-12 production. Several patients fall outside the control IQR, with an apparent clustering of high and low IL-12 producers. The box-and-whisker plot shows the $10^{th}$ to $90^{th}$ percentile of the data. The rectangular part of the box-plot represents the IQR of the data, with the line in the middle representing the median. Outliers are shown as dots.

## Case-by-case results

Composite data sets for IFN-γR1 and IL-12Rβ1 percentage positive and receptor density (MFI) expression, fold changes in pSTAT1 and pSTAT4 detection, as well as the IL-12-induced IFN-γ and IFN-γ-induced IL-12 production results for each patient can be found in Appendix E. A short summary of the functional data for the major cell subsets for each patient can be found in Table 4.6 on page 85.

### PID01 - *IFNGR1* (c.818del4)

PID01 had very high levels, above 95.40%, CD119 expression across all cell subsets. IFN-γR1 density was also very high across all cell subsets, with an MFI of 5451 on CD14+ monocytes and an MFI of 707 on CD19+ (B) cells, which is significantly higher than the controls. Contrastingly, fold change in pSTAT1 was lower than the normal ranges for CD14+ monocytes, as well as for various lymphocyte subsets including CD3+CD56+ (NKT) cells, total CD3+ T cells, CD4+, CD8+, CD4-CD8- (γδ) T cells and CD20+ (B) cells. This enhanced expression and decreased signalling was also observed for the patients' child. PID01 also had decreased CD212 percentage expression on CD56+ (NK), CD3+CD56+ (NKT) and CD4-CD8- T cells. Fold change in pSTAT4 was normal for most cell subsets although slightly increased on CD20+ (B) cells. PID01's child also displayed similar CD212 expression and signalling.

PID01 had normal levels of IFN-γ production in response to IL-12 stimulation, although there was no IL-12 produced in response to IFN-γ stimulation. The same cytokine responses were observed in PID01's child. A graphical summary of the functional results for PID01 and their child can be found in Figure 4.15.

A

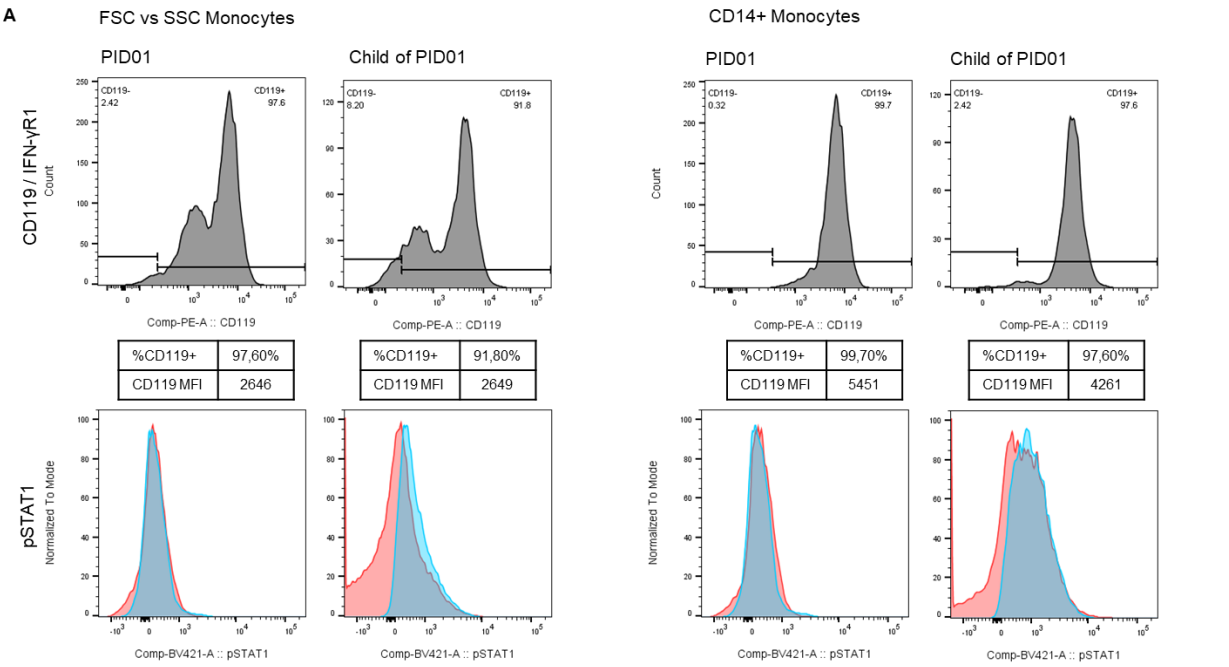


| Sample | MFI |
|---|---|
| Unstimulated | 232 |
| IFN-γ stimulated | 248 |
| Fold-change in pSTAT1: | **1,07** |

| Sample | MFI |
|---|---|
| Unstimulated | 550 |
| IFN-γ stimulated | 277 |
| Fold-change in pSTAT: | **0,50** |

| Sample | MFI |
|---|---|
| Unstimulated | 274 |
| IFN-γ stimulated | 329 |
| Fold-change in pSTAT1: | **1,20** |

| Sample | MFI |
|---|---|
| Unstimulated | 946 |
| IFN-γ stimulated | 758 |
| Fold-change in pSTAT1: | **0,80** |

B

| | IFN-γ production assay | | | | IL-12 production assay | | | |
|---|---|---|---|---|---|---|---|---|
| | NIL | PHA | PHA+IL-12 | Net IL-12-induced IFN-γ production | NIL | PHA | PHA+IFN-γ | Net IFN-γ-induced IL-12 production |
| PID01 | 0 pg/mL | 70,00 pg/mL | 425,40 pg/mL | 355,40 pg/mL | 0 pg/mL | 0,26 pg/mL | 0,69 pg/mL | 0,43 pg/mL |
| Child of PID01 | 0 pg/mL | 197,98 pg/mL | 343,70 pg/mL | 145,73 pg/mL | 0 pg/mL | 0,27 pg/mL | 2,06 pg/mL | 1,79 pg/mL |

**Figure 4.15: Summary of functional results for PID01 and their clinically unaffected child**. A. Very high levels of CD119 expression was observed across all cell subsets for both PID01 and their child (only FSC vs. SSC monocytes and CD14+ monocytes shown). Fold change in pSTAT1 was below the normal range for both PID01 and their child for CD14+ monocytes; B. There was very little to no IL-12 production induced by IFN-γ stimulation in both individuals.

## PID02 - *IFNGR1* (c.C864G) & *NOD2* (c.C374T)

PID02 had normal levels of CD119 and CD212 percentage expression for most cell subsets. CD119 was slightly below normal on CD56+ (NK) cells and slightly above the normal range on CD4+T cells and CD19+ (B) cells. Although PID02 had normal CD119 percentage expression on CD14+ monocytes, the receptor density was much higher than the controls (CD119 MFI: 1175). In contrast, the parent of PID02 with the same variant in *IFNGR1* had lower percentage CD119 expression on CD14+ monocytes compared to the patient, although receptor density was within the normal range (CD119 MFI: 702). PID02's fold change in pSTAT1 was below the normal range for CD14+ monocytes although it was within normal ranges their unaffected parent. pSTAT1 fold changes were higher in the unaffected parent compared to the patient for all cell subsets.

PID02 and their parent both had normal levels of CD212 expression, although they showed lower than normal fold changes in pSTAT4 in CD56+ (NK) cells.

PID02 and their unaffected parent both produced higher than normal levels of IFN-γ in response to IL-12 stimulation, with PID02's IFN-γ production being approximately 2.5 times higher than their unaffected parent (1451.80 pg/mL per $10^5$ IFN-γ produced by PID02 vs 538.96 pg/mL per $10^5$ IFN-γ produced by unaffected parent). IL-12 production in response to IFN-γ stimulation was within normal ranges. A graphical summary of the functional results for PID02 and their unaffected parent can be found in Figure 4.16.

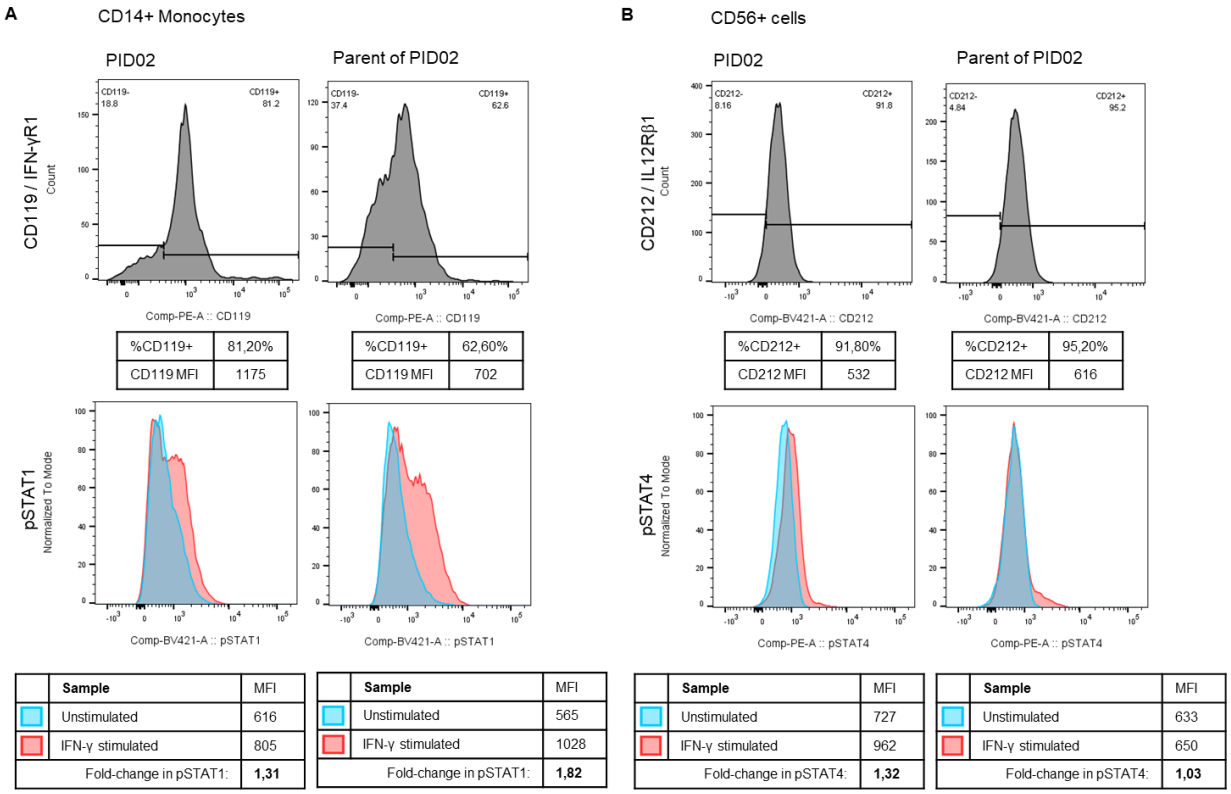


| Sample | MFI |
|---|---|
| Unstimulated | 616 |
| IFN-γ stimulated | 805 |
| Fold-change in pSTAT1: | **1,31** |

| Sample | MFI |
|---|---|
| Unstimulated | 565 |
| IFN-γ stimulated | 1028 |
| Fold-change in pSTAT1: | **1,82** |

| Sample | MFI |
|---|---|
| Unstimulated | 727 |
| IFN-γ stimulated | 962 |
| Fold-change in pSTAT4: | **1,32** |

| Sample | MFI |
|---|---|
| Unstimulated | 633 |
| IFN-γ stimulated | 650 |
| Fold-change in pSTAT4: | **1,03** |

C

| | IFN-γ production assay | | | | IL-12 production assay | | | |
|---|---|---|---|---|---|---|---|---|
| | NIL | PHA | PHA+IL-12 | Net IL-12-induced IFN-γ production | NIL | PHA | PHA+IFN-γ | Net IFN-γ-induced IL-12 production |
| PID02 | 0 pg/mL | 57,48 pg/mL | 1512,29 pg/mL | 1454,80 pg/mL | 0 pg/mL | 0,90 pg/mL | 22,14 pg/mL | 21,24 pg/mL |
| Parent of PID02 | 0 pg/mL | 57,18 pg/mL | 596,14 pg/mL | 538,96 pg/mL | 0 pg/mL | 0,38 pg/mL | 9,95 pg/mL | 9,57 pg/mL |

**Figure 4.16: Summary of functional results for PID02 and their clinically unaffected parent**. A. CD119 expression and fold changes in pSTAT1 for CD14+ monocytes were within the normal ranges, although there was a difference between parent and child for both receptor expression (CD119 expression is lower in the unaffected parent) and signalling (fold change in pSTAT1 is higher for the unaffected parent). B. CD212 expression was normal for both PID02 and their parent, and fold changes in pSTAT4 was below normal in CD56+ (NK) cells for both individuals. C. IFN-γ overproduction in response to IL-12 stimulation was observed for both PID02 and their parent. IL-12 production was normal.

## **PID03** - *IKZF1* (c.G1009A) & *IFNGR1* (c.C698T)

PID03 had lower than normal CD119 percentage expression on CD14+ Monocytes (51.5%), although the receptor density was higher than normal on the same subset (CD119 MFI: 588). Fold changes in pSTAT1 was within the normal range for all cell subsets.

CD212 expression for PID03 was low on CD14+ monocytes (23.2%; MFI: 1198), CD56+ (NK) cells (84.1%; MFI: 448), CD3+CD56+ (NKT) cells (83.0%; MFI: 373), and CD4-CD8- T cells (78.3%;

MFI: 252). Fold changes in pSTAT4 were lower than the normal ranges for all subsets except for CD8+ T cells and CD20+ (B) cells, which was normal.

PID03 produced higher than normal concentrations of levels of IL-12 in response to PHA stimulation and the net IFN-γ-induced IL-12 production levels were also elevated. IFN-γ production in response to IL-12 stimulation was slightly lower than the normal control ranges. A graphical summary of the functional results for PID03 can be found in Figure 4.17.

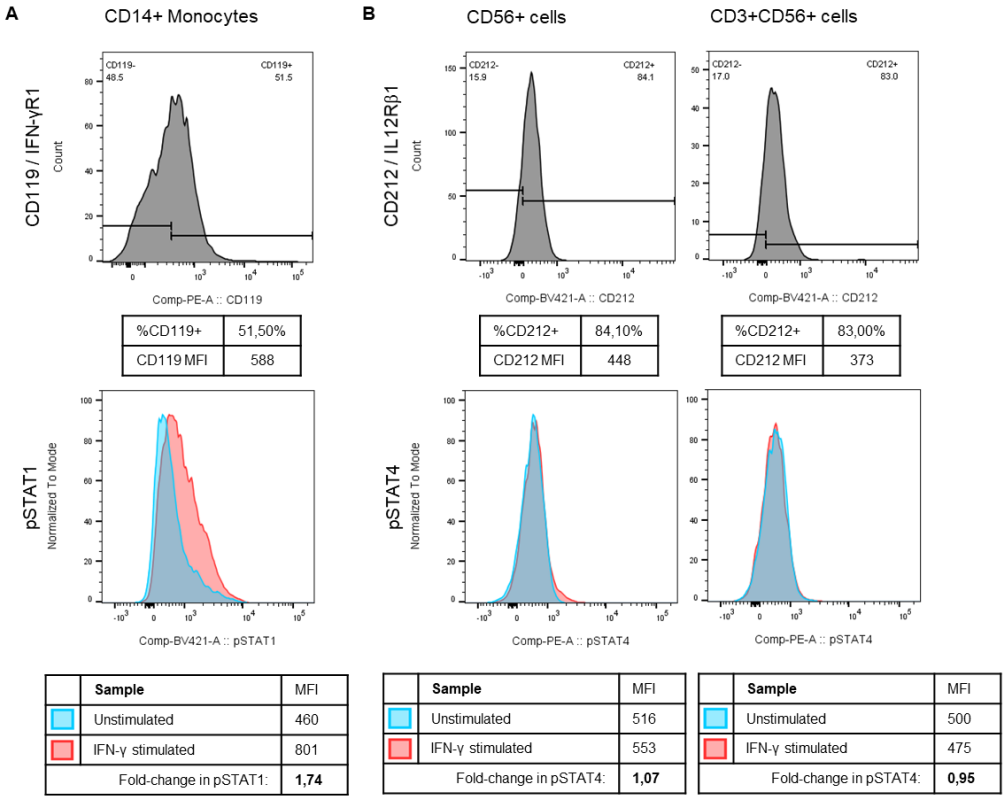


C

| IFN-γ production assay | | | | IL-12 production assay | | | |
|---|---|---|---|---|---|---|---|
| NIL | PHA | PHA+IL-12 | Net IL-12-induced IFN-γ production | NIL | PHA | PHA+IFN-γ | Net IFN-γ-induced IL-12 production |
| 0 pg/mL | 480,56 pg/mL | 619,99 pg/mL | 139,43 pg/mL | 0 pg/mL | 18,63 pg/mL | 38,83 pg/mL | 20,20 pg/mL |

**Figure 4.17: Summary of functional results for PID03**. A. CD119 expression was lower than normal on CD14+ monocytes, although the fold change in pSTAT1 was within the normal range; B. CD212 expression was low on CD56+ (NK) cells and CD3+CD56+ (NKT) cells, and pSTAT4 fold changes were also below the normal range for both subsets; C. Higher than normal levels of and IL-12 was produced upon PHA stimulation and IFN-γ co-stimulation. The net IL-12-induced IFN-γ production was slightly below the normal range.

## PID04 - *IL12RB1* (c.G684C)

PID04 had normal levels of CD119 percentage expression on most cell subsets, although the receptor density was very high on CD14+ monocytes (CD119 MFI: 917). Fold changes in pSTAT1 were much higher than normal for CD14+ monocytes, CD56+ (NK) cells and CD20+ (B) cells.

PID04 had decreased expression of CD212 on all lymphocyte subsets, except for CD4+ T cells, which was normal. IL12Rβ1 receptor density was also decreased for all lymphocyte subsets but CD4+ T cells. In contrast to the reduced CD212 expression, fold changes in pSTAT4 were very high

for all lymphocyte subsets. pSTAT4 fold changes were highest in CD56+ (NK) cells (9.21), CD8+ T cells (4.95), CD4-CD8- T cells (3.62), and CD20+ (B) cells (14.14).

PID04 had higher than normal levels of IL-12-induced IFN-γ production (546.91 pg/mL per $10^5$ cells) and IFN-γ-induced IL-12 production (35.06 pg/mL per $10^5$ cells). IFN-γ production in response to PHA stimulation was below the normal range (15.85 pg/mL per $10^5$ cells). A graphical summary of the functional results for PID04 can be found in Figure 4.18.

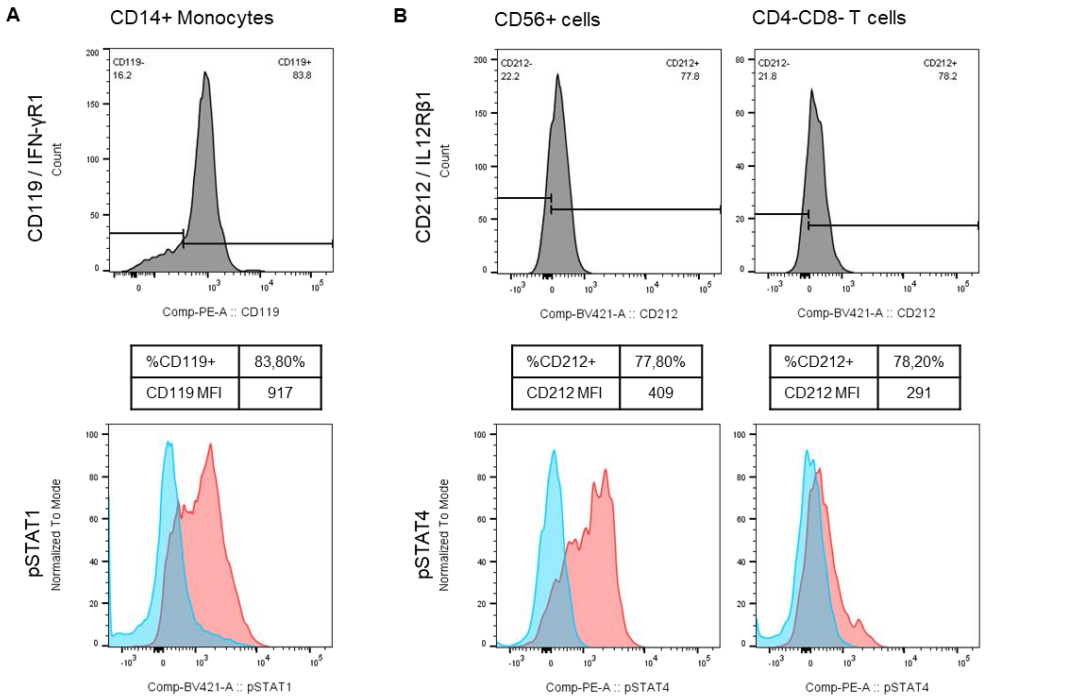


C

| IFN-γ production assay | | | | IL-12 production assay | | | |
|---|---|---|---|---|---|---|---|
| NIL | PHA | PHA+IL-12 | Net IL-12-induced IFN-γ production | NIL | PHA | PHA+IFN-γ | Net IFN-γ-induced IL-12 production |
| 0 pg/mL | 15,85 pg/mL | 562,76 pg/mL | 546,91 pg/mL | 0 pg/mL | 1,84 pg/mL | 36,90 pg/mL | 35,06 pg/mL |

**Figure 4.18: Summary of functional results for PID04**. A. Percentage CD119 expression was normal on CD14+ monocytes, although CD119 density (MFI) was higher than for the controls. Fold change in pSTAT1 was much higher than normal in CD14+ monocytes; B. CD212 expression was decreased on CD56+ (NK) and CD4-CD8- (γδ) T cells, although contrastingly, pSTAT4 fold changes were much higher than normal; C. IFN-γ production in response to PHA only was lower than normal, however, IL-12-induced IFN-γ production was higher than normal. IFN-γ-induced IL-12 production was also higher than normal.

## **PID05** - *IL12RB1* (c.C139T)

PID05 had decreased percentage CD119 expression on CD14+ monocytes (46.9%), CD56+ (NK) cells (30.9%), CD3+CD56+ (NKT) cells (27.1%), total CD3+ (19.5%), CD4+ (17.8%) and CD8+ T cells (17.6%), however, the overall receptor density was higher than the normal controls (CD119 MFI: 704, 67, 146, 122, 103, and 151 respectively). Fold changes in pSTAT1 were slightly elevated in CD56+ (NK) cells, total CD3+, CD4+ and CD8+ T cell subsets compared to the controls.

PID05 had very low levels of CD212 percentage expression and receptor density on CD56+ (NK) cells (72.5%; MFI: 395), CD3+CD56+ (NKT) cells (66.0%; MFI: 245), CD8+ T cells (70.9%; MFI: 195), CD4-CD8- T cells (66.8%; MFI: 171), and CD19+ (B) cells (71.5%; MFI: 182). Fold changes in pSTAT4 were decreased in nearly all cell subsets, with the lowest response being in CD56+ (NK) cells (1.19), CD3+CD56+ (NKT) cells (0.98), and CD20+ (B) cells (0.82).

PID05 had very high levels of IFN-γ production in response to IL-12 stimulation (686.56 pg/mL per $10^5$ cells) and very little IL-12 production in response to IFN-γ stimulation (2.28 pg/mL per $10^5$ cells). A graphical summary of the functional results for PID05 can be found in Figure 4.19.

**PID06 - *IL12B* (c.A320G) & *NFKB2* (c.C2042T)**

CD119 percentage expression was normal on all cell subsets for PID06, although the receptor density was elevated for most cell subsets (e.g. CD14+ monocytes CD119 MFI: 820). Fold change in pSTAT1 was higher than normal for CD20+ (B) cells (2.55), but within the normal range for all other subsets. PID06 had lower than normal levels of CD212 percentage expression and receptor density on CD56+ (NK) cells (84.1%; MFI: 471), CD3+CD56+ (NKT) cells (78.0%; MFI: 362), CD4-CD8- T cells (72.9%; MFI: 228), and CD19+ (B) cells (71.3%; MFI: 195). pSTAT4 fold changes were normal for all cell subsets.

PID06 had lower than normal IFN-γ production in response to IL-12 stimulation (48.56 pg/mL per $10^5$ cells), as well as essentially no IL-12 produced in response to IFN-γ stimulation (1.07 pg/mL per $10^5$ cells). Interestingly, PID06 had higher than normal IFN-γ levels (11.54 pg/mL per $10^5$ cells) in the unstimulated well of the cytokine assay, although there was no IFN-γ detected in the blood plasma indicating in vitro culture-induced production.

A

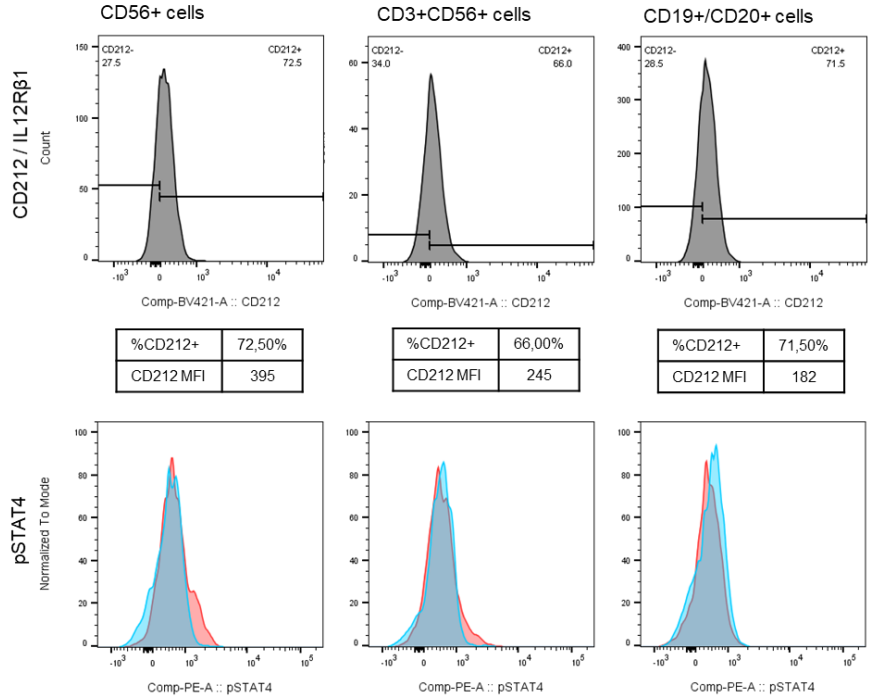


| | |
|---|---|
| %CD212+ | 72,50% |
| CD212 MFI | 395 |

| | |
|---|---|
| %CD212+ | 66,00% |
| CD212 MFI | 245 |

| | |
|---|---|
| %CD212+ | 71,50% |
| CD212 MFI | 182 |

| Sample | MFI |
|---|---|
| Unstimulated | 519 |
| IFN-γ stimulated | 617 |
| Fold-change in pSTAT4: | **1,19** |

| Sample | MFI |
|---|---|
| Unstimulated | 524 |
| IFN-γ stimulated | 513 |
| Fold-change in pSTAT4: | **0,98** |

| Sample | MFI |
|---|---|
| Unstimulated | 500 |
| IFN-γ stimulated | 412 |
| Fold-change in pSTAT4: | **0,82** |

B

| IFN-γ production assay | | | | IL-12 production assay | | | |
|---|---|---|---|---|---|---|---|
| NIL | PHA | PHA+IL-12 | Net IL-12-induced IFN-γ production | NIL | PHA | PHA+IFN-γ | Net IFN-γ-induced IL-12 production |
| 0 pg/mL | 68,75 pg/mL | 755,31 pg/mL | 686,56 pg/mL | 0 pg/mL | 0,19 pg/mL | 2,47 pg/mL | 2,28 pg/mL |

**Figure 4.19: Summary of functional results for PID05**. A. CD212 expression was lower than normal on CD56+ (NK), CD3+CD56+ (NKT) and CD19+ (B) cells. Fold changes in pSTAT4 were also below the normal ranges for these subsets. B. IFN-γ production in response to IL-12 stimulation was higher than normal, and IFN-γ-induced IL-12 production was lower than normal.

## **PID07** - ***IL12B*** **(c.G863C)**

PID07 had lower than normal levels of CD119 percentage expression, with variable receptor density on CD56+ (NK) cells (31.5%; MFI: 39.4), CD3+CD56+ (NKT) cells (28.6%; MFI: 117), CD8+ T cells (19.0%; MFI: 128) and CD19+ (B) cells (60.5%; MFI: 94.10). Fold change in pSTAT1 was only slightly higher than the normal ranges in CD14+ monocytes (2.19) and CD3+CD56+ (NKT) cells (1.96). Additionally, PID07 also had decreased levels of CD212 percentage expression, but normal receptor densities on CD56+ (NK) cells (86.6%), CD3+CD56+ (NKT) cells (82.4%), CD4-CD8- T cells (80.4%), and CD19+ (B) cells (71.8%). Fold changes in pSTAT4 were elevated in CD14+ monocytes (2.35), CD4+ T cells (1.53), and CD4-CD8- T cells (5.02).

PID07 produced normal levels of IFN-γ in response to IL-12 stimulation (294.42 pg/mL per $10^5$ cells), although the IFN-γ produced in response to PHA stimulation alone was below the normal range (5.49 pg/mL per $10^5$ cells). There was very little IL-12 production induced upon IFN-γ stimulation (4.61 pg/mL per $10^5$ cells). A graphical summary of the functional results for PID07 can be found in Figure 4.20.

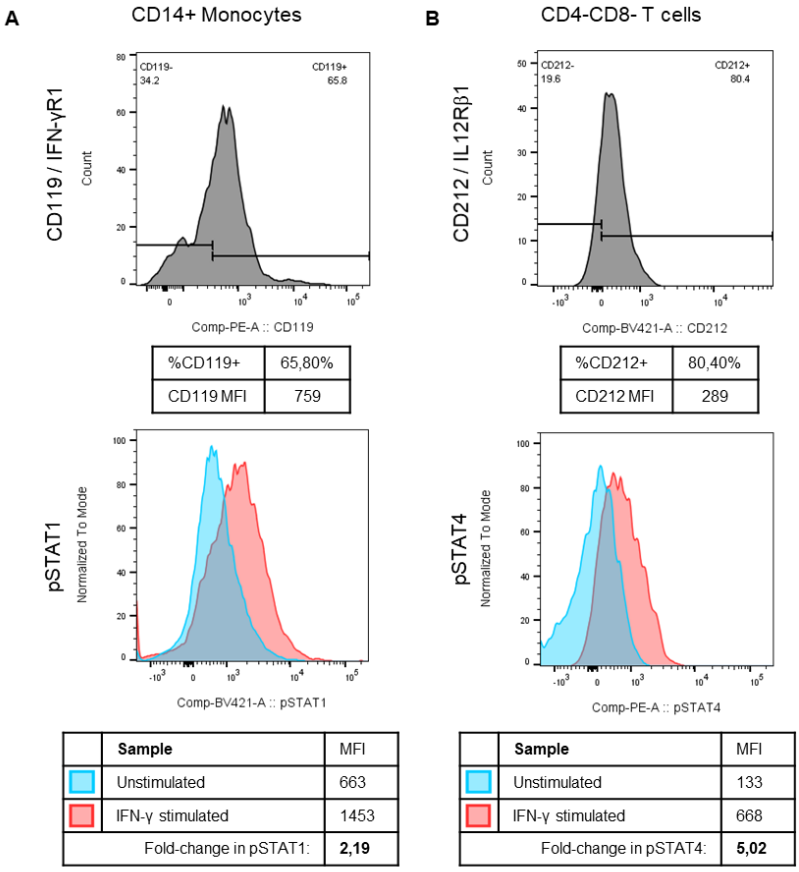


C

| IFN-γ production assay | | | | IL-12 production assay | | | |
|---|---|---|---|---|---|---|---|
| NIL | PHA | PHA+IL-12 | Net IL-12-induced IFN-γ production | NIL | PHA | PHA+IFN-γ | Net IFN-γ-induced IL-12 production |
| 0 pg/mL | 5,49 pg/mL | 299,91 pg/mL | 294,42 pg/mL | 0 pg/mL | 0,21 pg/mL | 4,81 pg/mL | 4,61 pg/mL |

**Figure 4.20: Summary of functional results for PID07.** A. CD119 expression was normal on CD14+ monocytes, although fold change in pSTAT1 was slightly elevated; B. CD212 percentage expression was slightly decreased on CD4-CD8- T cells, and the fold changes in pSTAT4 were higher than the controls; C. IFN-γ production in response to IL-12 stimulation was within the normal range, while IFN-γ-induced IL-12 production was lower than normal.

## **PID08** - *IFNGR2* (c.A708T)

Although the detection of IFN-γR2 (as opposed to IFN-γR1) was not part of the current study, CD119 (IFN-γR1) expression was found to be decreased on CD14+ monocytes (56.5%; MFI: 536) and CD3+CD56+ (NKT) cells (25.8%; MFI: 144). CD119 receptor density was elevated on all lymphocyte subsets. CD119 percentage expression was slightly elevated only on CD56+ and CD19+ (B) cells in this patient, and normal on other subsets. Fold changes in pSTAT1 was low for CD14+ monocytes (1.03). PID08 had decreased CD212 expression on CD56+ (NK) cells (80.0%; MFI: 430), CD3+CD56+ (NKT) cells (83.3%; MFI: 423), and CD19+ (B) cells (72.0%; MFI: 186). Decreased fold changes in pSTAT4 detection was observed on CD56+ (NK) cells (1.51) and CD3+CD56+ (NKT) cells (1.12) compared to the controls.

PID08 had very low levels of IFN-γ production in response to IL-12 stimulation (25.55 pg/mL per $10^5$ cells), as well as very little IL-12 production in response to IFN-γ stimulation (3.44 pg/mL per $10^5$ cells). PID08 was the only patient that had detectable levels of IFN-γ present in their blood plasma

(18.59 pg/mL) which relates to the high baseline IFN-γ production seen in the unstimulated well for the cytokine assay (10.31 pg/mL per $10^5$ cells). A graphical summary of the functional results for PID08 can be found in Figure 4.21.

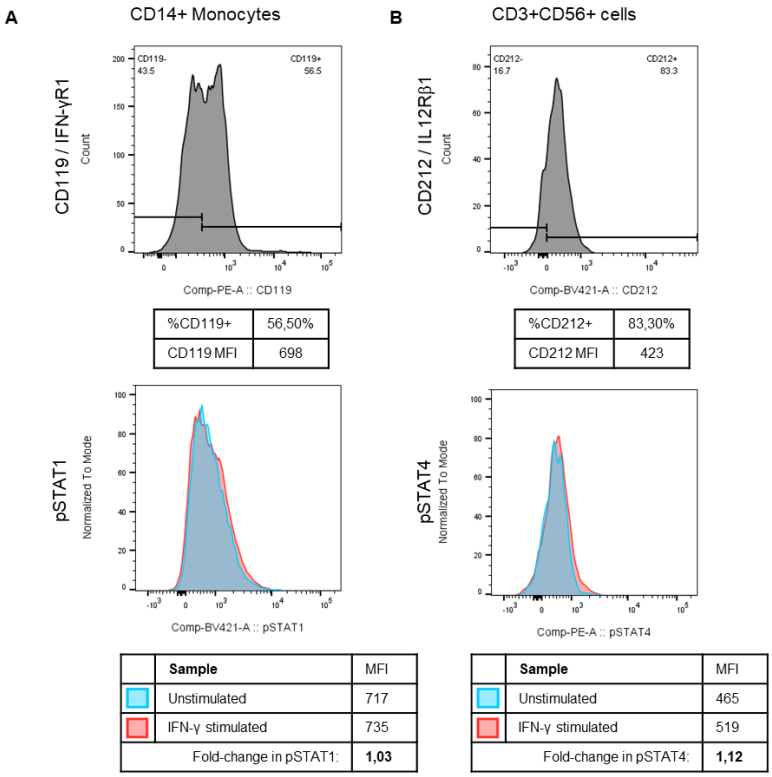


C

| IFN-γ production assay | | | | IFN-γ levels in plasma | IL-12 production assay | | | |
|---|---|---|---|---|---|---|---|---|
| NIL | PHA | PHA+IL-12 | Net IL-12-induced IFN-γ production | | NIL | PHA | PHA+IFN-γ | Net IFN-γ-induced IL-12 production |
| 10,31 pg/mL | 0 pg/mL | 25,55 pg/mL | 25,55 pg/mL | 18,59 pg/mL | 0 pg/mL | 0,27 pg/mL | 3,72 pg/mL | 3,44 pg/mL |

**Figure 4.21: Summary of functional results for PID08**. A. CD119 expression was decreased on CD14+ monocytes, and the fold change in pSTAT1 was also below the normal range; B. CD212 expression on CD3+CD56+ (NKT) cells was decreased, and the fold change in pSTAT4 was also lower than normal; C. IL-12-induced IFN-γ production was lower than normal. There was also very little IL-12 production upon IFN-γ stimulation. PID08 was the only participant that had detectable levels of IFN-γ present in their blood plasma.

## **PID09** - *CYBB* (c. A302G)

PID09 had normal CD119 expression levels on most cell subsets, although it was slightly higher than normal on total CD3+ T cells (27.4%; MFI: 86.4), CD4+ T cells (25.1%; MFI: 82.1), and CD8+ T cells (29.1%; MFI: 115). Fold changes in pSTAT1 was also normal on all subsets except for CD20+ (B) cells, which was higher than normal (2.23). CD212 expression was slightly decreased on CD3+CD56+ (NKT) cells (80.4%; MFI: 395) and CD4-CD8- T cells (78.9%; MFI: 301) for PID09. Fold changes in pSTAT4 were decreased in all cell subsets except for CD20+ (B) cells.

PID09 produced higher than normal levels of both IFN-γ (646.85 pg/mL per $10^5$ cells) and IL-12 (47.19 pg/mL per $10^5$ cells) in response to IL-12 and IFN-γ stimulation, respectively. IFN-γ production in the unstimulated (NIL) well was also high (47.72 pg/mL per $10^5$ cells), although no IFN-γ was detected in the blood plasma.

**PID10 - *IKBKB* (c.G2257A) & *NFKB2* (c.C2042T)**

PID10 had higher expression levels of CD119 on CD14+ monocytes (84.7%; MFI: 827), and pSTAT1 fold change was also higher than normal for this subset (2.19) as well as in CD20+ (B) cells (2.00). PID10 had decreased CD212 expression on CD56+ (NK) cells (83.1%; MFI: 470), CD3+CD56+ (NKT) cells (80.0%; MFI: 401), CD4-CD8- T cells (77.0%: MFI: 285), and CD19+ (B) cells (68.1%; MFI: 170). Fold changes in pSTAT4 was lower than normal for CD56+ (NK) cells (1.43), CD3+CD56+ (NKT) cells (1.15), and CD4-CD8- T cells (1.22).

PID10 produced normal levels of IFN-γ (379.97 pg/mL per $10^5$ cells) in response to IL-12 stimulation, although the IFN-γ production in response to PHA only was lower than the normal range (19.57 pg/mL per $10^5$ cells). There was very little to no IL-12 production (1.54 pg/mL per $10^5$ cells) in response to IFN-γ stimulation.

**PID11 - *IRAK1* (c.C1939T)**

PID11 had slightly lower CD119 percentage expression on CD56+ (NK) cells (37.9%), CD3+CD56+ (NKT) cells (25.4%), total CD3+ T cells (20.5 %), CD8+ T cells (18.7%), and CD19+ (B) cells (63.7%), although CD119 receptor densities on these cell subsets were within the normal ranges. Fold changes in pSTAT1 were moderately increased on CD14+ monocytes (2.30), CD3+CD56+ (NKT) cells (2.22), total CD3+ T cells (2.25), CD4+ T cells (2.30), and CD8+ T cells (2.34). PID11 had slightly increased CD212 expression on CD14+ monocytes (86.2%; MFI: 3000), but slightly decreased expression on CD4-CD8- T cells (81.0%; MFI: 302) and CD19+ (B) cells (68.30%; MFI: 136). Fold changes in pSTAT4 were normal for all cell subsets. PID11 had normal IFN-γ production (229.16 pg/mL per $10^5$ cells) in response to IL-12 stimulation. IL-12 production (10.12 pg/mL per $10^5$ cells) in response to IFN-γ stimulation was, however, slightly below normal levels.

**PID12 - No result from WES**

CD119 expression was higher than normal on total CD3+ T cells (27.2%; MFI: 120) and CD19+ (B) cells (87.4%; MFI: 168) for PID12, and CD119 receptor density was decreased on CD14+ monocytes (MFI: 519). Fold change in pSTAT1 was higher than normal in CD20+ (B) cells (1.92), although normal in all other cell subsets. PID12 had decreased CD212 expression on CD56+ (NK) cells (86.8%; MFI: 544), CD3+CD56+ (NKT) cells (82.7%; MFI: 417), and CD4-CD8- T cells (79.5%; MFI: 262). Fold changes in pSTAT4 were decreased in CD14+ monocytes (1.02), CD3+CD56+ (NKT) cells (0.95), total CD3+ (0.83), CD4+ (0.84), CD8+ (0.82), and CD4-CD8- T cells (0.85).

PID12 had lower than normal IFN-γ production (103.39 pg/mL per $10^5$ cells) in response to IL-12 stimulation. The IL-12 production (29.26 pg/mL per $10^5$ cells) in response to IFN-γ stimulation was

higher than normal. A graphical summary of the functional results for PID12 can be found in Figure 4.22.

A

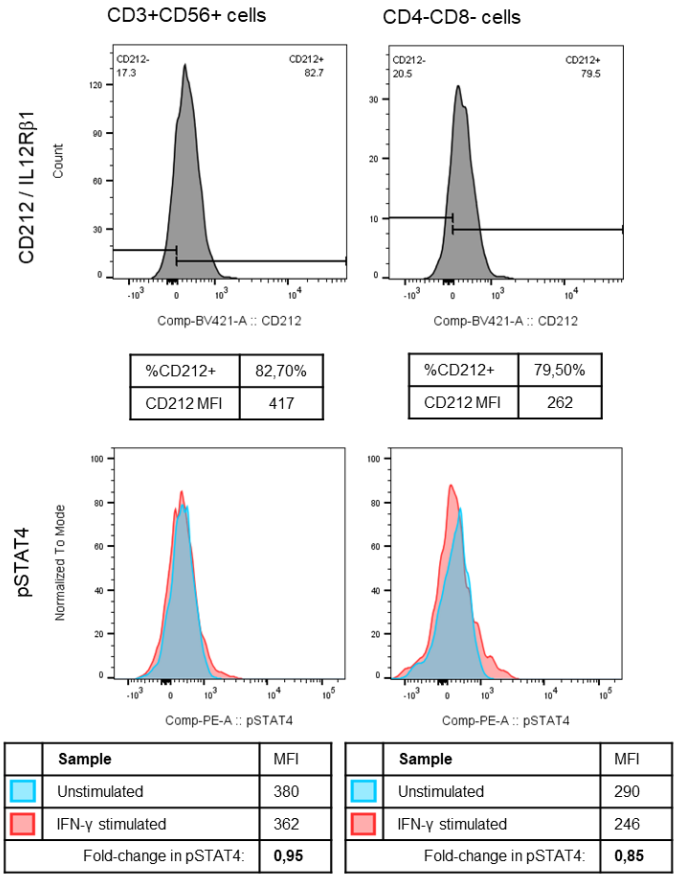


| | |
|---|---|
| %CD212+ | 82,70% |
| CD212 MFI | 417 |

| | |
|---|---|
| %CD212+ | 79,50% |
| CD212 MFI | 262 |

| | Sample | MFI |
|---|---|---|
| | Unstimulated | 380 |
| | IFN-γ stimulated | 362 |
| | Fold-change in pSTAT4: | **0,95** |

| | Sample | MFI |
|---|---|---|
| | Unstimulated | 290 |
| | IFN-γ stimulated | 246 |
| | Fold-change in pSTAT4: | **0,85** |

B

| IFN-γ production assay | | | | IL-12 production assay | | | |
|---|---|---|---|---|---|---|---|
| NIL | PHA | PHA+IL-12 | Net IL-12-induced IFN-γ production | NIL | PHA | PHA+IFN-γ | Net IFN-γ-induced IL-12 production |
| 0 pg/mL | 2,09 pg/mL | 106,02 pg/mL | 103,93 pg/mL | 0 pg/mL | 0,87 pg/mL | 30,49 pg/mL | 29,62 pg/mL |

**Figure 4.22: Summary of functional results for PID12.** A. CD212 expression was lower than normal on CD3+CD56+ (NKT) and CD4-CD8- (γδ) T cells. Fold changes in pSTAT4 was below the normal ranges for CD3+CD56+ (NKT) and CD4-CD8- (γδ) T cells; B. IL-12-induced IFN-γ production was lower than normal, and IFN-γ-induced IL-12 production was higher than normal.

## PID13 - WES not performed

For PID13, CD119 expression was low on CD14+ monocytes (32.6%; MFI: 394), CD56+ (NK) cells (37.6%; MFI: 46.8), and CD19+ (B) cells (59.1%; MFI: 84.4). Fold changes in pSTAT1 were normal for all cell subsets. CD212 expression was low on CD56+ (NK) cells (81.7%; MFI: 459), CD3+CD56+ (NKT) cells (69.2%; MFI:282), CD8+ T cells (69.9%; MFI:190), CD4-CD8- T cells (67.0%; MFI:190), and CD19+ (B) cells (64.4%; MFI:153). Fold changes in pSTAT4 were decreased in CD56+ (NK) cells (1.53), but normal in other cell subsets.

PID13 had slightly higher than normal levels of both IL-12-induced IFN-γ production (485.86 pg/mL per $10^5$ cells) and IFN-γ-induced IL-12 production (23.61 pg/mL per $10^5$ cells).

## PID14 - WES not performed

PID14 had decreased CD119 expression on CD14+ monocytes (48.8%; MFI: 563) and CD56+ (NK) cells (35.6%; MFI: 40.60), although fold changes in pSTAT1 were normal for all cell subsets. PID14 had low levels of CD212 expression on nearly all cell subsets, including CD14+ monocytes (10.6%; MFI: 943), CD56+ (NK) cells (75.7%; MFI: 445), CD3+CD56+ (NKT) cells (72.0%; MFI: 296), CD8+ (70.5%; MFI: 203), CD4-CD8- T cells (66.8%; MFI: 184) and CD19+ (B) cells (65.8%; MFI: 154). Fold changes in pSTAT4 were decreased for all non-B lymphocyte subsets, i.e. CD56+ (NK) cells (1.88), CD3+CD56+ (NKT) cells (0.82), total CD3+ (0.69), CD4+ (0.68), CD8+(0.69), and CD4-CD8- T cells (0.83). Fold changes in pSTAT4 were normal for monocytes and CD20+ (B) cells

PID14 had normal IFN-γ production (203.47 pg/mL per $10^5$ cells) in response to IL-12 stimulation. There was very little IL-12 production (2.75 pg/mL per $10^5$ cells) in response to IFN-γ stimulation. A graphical summary of the functional results for PID14 can be found in Figure 4.23.

A

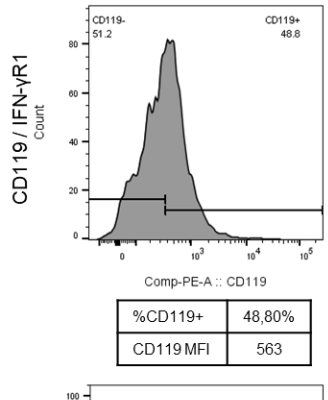


| | |
|---|---|
| %CD119+ | 48,80% |
| CD119 MFI | 563 |

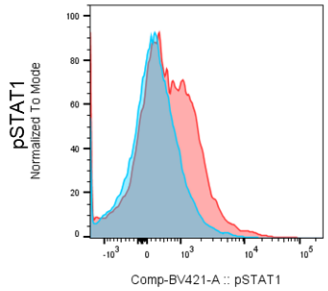


| | Sample | MFI |
|---|---|---|
| | Unstimulated | 333 |
| | IFN-γ stimulated | 646 |
| | Fold-change in pSTAT1: | **1,94** |

B

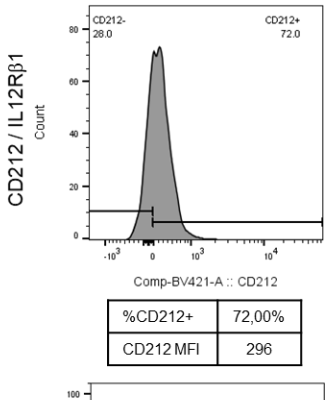


| | |
|---|---|
| %CD212+ | 72,00% |
| CD212 MFI | 296 |

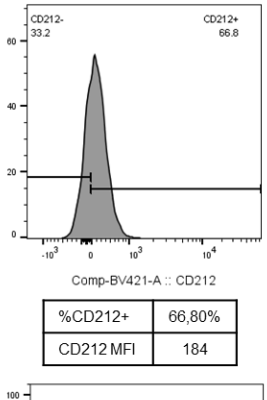


| | |
|---|---|
| %CD212+ | 66,80% |
| CD212 MFI | 184 |

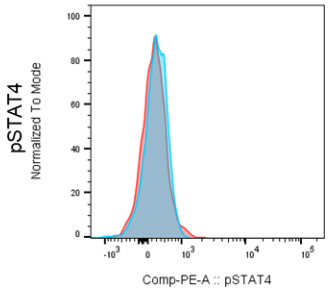


| | Sample | MFI |
|---|---|---|
| | Unstimulated | 308 |
| | IFN-γ stimulated | 252 |
| | Fold-change in pSTAT4: | **0,82** |

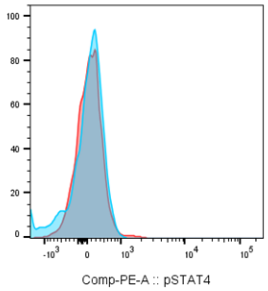


| | Sample | MFI |
|---|---|---|
| | Unstimulated | 192 |
| | IFN-γ stimulated | 160 |
| | Fold-change in pSTAT4: | **0,83** |

C

| IFN-γ production assay | | | | IL-12 production assay | | | |
|---|---|---|---|---|---|---|---|
| NIL | PHA | PHA+IL-12 | Net IL-12-induced IFN-γ production | NIL | PHA | PHA+IFN-γ | Net IFN-γ-induced IL-12 production |
| 0 pg/mL | 12,32 pg/mL | 215,79 pg/mL | 203,47 pg/mL | 0 pg/mL | 0,04 pg/mL | 2,79 pg/mL | 2,75 pg/mL |

**Figure 4.23: Summary of functional results for PID14**. A. CD119 expression was decreased on CD14+ monocytes, although the fold change in pSTAT1 was within the normal range. B. CD212 expression was decreased on CD3+CD56+ (NKT) cells and CD4-CD8- (γδ) T cells and the fold changes in pSTAT4 for these subsets were also below the normal ranges. C. IL-12-induced IFN-γ production was within the normal range, although there was very little IL-12 production in response to IFN-γ stimulation.

**PID15 - WES not performed**

PID15 had lower than normal levels of CD119 percentage expression on CD56+ (NK) cells (33.2%), CD3+ (19.9%), CD8+ (18.9%) and CD4-CD8- T cells (17.2%), although the receptor densities were normal on these cells. The CD119 receptor density was higher than normal on CD14+ monocytes (MFI: 917) even though the percentage of CD119 positive monocytes were within the normal range. The fold changes in pSTAT1 were higher than normal in CD14+ monocytes (2.84), CD3+CD56+ (NKT) cells (1.93), total CD3+ (2.65), CD4+ (2.86), and CD8+ cells (2.46).

CD212 expression was lower than normal on CD56+ (NK) cells (75.2%; MFI: 479), CD4-CD8- T cells (67.0%; MFI: 217) and CD19+ (B) cells (62.5%; MFI: 165). Fold changes in pSTAT4 were decreased in CD14+ monocytes (0.97) and CD56+ (NK) cells (1.56) although it was increased in CD4-CD8- T cells (3.63).

PID15 produced higher than normal levels of IFN-γ (873.90 pg/mL per $10^5$ cells) in response to IL-12 stimulation even though the IFN-γ production in response to PHA only was below the normal ranges (27.92 pg/mL per $10^5$ cells). IL-12 production (16.92 pg/mL per $10^5$ cells) in response to IFN-γ stimulation was normal.

**PID16 - WES not performed**

PID16 had below normal percentage expression of CD119 on CD56+ (NK) cells (19.3%) and CD3+ (17.8%), CD4+ (16.9%), CD8+ (17.0%) and CD4-CD8- (17.5%) T cells, although fold changes in pSTAT1 were normal for all these subsets. The fold change in pSTAT1 for CD14+ monocytes (1.14) was lower than the normal range. Expression of CD212 was slightly elevated on CD14+ monocytes (68.5%; MFI: 2200) and CD8+ T cells (92.1%; MFI: 516). Fold changes in pSTAT4 were below normal for all cell subsets (see Appendix E).

IFN-γ production (402.02 pg/mL per $10^5$ cells) in response to IL-12 stimulation was normal for PID16, however, IL-12 production (28.77 pg/mL per $10^5$ cells) in response to IFN-γ stimulation was higher than normal. A graphical summary of the functional results for PID16 can be found in Figure 4.24.

A

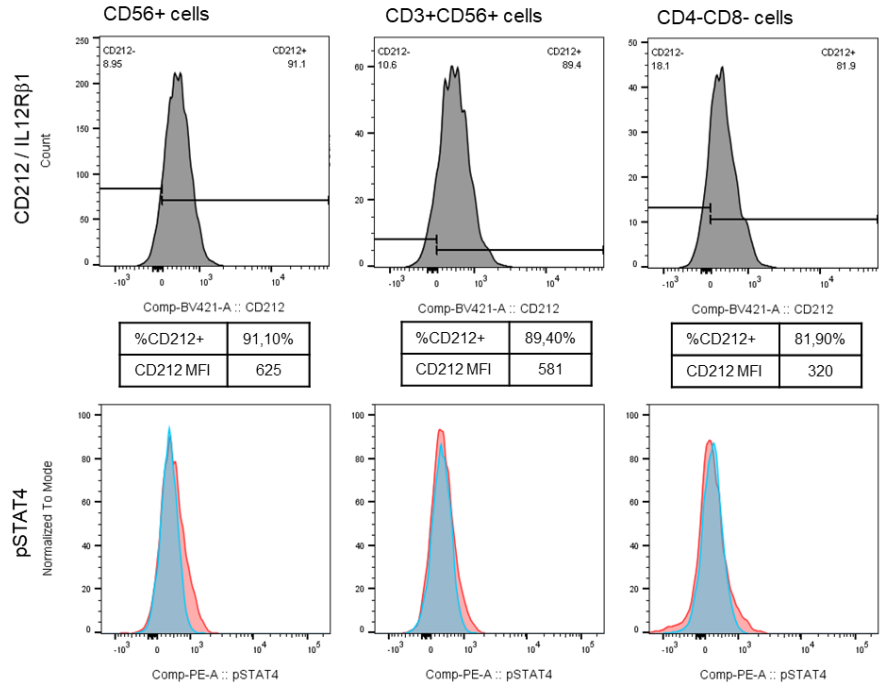


| | |
|---|---|
| %CD212+ | 91,10% |
| CD212 MFI | 625 |

| | |
|---|---|
| %CD212+ | 89,40% |
| CD212 MFI | 581 |

| | |
|---|---|
| %CD212+ | 81,90% |
| CD212 MFI | 320 |

| Sample | MFI |
|---|---|
| Unstimulated | 387 |
| IFN-γ stimulated | 457 |
| Fold-change in pSTAT4: | **1,18** |

| Sample | MFI |
|---|---|
| Unstimulated | 354 |
| IFN-γ stimulated | 371 |
| Fold-change in pSTAT4: | **1,05** |

| Sample | MFI |
|---|---|
| Unstimulated | 273 |
| IFN-γ stimulated | 241 |
| Fold-change in pSTAT4: | **0,88** |

B

| IFN-γ production assay | | | | IL-12 production assay | | | |
|---|---|---|---|---|---|---|---|
| NIL | PHA | PHA+IL-12 | Net IL-12-induced IFN-γ production | NIL | PHA | PHA+IFN-γ | Net IFN-γ-induced IL-12 production |
| 0 pg/mL | 23,09 pg/mL | 425,11 pg/mL | 402,02 pg/mL | 0 pg/mL | 0,41 pg/mL | 29,18 pg/mL | 28,77 pg/mL |

**Figure 4.24: Summary of functional results for PID16**. A. CD212 expression was normal for all cell subsets, however, the fold changes in pSTAT1 detection was below normal for nearly all subsets [CD56+ (NK) cells, CD3+CD56+ (NKT) cells and CD4-CD8- (γδ) T cells shown]; B. IFN-γ production was normal, however IFN-γ-induced IL-12 production was higher than normal.

## PID17 - WES not performed

CD119 expression was slightly lower than control ranges on CD3+CD56+ (NKT) cells (23.8%; MFI: 77.8) and CD19+ (B) cells (60.1%; MFI: 85.4) for PID17. Fold changes in pSTAT1 were slightly lower than normal in CD3+CD56+ (NKT) cells (0.97) but elevated in CD14+ monocytes (2.65) and CD4-CD8- T cells (5.86). CD212 percentage expression was low in all lymphocyte subsets except CD4+ T cells. CD212 receptor densities were also lower than the normal ranges for all lymphocyte subsets. Fold changes in pSTAT4 were decreased in CD14+ monocytes (1.23), CD56+ (NK) cells (1.43), CD3+CD56+ (NKT) cells (0.51), CD4+ T cells (1.09), and CD4-CD8- T cells (0.57).

PID17 had normal IFN-γ production (288.80 pg/mL per $10^5$ cells) in response to IL-12, although IL-12 production (8.74 pg/mL per $10^5$ cells) in response to IFN-γ stimulation was lower than normal. A graphical summary of the functional results for PID17 can be found in Figure 4.25.

A

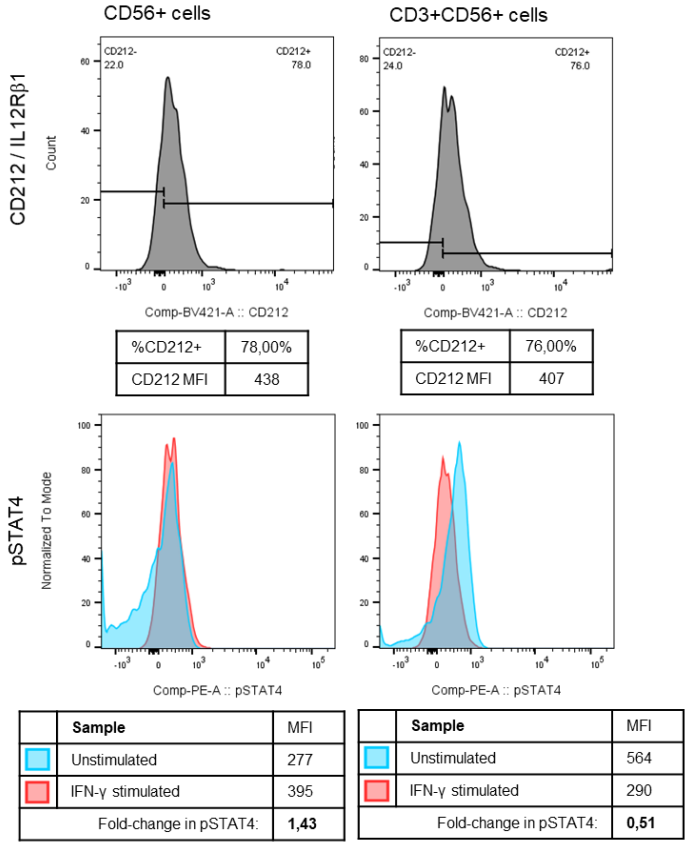


| | |
|---|---|
| %CD212+ | 78,00% |
| CD212 MFI | 438 |

| | |
|---|---|
| %CD212+ | 76,00% |
| CD212 MFI | 407 |

| | Sample | MFI |
|---|---|---|
| | Unstimulated | 277 |
| | IFN-γ stimulated | 395 |
| | Fold-change in pSTAT4: | **1,43** |

| | Sample | MFI |
|---|---|---|
| | Unstimulated | 564 |
| | IFN-γ stimulated | 290 |
| | Fold-change in pSTAT4: | **0,51** |

B

| IFN-γ production assay | | | | IL-12 production assay | | | |
|---|---|---|---|---|---|---|---|
| NIL | PHA | PHA+IL-12 | Net IL-12-induced IFN-γ production | NIL | PHA | PHA+IFN-γ | Net IFN-γ-induced IL-12 production |
| 0 pg/mL | 24,03 pg/mL | 312,83 pg/mL | 288,80 pg/mL | 0 pg/mL | 0,24 pg/mL | 8,98 pg/mL | 8,74 pg/mL |

**Figure 4.25: Summary of functional results for PID17**. A. CD212 expression was decreased on CD56+ (NK) and CD3+CD56+ (NKT) cells, and the fold changes in pSTAT4 detection were also below the normal ranges in these cell subsets; B. IL-12-induced IFN-γ production was normal, however, IFN-γ-induced IL-12 production below the normal range for PID17.

**Table 4.6: Basic summary of functional results for all 17 patients**.

| Patient ID | Genetic Variant(s) | IFN-γR1 | IFN-γ signalling | IFN-γ-induced IL-12 production | IL-12Rβ1 | IL-12 signalling | IL-12-induced IFN-γ production | Baseline IFN-γ |
|---|---|---|---|---|---|---|---|---|
| PID01 | *IFNGR1* | +++ | - - | - - | - - | + | + | ND |
| Child of PID01 | *IFNGR1* | +++ | - - | - - | - | + | - | ND |
| PID02 | *IFNGR1 / NOD2* | + | - | ++ | + | - | +++ | ND |
| Parent of PID02 | *IFNGR1* | + | + | - | + | - | +++ | ND |
| PID03 | *IFNGR1 / IKZF1* | - | + | ++ | - - | - | - | ND |
| PID04 | *IL12RB1* | +++ | +++ | ++ | - - | +++ | +++ | ND |
| PID05 | *IL12RB1* | - - | + | - - | - - | - - | +++ | ND |
| PID06 | *IL12B / NFKB* | + | + | - - | - - | + | - | ND |
| PID07 | *IL12B* | + | ++ | - | - - | + | + | ND |
| PID08 | *IFNGR2* | - | - - | - - | - | + | - | +++ |
| PID09 | *CYBB* | + | + | +++ | + | - | +++ | ND |
| PID10 | *IKBKB / NFKB2* | +++ | ++ | - - | - - | - | + | ND |
| PID11 | *IRAK1* | + | ++ | - | - | + | + | ND |
| PID12 | No result | + | + | +++ | - | - | - | ND |
| PID13 | WES NP | - - | + | ++ | - - | - | ++ | ND |
| PID14 | WES NP | - - | + | - - | - - | - | + | ND |
| PID15 | WES NP | + | ++ | + | - - | + | +++ | ND |
| PID16 | WES NP | + | - | +++ | + | - - | + | ND |
| PID17 | WES NP | + | ++ | - - | - - | - - | + | ND |

This is an overall representation of the functional results for the major cell subsets. Results for IFN-γR1 expression and IFN-γ signalling in the table represent the CD14+ monocyte subset, while the CD56+ (NK) cells and CD4-CD8- (γδ) T cells are used as representatives for IL-12Rβ1 expression and IL-12 signalling results.

WES NP: WES Not Performed; ND: Not Detected

- - Significantly decreased (Patient values below 10$^{th}$ percentile of control values)
- Decreased (Patient values fall outside 'normal' IQR, but above 10$^{th}$ percentile)
+ Normal (Patient values within IQR of control data)
++ Elevated (Patient values fall outside 'normal' IQR, but below 90$^{th}$ percentile)
+++ Significantly elevated (Patient values above 90$^{th}$ percentile of control values)

# Chapter 5 Discussion

This chapter is presented in four sections. The first section (5.1) discusses the study participants and their genetic results. The second section (5.2) focusses discussion on the optimisation of the flow cytometric assays and the third section (5.3) discusses the results obtained for each of the respective functional assays. The final section (5.4) is an overarching discussion of the entire study.

## 5.1. Participants

### 5.1.1. Case Reports and Routine Laboratory Findings

Recurrent TB was the most common clinical presentation amongst the participants in this study. Two of the participants with suspected MSMD had a positive family history suggestive of PID, PID08 had a sibling that died in infancy and PID16 has a history of severe and recurrent TB on the paternal side of the family.

Most PID studies show a male gender predominance, due to X-linked disorders (Naidoo et al. 2010). Although some X-linked MSMD-associated genes have been described, there was no gender predominance in the current study, and only one of the patients, PID09, was found to have an X-linked PID (Bustamante et al. 2011).

All the participants were BCG vaccinated, but only one presented with likely BCGosis, which is one of the most common described presentations of MSMD. To date, BCGosis has not been as common in reported South African MSMD cases as compared to those in developed countries (Esser et al. 2016; Caragol and Casanova 2003). Seeing as various countries vaccinate with different strains of BCG, it is possible that the BCG strain (Danish 1331) used in South Africa is more attenuated or less virulent than those used in countries where TB is less prevalent. It has been previously described that BCG vaccination is not entirely effective at preventing TB infection, although it is still used routinely due to its ability to prevent severe TB and disseminated TB in children (World Health Organization 2017; Esser et al. 2015; Sasaki et al. 2002). In the current cohort of PID patients, it appears that the BCG vaccination had no protective effect as it did not prevent TB disease or even severe and disseminated TB in multiple cases.

Only 2 patients presented with non-tuberculous mycobacterial infections, namely PID01 and PID09. PID01 had concurrent pulmonary TB and disseminated *M.avium* infection, while PID09 had disseminated Mycobacterium complex infection, which was suspected to be BCG. Unfortunately, the routine laboratories were unable to culture and identify the causative Mycobacterium in PID09. Only 1 patient presenting with recurrent Salmonella infection, which is one of the most common described presentations in *IL12RB1* and *IL12B* deficiencies, was documented (Robinson 2015).

Negative QFT-plus results i.e. lack of IFN-γ production in response to TB antigens, in the 3 participants that had confirmed TB episodes (PID03, PID08 and PID12) are a clear indication that there is a defect related to IFN-γ production (i.e. in the IL-12-IFN-γ pathways) in response to TB antigenic stimulation. This shows that the routine QFT-plus TB diagnostic test is a useful tool to identify potential PID in patients with known TB.

### 5.1.2. Genetic Findings

WES in the combination with TAPER™ pipeline was very efficient in finding plausible disease-causing variants, with 8 of the participants having gene variants in known MSMD-associated genes identified. All but one of these variants, *IFNGR1* (c.818del4), are novel and have not been reported before.

The *IFNGR1* (c.818del4) variant is known to be a partial dominant disease-causing variant. Most described cases of 818del4 present with BCGosis or with *M.avium* infection (Wang et al. 2012). PID01 is the first patient described with this variant that also presented with 'regular' pulmonary TB (Glanzmann et al. 2018a). PID01's daughter was screened for the 818del4 variant when she was only 1 month old, and it was revealed that she also had the variant. The child is being closely monitored by her mother and physician for any signs of TB or *M.avium* infection. The early diagnosis of the young child may be beneficial in the long-term management of the condition.

The effect of the other novel variants in MSMD-associated genes are unknown, although they were all predicted to be pathogenic or likely pathogenic by various *in silico* prediction tools. It was expected, and to some extent confirmed in this study, that variants in *IFNGR1* or *IL12RB1* would impair the response to IFN-γ or IL-12, and variants in IL12B would lead to lack of IL-12 production as well as an overall lack of response to IFN-γ, similar to what has been described in other variants within the same genes (Bustamante et al. 2014). PID09 is the first patient with *CYBB* mutation, usually leading to CGD, that presented with mycobacterial disease in South Africa (Glanzmann et al. 2018b; Reed and Dolen 2018).

The other, non-MSMD associated variants identified could potentially also lead to the disease phenotype since these genes encode for proteins that are essential for the immune response against TB. For instance, *IKZF1* encodes for a zinc finger transcription factor, which plays an important role in lymphocyte development and differentiation (Boutboul et al. 2018; Cytlak et al. 2018; Bonilla et al. 2015). Therefore, it is possible that a defect in *IKZF1* could impact the ability of lymphocytes to respond to IL-12 or to produce IFN-γ. *NOD2* encodes for an important pattern recognition receptor, which is essential for the recognition *M.tb* and induction of IL-12 (Mishra et al. 2017; Naranbhai 2016). IRAK1, is an important part of the NF-κB pathway and is known to interact with the protein NEMO, which is a described MSMD-associated variant (Bustamante et al. 2019; Ghosh and Dass 2016). The proteins encoded by *IKBKB* and NFKB2 also interact with NEMO

(Boisson-dupuis et al. 2015). It is not known if or how these non-MSMD-associated variants would impact on the IL-12-IFN-γ cytokine pathways.

The genetic results for each patient will be further discussed in section 5.3, along with the respective functional data for each patient.

## 5.2. Optimisation of flow cytometric assays

### 5.2.1. Receptor panel

PHA stimulation upregulated expression of CD212. The upregulation was similar, although slightly to a lesser degree than what has previously been described by Esteve-Solé et al. (2018), Fieschi (2004), and Altare et al. (2001), where PBMCs were stimulated with both IL-2 and PHA. Although the 24-hour PHA stimulation without IL-2 stimulation in the current study was shorter than the stimulation in preciously published methods, it still allowed sufficient expression of CD212 for detection by flow cytometry, and also allows for faster processing time.

The effect of PHA stimulation on CD119 has not previously been described and was assessed in this study in order to determine whether both CD119 and CD212 expression on PBMCs could be measured simultaneously. PHA pre-stimulation for 24 hours appeared to significantly downregulate CD119 expression on monocytes, although expression started to increase again after 48 hours of PHA stimulation. PHA is a mitogen that acts on lymphocytes, and it is likely that upon the activation of the lymphocytes with PHA these lymphocytes secrete cytokines and other mediators which can alter the phenotype and activity of monocytes *in vitro*. Additionally, culturing of monocytes *in vitro* also leads to their differentiation into macrophages, which have a very different phenotype to circulating monocytes (Movafagh et al. 2011).

Based on the findings of this study, it is not advisable to assess both CD119 and CD212 expression simultaneously, due to the effect of PHA on CD119 expression. Therefore, for the optimal detection of CD212, PBMCs were pre-stimulated for 24 hours while additional PBMCs were left unstimulated for optimal detection of CD119.

### 5.2.2. Phosflow panel

The Phosflow protocol is much harsher on cells compared to regular surface staining protocols and this is evident by the loss of surface marker fluorescent signal observed when using either of the Perm buffers. Both the fixation and permeabilisation steps result in destruction of surface epitopes, which explains the decreased signals of the surface markers. Perm IV resulted in a lower loss-of-signal of surface markers compared to Perm III. Perm IV is a detergent-based buffer and is less harsh on the cells than the alcohol-based Perm III. It was initially assumed that Perm III would allow better pSTAT detection, due to its harsher, often more effective, permeabilisation capabilities.

However, it was found that Perm IV allows equivalent, if not slightly better, pSTAT1 and pSTAT4 detection in these conditions.

All of the cytokine stimulation concentrations tested in this study resulted in a similar signal, which differs from what has been described by other studies (Fieschi 2004; Uzel et al. 2001; Fleisher et al. 1999). Usually, different concentrations for stimulation results in different degrees of phosphorylation of STATs. Different permeabilisation methods and sample types were used in these other studies. For instance, both Uzel et al (2001) and Fleisher et al. (1999) used methanol to permeablise cells for pSTAT1 or pSTAT4 detection. Uzel et al. (2001) also used PBMC-derived PHA/IL-2 blast cells as opposed to regular, untreated PBMCs for pSTAT4 detection.

Stimulation of PBMCs with PHA prior to the Phosflow protocol allowed much better detection of pSTAT4, although once again these results are not equivalent to that of other studies, where PBMCs were co-cultured with PHA and IL-2 for 72 hours prior to the cytokine stimulation (Fieschi 2004; Uzel et al. 2001). Although the detection of pSTAT4 in this study was not perfectly aligned with that in other studies, the overall trends and outcomes of the assays were similar.

## 5.3. Implementation of the Assays

## 5.3.1. Controls

### Receptor Panel

CD119 expression was highest on monocytes, which was expected, since these cells are the main producers of IL-12 and are they are dependent on IFN-γ for induction of various functions (Lammas et al. 2000). CD119 expression was also present on most lymphocytes. IFN-γ is important for lymphocyte functions and plays roles in promoting NK cell activity, leukocyte migration and even enhances further differentiation of CD4+ T cells into IFN-γ producing Th1 cells (Bhat et al. 2017). CD119 percentage expression was high on B cells, similar percentage expression on monocytes, although the receptor density (MFI) on B cells were comparable to other lymphocytes. IFN-γR1 expression on B cells has not been well described before, and the role of IFN-γ in B cell function is not as well know but it is likely related to the induction or regulation of antibody production (Chan et al. 2014; Nimmerjahn and Ravetch 2008).

Percentage CD212, or IL-12Rβ1, expression was very high on all PHA pre-stimulated lymphocytes, likely due to the important role that IL-12 plays in lymphocyte differentiation and induction cytotoxic activity (Losana et al. 2002; Lammas et al. 2000). Percentage IL-12Rβ1 expression was highest in NK, NKT, CD8+ T cells and CD4-CD8- (γδ) T cells, likely to the inducible cytotoxic activity of these cells. These cytotoxic lymphocytes are also known to be the main producers of IFN-γ.

## Signalling Panel

The fold changes in pSTAT1 was highest in CD14+ monocytes and B cells, which agrees with the higher levels of CD119 (IFN-γR1) expression observed in these cells. Likewise, fold changes in pSTAT4 was highest in the lymphocytes with higher levels of CD212 (IL-12Rβ1) expression, especially NK cells and double negative / γδ T cells. Unlike receptor expression, the differences in pSTAT detection did not differ significantly between the various cell subsets. Due to the lack of difference in fold changes between the different cell subsets, it appears that a similar degree of 'signal' is transferred through the cytokine receptors, regardless of the levels of receptor expression.

IFN-γ signalling (fold change in pSTAT1) showed no correlation with the levels of IFN-γR1 expression. IL-12 signalling (fold change in pSTAT4) showed a positive correlation to the levels of IL-12Rβ1 expression, indicating that cells with higher levels of IL-12Rβ1 expression tend to have slightly enhanced IL-12 signalling. This could potentially explain why lymphocytes, which are more dependent of IL-12 for their function, and not monocytes have relatively high levels of IL-12Rβ1 expression.

## Cytokine Assay

### *Cytokine-induced cytokine production*

As expected, PHA induced a moderate amount of IFN-γ production, while co-stimulation with IL-12 enhanced the levels of IFN-γ production. Similarly, IL-12 was produced upon PHA and IFN-γ co-stimulation but not with PHA alone, which confirms the findings described by other authors (Dorman and Holland 1998). The results generated by this assay are comparable to other previously published experiments where PHA was used to activate PBMCs as well as to the 'gold standard' cytokine assay developed by Feinberg et al. (2004) for the study of the integrity of the IFN-γ pathway which uses BCG to activate the cells.

This cytokine assay can easily detect complete defects, but it is often difficult to identify partial defects in this manner. PHA co-stimulation has previously been shown to be less effective than BCG stimulation for the detection of partial deficiencies of *IFNGR1* or *IL12RB1*. This is due to the fact that PHA induces a 'general' type of immune response (mitogenic "global" T cell stimulation), unlike BCG, which induces a mycobacterial pathogen-specific immune response (Esteve-Solé et al. 2018).

Unlike the flow cytometry-based methods, the cytokine production is measured for total PBMCs and not for each of the relevant cell subsets. IL-12 is produced mainly by monocytes and DCs, which make up about 10% of total PBMCs, whereas the main producers of IFN-γ, T cells, make up about 60-70% of PBMCs. The ratios of IL-12 and IFN-γ producing cells in the PBMCs would be expected to impact on the levels of cytokines that were detected. The state of the immune cells, i.e. if anergic or exhausted or activated due to underlying conditions or active infections, would also impact on

cell responsiveness to stimulation. For future studies it may be beneficial to rather measure intracellular cytokine production after stimulation by means of flow cytometry. Alternatively, cell subsets can be separated, through fluorescent or magnetic cell sorting prior to stimulation and assay readout through ELISA.

#### *Baseline IFN-γ levels*

In healthy individuals, IFN-γ is undetectable in blood plasma. No IFN-γ was detected in the blood plasma of the laboratory volunteers, and for this reason any IFN-γ detected in the plasma in succeeding experiments was considered abnormal.

IFN-γ is usually only increased in patients with active infection or chronic inflammation, such as during HIV infection, although elevated IFN-γ in blood plasma has been described in various cases of IFN-γR deficiencies (Esteve-Solé et al. 2018; Fieschi et al. 2001). The increased IFN-γ present in plasma of patients with IFN-γR deficiencies is due to the accumulation of IFN-γ in the plasma as a result of the inability of IFN-γ to bind to its receptor or as a result of IFN-γ overproduction by the host's immune system. This latter phenomenon is an attempt to compensate for either low binding affinity of IFN-γ to its receptor or lack of signal transduction though the receptor.

## 5.3.2. Patients

Receptor expression, signalling through the receptor, and downstream cytokine production was not significantly different between the control group and the combined patient group. Although there were no significant differences, there was a lot more variation in the patient group compared to the controls with the patient group showing much larger ranges of receptor expression, signalling and cytokine production. In the IL-12 production assay, there appeared to be a clustering of distinct high and low IL-12 producers in the patient group, which was absent in the control group.

### Case-by-case patient results

#### *IFNGR1*

A well described heterozygous mutation in *IFNGR1* (c.818del4) was identified in PID01 and her infant daughter. The functional assays in this study, which revealed very high levels of IFN-γR1 expression on all cell subsets along with lack of signalling though the receptor as well as a lack of IL-12 production upon IFN-γ stimulation, were in agreement with what has previously been published on this specific variant. It has been well described that the 818del4 variant in *IFNGR1* results in high levels of non-functional IFN-γR1 expression on the surfaces of immune cells (Esteve-Solé et al. 2018). The non-functional IFN-γR is capable of binding IFN-γ but no signal is transduced through the receptor due to a lack of Janus Kinase (JAK1)/STAT1 binding sites in the intracellular domain of the IFN-γR. The 818del4 variant has been associated with *M.avium* infection but not with TB (Wang et al. 2012; Sasaki et al. 2002; Villella et al. 2001; Jouanguy et al. 1999). PID01 is the

first person with an 818del4 *IFNGR1* variant that presented with both pulmonary TB and *M.avium* infection. PID01 successfully cleared the TB infection on standard treatment, however her *M.avium* infection recurs whenever *M.avium* treatment is terminated. As a result, the patient has been placed on prophylactic treatment permanently. Early identification of this IFN-γR1 defect in PID01's daughter may prove to be beneficial in future management.

Novel heterozygous variants in both *IFNGR1* (c.C864G) and *NOD2* (c.C374T) were identified in PID02 and PID02's father had the same variant in *IFNGR1*. IFN-γ signalling was decreased in PID02 but not in her father, however IL-12 production was normal for both the patient and her father, indicating that the observed defect in IFN-γ signalling is potentially not as harmful as with the 818del4 variant in PID01. The overproduction of IFN-γ by both PID02 and her father could potentially be an immune compensatory mechanism, where the host is overproducing IFN-γ to compensate for lack of receptor expression or binding affinity or even signalling through the receptor. The *NOD2* variant, which encodes for a pattern recognition receptor belonging to the NOD-like family of receptors, might explain the decreased function in PID01 compared to her father. NOD receptors are important for activation of the NF-κB pathway, which in turn plays an important role in T cell development, maturation and proliferation (Pellegrini et al. 2018; Mishra et al. 2017; Ghosh and Dass 2016).

Two novel variants were identified in PID03, a heterozygous variant in *IFNGR1* (c.C698T) as well as a homozygous variant in *IKZF1* (c.G1009A). The decreased IFN-γ production observed agrees with the negative QFT-plus result that showed lack of IFN-γ production upon stimulation of immune cells with TB antigens. The lack of IL-12 receptor expression and signalling could possibly be explained by the *IKZF1* variant, which encodes for DNA-binding protein Ikaros, also known as Ikaros family zinc finger protein 1. *IKZF1* plays important roles in lymphocyte development and differentiation (Boutboul et al. 2018; Cytlak et al. 2018; Bonilla et al. 2015).

Variants in the same gene, *IFNGR1*, were identified in PID01, PID02, and PID03. Although these patients all had variants in the same gene, they had very different clinical presentation and functional immune profiles. This shows that it is important to always assess immune functionality *in vitro*, rather than assuming that variants within the same gene will lead to similar phenotypes. The novel *IFNGR1* variants in PID02 and PID03 may need to be further investigated in order to determine exactly how the variants affect IFN-γR1 expression and functionality. This may include further investigations such as ligand affinity binding assays as well as biochemical modelling to assess potential changes in protein structure induced by the variants.

***IL12RB1***

Plausible disease-causing mutations were identified in *IL12RB1* for both PID04 (c.G684C) and PID05 (c.C139T), although they had very different clinical presentations – Inflammatory bowel disease (IBD) phenotype and recurrent Salmonella infection in PID04 versus recurrent pulmonary

TB in PID05. PID05 had decreased IL-12Rβ1 expression and decreased IL-12 signalling, similar to what has been described in other non-complete defects in *IL12RB1* (Fieschi 2004). The cytokine production assay results for PID05 were contradictory, and not in agreement with previously described *IL12RB1* variants, with IFN-γ-induced IL-12 production being very low, whilst IL-12-induced IFN-γ production was higher than controls (Esteve-Solé et al. 2018; Fieschi 2004). The contradictory cytokine production results could be due to the fact that the cytokine assays are PBMC based rather than immune cell subset based. The results may be unusual if the ratios of cell subsets are skewed significantly or if the responder cells are anergic or exhausted due to other underlying conditions. A possible confounding factor for PID05 could be the Shprintzen–Goldberg syndrome previously diagnosed in this patient. PID05 generally responds well to standard TB treatment regimens and is therefore treated in the standard way for each recurring TB episode.

Recurrent Salmonella infection is common amongst patients with mutations in *IL12RB1*, with about 62% of described cases presenting with this clinical phenotype (Haverkamp et al. 2014; Ramirez-Alejo and Santos-Argumedo 2014; Qu et al. 2011). Unlike previously described *IL12RB1* variants, the heterozygous variant identified in PID04 (c.G684C) resulted in an immunological phenotype that has never been described before. PID04 had lower IL-12Rβ1 expression (percentage positive cells as well as receptor density per cell), similar to previously described IL12RB1 variants and PID05; however, PID04 had very high levels of IL-12 signalling through the receptor, which resulted in high levels of IFN-γ production upon IL-12 stimulation. A gain-of-function variant in *IL12RB1* has never been described before, even though several case studies of *IL12RB1* variants with clinical presentation similar to that of PID04 have been published (Göktürk et al. 2016; Robinson 2015; de Beaucoudrey et al. 2011). These other case studies, however, only assessed IL-12Rβ1 expression levels and not receptor functionality, and therefore it is possible that a gain-of-function mutation may have been overlooked. PID04 also had higher levels of IFN-γ signalling as well as IL-12 production after IFN-γ stimulation when compared to controls. The higher levels of cytokine signalling as well as increased cytokine production may explain the IBD-like presentation that PID04 has had from a very young age. It is likely that this possible gain-of-function *IL12RB1* variant presents as both immunodeficiency, as evidenced by susceptibility to Salmonella (and potentially mycobacteria), and autoimmunity. Other PIDs, such as IPEX syndrome and IL10/IL10R deficiencies have previously been shown to present with both autoimmunity and immunodeficiencies, and this dual-presentation is becoming more commonly recognized as more PIDs relating to immune dysregulation are identified (Carneiro-Sampaio and Coutinho 2015).

After the initial genetics-based diagnosis of *IL12RB1,* PID04 received a HSCT from a well-matched donor at the age of 3 and a half years. This was the first HSCT transplant in South Africa for a patient with *IL12RB1* diagnosis. Shortly after the transplant, his condition deteriorated, and he presented with very high fevers. It was initially assumed to be a sign of rejection, due to the lack of any obvious infections. An IL-12/23 blocker, Ustekinumab, was administered and the fever improved

after about 10 hours, and he started engrafting host cells. It is now suspected that due the over-responsiveness of his immune cells to IL-12, as evidenced by the pre-HSCT functional assays, there was an increased induction of various inflammatory cytokines resulting in a 'cytokine storm' type response. He is currently (2 months post-transplant) doing well and recovering at home, however, it is unknown whether he will develop a fully competent immune system and is therefore closely monitored by various physicians. The potential gain-of-function *IL12RB1* variant will be investigated further in cell-lines altered by site-directed mutagenesis as well as in animal models.

Similar to the *IFNGR1* variants described earlier, different variants in *IL12RB1* resulted in varying clinical presentation and immune functionality, once again highlighting the importance of in-depth *in vitro* assessment of immune functionality.

***IL12B***

All reported variants in *IL12B,* which encodes for the IL-12p40 subunit, are autosomal recessive loss-of-function and are characterised by lack of IL-12 production by immune cells (Al-Muhsen and Casanova 2008; Picard et al. 2002). Similar to previously reported *IL12B* variants, both PID06 [*IL12B* (c.A320G) and *NFKB2* (c.C2042T), both heterozygous] and PID07 [*IL12B* (c.G863C) homozygous] had very low levels of IL-12 production upon IFN-γ stimulation. The slightly higher signalling, for both IFN-γ and IL-12, observed in these patients could potentially be an immune compensatory mechanism for the lack of IL-12 production by host cells. From the functional assay results for PID07, it can be assumed that the c.C863C variant also acts in an autosomal recessive manner as previously reported *IL12B* mutations (Al-Muhsen and Casanova 2008; Picard et al. 2002). PID06's immune function results were very similar to PID07's, although PID06's *IL12B* variant (c.A320G) is present in heterozygous form – which has never before been reported to be associated with MSMD. It is possible that the additional variant in PID06, *NFKB2* (c.C2042T), may have a compound heterozygous effect on the *IL12B* variant, which could lead to the clinical disease phenotype. PID06 had lower than normal levels of IFN-γ production in response to PHA and IL-12 co-stimulation, which may potentially also be explained by the compounded effects of the heterozygous *IL12B* and *NKFB2* variants. *NFKB2* forms a crucial part of the non-canonical NF-κB pathway, which is essential for immunity and cell survival. Dysregulation of the NF-κB pathway has previously been associated with improper immune development leading to increased susceptibility to infections or autoimmune manifestations (Ghosh and Dass 2016; Shi et al. 2016).

***IFNGR2***

Very few *IFNGR2* mutations have been described to date, but all these result in phenotypes similar to the more commonly observed *IFNGR1* mutations (Parvaneh et al. 2015; Kong et al. 2013). PID08's immunological phenotype is very similar to the first reported *IFNGR2* mutation, by Dorman and Holland (1998), where IFN-γR1 was detectable on immune cells but there was a lack of response to IFN-γ, indicating that the IFN-γR is non-functional. PID08 had very high levels of IFN-γ

present in blood plasma, similar to what has been observed in various IFN-γR deficiencies (Apt et al. 2017), which indicates that there is either a build-up of IFN-γ due to lack of binding to its receptor or the host cells are overproducing IFN-γ in an attempt to compensate for lack of signal transduction through the IFN-γR. Kotenko et al. (1995) have shown that the association of IFN-γR1 and IFN-γR2, to form the IFN-γR complex, is needed for signal transduction and that the IFN-γR2 intracellular domain plays an essential role in IFN-γ signalling. Further research on the *IFNGR2* variant (c.A708T) found in PID08 is needed in order to determine the exact impact of the variant on IFN-γR2 protein expression and folding, which may contribute to a better understanding of the dependence on IFN-γR components for IFN-γ signalling.

***CYBB***

Most *CYBB* mutations are associated with CGD and approximately 70% of CGD patients harbour mutations in *CYBB* (Ochs and Petroni 2017). There are also other reported cases of *CYBB* mutations, which lead to a defective IFN-γ dependant respiratory burst response in macrophages, that has been associated with a selective susceptibility to mycobacterial infections, usually BCGosis (Abel et al. 2017; Al-Herz et al. 2015; Wu and Holland 2015). PID09 presented with disseminated mycobacterial disease and not the traditional CGD presentation of recurrent staphylococcal or fungal infections , indicating that the CYBB (c.A302G) variant may be associated with MSMD. IFN-γR1 and IL-12Rβ1 expression and IFN-γ signalling was mostly normal for PID09, and IL-12 signalling was slightly decreased, which was expected since the gp91phox protein, encoded by CYBB, is not expected to alter cytokine receptor expression and signalling.

***Variants in NF-κB pathway – not previously associated with MSMD***

Variants in two separate genes that are important for the functionality of the NF-κB pathway, *IKBKB* (c.G2257A) homozygous and *NFKB2* (c.C2042) heterozygous, were identified in PID10. *IKBKB* encodes for the IKK-β subunit of the IκB kinase, or IKK, an enzyme complex located upstream of the NF-κB signalling cascade. Upon binding of IKK to NEMO (NF-κB essential modulator, also known as IKK-γ), NF-κB is activated resulting in transcription of various immunological genes (Rothwarf et al. 1998). NF-κB deficiencies, brought upon by mutations in *NFKB1 or NFKB2*, have been associated with CVID (Shi et al. 2016; Chen et al. 2013).

IL-12 production upon IFN-γ stimulation was impaired in PID10, likely due to the IKBKB variant, which is involved to some extent in downstream IFN-γ signalling events (Boisson-dupuis et al. 2015). The higher expression levels of IFN-γR1 as well as enhanced IFN-γ signalling observed in PID10 could be a potential immune compensatory mechanism due to defects in the downstream IFN-γ signalling cascade. The decreased IL-12Rβ1 expression and IL-12 signalling could be due to the additional heterozygous *NFKB2* variant, since NF-κB is essential for lymphocyte development and functions (Ghosh and Dass 2016; Shi et al. 2016; Chen et al. 2013). Interestingly the *NFKB2* variant in PID10 was the exact same variant as in PID06, and both patients showed a similar change in

lymphocyte phenotypes and cytokine production. The functional assays in this study were not able to define the exact effect of *NFKB2* variants since the assays are focussed around the IL-12 and IFN-γ pathways and not the NF-κB pathway. Further research on this *NFKB* variant is needed in order to determine the extent of the resulting immune deficit.

*IRAK1* encodes for an enzyme that functions downstream of IL-1, and is partially responsible for IL-1 induced activation of NF-κB (Bustamante et al. 2019; Ghosh and Dass 2016). IRAK1 associates with IKK and in turn with NEMO, and therefore it was expected that the functional phenotype of the *IRAK* variant in PID11 (c.C1939T) would be similar, although to a lesser extent, to the *IKBKB* variant in PID10. PID11 did have slightly lower than normal IFN-γ-induced IL-12 production, although not as low as PID10. PID11 also had enhanced IFN-γ signalling, similar to PID10. The results from PID11's functional assays were not as clear-cut as PID10's, with contradictory up- and down regulation of cytokine receptor expression and signalling on the different cell subsets making it harder to make a definitive call on the likely effect of this *IRAK1* variant on the IL-12-IFN-γ pathway. More research is needed on *IRAK1*, as with *IKBKB* and *NFKB2*, to determine the exact pathophysiology of associated immune defects.

***Patients without genetic results***

WES and the subsequent bioinformatics pipeline were unable to identify plausible disease-causing variants for PID12. Several other variants in a wide array of genes were identified that have never been associated with PID, however, re-analysis of the WES data at a later point may be able to identify newly described variants associated with PID. It is also possible that a potential PID-causing defect in PID12 may not be located in their exome but rather in non-coding regulatory elements of the DNA. Defects in non-coding regions of the DNA could potentially lead to alteration(s) in expression levels, exporting, or homing of immunological protein(s), and can be assessed by means of RNA-sequencing (Naranbhai 2016). PID12 had lower than control levels of IL-12Rβ1 expression, as well as decreased IL-12 signalling and IL-12-induced IFN-γ production. The defective IFN-γ production revealed by these functional assays support the negative QFT-plus result that this patient had, despite several culture-confirmed TB episode. The functional phenotype of PID12 is reminiscent of that of a loss-of-function defect in *IL12RB1*, although no plausible disease-causing mutation was found in *IL12RB1*. It is likely that this patient has a regulatory defect relating to IL-12Rβ1 expression and function or perhaps a more complex defect that relates to overall lymphocyte function. The over-production of IL-12 upon IFN-γ stimulation, could potentially represent an immune compensatory mechanism to counteract the lack of lymphocyte responsiveness to IL-12.

Patients PID13 - PID17 have not yet undergone WES, due to funding constraints however the functional assays in this study revealed likely defects in or closely related to the IL-12-IFN-γ pathway.

In PID13, IL-12Rβ1 expression was low on various lymphocyte subsets, however, IL-12 signalling was low only on NK cells, suggesting that he may potential have an immune deficiency relating specifically to NK cells development and function. The slightly higher than normal levels of both IFN-γ-induced IL-12 production and IL-12-induced IFN-γ production in PID13 cannot be explained based solely on the decreased IL-12 responsiveness of NK cells and further investigations may be needed to explain the overproduction of these cytokines.

PID14 had decreased levels of IFN-γR1 expression, although signalling though the receptor was within the normal range. Additionally, IFN-γ-induced IL-12 production was lower than normal, which is in alignment with the overall functional phenotype seen in some cases of *IFNGR1/2* and all *IL12B* mutations (Esteve-Solé et al. 2018). Interestingly, PID14 also had lower than normal levels of IL-12Rβ1 expression and IL-12 signalling in nearly all lymphocyte subsets, similar to previously reported loss-of-function *IL12RB1* mutations, although in this case the IL-12-induced IFN-γ production was normal (Robinson 2015). It is likely that PID14 has a defect in *IL12B* based on the similarity of the immune functional readouts to that of PID07, which had a homozygous variant in *IL12B*. Both PID14 and PID17 showed decreased IL-12Rβ1 expression and IL-12 signalling, especially in NK cells. Alternatively, PID14 may have a defect in some part of the NF-κB pathway or another immune pathway essential for lymphocyte development and function.

PID15's clinical phenotype, unusual TBM in a 9-year-old, was very similar to that of PID02 (*IFNGR1* variant) and both of these patients had very high levels of IL-12-induced IFN-γ production. Unlike PID02, however, PID15 had higher than normal density of IFN-γR1 expression and IFN-γ signalling in monocytes as well as decreased of IL-12Rβ1 expression and IL-12 signalling in NK cells, similar to what was observed for PID11, who had variants in both *IKBKB* and *NFKB2*. IL-12 production was normal for PID15, unlike for PID11 and PID02. It is possible that PID15 has a defect in the NF-κB pathway that relates to defective lymphocyte development and function – the enhanced IFN-γ production and signalling may be a potential compensatory mechanism of the host immune cells, however, further research and genetic investigation is needed in order to confirm the diagnosis.

Higher than normal levels of IFN-γ-induced IL-12 production as well as the decreased IL-12 signalling observed in all cell subsets for PID16, is very similar to the immunological phenotypes of loss-of-function *IL12RB1* mutations (Robinson 2015), however PID16 had contradictory, normal IL-12-induced IFN-γ production. Mutations in *IL12RB1* are usually associated with BCGosis or non-tuberculous mycobacterial and Salmonella infections and would therefore not, however, explain the severe clinical phenotype of recurrent and disseminated TB infection that was non-responsive to treatment which eventually lead to the demise of PID16 (Ramirez-Alejo and Santos-Argumedo 2014). The functional results suggest that PID16 most likely had an immune defect relating to defective lymphocyte responses, although further research, including genetic analysis, is needed in order to diagnose the potential PID.

PID17 had lower than normal levels of IL-12Rβ1 expression and IL-12 signalling in nearly all lymphocyte subsets although IL-12-induced IFN-γ production was normal, similar to PID14. It is therefore likely that PID17 has a PID similar to that of PID14, which is likely related to *IL12B* expression or function.

## 5.4. Combined Discussion

WES and the TAPER™ bioinformatics pipeline is a very efficient tool for identifying genetic variants associated to PID. Plausible-disease causing variants were identified in all but one of the participants that underwent WES. Most of the variants identified though WES were novel and would likely have been missed by commercially available gene panels. Several variants that do not fall within the conventional IL-12-IFN-γ pathway were also identified. Plausible disease-causing variants that fall within the NF-κB pathway were identified in 4 of the 11 patients that underwent WES. This indicates that mycobacterial susceptibility may also be associated with defects in the NF-κB pathway.

The combination of the three functional assays for the assessment of the integrity of the IL-12-IFN-γ pathway was successful in identifying immune deficits in essentially all of the participants. The results generated by the functional assays were variable, and in several cases the functional data alone could not fully explain the disease phenotypes, especially in patients for which no plausible disease-causing variant(s) were yet identified. The functional assays were easier to interpret if a plausible variant/gene had been identified; however, even in the absence of genetic data the functional assays provided some clues as to the likely defect.

The functional assays did not always correlate well with each other, for instance, PID05 had lower than normal levels of IL-12Rβ1 expression (percentage positive cells as well as receptor density per cell) and IL-12 signalling, however IFN-γ production upon IL-12 stimulation was paradoxically higher than normal. In several cases, the cytokine assay did not correlate well to the cytokine receptor and signalling readouts. This may be an unexpected but accurate observation of the immune functionality of the immune cells *in vitro*, however, it could also be due to the non-mycobacterial-specificity of the cytokine assays or the fact that the cytokine production is measured for total PBMCs and not for each respective cell subset as with the flow cytometric assays. The percentages of constituent cell subsets in the PBMCs of each patient may differ and this may significantly impact the final readout of the cytokine assay.

The clinical and molecular phenotypes of the patients that shared variants in the same genes, for instance *IFNGR1* and *IL12B*, were highly variable. Different variants in *IFNGR1*, identified in patients with distinctly different clinical presentations (PID01-PID03), led to variable levels of IFN-γR1 expression and functionality (signalling) as well as downstream cytokine production. Similarly, the different variants in *IL12RB1* (PID04 and PID05) also lead to varying levels of IL-12Rβ1 expression,

functionality, and downstream cytokine production in patients with different clinical disease presentation. Although both PID04 and PID05 had decreased IL-12Rβ1 expression levels, PID04 had decreased IL-12 signalling similar to previously reported loss-of-function *IL12RB1* mutations, whereas PID05 had enhanced IL-12 signalling, suggesting a never-before encountered gain-of-function variant (Robinson 2015). Due to the variability of the molecular phenotypes associated with variants within the same gene, it is important to assess the immune functionality for all likely disease-causing variants rather than assuming that variants within the same gene would lead to similar phenotypes.

# Chapter 6 Conclusions and Future Perspectives

Evidence of functional abnormalities is essential in confirming whether a potentially pathogenic variant identified by WES manifests as truly pathogenic *in vitro*. The functional assays implemented and optimised in this study were able to identify immune deficits relating to the IL-12-IFN-γ pathway for nearly all the participants with suspected MSMD.

Although functional assays alone could not always provide a clear diagnosis, they do give an overview of the integrity of the IL-12-IFN-γ pathway. It would be beneficial to apply these assays routinely for patients with suspected PID relating to mycobacterial susceptibility. Abnormalities observed in these 'routine' functional readouts can be used to pre-select patients for subsequent genetic analysis. If the functional readout is similar to well-defined, previously described cases associated with certain genetic mutations e.g. IFNGR1 (c.818del4), it may speed up the genetic diagnosis of the patient as they can likely be diagnosed by Sanger sequencing or commercial gene panels rather than undergoing costly, complex and time-consuming WES. If the functional readouts show no abnormalities or abnormalities that do not fit characteristic patterns, it may earmark these patients for further investigation through WES or RNA-sequencing.

Several of the plausible disease-causing variants that were identified in the participants form part of the NF-κB signalling pathways, which is essential for T cell development and function (Pellegrini et al. 2018; Mishra et al. 2017; Ghosh and Dass 2016; Lee et al. 2011). This suggests that mycobacterial susceptibility, especially in a TB endemic area, could also be caused by defects in pathways other than the IL-12-IFN-γ pathway. Defects in the NF-κB pathway have previously been associated with CVID (Chen et al. 2013), but further research is required to investigate the pathophysiology of mycobacterial susceptibility relating to the NF-κB pathway.

A molecular diagnosis paves the way for better treatment options for the patients, based on a better understanding of the molecular mechanism that leads to disease. Molecular diagnoses also allow genetic counselling of affected family members, which increases awareness for the specific disorder within the family.

The flow cytometry-based assays implemented in this study differ slightly from previously published methods that also assess IL-12 and IFN-γ receptor expression and functionality. The assays optimised in this study have much faster turn-around times, although potentially sub-optimal stimulation conditions when compared to others.

Due to problems accessing standardised viable titred stocks of BCG, PHA was used to activate PBMCs during the cytokine assays. This has been shown to be less efficient at detecting partial defects in the IL-12-IFN-γ pathways. Using BCG instead of PHA would have been preferable, due

to the induction of a mycobacterial specific immune activation state. Future studies will incorporate BCG stimulation to activate PBMCs.

The 10 controls used to establish normal ranges for receptor expression, signalling, and cytokine production, were not age matched to the participants. For future, larger scale studies, it would be better to have more controls that are age-matched to the participants in order to have more reliable comparative data.

PBMCs were isolated from patient blood collected during clinic visits or hospitalisation. The activation status of the patients' PBMCs at the time of collection, due to active diseased state, could have potentially affected the functional assay readouts.

## Final Concluding Remarks

The current study has led to the implementation of functional immune assays which allowed for the evaluation of the functional impact of both novel and previously described genetic variants on the IL-12-IFN-γ pathways. These functional assays aided in the identification and confirmation of immune deficits in all participants in this study. This is the first documented study with such a diverse cohort of MSMD patients – in terms of clinical presentation and genetic phenotypes – with readouts of immune functionality. These assays have direct clinical relevance and treatment implications, as seen in this study with patients PID01 and PID04. This IL-12-IFN-γ pathway functional 'screening' could potentially also be used to pre-select patients for further genetic investigations and might provide a much faster and cost-effective approach to diagnosing PIDs associated with mycobacterial infections

This study further emphasises the importance of investigating PID and TB susceptibility in TB endemic regions. Most features that have been previously described for MSMD – such as the predisposition to unusual mycobacterial infections – resulted from studies done in developed first world settings or areas where TB is rare. MSMD and other previously described PIDs relating to TB susceptibility may present differently in TB endemic areas such as South Africa. It is therefore important to have access to *in vitro* functional investigations to better understand the functional impact of both novel and previously described MSMD variants. The functional definition of novel variants associated with mycobacterial susceptibility will also contribute towards the understanding of host immune responses to mycobacteria.

# References

Abel L, Fellay J, Haas DW, Schurr E, Srikrishna G, Urbanowski M, et al. 2017. Genetics of human susceptibility to active and latent tuberculosis: Present knowledge and future perspectives. Lancet Infect Dis 3099:1–12; doi:10.1016/S1473-3099(17)30623-0.

Abraham RS, Aubert G. 2016. Flow Cytometry , a Versatile Tool for Diagnosis and Monitoring of Primary Immunodeficiencies. Clin Vaccine Immunol 23:254–271; doi:10.1128/CVI.00001-16.Editor.

Adzhubei IA, Schmidt S, Peshkin L, Ramensky VE, Gerasimova A, Bork P, et al. 2010. A method and server for predicting damaging missense mutations. Nat Methods 7:248–249; doi:10.1038/nmeth0410-248.

Al-Herz W, Bousfiha A, Casanova J-L, Chatila T, Conley ME, Cunningham-Rundles C, et al. 2015. Primary Immunodeficiency Diseases: an Update on the Classification from the International Union of Immunological Societies Expert Committee for Primary Immunodeficiency 2015. J Clin Immunol 35:696–726; doi:10.1007/s10875-015-0201-1.

Al-Mousa H, Al-Saud B. 2017. Primary immunodeficiency diseases in highly consanguineous populations from Middle East and North Africa: Epidemiology, diagnosis, and care. Front Immunol 8:1–7; doi:10.3389/fimmu.2017.00678.

Al-Muhsen S, Casanova JL. 2008. The genetic heterogeneity of mendelian susceptibility to mycobacterial diseases. J Allergy Clin Immunol 122:1043–1051; doi:10.1016/j.jaci.2008.10.037.

Alinejad Dizaj M, Mortaz E, Mahdaviani SA, Mansouri D, Mehrian P, Verhard EM, et al. 2018. Susceptibility to mycobacterial disease due to mutations in IL-12Rβ1 in three Iranian patients. Immunogenetics 70:373–379; doi:10.1007/s00251-017-1041-3.

Altare F, Ensser A, Breiman A, Reichenbach J, Baghdadi JE, Fischer A, et al. 2001. Interleukin-12 Receptor β1 Deficiency in a Patient with Abdominal Tuberculosis. J Infect Dis 184:231–236; doi:10.1086/321999.

Apt AS, Logunova NN, Kondratieva TK. 2017. Host genetics in susceptibility to and severity of mycobacterial diseases. Tuberculosis 106:1–8; doi:10.1016/j.tube.2017.05.004.

Arkwright PD, Gennery AR. 2011. Ten warning signs of primary immunodeficiency: A new paradigm is needed for the 21st century. Ann N Y Acad Sci 1238:7–14; doi:10.1111/j.1749-6632.2011.06206.x.

BD Biosciences. 2018. BD Spectrumviewer. Available: http://www.bdbiosciences.com/us/s/spectrumviewer [accessed 6 November 2018].

Bhat P, Leggatt G, Waterhouse N, Frazer IH. 2017. Interferon-γ derived from cytotoxic lymphocytes directly enhances their motility and cytotoxicity. Cell Death Dis 8:e2836; doi:10.1038/cddis.2017.67.

Blouin Y, Hauck Y, Soler C, Fabre M, Vong R, Dehan C, et al. 2012. Significance of the Identification in the Horn of Africa of an Exceptionally Deep Branching Mycobacterium tuberculosis Clade. I. Mokrousov, ed PLoS One 7:e52841; doi:10.1371/journal.pone.0052841.

Bluestone JA, Cron RQ, Cotterman M, Houlden BA, Matis LA. 1988. Structure and specificity of T cell receptor gamma/delta on major histocompatibility complex antigen-specific CD3+, CD4-, CD8- T lymphocytes. J Exp Med 168:1899–1916; doi:10.1084/jem.168.5.1899.

Boisson-Dupuis S, Baghdadi JE, Parvaneh N, Bousfiha A, Bustamante J, Feinberg J, et al. 2011. IL-12RB1

deficiency in two of fifty children with severe tuberculosis from Iran, Morocco, and Turkey. PLoS One 6:1–7; doi:10.1371/journal.pone.0018524.

Boisson-Dupuis S, Bustamante J, El-Baghdadi J, Camcioglu Y, Parvaneh N, Azbaoui S El, et al. 2015. Inherited and acquired immunodeficiencies underlying tuberculosis in childhood. Immunol Rev 264:103–120; doi:10.1111/imr.12272.Inherited.

Bonilla FA, Khan DA, Ballas ZK, Chinen J, Frank MM, Hsu JT, et al. 2015. Practice parameter for the diagnosis and management of primary immunodeficiency. J Allergy Clin Immunol 136:1186–1205.e78; doi:10.1016/j.jaci.2015.04.049.

Bonilla LE, Means GD, Lee KA, Patterson SD. 2008. The evolution of tools for protein phosphorylation site analysis: From discovery to clinical application. Biotechniques 44:671–679; doi:10.2144/000112800.

Bousfiha A, Jeddane L, Al-Herz W, Ailal F, Casanova JL, Chatila T, et al. 2015. The 2015 IUIS Phenotypic Classification for Primary Immunodeficiencies. J Clin Immunol 35:727–738; doi:10.1007/s10875-015-0198-5.

Bousfiha AA, Jeddane L, Ailal F, Benhsaien I, Mahlaoui N, Casanova J-L, et al. 2013. Primary Immunodeficiency Diseases Worldwide: More Common than Generally Thought. J Clin Immunol 33:1–7; doi:10.1007/s10875-012-9751-7.

Boutboul D, Kuehn HS, Van De Wyngaert Z, Niemela JE, Callebaut I, Stoddard J, et al. 2018. Dominant-negative IKZF1 mutations cause a T, B, and myeloid cell combined immunodeficiency. J Clin Invest 128:3071–3087; doi:10.1172/JCI98164.

Boyum A. 1976. Isolation of Lymphocytes, Granulocytes and Macrophages. Scand J Immunol 5:9–15; doi:10.1111/j.1365-3083.1976.tb03851.x.

Braue J, Murugesan V, Holland S, Patel N, Naik E, Leiding J, et al. 2015. NF-κB essential modulator deficiency leading to disseminated cutaneous atypical mycobacteria. Mediterr J Hematol Infect Dis 7:2–7; doi:10.4084/mjhid.2015.010.

Brent AJ, Mugo D, Musyimi R, Mutiso A, Morpeth S, Levin M, et al. 2017. Bacteriological diagnosis of childhood TB: a prospective observational study. Sci Rep 7:11808; doi:10.1038/s41598-017-11969-5.

Brown AE, Holzer TJ, Andersen BR. 1987. Capacity of human neutrophils to kill Mycobacterium tuberculosis. J Infect Dis 156: 985–989.

Bustamante J, Boisson-dupuis S, Abel L, Casanova J-L. 2014. Mendelian susceptibility to mycobacterial disease : Genetic , immunological , and clinical features of inborn errors of IFN-γ immunity. Semin Immunol 26:454–470; doi:10.1016/j.smim.2014.09.008.

Bustamante J, Picard C, Boisson-Dupuis S, Abel L, Casanova J-L. 2011. Genetic lessons learned from X-linked Mendelian susceptibility to mycobacterial diseases. Ann N Y Acad Sci 1246:92–101; doi:10.1111/j.1749-6632.2011.06273.x.

Bustamante J, Zhang S-Y, Boisson B, Ciancanelli M, Jouanguy E, Dupuis-Boisson S, et al. 2019. *Immunodeficiencies at the Interface of Innate and Adaptive Immunity*. Fifth Edit. R.R. Rich, T.A. Fleisher, W.T. Shearer, H.W. Schroeder, A.J. Frew, and C.M. Weyand, eds. Elsevier Ltd.

Caragol I, Casanova J-L. 2003. Inherited disorders of the Interleukin-12 / Interferon-gamma axis : Mendelian predisposition to mycobacterial disease in man. Inmunologia 22: 263–276.

Caragol I, Raspall M, Fieschi C, Feinberg J, Larrosa MN, Hernandez M, et al. 2003. Clinical Tuberculosis in 2 of 3 Siblings with Interleukin-12 Receptor 1 Deficiency. Clin Infect Dis 37:302–306; doi:10.1086/375587.

Carneiro-Sampaio M, Coutinho A. 2015. Early-Onset Autoimmune Disease as a Manifestation of Primary Immunodeficiency. Front Immunol 6; doi:10.3389/fimmu.2015.00185.

Casanova J-L. 2015. Severe infectious diseases of childhood as monogenic inborn errors of immunity. Proc Natl Acad Sci 1:201521651; doi:10.1073/pnas.1521651112.

Casanova J-L, Abel L. 2002. Genetic Dissection of Immunity to Mycobacteria: The Human Model. Annu Rev Immunol 20:581–620; doi:10.1146/annurev.immunol.20.081501.125851.

Casanova JL, Abel L, Quintana-Murci L. 2013. Immunology taught by human genetics. Cold Spring Harb Symp Quant Biol 78:157–172; doi:10.1101/sqb.2013.78.019968.

Chan J, Mehta S, Bharrhan S, Chen Y, Achkar JM, Casadevall A, et al. 2014. The role of B cells and humoral immunity in Mycobacterium tuberculosis infection. Semin Immunol 26:588–600; doi:10.1016/j.smim.2014.10.005.The.

Chapel H, Prevot J, Gaspar HB, Español T, Bonilla FA, Solis L, et al. 2014. Primary Immune Deficiencies - Principles of Care. Front Immunol 5:1–12; doi:10.3389/fimmu.2014.00627.

Chapgier A, Wynn RF, Jouanguy E, Filipe-Santos O, Zhang S, Feinberg J, et al. 2006. Human Complete Stat-1 Deficiency Is Associated with Defective Type I and II IFN Responses In Vitro but Immunity to Some Low Virulence Viruses In Vivo. J Immunol 176:5078–5083; doi:10.4049/jimmunol.176.8.5078.

Chen K, Coonrod EM, Kumánovics A, Franks ZF, Durtschi JD, Margraf RL, et al. 2013. Germline Mutations in NFKB2 Implicate the Noncanonical NF-kB Pathway in the Pathogenesis of Common Variable Immunodeficiency. Am J Hum Genet 93:812–824; doi:10.1016/j.ajhg.2013.09.009.

CIA World Factbook. 2018. South Africa. World Factbook 2018. https://www.cia.gov/library/publications/the-world-factbook/geos/sf.html

Colditz GA, Brewer TF, Berkey CS, Wilson ME, Burdick E, Fineberg H V, et al. 1994. Efficacy of BCG vaccine in the prevention of tuberculosis. Meta-analysis of the published literature. JAMA 271: 698–702.

Comas I, Coscolla M, Luo T, Borrell S, Holt KE, Kato-Maeda M, et al. 2013. Out-of-Africa migration and Neolithic coexpansion of Mycobacterium tuberculosis with modern humans. Nat Genet 45:1176–1182; doi:10.1038/ng.2744.

Connor LM, Harvie MC, Rich FJ, Quinn KM, Brinkmann V, Le Gros G, et al. 2010. A key role for lung-resident memory lymphocytes in protective immune responses after BCG vaccination. Eur J Immunol 40:2482–2492; doi:10.1002/eji.200940279.

Cooke GS, Campbell SJ, Sillah J, Gustafson P, Bah B, Sirugo G, et al. 2006. Polymorphism within the Interferon-γ/Receptor Complex Is Associated with Pulmonary Tuberculosis. Am J Respir Crit Care Med 174:339–343; doi:10.1164/rccm.200601-088OC.

Cooper AM. 2009. Cell mediated immune responses in Tuberculosis. Annu Rev Immunol 27:393–422; doi:10.1146/annurev.immunol.021908.132703.Cell.

Cooper AM, Solache A, Khader SA. 2007. Interleukin-12 and tuberculosis: an old story revisited. Curr Opin Immunol 19:441–447; doi:10.1016/j.coi.2007.07.004.

Cossarizza A, Chang H-D, Radbruch A, Akdis M, Andrä I, Annunziato F, et al. 2017. Guidelines for the use of flow cytometry and cell sorting in immunological studies. Eur J Immunol 47:1584–1797; doi:10.1002/eji.201646632.

Cottle LE. 2011. Mendelian susceptibility to mycobacterial disease. Clin Genet 79:17–22; doi:10.1111/j.1399-0004.2010.01510.x.

Cytlak U, Resteu A, Bogaert D, Kuehn HS, Altmann T, Gennery A, et al. 2018. Ikaros family zinc finger 1 regulates dendritic cell development and function in humans. Nat Commun 9:1239; doi:10.1038/s41467-018-02977-8.

Darrah PA, Patel DT, De Luca PM, Lindsay RWB, Davey DF, Flynn BJ, et al. 2007. Multifunctional TH1 cells define a correlate of vaccine-mediated protection against Leishmania major. Nat Med 13:843–850; doi:10.1038/nm1592.

Davies R, Vogelsang P, Jonsson R, Appel S. 2016. An optimized multiplex flow cytometry protocol for the analysis of intracellular signaling in peripheral blood mononuclear cells. J Immunol Methods 436:58–63; doi:10.1016/j.jim.2016.06.007.

de Beaucoudrey L, Samarina A, Bustamante J, Abel L, Sanal O, Casanova J-L, et al. 2011. Revisiting Humal IL-12RB1 Deficiency: A Survey of 141 Patients From 30 Countries. Med 89:381–402; doi:10.1097/MD.0b013e3181fdd832.Revisiting.

de Vor IC, van der Meulen PM, Bekker V, Verhard EM, Breuning MH, Harnisch E, et al. 2016. Deletion of the entire interferon-γ receptor 1 gene causing complete deficiency in three related patients. J Clin Immunol 36:195–203; doi:10.1007/s10875-016-0244-y.

de Vries E, Alvarez Cardona A, Abdul Latiff AH, Badolato R, Brodszki N, Cant AJ, et al. 2012. Patient-centred screening for primary immunodeficiency, a multi-stage diagnostic protocol designed for non-immunologists: 2011 update. Clin Exp Immunol 167:108–119; doi:10.1111/j.1365-2249.2011.04461.x.

Demangel C, Bertolino P, Britton WJ. 2002. Autocrine IL-10 impairs dendritic cell (DC)-derived immune responses to mycobacterial infection by suppressing DC trafficking to draining lymph nodes and local IL-12 production. Eur J Immunol 32:994–1002; doi:10.1002/1521-4141(200204)32:4<994::AID-IMMU994>3.0.CO;2-6.

Denis M. 1991. Human neutrophils, activated with cytokines or not, do not kill virulent Mycobacterium tuberculosis. J Infect Dis 163:919; doi:10.1093/infdis/163.4.919.

Depner M, Fuchs S, Raabe J, Frede N, Glocker C, Doffinger R, et al. 2016. The Extended Clinical Phenotype of 26 Patients with Chronic Mucocutaneous Candidiasis due to Gain-of-Function Mutations in STAT1. J Clin Immunol 36:73–84; doi:10.1007/s10875-015-0214-9.

Dorman SE, Holland SM. 2000. Interferon-γ and interleukin-12 pathway defects and human disease. Cytokine Growth Factor Rev 11:321–333; doi:10.1016/S1359-6101(00)00010-1.

Dorman SE, Holland SM. 1998. Mutation in the signal-transducing chain of the interferon-γ receptor and susceptibility to mycobacterial infection. J Clin Invest 101:2364–2369; doi:10.1172/JCI2901.

El Azbaoui S, Sabri A, Ouraini S, Hassani A, Asermouh A, Agadr A, et al. 2016. Utility of the QuantiFERON®-TB Gold In-Tube assay for the diagnosis of tuberculosis in Moroccan children. Int J Tuberc Lung Dis 20:1639–1646; doi:10.5588/ijtld.16.0382.

Eley B, Esser M. 2014. Investigation and management of primary immunodeficiency in South African children. S Afr Med J 104:1–4; doi:10.7196/samj.8946.

Esser MM, Banda E, Moller M, Nortje R. 2015. Primary immunodeficiency disease management in tuberculosis endemic regions – are we aware enough and how does a registry assist? S Afr Med J 57–61.

Esser MM, Potter P, Nortje R. 2016. Meeting the needs of Primary Immunodeficiency pathients in South Africa - Some findings from the South African Registry. Curr Allergy Clin Immunol 29: 56–60.

Esteve-Solé A, Sologuren I, Martínez-Saavedra MT, Deyà-Martínez À, Oleaga-Quintas C, Martinez-Barricarte R, et al. 2018. Laboratory evaluation of the IFN-γ circuit for the molecular diagnosis of Mendelian susceptibility to mycobacterial disease. Crit Rev Clin Lab Sci 55:184–204; doi:10.1080/10408363.2018.1444580.

Eum S-Y, Kong J-H, Hong M-S, Lee Y-J, Kim J-H, Hwang S-H, et al. 2010. Neutrophils are the predominant infected phagocytic cells in the airways of patients with active pulmonary TB. Chest 137:122–128; doi:10.1378/chest.09-0903.

Feinberg J, Fieschi C, Doffinger R, Feinberg M, Leclerc T, Boisson-Dupuis S, et al. 2004. Bacillus Calmette Guérin triggers the IL-12/IFN-γ axis by an IRAK-4- and NEMO-dependent, non-cognate interaction between monocytes, NK, and T lymphocytes. Eur J Immunol 34:3276–3284; doi:10.1002/eji.200425221.

Ferguson JS, Voelker DR, McCormack FX, Schlesinger LS. 1999. Surfactant protein D binds to Mycobacterium tuberculosis bacilli and lipoarabinomannan via carbohydrate-lectin interactions resulting in reduced phagocytosis of the bacteria by macrophages. J Immunol 163: 312–321.

Fieschi C. 2004. A novel form of complete IL-12/IL-23 receptor 1 deficiency with cell surface-expressed nonfunctional receptors. Blood 104:2095–2101; doi:10.1182/blood-2004-02-0584.

Fieschi C, Dupuis S, Picard C, Smith CIE, Holland SM, Casanova J-L. 2001. High Levels of Interferon Gamma in the Plasma of Children With Complete Interferon Gamma Receptor Deficiency. Pediatrics 107:e48–e48; doi:10.1542/peds.107.4.e48.

Fleisher TA, Dorman SE, Anderson JA, Vail M, Brown MR, Holland SM. 1999. Detection of Intracellular Phosphorylated STAT-1 by Flow Cytometry. Clin Immunol 90:425–430; doi:10.1006/clim.1998.4654.

Flynn JL, Chan J. 2001. Immunology of tuberculosis. Annu Rev Immunol 19:93–129; doi:10.1146/annurev.immunol.19.1.93.

Fogel N. 2015. Tuberculosis: A disease without boundaries. Tuberculosis 95:527–531; doi:10.1016/j.tube.2015.05.017.

Fraser DA, Bulat-kardum L, Knezevic J, Babarovic P, Dellacasagrande J, Matanic D, et al. 2003. Interferon-g Receptor-1 Gene Polymorphism in Tuberculosis Patients from Croatia. Scand J Immunol 57: 480–484.

Gallo V, Dotta L, Giardino G, Cirillo E, Lougaris V, D'Assante R, et al. 2016. Diagnostics of Primary Immunodeficiencies through Next-Generation Sequencing. Front Immunol 7:1–10; doi:10.3389/fimmu.2016.00466.

Gaynor CD, McCormack FX, Voelker DR, McGowan SE, Schlesinger LS. 1995. Pulmonary surfactant protein A mediates enhanced phagocytosis of Mycobacterium tuberculosis by a direct interaction with human

macrophages. J Immunol 155: 5343-5351.

Ge L, Ma J-C, Han M, Li J-L, Tian J-H. 2014. Interferon-gamma release assay for the diagnosis of latent Mycobacterium tuberculosis infection in children younger than 5 years: a meta-analysis. Clin Pediatr (Phila) 53:1255–1263; doi:10.1177/0009922814540040.

Ghosh S, Dass JFP. 2016. Study of pathway cross-talk interactions with NF-κB leading to its activation via ubiquitination or phosphorylation: A brief review. Gene 584:97–109; doi:10.1016/j.gene.2016.03.008.

Ghosh S, Gaspar HB. 2017. Gene Therapy Approaches to Immunodeficiency. Hematol Oncol Clin North Am 31:823–834; doi:10.1016/j.hoc.2017.05.003.

Glanzmann B, Herbst H, Kinnear CJ, Möller M, Gamieldien J, Bardien S. 2016. A new tool for prioritization of sequence variants from whole exome sequencing data. Source Code Biol Med 11:10; doi:10.1186/s13029-016-0056-8.

Glanzmann B, Möller M, Moncada-Velez M, Peter J, Urban M, van Helden PD, et al. 2018a. Autosomal Dominant IFN-γR1 Deficiency Presenting with both Atypical Mycobacteriosis and Tuberculosis in a BCG-Vaccinated South African Patient. J Clin Immunol 38:460–463; doi:10.1007/s10875-018-0509-8.

Glanzmann B, Uren C, de Villiers N, van Coller A, Glashoff RH, Urban M, et al. 2018b. Primary immunodeficiency diseases in a tuberculosis endemic region: challenges and opportunities. Genes Immun; doi:10.1038/s41435-018-0041-0.

Göktürk B, Reisli İ, Çalışkan Ü, Oleaga-quintas C, Deswarte C, Turul-özgür T, et al. 2016. Infectious diseases , autoimmunity and midline defect in a patient with a novel bi-allelic mutation in IL12RB1 gene. Turk J Pediatr 58: 331–336.

Gold MC, Cerri S, Smyk-Pearson S, Cansler ME, Vogt TM, Delepine J, et al. 2010. Human Mucosal Associated Invariant T Cells Detect Bacterially Infected Cells. P. Marrack, ed PLoS Biol 8:e1000407; doi:10.1371/journal.pbio.1000407.

Gray D, Gray M, Barr T. 2007. Innate responses of B cells. Eur J Immunol 37:3304–3310; doi:10.1002/eji.200737728.

Green RC, Berg JS, Grody WW, Kalia S, Korf BR, Martin CL, et al. 2013. ACMG Recommendations for Reporting of Incidental Findings in Clinical Exome and Genome Sequencing. Genet Med 15:565–574; doi:10.1038/gim.2013.73.ACMG.

Gupta A, Kaul A, Tsolaki AG, Kishore U, Bhakta S. 2012. Mycobacterium tuberculosis: Immune evasion, latency and reactivation. Immunobiology 217:363–374; doi:10.1016/j.imbio.2011.07.008.

Harriff MJ, Purdy GE, Lewinsohn DM. 2012. Escape from the phagosome: The explanation for MHC-I processing of mycobacterial antigens? Front Immunol 3:1–11; doi:10.3389/fimmu.2012.00040.

Harris DP, Goodrich S, Gerth AJ, Peng SL, Lund FE. 2005. Regulation of IFN-gamma production by B effector 1 cells: essential roles for T-bet and the IFN-gamma receptor. J Immunol 174: 6781–6790.

Harris DP, Haynes L, Sayles PC, Duso DK, Eaton SM, Lepak NM, et al. 2000. Reciprocal regulation of polarized cytokine production by effector B and T cells. Nat Immunol 1:475–482; doi:10.1038/82717.

Haverkamp MH, van de Vosse E, van Dissel JT. 2014. Nontuberculous mycobacterial infections in children with inborn errors of the immune system. J Infect 68:S134–S150; doi:10.1016/j.jinf.2013.09.024.

Henao-Tamayo M, Ordway DJ, Orme IM. 2014. Memory T cell subsets in tuberculosis: what should we be targeting? Tuberculosis (Edinb) 94:455–461; doi:10.1016/j.tube.2014.05.001.

Hershberg R, Lipatov M, Small PM, Sheffer H, Niemann S, Homolka S, et al. 2008. High Functional Diversity in Mycobacterium tuberculosis Driven by Genetic Drift and Human Demography. PLoS Biol 6:e311; doi:10.1371/journal.pbio.0060311.

Holland SM. 2007. Interferon gamma, IL-12, IL-12R and STAT-1 immunodeficiency diseases: disorders of the interface of innate and adaptive immunity. Immunol Res 38:342–346; doi:10.1007/s12026-007-0045-8.

Holland SM. 2000. Treatment of infections in the patient with Mendelian susceptibility to mycobacterial infection. Microbes Infect 2:1579–1590; doi:10.1016/S1286-4579(00)01314-9.

Hønge BL, Petersen MS, Olesen R, Møller BK, Erikstrup C. 2017. Optimizing recovery of frozen human peripheral blood mononuclear cells for flow cytometry. PLoS One 12:e0187440; doi:10.1371/journal.pone.0187440.

Howley MM, Painter JA, Katz DJ, Graviss EA, Reves R, Beavers SF, et al. 2015. Evaluation of QuantiFERON-TB gold in-tube and tuberculin skin tests among immigrant children being screened for latent tuberculosis infection. Pediatr Infect Dis J 34:35–39; doi:10.1097/INF.0000000000000494.

Immune Deficiency Foundation. 2009. *Diagnostic & Clinical Care Guidelines for primary immunodeficiency diseases*. 2nd ed. R.H. Buckley, ed. Immune Deficiency Foundation:Maryland.

Jasenosky LD, Scriba TJ, Hanekom WA, Goldfeld AE. 2015. T cells and adaptive immunity to Mycobacterium tuberculosis in humans. Immunol Rev 264:74–87; doi:10.1111/imr.12274.

Jouanguy E, Lamhamedi-Cherradi S, Altare F, Fondanèche MC, Tuerlinckx D, Blanche S, et al. 1997. Partial interferon-γ receptor 1 deficiency in a child with tuberculoid bacillus Calmette-Guerin infection and a sibling with clinical tuberculosis. J Clin Invest 100:2658–2664; doi:10.1172/JCI119810.

Jouanguy E, Lamhamedi-Cherradi S, Lammas D, Dorman SE, Fondaneche MC, Dupuis S, et al. 1999. A human IFNGR1 small deletion hotspot associated with dominant susceptibility to mycobacterial infection. Nat Genet 21:370–378; doi:10.1038/7701.

Kaufmann SHE, Hussey G, Lambert P-H. 2010. New vaccines for tuberculosis. Lancet (London, England) 375:2110–2119; doi:10.1016/S0140-6736(10)60393-5.

Keshavjee S, Farmer PE. 2012. Tuberculosis, Drug Resistance, and the History of Modern Medicine. N Engl J Med 367:931–936; doi:10.1056/NEJMra1205429.

Khader SA, Partida-Sanchez S, Bell G, Jelley-Gibbs DM, Swain S, Pearl JE, et al. 2006. Interleukin 12p40 is required for dendritic cell migration and T cell priming after Mycobacterium tuberculosis infection. J Exp Med 203:1805–1815; doi:10.1084/jem.20052545.

Khader SA, Pearl JE, Sakamoto K, Gilmartin L, Bell GK, Jelley-Gibbs DM, et al. 2005. IL-23 compensates for the absence of IL-12p70 and is essential for the IL-17 response during tuberculosis but is dispensable for protection and antigen-specific IFN-gamma responses if IL-12p70 is available. J Immunol 175: 788–795.

Kircher M, Witten DM, Jain P, O'Roak BJ, Cooper GM, Shendure J. 2014. A general framework for estimating the relative pathogenicity of human genetic variants. Nat Genet 46:310–315; doi:10.1038/ng.2892.

Kobashi Y, Mouri K, Yagi S, Obase Y, Miyashita N, Okimoto N, et al. 2009. Clinical evaluation of the QuantiFERON-TB Gold test in patients with non-tuberculous mycobacterial disease. Int J Tuberc Lung Dis 13: 1422–1426.

Kong X-F, Vogt G, Itan Y, Macura-Biegun A, Szaflarska A, Kowalczyk D, et al. 2013. Haploinsufficiency at the human IFNGR2 locus contributes to mycobacterial disease. Hum Mol Genet 22:769–781; doi:10.1093/hmg/dds484.

Kotenko S V, Izotova LS, Pollack BP, Mariano TM, Donnelly RJ, Muthukumaran G, et al. 1995. Interaction between the components of the interferon gamma receptor complex. J Biol Chem 270: 20915–20921.

Kozakiewicz L, Phuah J, Flynn J, Chan J. 2013. The Role of B Cells and Humoral Immunity in Mycobacterium tuberculosis Infection. In: *The New Paradigm of Immunity to Tuberculosis, Advances in Experimental Medicine and Biology* (M. Divangahi, ed). Vol. 783 of *Advances in Experimental Medicine and Biology*. Springer New York:New York, NY. 225–250.

Kumar P, Henikoff S, Ng PC. 2009. Predicting the effects of coding non-synonymous variants on protein function using the SIFT algorithm. Nat Protoc 4:1073–1081; doi:10.1038/nprot.2009.86.

Kurt-Jones EA, Liano D, HayGlass KA, Benacerraf B, Sy MS, Abbas AK. 1988. The role of antigen-presenting B cells in T cell priming in vivo. Studies of B cell-deficient mice. J Immunol 140: 3773–3778.

Lammas DA, Casanova JL, Kumararatne DS. 2000. Clinical consequences of defects in the IL-12-dependent interferon-gamma (IFN-γ) pathway. Clin Exp Immunol 121:417–425; doi:10.1046/j.1365-2249.2000.01284.x.

Lavalett L, Rodriguez H, Ortega H, Sadee W, Schlesinger LS, Barrera LF. 2017. Alveolar macrophages from tuberculosis patients display an altered inflammatory gene expression profile. Tuberculosis 107:156–167; doi:10.1016/j.tube.2017.08.012.

Lee WI, Huang JL, Yeh KW, Jaing TH, Lin TY, Huang YC, et al. 2011. Immune defects in active mycobacterial diseases in patients with primary immunodeficiency diseases (PIDs). J Formos Med Assoc 110:750–758; doi:10.1016/j.jfma.2011.11.004.

Lerner TR, Borel S, Gutierrez MG. 2015. The innate immune response in human tuberculosis. Cell Microbiol 17:1277–1285; doi:10.1111/cmi.12480.

Li Y, Wang Y, Liu X. 2012. The Role of Airway Epithelial Cells in Response to Mycobacteria Infection. Clin Dev Immunol 2012:1–11; doi:10.1155/2012/791392.

Liu Y, Wu Y, Ramarathinam L, Guo Y, Huszar D, Trounstine M, et al. 1995. Gene-targeted B-deficient mice reveal a critical role for B cells in the CD4 T cell response. Int Immunol 7: 1353–1362.

Losana G, Rigamonti L, Borghi I, Assenzio B, Ariotti S, Jouanguy E, et al. 2002. Requirement for both IL-12 and IFN-g signaling pathways in optimal IFN-g production by human T cells. Eur J Immunol 32:693–700; doi:10.1002/1521-4141(200203)32:3<693::AID-IMMU693>3.0.CO;2-Q [pii].

Lund FE, Randall TD. 2010. Effector and regulatory B cells: modulators of CD4+ T cell immunity. Nat Rev Immunol 10:236–247; doi:10.1038/nri2729.

Madkaikar M, Mishra A, Ghosh K. 2013. Diagnostic approach to primary immunodeficiency disorders. Indian Pediatr 50:579–86; doi:10.1007/s13312-013-0171-4.

Maglione PJ, Xu J, Casadevall A, Chan J. 2008. Fc gamma receptors regulate immune activation and susceptibility during Mycobacterium tuberculosis infection. J Immunol 180: 3329–3338.

Marino S, Pawar S, Fuller CL, Reinhart TA, Flynn JL, Kirschner DE. 2004. Dendritic cell trafficking and antigen presentation in the human immune response to Mycobacterium tuberculosis. J Immunol 173: 494–506.

Martinot AJ. 2017. Microbial Offense vs Host Defense: Who Controls the TB Granuloma? Vet Pathol 300985817705177; doi:10.1177/0300985817705177.

Masserot C, Hachemane S, Casanova J, Coulomb A. 2017. Disseminated Bacillus Calmette-Gue Osteomyelitis in Twin Sisters Related to STAT1 Gene Deficiency. Pediatr Dev Pathol 1–5; doi:10.1177/1093526616686255.

Mauri C, Bosma A. 2012. Immune regulatory function of B cells. Annu Rev Immunol 30:221–241; doi:10.1146/annurev-immunol-020711-074934.

Mazurek GH, Jereb J, Lobue P, Iademarco MF, Metchock B, Vernon A. 2005. Guide- lines for using the QuantiFERON-TB Gold test for detecting Mycobacterium tuberculosis infection, United States. MMWR Recomm Rep 54: 49–55.

Merchant RH, Ahmed J, Ahmad N. 2013. XDR TB in a case of IL12RB1 deficiency: A case report of mendelian susceptibility to mycobacterial disease from India. Indian J Pediatr 80:781–782; doi:10.1007/s12098-012-0806-9.

Middleton AM, Chadwick M V, Nicholson AG, Dewar A, Feldman C, Wilson R. 2003. Investigation of mycobacterial colonisation and invasion of the respiratory mucosa. Thorax 58: 246–251.

Mishra A, Akhtar S, Jagannath C, Khan A. 2017. Pattern recognition receptors and coordinated cellular pathways involved in tuberculosis immunopathogenesis: Emerging concepts and perspectives. Mol Immunol 87:240–248; doi:10.1016/j.molimm.2017.05.001.

Modell V, Quinn J, Orange J, Notarangelo LD, Modell F. 2016. Primary immunodeficiencies worldwide: an updated overview from the Jeffrey Modell Centers Global Network. Immunol Res 64:736–753; doi:10.1007/s12026-016-8784-z.

Moliva JI, Turner J, Torrelles JB. 2017. Immune Responses to Bacillus Calmette–Guérin Vaccination: Why Do They Fail to Protect against Mycobacterium tuberculosis? Front Immunol 8; doi:10.3389/fimmu.2017.00407.

Mosmann T. 2000. Complexity or coherence? Cytokine secretion by B cells. Nat Immunol 1:465–466; doi:10.1038/82707.

Movafagh A, Heydary H, Mortazavi-tabatabaei SA. 2011. The Significance Application of Indigenous Phytohemagglutinin ( PHA ) Mitogen on Metaphase and Cell Culture Procedure. Iran J Pharm Res 10: 895–903.

Naidoo R, Ungerer L, Cooper M, Pienaar S, Eley BS. 2010. Primary immunodeficiencies: A 27-year review at a tertiary paediatric hospital in Cape Town, South Africa. J Clin Immunol 31:99–105; doi:10.1007/s10875-010-9465-7.

Naranbhai V. 2016. The Role of Host Genetics (and Genomics) in Tuberculosis. Microbiol Spectr 4:1–36; doi:10.1128/microbiolspec.TBTB2-0011-2016.

Neehus AL, Lam J, Haake K, Merkert S, Schmidt N, Mucci A, et al. 2017. Impaired IFNγ-Signaling and Mycobacterial Clearance in IFNγR1-Deficient Human iPSC-Derived Macrophages. Stem Cell Reports 10:7–16; doi:10.1016/j.stemcr.2017.11.011.

Nimmerjahn F, Ravetch J V. 2008. Fcgamma receptors as regulators of immune responses. Nat Rev Immunol 8:34–47; doi:10.1038/nri2206.

North RJ, Jung Y-J. 2004. Immunity to tuberculosis. Annu Rev Immunol 22:599–623; doi:10.1146/annurev.immunol.22.012703.104635.

Nykamp K, Anderson M, Powers M, Garcia J, Herrera B, Ho YY, et al. 2017. Sherloc: A comprehensive refinement of the ACMG-AMP variant classification criteria. Genet Med 19:1105–1117; doi:10.1038/gim.2017.37.

O'Garra A, Redford PS, McNab FW, Bloom CI, Wilkinson RJ, Berry MP. 2013. The immune response in tuberculosis. Annu Rev Immunol 31:475–527; doi:10.1146/annurev-immunol-032712-095939.

Ochs HD, Hagin D. 2014. Primary immunodeficiency disorders: general classification, new molecular insights, and practical approach to diagnosis and treatment. Ann Allergy, Asthma Immunol 112:489–495; doi:10.1016/j.anai.2014.04.007.

Ochs HD, Petroni D. 2017. From clinical observations and molecular dissection to novel therapeutic strategies for primary immunodeficiency disorders. Am J Med Genet Part A 1–20; doi:10.1002/ajmg.a.38480.

Oliveira JB, Fleisher TA. 2010. Laboratory evaluation of primary immunodeficiencies. J Allergy Clin Immunol 125:S297-305; doi:10.1016/j.jaci.2009.08.043.

Orme IM, Andersen P, Boom WH. 1993. T cell response to Mycobacterium tuberculosis. J Infect Dis 167: 1481–1497.

Ozbek N, Fieschi C, Yilmaz BT, de Beaucoudrey L, Demirhan B, Feinberg J, et al. 2005. Interleukin-12 Receptor 1 Chain Deficiency in a Child with Disseminated Tuberculosis. Clin Infect Dis 40:e55–e58; doi:10.1086/427879.

Parvaneh N, Pourakbari B, Rezaei N, Omidvar A, Sabouni F, Mahmoudi S, et al. 2015a. Impaired in-vitro responses to IL-12 and IFN-?? in Iranian patients with Mendelian susceptibility to mycobacterial disease. Allergol Immunopathol (Madr) 43:456–460; doi:10.1016/j.aller.2014.05.008.

Pellegrini E, Desfosses A, Wallmann A, Schulze WM, Rehbein K, Mas P, et al. 2018. RIP2 filament formation is required for NOD2 dependent NF-κB signalling. Nat Commun 9:4043; doi:10.1038/s41467-018-06451-3.

Pertovaara M, Silvennoinen O, Isomäki P. 2016. Cytokine-induced STAT1 activation is increased in patients with primary Sjögren's syndrome. Clin Immunol 165:60–67; doi:10.1016/j.clim.2016.03.010.

Picard C, Bobby Gaspar H, Al-Herz W, Bousfiha A, Casanova J-L, Chatila T, et al. 2018. International Union of Immunological Societies: 2017 Primary Immunodeficiency Diseases Committee Report on Inborn Errors of Immunity. J Clin Immunol 38:96–128; doi:10.1007/s10875-017-0464-9.

Picard C, Fieschi C, Altare F, Al-Jumaah S, Al-Hajjar S, Feinberg J, et al. 2002. Inherited Interleukin-12 Deficiency: IL12B Genotype and Clinical Phenotype of 13 Patients from Six Kindreds. Am J Hum Genet 70:336–348; doi:10.1086/338625.

Principi N, Esposito S. 2014. Vaccine use in primary immunodeficiency disorders. Vaccine 32:3725–3731; doi:10.1016/j.vaccine.2014.05.022.

Qiagen®. 2015. QuantiFERON®-TB Gold Plus (QFT®-Plus) ELISA Package. 45.

Qu HQ, Fisher-Hoch SP, McCormick JB. 2011. Molecular immunity to mycobacteria: Knowledge from the mutation and phenotype spectrum analysis of Mendelian susceptibility to mycobacterial diseases. Int J Infect Dis 15:e305–e313; doi:10.1016/j.ijid.2011.01.004.

Queval CJ, Brosch R, Simeone R. 2017. The Macrophage: A Disputed Fortress in the Battle against Mycobacterium tuberculosis. Front Microbiol 8:1–11; doi:10.3389/fmicb.2017.02284.

Ramirez-Alejo N, Santos-Argumedo L. 2014. Innate Defects of the IL-12/IFN-γ Axis in Susceptibility to Infections by Mycobacteria and Salmonella. J Interf Cytokine Res 34:307–317; doi:10.1089/jir.2013.0050.

Reed B, Dolen WK. 2018. The Child with Recurrent Mycobacterial Disease. Curr Allergy Asthma Rep 18; doi:10.1007/s11882-018-0797-3.

Riazi S, Zeligs B, Yeager H, Peters SM, Benavides GA, Di Mita O, et al. 2012. Rapid diagnosis of Mycobacterium tuberculosis infection in children using interferon-gamma release assays (IGRAs). Allergy asthma Proc 33:217–226; doi:10.2500/aap.2012.33.3574.

Riedel DD, Kaufmann SH. 1997. Chemokine secretion by human polymorphonuclear granulocytes after stimulation with Mycobacterium tuberculosis and lipoarabinomannan. Infect Immun 65: 4620–4623.

Rivas-Santiago B, Schwander SK, Sarabia C, Diamond G, Klein-Patel ME, Hernandez-Pando R, et al. 2005. Human {beta}-defensin 2 is expressed and associated with Mycobacterium tuberculosis during infection of human alveolar epithelial cells. Infect Immun 73:4505–4511; doi:10.1128/IAI.73.8.4505-4511.2005.

Robinson RT. 2015. IL12RB1: The cytokine receptor that we used to know. Cytokine 71:348–359; doi:10.1016/j.cyto.2014.11.018.

Roederer M. 2001. Spectral compensation for flow cytometry: Visualization artifacts, limitations, and caveats. Cytometry 45:194–205; doi:10.1002/1097-0320(20011101)45:3<194::AID-CYTO1163>3.0.CO;2-C.

Rothwarf DM, Zandi E, Natoli G, Karin M. 1998. IKK-γ is an essential regulatory subunit of the IκB kinase complex. Nature 395: 297.

Routes J, Abinun M, Al-Herz W, Bustamante J, Condino-Neto A, De La Morena MT, et al. 2014. ICON: The early diagnosis of congenital immunodeficiencies. J Clin Immunol 34:398–424; doi:10.1007/s10875-014-0003-x.

Sasaki Y, Nomura A, Kusuhara K, Takada H, Ahmed S, Obinata K, et al. 2002. Genetic Basis of Patients with Bacille Calmette-Guérin Osteomyelitis in Japan: Identification of Dominant Partial Interferon-γ Receptor 1 Deficiency as a Predominant Type. J Infect Dis 185:706–709; doi:10.1086/339011.

Schluger NW, Rom WN. 1998. State of the Art The host: Immune response to tuberculosis. Am J Respir Crit Care Med 157:679–691; doi:10.1164/ajrccm.157.3.9708002.

Schwarz JM, Cooper DN, Schuelke M, Seelow D. 2014. MutationTaster2: mutation prediction for the deep-sequencing age. Nat Methods 11: 361–362.

Sharfe N, Nahum A, Newell A, Dadi H, Ngan B, Pereira SL, et al. 2014. Fatal combined immunodeficiency

associated with heterozygous mutation in STAT1. J Allergy Clin Immunol 133:807–817; doi:10.1016/j.jaci.2013.09.032.

Shen Y, Zhou D, Qiu L, Lai X, Simon M, Shen L, et al. 2002. Adaptive immune response of Vgamma2Vdelta2+ T cells during mycobacterial infections. Science 295:2255–2258; doi:10.1126/science.1068819.

Shi C, Wang F, Tong A, Zhang X, Song H, Liu Z-Y, et al. 2016. NFKB2 mutation in common variable immunodeficiency and isolated adrenocorticotropic hormone deficiency. Medicine (Baltimore) 95:e5081; doi:10.1097/MD.0000000000005081.

Srivastava S, Ernst JD, Desvignes L. 2014. Beyond macrophages: the diversity of mononuclear cells in tuberculosis. Immunol Rev 262:179–192; doi:10.1111/imr.12217.

Stray-Pedersen A, Sorte HS, Samarakoon P, Gambin T, Chinn IK, Coban Akdemir ZH, et al. 2017. Primary immunodeficiency diseases: Genomic approaches delineate heterogeneous Mendelian disorders. J Allergy Clin Immunol 139:232–245; doi:10.1016/j.jaci.2016.05.042.

Tiruviluamala P, Reichman LB. 2002. Tuberculosis. Annu Rev Public Health 23:403–426; doi:10.1146/annurev.publhealth.23.100901.140519.

Trunz BB, Fine P, Dye C. 2006. Effect of BCG vaccination on childhood tuberculous meningitis and miliary tuberculosis worldwide: a meta-analysis and assessment of cost-effectiveness. Lancet (London, England) 367:1173–1180; doi:10.1016/S0140-6736(06)68507-3.

Uzel G, Frucht DM, Fleisher TA, Holland SM. 2001. Detection of Intracellular Phosphorylated STAT-4 by Flow Cytometry. Clin Immunol 100:270–276; doi:10.1006/clim.2001.5078.

van de Vosse E, Ottenhoff THM. 2006. Human host genetic factors in mycobacterial and Salmonella infection: lessons from single gene disorders in IL-12/IL-23-dependent signaling that affect innate and adaptive immunity. Microbes Infect 8:1167–1173; doi:10.1016/j.micinf.2005.10.032.

van de Vosse E, van Dissel JT, Ottenhoff TH. 2009. Genetic deficiencies of innate immune signalling in human infectious disease. Lancet Infect Dis 9:688–698; doi:10.1016/S1473-3099(09)70255-5.

van den Berg S, van Rooyen C, Green RJ. 2017. We can do more to Identify Patients with Primary Immunodeficiencies. Curr Allergy Clin Immunol 30: 44–52.

Vankayalapati R, Barnes PF. 2009. Innate and adaptive immune responses to human Mycobacterium tuberculosis infection. Tuberculosis 89:S77–S80; doi:10.1016/S1472-9792(09)70018-6.

Villella A, Picard C, Jouanguy E, Dupuis S, Popko S, Abughali N, et al. 2001. Recurrent Mycobacterium avium Osteomyelitis Associated With a Novel Dominant Interferon Gamma Receptor Mutation. Pediatrics 107: 1–3.

Vinuesa CG, Tangye SG, Moser B, Mackay CR. 2005. Follicular B helper T cells in antibody responses and autoimmunity. Nat Rev Immunol 5:853–865; doi:10.1038/nri1714.

Volkman HE, Pozos TC, Zheng J, Davis JM, Rawls JF, Ramakrishnan L. 2010. Tuberculous granuloma induction via interaction of a bacterial secreted protein with host epithelium. Science 327:466–469; doi:10.1126/science.1179663.

Wang LH, Yen CL, Chang TC, Liu CC, Shieh CC. 2012. Impact of molecular diagnosis on treating Mendelian susceptibility to mycobacterial diseases. J Microbiol Immunol Infect 45:411–417;

doi:10.1016/j.jmii.2012.08.017.

WHO. 2016. Global Tuberculosis Report 2016. In: *Global Tuberculosis Report 2016*. World Health Organization. 214.

Wirth T, Hildebrand F, Allix-Béguec C, Wölbeling F, Kubica T, Kremer K, et al. 2008. Origin, spread and demography of the Mycobacterium tuberculosis complex. PLoS Pathog 4; doi:10.1371/journal.ppat.1000160.

World Health Organization. 2017. *Global Tuberculosis Report 2017: Leave no one behind - Unite to end TB*.

Wu U, Holland SM. 2015. Host susceptibility to non-tuberculous mycobacterial infections. Lancet Infect Dis 15:968–980; doi:10.1016/S1473-3099(15)00089-4.

Yao BB, Niu P, Surowy CS, Faltynek CR. 1999. Direct Interaction of STAT4 with the IL-12 Receptor. Arch Biochem Biophys 368:147–155; doi:10.1006/abbi.1999.1302.

# Appendix A

# PARTICIPANT INFORMATION AND INFORMED CONSENT FORM FOR RESEARCH INVOLVING GENETIC STUDIES

**TITLE OF RESEARCH PROJECT:**

**Identification of novel candidate genes for susceptibility to tuberculosis by identifying disease causing mutations in individuals with Primary Immunodeficiencies.**

**REFERENCE NUMBER:**

**PRINCIPAL INVESTIGATOR: Dr Craig Kinnear**

**ADDRESS: Department of Biomedical Sciences,**
**Faculty of Medicine and Health Sciences**
**Stellenbosch University**
**P.O. Box 19063**
**Tygerberg.**

**CONTACT NUMBER: (021) 938 9695/ 076 094 8957**

We would like to invite you to participate in a research study that involves genetic analysis and possible long-term storage of blood or tissue specimens. Please take some time to read the information presented here which will explain the details of this project. Please ask the study staff or doctor any questions about any part of this project that you do not fully understand. It is very important that you are fully satisfied that you clearly understand what this research entails and how you could be involved. Also, your participation is **entirely voluntary** and you are free to decline to participate. If you say no, this will not affect you negatively in any way whatsoever. You are also free to withdraw from the study at any point, even if you do agree to take part initially.

This research study has been approved by the ethics **Health Research Ethics Committee at Stellenbosch University** and it will be conducted according to international and locally accepted ethical guidelines for research, namely the Declaration of Helsinki, and the SA Department of Health's 2004 Guidelines: *Ethics in Health Research: Principles, Structures and Processes.*

**What is Genetic research?**
Genetic material, also called DNA or RNA, is usually obtained from a small blood sample. Occasionally genetic material is obtained from other sources such as saliva or biopsy specimens. (A biopsy is a tiny piece of tissue that is cut out e.g. from the skin or from a lump, to help your doctor make a diagnosis.) Genes are found in every cell in the human body. The genes are the instructions that tell the body how to grow and function. The genes determine what we look like and sometimes what kind of diseases we may be susceptible to. Worldwide, researchers in the field of genetics are continuously discovering new

information that may be of great benefit to future generations and also that may benefit people today, who suffer from particular diseases or conditions.

**What does this particular research study involve?**

- The immune system refers to the body cells that fight infection. A person with a faulty immune system will get infections much more easily than other people. This person has an 'immune deficiency'. There are many causes of immune deficiency, and we still don't know all the possible causes. Some immune deficiencies are caused by 'faulty genes' as described below.
- The genes are instructions that are passed on from parent to child in the egg cell and sperm cell. Some of these instructions are for how the immune system will work, and each gene tells a specific part of the immune system how to work.
- If there is a fault (mutation) in one of these genes, the person will have an immune deficiency.
- Currently we do not know all of the genes and gene faults that cause immune deficiency. Therefore, we are aiming to find out more about:
  - The genes that cause immune deficiency.
  - The gene fault(s) causing immune deficiency in your family.
- We will do genetic testing to try and identify the cause of immune deficiency in each affected person who participates in the study. The type of genetic test will vary in different people.
  - In some people the test might target certain known genes in the immune system.
  - In other people we will do a much broader screen for gene faults (mutations), to see if we can identify the cause of the immune deficiency. This test is called 'exome sequencing'. Exome sequencing screens all or most of the known genes in the body, because we don't yet know the functions of all these genes. This allows us to test for a lot more gene faults to see if these are causing the immune deficiency. However, exome sequencing may also detect faults in genes that can cause a different disease.

**Why have you been invited to participate?**

- Your child has an immune deficiency that might be caused by a gene fault. However, we do not know what this gene fault is.
- We would like to do genetic tests to try and identify the gene fault (mutation).

**What procedures will be involved in this research?**

- A doctor or nurse will draw 5ml (one teaspoon) of blood from your child so that we can extract the DNA. We will then do all our genetic tests on your child's DNA.
- In some cases we may also draw 5-10ml (one to two teaspoons) of blood at a later stage from you (the available parents of the child) for comparison purposes.

**Are there any risks involved in genetic research?**

- If exome sequencing is conducted, there is a small chance that we will detect a gene fault that shows susceptibility to another condition (e.g. for developing cancer). Some of these conditions may only be expected to develop in adulthood and may therefore have no immediate importance to a child with immunodeficiency. However the same fault may be present in a parent and perhaps other family members.
- It may therefore be beneficial for you to know about such gene faults, especially if they can cause a condition that can be prevented or treated. However, knowledge of such gene faults can sometimes have negative effects:
    - It may cause anxiety or other negative feelings.
    - There is chance that a person who carries such a gene fault may be stigmatised in some way, e.g. within the family.
    - This can apply to the child or to adults found to have gene faults.
- We therefore ask you to decide in advance whether you want us to inform you, if we detect such other (incidental) gene faults.
- Results will be made known **only if they indicate**:
    - A definite risk for developing a particular disorder.
    - Require genetic counselling.
- In addition, if we do genetic tests on the parents as well as the child, there is a chance that it will give us unexpected information about the family, e.g. that the father is not the biological of the child. We do not specifically report this information, but there is a chance it will be apparent from genetic information we report back regarding gene faults detected in the family.
- We further request your consent to enter your information onto the South African PID and linked international databases. The database will contain information about you and your attending doctors as well as laboratory results, relative clinical findings and treatment used. This will be followed up at 6 or 12 monthly intervals. If you agree and if the genetic mutations (changes in the normal inheritance pattern) causing you/your child's medical condition are known, they can be stored anonymously in a European database for the documentation and analysis of mutations involved in immunodeficiencies. This database is hosted by the Institute of Medical Technology at the University of Tampere, Finland (http://bioinf.uta.fi/idr/) with the aim of collecting immunodeficiency data to improve the understanding of PID and ultimately improve the treatment of these diseases. Mutation data is transferred anonymously to this database through a secure connection from the ESID (European Society for Immunodeficiency Diseases) database. For the South African database the data will be entered with patient name and residential address but for international registries such as the ESID or African Society for Immunodeficiencies (ASID), patient information will be anonymous without the name or address given. Your/ your child's data will only be made available on request for research purposes with the permission of the Registry panel. If you decide not to agree to have your/ your child's information stored in these databases, it will not affect you negatively and you/your child will still be able to take part in the study.

**Tick the options you choose:**

I **AGREE** that my/my child's information be stored in the databases as explained above ☐

**OR**

I **DO NOT AGREE** that my/my child's information be stored in the databases as explained above ☐

**Are there any benefits to your taking part in this study and will you get told your results?**

- We will inform you if we detect the gene faults causing immune deficiency in your child. If we do detect a specific gene fault, this knowledge:
  - May or may not make a difference to the treatment we offer your child.
  - May allow us to offer genetic testing in the family (e.g. for prenatal diagnosis of future pregnancies).
- Please note that we cannot guarantee that we will get any results which we can feed back, or how long it will take.
- We will inform you of coincidental gene faults we detect that may cause other conditions - if you have indicated that you want to be informed.
- Please note that if we do not detect any gene faults, this does not guarantee that none are present, because not all gene faults can be detected by current methods.
- Any results reported back to you will be discussed with you by a genetic counselling professional (genetic counsellor/clinical geneticist), who will also inform you about any implications for the family.
- Findings from this study may benefit people with immune deficiencies in the future.

**How long will your blood be stored and where will it be stored?**

- DNA will be stored at the University of Stellenbosch until we have detected the gene faults causing immune deficiency in your family.
- Afterwards it may continue to be stored and used to help establish tests for other people with immune deficiencies. If you do not wish your blood specimen to be stored after this research study is completed you will have an opportunity to request that it be discarded when you sign the consent form.
- We work together with colleagues in South Africa and overseas. Your DNA samples may be sent to such colleagues for further testing.

**If your blood is to be stored is there a chance that it will be used for other research?**

Your and your child's blood will only be used for genetic research that is directly related to immune deficiency.

**How will your confidentiality be protected?**

- We will keep your genetic information private. DNA samples are identified only by a study number. This is linked to your personal information on a database that is kept private and protected by a password.
- If your sample is sent to any other colleagues, they will have access to your study number, and to details of the condition we are looking for, but not to your personal details.
- If we do find any gene faults we will do our best to contact you using the contact details you supply us. Please contact us with any change in your contact details using the contact details on this form.

**Will you or the researchers benefit financially from this research?**

You will not be paid to take part in this study.

**Important information: In the unlikely event that this research leads to the development of a commercial application or patent, you or your family will not receive any profits or royalties**

**Is there anything else that you should know or do?**

- You should inform your family practitioner or usual doctor that you are taking part in a research study. (*Include if applicable*)
- You should also inform your medical insurance company that you are participating in a research study.
- While you are not required to inform any current insurance company about any incidental findings, you would be required to inform any future insurance company about any incidental findings that may increase your risk of developing pathological conditions.
- You can contact Dr Craig Kinnear at tel (021) 938 9695, Dr Monika Esser at 021-938-5995, Dr Mike Urban at 021-938-9807 or Mardelle Schoeman at 021-938-9807 if you have any further queries or encounter any problems.
- You can contact the Health Research Ethics Committee at 021-938 9207 if you have any concerns or complaints that have not been adequately addressed by your study doctor.
- You will receive a copy of this information and consent form for your own records.

## Declaration by participant

By signing below, I ……..…… agree to take part in a genetic research study entitled *(Identification of novel candidate genes for susceptibility to tuberculosis by identifying disease causing mutations in individuals with Primary Immunodeficiencies)*.

I declare that:

- I have read or had read to me this information and consent form and it is written in a language with which I am fluent and comfortable.
- I have had a chance to ask questions and all my questions have been adequately answered.
- I understand that taking part in this study is voluntary and I have not been pressurised to take part.
- I have received a signed duplicate copy of this consent form for my records.

**Tick the options you choose:**

☐ **I agree that blood or tissue samples can be stored on my child ..... / myself indefinitely / stored for ……years,** but I can choose to request at any time that my stored sample be destroyed. My sample will be identified with a special study number that will remain linked to my name and contact details. I have the right to receive confirmation that my request has been carried out.

By choosing this option I indicate that I wish to receive results regarding the gene fault detected that may be causing the immune deficiency in my family.

In addition I choose:

☐ To receive other coincidentally detected results

☐ Not to receive other coincidentally detected results

**OR**

☐ **I agree that blood or tissue sample can be stored on my child …….. / myself indefinitely / stored for ……years** after the project is completed but that it is anonymised with all possible links to my identity removed, and that the researchers may then use it for additional research in this or a related field. Once my sample is anonymised, my rights to that sample are waivered. My sample may be shipped to another laboratory in SA or abroad to be used in other research projects in this or a related field

**OR**

☐ Please destroy my blood sample as soon as the current research project has been completed.

Signed at (*place*) ..... on (*date*) .....

..... .....

**Signature of participant** **Signature of witness**

## Declaration by investigator

I *(name)* …… declare that:

- I explained the information in this document to ……..……...
- I encouraged him/her to ask questions and took adequate time to answer them.
- I am satisfied that he/she adequately understands all aspects of the research as discussed above.
- I did/did not use a interpreter. (*If a interpreter is used then the interpreter must sign the declaration below.*

Signed at (*place*) .....…….....…….. on (*date*) ……...…….. .

..... .....
**Signature of investigator** **Signature of witness**

## Declaration By Interpreter

I *(name)* …… declare that:

- I assisted the investigator (*name*) ……. to explain the

  information in this document to (*name of participant*) ……..

  using the language medium of Afrikaans/Xhosa.

- We encouraged him/her to ask questions and took adequate time to answer them.
- I conveyed a factually correct version of what was related to me.
- I am satisfied that the participant fully understands the content of this informed consent document and has had all his/her question satisfactorily answered.

Signed at (*place*) .....…….....…….. on (*date*) ……...……...

..... .....
**Signature of interpreter** **Signature of witness**

# Appendix B

# PARTICIPANT INFORMATION AND INFORMED CONSENT FORM FOR RESEARCH INVOLVING IMMUNE FUNCTION STUDIES

**TITLE OF RESEARCH PROJECT:**

Identification of novel candidate genes for susceptibility to tuberculosis by identifying disease causing mutations in individuals with primary Immunodeficiencies – Functional Studies

**REFERENCE NUMBER: N13/05/075**

We would like to invite you to participate in a research study that involves functional immune analysis of blood specimens. Please take some time to read the information presented here which will explain the details of this project. Please ask the study staff or doctor any questions about any part of this project that you do not fully understand. It is very important that you are fully satisfied that you clearly understand what this research entails and how you could be involved. Also, your participation is **entirely voluntary,** and you are free to decline to participate. If you say no, this will not affect you negatively in any way whatsoever. You are also free to withdraw from the study at any point, even if you do agree to take part initially.

This research study has been approved by the ethics **Committee for Human Research at Stellenbosch University** and it will be conducted according to international and locally accepted ethical guidelines for research, namely the Declaration of Helsinki, and the SA Department of Health's 2004 Guidelines: *Ethics in Health Research: Principles, Structures and Processes.*

**What does this particular research study involve?**

- The immune system refers to the body cells that fight infection. A person with a faulty immune system will get infections much more easily than other people. This person has an 'immune deficiency'. There are many causes of immune deficiency, and we still don't know all the possible causes. Some immune deficiencies are caused by 'faulty genes' as described below.

- The genes are instructions that are passed on from parent to child in the egg cell and sperm cell. Some of these instructions are for how the immune system will work, and each gene tells a specific part of the immune system how to work.
- If there is a fault (mutation) in one of these genes, the person will have an immune deficiency.
- Currently we do not know all of the genes and gene faults that cause immune deficiency. Therefore, we are aiming to find out more about:
    - The genes that cause immune deficiency.
    - The gene fault(s) causing immune deficiency in your family.
- We will do genetic testing to try and identify the cause of immune deficiency in each affected person who participates in the study. The type of genetic test will vary in different people.
    - In some people the test might target certain known genes in the immune system.
    - In other people we will do a much broader screen for gene faults (mutations), to see if we can identify the cause of the immune deficiency. This test is called 'exome sequencing'. Exome sequencing screens all or most of the known genes in the body, because we don't yet know the functions of all these genes. This allows us to test for a lot more gene faults to see if these are causing the immune deficiency. However, exome sequencing may also detect faults in genes that can cause a different disease.
- When a genetic mutation is found, further research is done in order to describe the effect of the mutation on immune function.

**Why have you been invited to participate?**

You are a healthy volunteer, and you are therefore the ideal person to participate in this study as a 'healthy control'. Approximately 6-15 healthy controls will participate in this particular project.

**What procedures will be involved in this research?**

For getting the blood samples, a sterile needle will be used to draw blood from a vein in the arm. The amount of blood drawn will be 5-15ml, depending on age and body weight. This is not an amount that poses any dangers to a healthy adult.

White blood cells, or peripheral blood mononuclear cells (PBMCs), will be extracted from the blood for immune functional investigation.

**Are there any risks involved in this research?**

You may experience minor pain and/or bruising at the site where blood is taken. Any related injury, which is highly unlikely, will be managed by the nurse or doctor taking the blood.

Some insurance companies may mistakenly assume that taking part in genetic research indicates a higher risk for disease. Thus, no information about you or your family will be shared with such companies.

Controls for functional studies are NOT genetically analysed, therefore risks associated with genetic studies does not apply.

## Are there any benefits to your taking part in this study and will you get told your results?

While the research project may not be directly beneficial to you, the results of the research will help us to understand how the immune system functions and this information may help us in the future to diagnose patients with immune defects related to TB susceptibility.

Your personal results will be made known to you **only if they indicate** that you may:

- Have a definite risk for developing a particular disorder.
- Have a condition or predisposition to developing a condition that is treatable or avoidable e.g. by a lifestyle modification.
- Need genetic counselling.

## How long will your blood be stored and is there a chance that it will be used for other research?

PBMCs may be stored to be tested at a later date, however ALL remaining control samples will be destroyed upon completion of functional studies.

Your blood will not be used in any other studies.

## How will your confidentiality be protected?

All personal information obtained from this study will be strictly confidential. Only the Principal Investigators at Stellenbosch University and the nursing sister who takes consent from you will have access to the information that links the blood samples to the nominal data (names and addresses). Confidentiality will be protected by the Health Professionals Council of South Africa's guidelines. The results of the study will be published in medical or science journals, but without mentioning the name of any person on whom blood was taken. Research Ethics Committee members may need to inspect research records. This committee can be contacted at 021 938 9207.

**Will you or the researchers benefit financially from this research?**

You will not be paid to take part in this study.

**Important information: In the unlikely event that this research leads to the development of a commercial application or patent, you or your family will not receive any profits or royalties**

## Declaration by participant

By signing below, I ……..……. agree to take part in a genetic research study entitled:

**Identification of novel candidate genes for susceptibility to tuberculosis by identifying disease causing mutations in individuals with primary Immunodeficiencies – Functional Studies**

I declare that:

- I have read or had read to me this information and consent form and it is written in a language with which I am fluent and comfortable.
- I have had a chance to ask questions and all my questions have been adequately answered.
- I understand that taking part in this study is voluntary and I have not been pressurised to take part.
- I have received a signed duplicate copy of this consent form for my records.

Signed at (*place*) ..... on (*date*) .....

..... .....

**Signature of participant** **Signature of witness**

## Declaration by investigator

I *(name)* …… declare that:

- I explained the information in this document to ……..……...
- I encouraged him/her to ask questions and took adequate time to answer them.
- I am satisfied that he/she adequately understands all aspects of the research as discussed above.
- I did/did not use a interpreter. (*If an interpreter is used then the interpreter must sign the declaration below.*

Signed at (*place*) .....…..…….. on (*date*) ……...…….. 2005.

| | |
|---|---|
| ..... | ..... |
| **Signature of investigator** | **Signature of witness** |

# Appendix C

## *In-silico* prediction tools for characterising genetic variants

**Table C.1: Description of each of the *in-silico* prediction tools used in this study to determine pathogenicity of identified variants**

| | |
|---|---|
| SIFT | The Sorting Intolerant from Tolerant, or SIFT, tool predicts the functional importance of amino acid substitution based on the alignment of paralogous and/or orthologous protein sequences |
| PolyPhen | Polymorphism Phenotyping, or PolyPhen, tool can predict the functional importance of an amino acid substitution by considering evolutionary conservation, physiochemical differences and proximity of substitution to predicted functional or structural domains |
| MutationTaster2 | MutationTaster can predict the functional consequences of not only amino acid substitutions but also intronic and synonymous alterations, short insertions and/or deletion (indel) mutations and variants that span intron-exon borders. |
| CADD Score | The Combined Annotation-Dependent Depletion (CADD) method integrates many diverse annotations of genetic variations into a single measurement, a CADD score, for each variant. CADD scores correlate with allelic diversity, pathogenicity, disease severity, etc. |
| | |
| ACMG Criteria | The American College of Medical Genetics and Genomics (ACMG) criteria provides guidance for the interpretation of sequence variants. The ACMG criteria describes genetic variants as “pathogenic”, “likely pathogenic”, “uncertain significance”, “likely benign”, and “benign” based on five different categories of evidence: functional data, population data, computational data and segregation data. |
| Sherloc Criteria | Sherloc (semiquantitative, hierarchical evidence-based rules for locus interpretation) is a variant classification framework that is essentially a refinement of the ACMG criteria. |

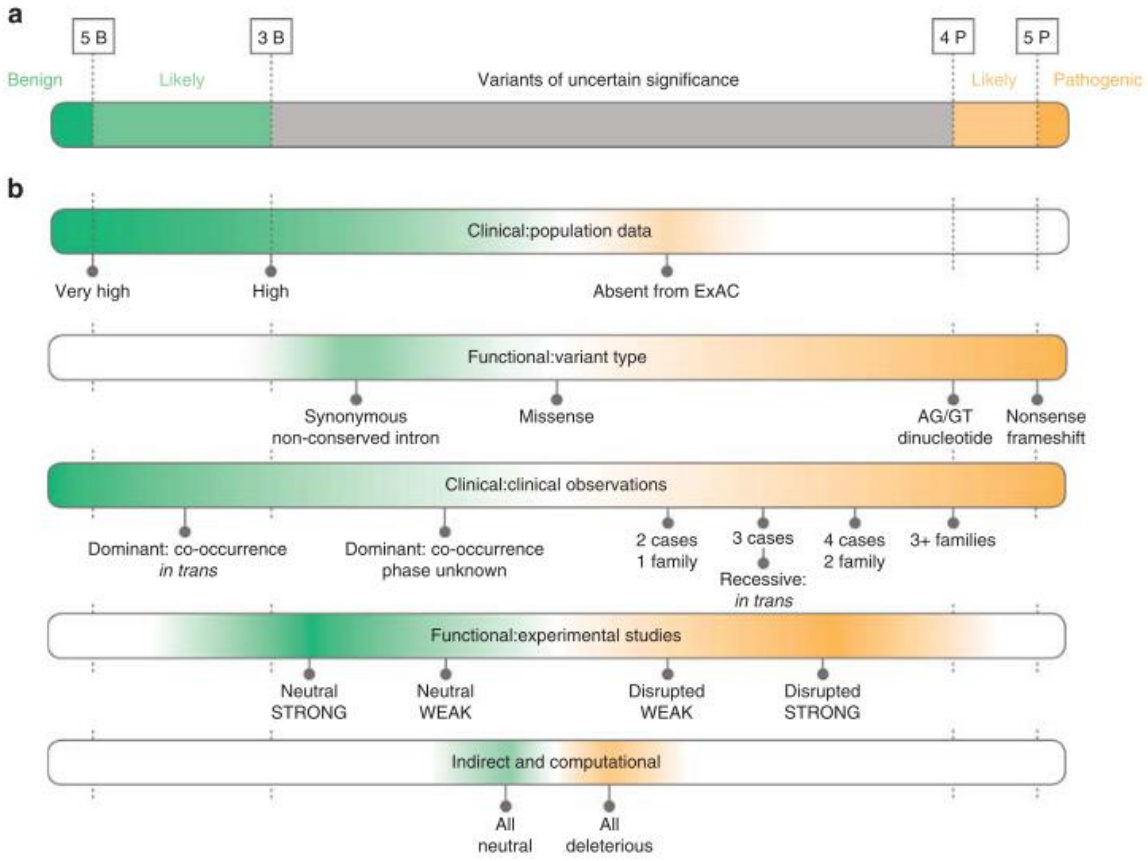


**Figure C.1: Scoring thresholds and evidence categories used for assessment of genetic variants**. (a) Thresholds for scoring variants as pathogenic, likely pathogenic, uncertain significance, likely benign, and benign. (b) Evidence, in the order that they are evaluated, that is used to score genetic variants (Nykamp et al. 2017)

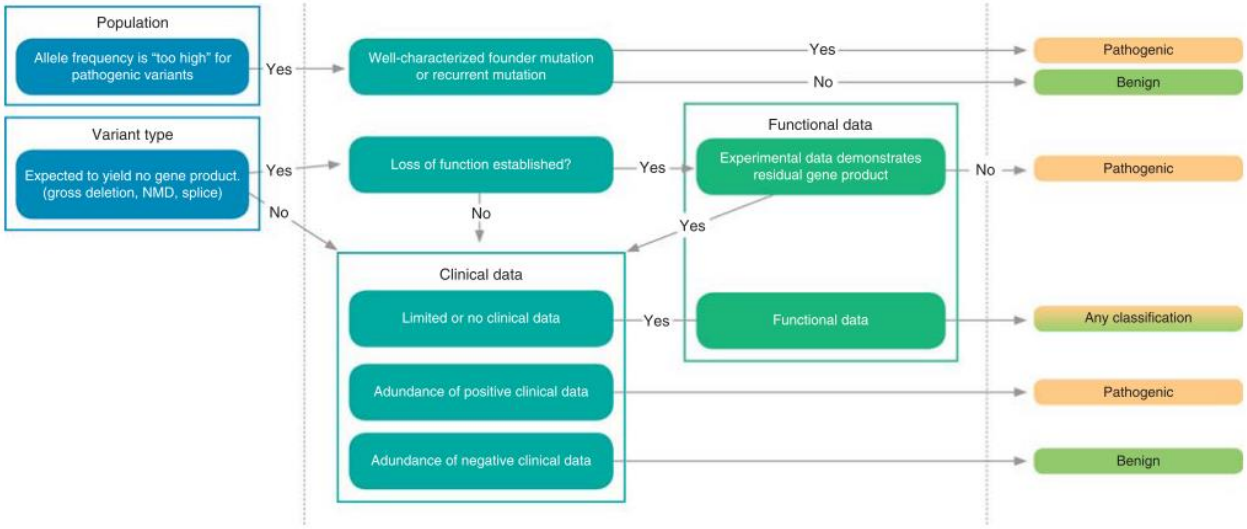


**Figure C.2: Hierarchical approach to efficient variant research**, as suggested by Nykamp et al. (2017). Evaluation of evidence for pathogenicity prediction usually goes from the simplest type (i.e. population data and variant type) to the more complex type evidence (i.e. clinical data and functional data).

# Appendix D

## Primers used for Sanger Sequencing

***IFNGR1*** **PID01**

| | Start | Stop | Length | Tm | GC% |
|---|---|---|---|---|---|
| Forward CCTAACTTCTGCTTCCTTCAGT (Sense) | 64 | 86 | 22 | 62 | 45.5 |
| Reverse GCAGGTGACATCTTGTTGAATATC (AntiSense) | 426 | 450 | 24 | 62 | 41.7 |

***NOD2*** **PID02**

| | Start | Stop | Length | Tm | GC% |
|---|---|---|---|---|---|
| Forward CTGGACACCGTCTGGAATAAG (Sense) | 323 | 344 | 21 | 62 | 52.4 |
| Reverse TTTCCTGCCAAGAGTCAAGAG (AntiSense) | 744 | 765 | 21 | 62 | 47.6 |

***IFNGR1*** **PID02**

| | Start | Stop | Length | Tm | GC% |
|---|---|---|---|---|---|
| Forward CCCATAGATCTCTGTGGTAAGAAG (Sense) | 75 | 99 | 24 | 62 | 45.8 |
| Reverse GGTGAAGAACTCTCTCTCTCTATTG (AntiSense) | 338 | 363 | 25 | 62 | 44 |

***IKZF1*** **PID03**

| | Start | Stop | Length | Tm | GC% |
|---|---|---|---|---|---|
| Forward GCTACGAGAAGGAGAACGAAAT (Sense) | 209 | 231 | 22 | 62 | 45.5 |
| Reverse CTGCTCCTCGTTGTTGCT (AntiSense) | 520 | 538 | 18 | 62 | 55.6 |

***IFNGR1*** **PID03**

| | Start | Stop | Length | Tm | GC% |
|---|---|---|---|---|---|
| Forward ATACTCACGCAGAAGGAAGATG (Sense) | 239 | 261 | 22 | 62 | 45.5 |
| Reverse CCATCACATGGCTTTCCAAATTA (AntiSense) | 607 | 630 | 23 | 62 | 39.1 |

***IL12RB1*** **PID04**

| | Start | Stop | Length | Tm | GC% |
|---|---|---|---|---|---|
| Forward GCCAAGTCCTGGACAATTCTTA (Sense) | 136 | 158 | 22 | 62 | 45.5 |
| Reverse ACTCCTGACCTCAAGTGATCT (AntiSense) | 553 | 574 | 21 | 62 | 47.6 |

***IL12RB1*** **PID05**

| | Start | Stop | Length | Tm | GC% |
|---|---|---|---|---|---|
| Forward GAAACAGCCAAACACAGACAC (Sense) | 36 | 57 | 21 | 62 | 47.6 |
| Reverse TTCCAGGCCATTACCCATTC (AntiSense) | 341 | 361 | 20 | 62 | 50 |

***IL12B* PID06**

| | Start | Stop | Length | Tm | GC% |
|---|---|---|---|---|---|
| Forward ACCAGAGCAGTGAGGTCTTA (Sense) | 285 | 305 | 20 | 62 | 50 |
| Reverse GTTGATAACCCAAAGGGTCCA (AntiSense) | 627 | 648 | 21 | 62 | 47.6 |

***NFKB2* PID06 & PID10**

| | Start | Stop | Length | Tm | GC% |
|---|---|---|---|---|---|
| Forward CTCCAGGCTGGGCAATAAG (Sense) | 17 | 36 | 19 | 62 | 57.9 |
| Reverse GTGGGTCAGGGCTAGGT (AntiSense) | 378 | 395 | 17 | 62 | 64.7 |

***IL12B* PID07**

| | Start | Stop | Length | Tm | GC% |
|---|---|---|---|---|---|
| Forward CTCAGCTTACCCTGTGACTATG (Sense) | 179 | 201 | 22 | 62 | 50 |
| Reverse TTCCTGCAATATCCCTGTGG (AntiSense) | 564 | 584 | 20 | 62 | 50 |

***IFNGR2* PID08**

| | Start | Stop | Length | Tm | GC% |
|---|---|---|---|---|---|
| Forward CCTTTCAGAAGCAACTCCATTTC (Sense) | 174 | 197 | 23 | 62 | 43.5 |
| Reverse TGCAGTTCAGCACTCTTCTC (AntiSense) | 436 | 456 | 20 | 62 | 50 |

***CYBB* PID09**

| | Start | Stop | Length | Tm | GC% |
|---|---|---|---|---|---|
| Forward GATGACTGCATCTCTCTGAACC (Sense) | 44 | 66 | 22 | 62 | 50 |
| Reverse CAACATATCCAACCACCACTTAATC (AntiSense) | 389 | 414 | 25 | 62 | 40 |

***IKBKB* PID10**

| | Start | Stop | Length | Tm | GC% |
|---|---|---|---|---|---|
| Forward TTGTCCTGATTTCCTCCTGAAG (Sense) | 55 | 77 | 22 | 62 | 45.5 |
| Reverse CTGCACAAGGCCTGCTAT (AntiSense) | 242 | 260 | 18 | 62 | 55.6 |

***IRAK1* PID11**

| | Start | Stop | Length | Tm | GC% |
|---|---|---|---|---|---|
| Forward CTGCCCTTGGACTTCTCTG (Sense) | 12 | 31 | 19 | 62 | 57.9 |
| Reverse CAGCTTCTGGACCATCTTCT (AntiSense) | 193 | 213 | 20 | 61 | 50 |

# Appendix E

**Table E.1: CD119/IFN-γR1 expression levels (%) and receptor densities (MFI) for each of the cell subsets**. Values in blue or red are either below or above the respective normal ranges.

| | FSC vs. SSC Monocytes | | CD14+ | | FSC vs. SSC Lymphocytes | | CD56+ | | CD3+CD56+ | | CD3+ | | CD4+ | | CD8+ | | CD4-CD8- | | CD19+ | |
|---|---|---|---|---|---|---|---|---|---|---|---|---|---|---|---|---|---|---|---|---|
| | %CD119 + IQR: 41-63 | CD119 MFI IQR: 310-474 | %CD119 + IQR: 57-83 | CD119 MFI IQR: 625-790 | %CD119 + IQR: 26-35 | CD119 MFI IQR: 71-87 | %CD119 + IQR: 39-50 | CD119 MFI IQR: 51-66 | %CD119 + IQR: 31-47 | CD119 MFI IQR: 96-119 | %CD119 + IQR: 24-27 | CD119 MFI IQR: 72-88 | %CD119 + IQR: 19-25 | CD119 MFI IQR: 67-79 | %CD119 + IQR: 21-28 | CD119 MFI IQR: 103-120 | %CD119 + IQR: 25-42 | CD119 MFI IQR: 59-98 | %CD119 + IQR: 68-81 | CD119 MFI IQR: 98-130 |
| **PID01** | 97.20 | 2646 | 99.30 | 5451 | 98.70 | 506 | 97.50 | 328 | 99.20 | 515 | 99.30 | 511 | 99.40 | 482 | 99.90 | 557 | 95.40 | 375 | 99.40 | 707 |
| **Child of PID01** | 91.10 | 2649 | 97.10 | 4261 | 95.40 | 380 | 87.40 | 253 | 97.70 | 397 | 98.30 | 397 | 98.60 | 395 | 99.70 | 423 | 90.60 | 297 | 91.60 | 226 |
| **PID02** | 49.00 | 447 | 81.20 | 1175 | 34.40 | 106 | 34.40 | 45 | 44.00 | 168 | 29.40 | 126 | 29.60 | 108 | 25.20 | 173 | 28.70 | 83 | 80.40 | 164 |
| **Parent of PID02** | 44.30 | 363 | 62.60 | 702 | 38.00 | 118 | 41.60 | 61 | 40.50 | 151 | 33.60 | 120 | 33.30 | 108 | 31.40 | 154 | 22.10 | 70 | 88.20 | 171 |
| **PID03** | 29.00 | 282 | 51.50 | 588 | 30.40 | 99 | 33.50 | 51 | 32.00 | 122 | 25.10 | 101 | 24.50 | 94 | 21.80 | 137 | 25.10 | 73 | 69.70 | 112 |
| **PID04** | 57.60 | 454 | 83.80 | 917 | 33.30 | 97 | 55.20 | 76 | 27.50 | 105 | 24.80 | 98 | 23.70 | 92 | 21.90 | 123 | 30.90 | 71 | 63.90 | 96 |
| **PID05** | 42.90 | 523 | 46.90 | 704 | 33.40 | 122 | 30.90 | 67 | 27.10 | 146 | 19.50 | 122 | 17.80 | 103 | 17.60 | 151 | 31.00 | 143 | 64.90 | 134 |
| **PID06** | 52.50 | 423 | 71.80 | 820 | 33.70 | 130 | 51.80 | 77 | 35.90 | 150 | 27.10 | 130 | 26.60 | 119 | 25.20 | 157 | 27.90 | 82 | 76.40 | 132 |
| **PID07** | 39.10 | 275 | 65.80 | 759 | 28.00 | 100 | 31.50 | 39 | 28.60 | 117 | 22.50 | 105 | 22.20 | 100 | 19.00 | 128 | 26.20 | 67 | 60.50 | 94 |
| **PID08** | 60.10 | 423 | 56.50 | 536 | 46.90 | 134 | 59.40 | 100 | 25.80 | 144 | 25.10 | 110 | 24.80 | 99 | 21.00 | 193 | 25.00 | 116 | 89.70 | 211 |
| **PID09** | 44.10 | 305 | 77.10 | 698 | 36.20 | 91 | 48.30 | 65 | 40.20 | 108 | 27.40 | 86 | 25.10 | 82 | 29.10 | 115 | 25.70 | 60 | 69.90 | 113 |
| **PID10** | 63.60 | 519 | 84.70 | 827 | 32.00 | 78 | 41.00 | 47 | 35.40 | 100 | 25.70 | 75 | 24.10 | 66 | 22.80 | 106 | 36.60 | 69 | 69.40 | 108 |
| **PID11** | 49.00 | 449 | 66.00 | 855 | 29.00 | 79 | 37.90 | 63 | 25.40 | 85 | 20.50 | 77 | 19.20 | 68 | 18.70 | 97 | 32.30 | 80 | 63.70 | 104 |
| **PID12** | 56.00 | 382 | 57.00 | 519 | 31.10 | 122 | 43.40 | 56 | 38.40 | 151 | 27.20 | 120 | 26.60 | 109 | 23.40 | 152 | 33.10 | 92 | 87.40 | 168 |
| **PID13** | 35.10 | 272 | 32.60 | 394 | 29.20 | 98 | 37.60 | 47 | 30.30 | 119 | 23.00 | 103 | 21.70 | 97 | 20.40 | 129 | 31.60 | 92 | 59.10 | 85 |
| **PID14** | 32.20 | 275 | 48.80 | 563 | 30.60 | 100 | 35.60 | 41 | 25.10 | 107 | 24.80 | 100 | 25.70 | 96 | 23.00 | 118 | 21.80 | 70 | 74.60 | 128 |
| **PID15** | 66.30 | 655 | 82.10 | 917 | 28.80 | 80 | 33.20 | 45 | 34.90 | 107 | 19.90 | 79 | 19.40 | 76 | 18.90 | 106 | 17.20 | 36 | 72.30 | 110 |
| **PID16** | 42.40 | 401 | 59.00 | 745 | 24.00 | 87 | 19.30 | 30 | 39.90 | 129 | 17.80 | 95 | 16.90 | 90 | 17.00 | 125 | 17.50 | 70 | 69.30 | 119 |
| **PID17** | 62.20 | 500 | 67.00 | 704 | 30.10 | 73 | 39.40 | 56 | 23.80 | 78 | 21.80 | 72 | 20.70 | 65 | 19.60 | 91 | 25.70 | 66 | 60.10 | 85 |

**Table E.2: CD212/IL-12Rβ1 expression levels (%) and receptor densities (MFI) for each of the cell subsets**. Values in blue or red are either below or above the respective normal ranges

| | FSC vs. SSC Monocytes | | CD14+ | | FSC vs. SSC Lymphocytes | | CD56+ | | CD3+CD56+ | | CD3+ | | CD4+ | | CD8+ | | CD4-CD8- | | CD19+ | |
|---|---|---|---|---|---|---|---|---|---|---|---|---|---|---|---|---|---|---|---|---|
| | %CD212 + IQR: 29-52 | CD212 MFI IQR: 1281-1763 | %CD212 + IQR: 24-60 | CD212 MFI IQR: 1446-2450 | %CD212 + IQR: 73-87 | CD212 MFI IQR: 239-427 | %CD212 + IQR: 90-95 | CD212 MFI IQR: 595-786 | %CD212 + IQR: 84-92 | CD212 MFI IQR: 465-661 | %CD212 + IQR: 71-86 | CD212 MFI IQR: 202-391 | %CD212 + IQR: 63-82 | CD212 MFI IQR: 168-361 | %CD212 + IQR: 78-92 | CD212 MFI IQR: 284-474 | %CD212 + IQR: 82-91 | CD212 MFI IQR: 333-485 | %CD212 + IQR: 73-87 | CD212 MFI IQR: 183-354 |
| **PID01** | 29.80 | 1257 | 35.00 | 1331 | 78.60 | 272 | 82.90 | 423 | 77.90 | 346 | 80.10 | 258 | 74.90 | 234 | 80.80 | 284 | 75.00 | 247 | 80.90 | 269 |
| **Child of PID01** | 32.30 | 1291 | 32.00 | 1289 | 84.60 | 316 | 88.60 | 549 | 82.50 | 589 | 87.20 | 316 | 86.20 | 322 | 89.30 | 382 | 78.40 | 241 | 75.60 | 201 |
| **PID02** | 32.70 | 1365 | 63.20 | 2088 | 85.20 | 357 | 91.80 | 532 | 88.10 | 457 | 82.80 | 264 | 78.30 | 238 | 83.90 | 295 | 81.00 | 291 | 81.30 | 259 |
| **Parent of PID02** | 35.70 | 1376 | 50.30 | 1751 | 86.70 | 377 | 95.20 | 616 | 88.30 | 457 | 85.30 | 309 | 81.50 | 279 | 86.50 | 355 | 83.20 | 292 | 84.50 | 290 |
| **PID03** | 9.91 | 921 | 23.20 | 1198 | 81.40 | 278 | 84.10 | 448 | 83.00 | 373 | 82.20 | 256 | 79.40 | 251 | 81.70 | 268 | 78.30 | 252 | 83.90 | 264 |
| **PID04** | 39.40 | 1402 | 71.80 | 2382 | 70.60 | 191 | 77.80 | 409 | 69.50 | 274 | 73.30 | 185 | 68.90 | 174 | 76.10 | 226 | 78.20 | 249 | 68.60 | 165 |
| **PID05** | 19.70 | 969 | 39.80 | 1445 | 70.60 | 198 | 72.50 | 395 | 66.00 | 245 | 72.10 | 180 | 68.30 | 171 | 70.90 | 195 | 66.80 | 171 | 71.50 | 182 |
| **PID06** | 51.60 | 1745 | 66.10 | 2355 | 75.00 | 245 | 84.10 | 471 | 78.00 | 362 | 76.30 | 227 | 71.20 | 202 | 80.20 | 284 | 72.90 | 228 | 71.30 | 195 |
| **PID07** | 31.60 | 1270 | 56.80 | 1952 | 78.50 | 261 | 86.60 | 558 | 82.40 | 411 | 81.10 | 261 | 77.50 | 242 | 84.50 | 321 | 80.40 | 289 | 71.80 | 192 |
| **PID08** | 55.90 | 1949 | 63.90 | 2230 | 76.70 | 257 | 80.00 | 430 | 83.30 | 423 | 78.80 | 244 | 70.20 | 191 | 90.10 | 363 | 85.60 | 291 | 72.00 | 186 |
| **PID09** | 36.10 | 1379 | 47.80 | 1663 | 79.90 | 292 | 91.10 | 611 | 80.40 | 395 | 80.70 | 277 | 78.10 | 265 | 83.00 | 328 | 78.90 | 301 | 76.10 | 228 |
| **PID10** | 15.80 | 1016 | 13.70 | 1069 | 75.60 | 231 | 83.10 | 470 | 80.00 | 401 | 78.80 | 235 | 75.20 | 221 | 79.70 | 265 | 77.00 | 285 | 68.10 | 170 |
| **PID11** | 60.90 | 1939 | 86.20 | 3000 | 76.00 | 228 | 88.80 | 616 | 81.80 | 532 | 77.20 | 205 | 71.90 | 175 | 80.40 | 257 | 81.00 | 302 | 68.30 | 136 |
| **PID12** | 20.30 | 1096 | 25.40 | 1207 | 77.30 | 247 | 86.80 | 544 | 82.70 | 417 | 77.80 | 217 | 71.90 | 194 | 80.50 | 259 | 79.50 | 262 | 80.10 | 242 |
| **PID13** | 21.90 | 991 | 26.80 | 1088 | 71.00 | 202 | 81.70 | 459 | 69.20 | 282 | 72.80 | 184 | 69.40 | 178 | 69.90 | 190 | 67.00 | 190 | 64.40 | 153 |
| **PID14** | 9.82 | 754 | 10.60 | 943 | 68.40 | 184 | 75.70 | 445 | 72.00 | 296 | 70.80 | 175 | 66.30 | 161 | 70.50 | 203 | 66.80 | 184 | 65.80 | 154 |
| **PID15** | 30.80 | 1320 | 39.50 | 1519 | 52.80 | 112 | 75.20 | 479 | 84.40 | 521 | 73.30 | 255 | 69.50 | 244 | 76.70 | 301 | 67.00 | 217 | 62.50 | 165 |
| **PID16** | 45.00 | 1616 | 68.50 | 2200 | 85.00 | 395 | 91.10 | 625 | 89.40 | 581 | 84.40 | 352 | 81.10 | 329 | 92.10 | 516 | 81.90 | 320 | 85.60 | 316 |
| **PID17** | 42.40 | 1527 | 51.30 | 1801 | 69.00 | 171 | 78.00 | 438 | 76.00 | 407 | 70.30 | 155 | 65.00 | 137 | 71.80 | 190 | 71.40 | 195 | 66.60 | 134 |

**Table E.3: Fold change in pSTAT1 for each of the cell subsets**. Values in blue or red are either below or above the respective normal ranges

| Patient ID | FSC vs. SSC Monocytes IQR: 0.97-1.75 | CD14+ IQR: 1.39-2.05 | FSC vs. SSC Lymphocytes IQR: 1.16-1.86 | CD56+ cells IQR: 0.89-1.34 | CD3+CD56+ cells IQR: 1.17-1.83 | CD3+ IQR: 1.20-1.98 | CD4+ IQR: 1.23-2.10 | CD8+ IQR: 1.17-1.82 | CD4-CD8- IQR: 0.96-2.33 | CD20+ IQR: 1.28-1.81 |
|---|---|---|---|---|---|---|---|---|---|---|
| **PID01** | 0.50 | 0.80 | 1.17 | 1.02 | 1.03 | 1.13 | 1.10 | 0.72 | 1.01 | 1.05 |
| **Child of PID01** | 1.07 | 1.20 | 1.18 | 1.04 | 1.02 | 0.86 | 1.13 | 1.10 | 0.86 | 1.18 |
| **PID02** | 1.11 | 1.31 | 1.34 | 1.11 | 1.16 | 1.42 | 1.44 | 1.45 | 1.22 | 1.59 |
| **Parent of PID02** | 1.54 | 1.82 | 1.63 | 1.24 | 1.37 | 1.70 | 1.71 | 1.76 | 1.26 | 2.14 |
| **PID03** | 1.41 | 1.74 | 1.27 | 1.15 | 1.21 | 1.30 | 1.33 | 1.27 | 1.13 | 1.51 |
| **PID04** | 3.57 | 4.23 | 2.14 | 2.00 | 2.23 | 1.95 | 1.88 | 2.32 | 1.92 | 4.24 |
| **PID05** | 1.65 | 1.84 | 2.02 | 1.40 | 1.82 | 2.18 | 2.23 | 2.13 | 1.74 | 1.97 |
| **PID06** | 1.48 | 1.64 | 1.54 | 1.36 | 1.57 | 1.51 | 1.51 | 1.47 | 1.45 | 2.55 |
| **PID07** | 1.67 | 2.19 | 1.77 | 1.18 | 1.96 | 1.83 | 1.97 | 1.47 | 2.26 | 1.64 |
| **PID08** | 0.86 | 1.03 | 1.23 | 0.92 | 0.92 | **1.20** | 1.29 | 0.95 | 0.89 | 1.66 |
| **PID09** | 1.55 | 1.95 | 1.53 | 1.24 | 1.60 | 1.50 | 1.53 | 1.41 | 1.65 | 2.23 |
| **PID10** | 1.61 | 2.19 | 1.33 | 1.14 | 1.37 | 1.33 | 1.34 | 1.32 | 1.24 | 2.00 |
| **PID11** | 2.79 | 2.30 | 2.21 | 1.51 | 2.22 | 2.25 | 2.30 | 2.34 | 1.44 | 1.74 |
| **PID12** | 1.46 | 1.71 | 1.69 | 1.19 | 1.48 | 1.73 | 1.81 | 1.65 | 1.39 | 1.92 |
| **PID13** | 1.39 | 1.56 | 1.50 | 1.00 | 1.50 | 1.62 | 1.72 | 1.53 | 1.64 | 1.58 |
| **PID14** | 1.18 | 1.94 | 1.29 | 1.14 | 1.57 | 1.29 | 1.32 | 1.21 | 0.98 | 1.34 |
| **PID15** | 2.24 | 2.84 | 2.44 | 1.15 | 1.93 | 2.65 | 2.86 | 2.46 | 1.94 | 1.69 |
| **PID16** | 0.44 | 1.14 | 1.44 | 0.99 | 1.52 | 1.49 | 1.64 | 1.26 | 0.98 | 1.54 |
| **PID17** | 3.74 | 2.65 | 1.37 | 1.00 | 0.97 | 1.31 | 1.27 | 1.17 | 5.86 | 1.33 |

**Table E.4: Fold change in pSTAT4 for each of the cell subsets**. Values in blue or red are either below or above the respective normal ranges

| Patient ID | FSC vs. SSC Monocytes<br>IQR: 1.53-2.07 | CD14+<br>IQR: 1.38-2.12 | FSC vs. SSC Lymphocytes<br>IQR: 1.19-1.58 | NK cells<br>IQR: 2.04-2.75 | NKT cells<br>IQR: 1.23-1.73 | CD3+<br>IQR: 1.20-1.65 | CD4+<br>IQR: 1.18-1.46 | CD8+<br>IQR: 1.33-2.19 | CD4-CD8-<br>IQR: 1.41-2.74 | CD20+<br>IQR: 0.98-1.53 |
|---|---|---|---|---|---|---|---|---|---|---|
| **PID01** | 1.58 | 1.58 | 1.45 | 1.83 | 1.55 | 1.39 | 1.32 | 1.48 | 1.74 | 2.15 |
| **Child of PID01** | 1.76 | 1.50 | 1.22 | 2.61 | 1.30 | 1.17 | 1.10 | 1.76 | 1.02 | 1.00 |
| **PID02** | 1.47 | 1.20 | 1.48 | 1.32 | 1.48 | 1.57 | 1.44 | 1.93 | 1.20 | 1.35 |
| **Parent of PID02** | 0.99 | 0.82 | 1.21 | 1.03 | 1.13 | 1.26 | 1.21 | **1.33** | 1.21 | 1.03 |
| **PID03** | 1.51 | 1.25 | 1.10 | 1.07 | 0.95 | 1.10 | 1.07 | 1.25 | 1.07 | 1.15 |
| **PID04** | 3.92 | 2.41 | 3.49 | 9.21 | 2.34 | 3.06 | 2.68 | 4.95 | 3.62 | 14.14 |
| **PID05** | 1.26 | 1.01 | 1.07 | 1.19 | 0.98 | 1.13 | 1.04 | 1.25 | 1.53 | 0.82 |
| **PID06** | 1.84 | 1.75 | 1.38 | 2.33 | 1.33 | 1.36 | 1.27 | 1.50 | 1.38 | 1.31 |
| **PID07** | 2.48 | 2.35 | 1.79 | 1.50 | 1.28 | 1.71 | 1.53 | 1.74 | 5.02 | 1.42 |
| **PID08** | 1.32 | 1.35 | 1.33 | 1.51 | 1.12 | 1.32 | 1.33 | 1.24 | 1.81 | 1.17 |
| **PID09** | 1.40 | 1.32 | 1.15 | 1.78 | 1.16 | 1.13 | 1.09 | **1.33** | 1.13 | 1.16 |
| **PID10** | 1.57 | 1.40 | 1.32 | 1.43 | 1.15 | 1.38 | 1.30 | 1.67 | 1.22 | 1.18 |
| **PID11** | 0.91 | 0.93 | 1.66 | 2.17 | 1.62 | 1.58 | 1.68 | 1.85 | 1.58 | **1.52** |
| **PID12** | 1.06 | 1.02 | 0.88 | 2.26 | 0.95 | 0.83 | 0.84 | 0.82 | 0.85 | 1.00 |
| **PID13** | 2.05 | 2.13 | 1.60 | 1.53 | 1.50 | 1.61 | 1.56 | 1.76 | 1.75 | 1.43 |
| **PID14** | 1.53 | 1.68 | 0.75 | 1.88 | 0.82 | 0.69 | 0.68 | 0.69 | 0.83 | 1.10 |
| **PID15** | 0.94 | 0.97 | 1.63 | 1.56 | 1.24 | 1.54 | 1.32 | 1.79 | 3.63 | 1.36 |
| **PID16** | 1.13 | 1.04 | 0.96 | 1.18 | 1.05 | 0.94 | 0.92 | 1.07 | 0.88 | **0.98** |
| **PID17** | 1.11 | 1.23 | 1.44 | 1.43 | 0.51 | 1.28 | 1.09 | 1.64 | 0.57 | 1.20 |

**Table E.5: Cytokine-induced cytokine production values for all participants.** Values in blue or red are either below or above the respective normal ranges

| Patient ID | IFN-γ production assay | | | | IL-12 production assay | | | |
|---|---|---|---|---|---|---|---|---|
| | NIL (pg/mL)<br>IQR: 0-0 | PHA (pg/mL)<br>IQR: 57-658 | PHA+IL-12 (pg/mL)<br>IQR: 545-692 | Net IL-12-induced IFN-γ production (pg/mL)<br>IQR: 176-443 | NIL (pg/mL)<br>IQR: 0-0 | PHA (pg/mL)<br>IQR: 0.13-1.69 | PHA+IFN-γ (pg/mL)<br>IQR: 11-19 | Net IFN-γ-induced IL-12 production (pg/mL)<br>IQR: 11-19 |
| **PID01** | 0.00 | 70.00 | 425.40 | 355.40 | 0.00 | 0.26 | 0.69 | 0.43 |
| **Child of PID01** | 0.00 | 197.98 | 343.70 | 145.73 | 0.00 | 0.27 | 2.06 | 1.79 |
| **PID02** | 0.00 | 57.49 | 1512.29 | 1454.80 | 0.00 | 0.90 | 22.14 | 21.24 |
| **Parent of PID02** | 0.00 | 57.18 | 596.14 | 538.96 | 0.00 | 0.38 | 9.95 | 9.57 |
| **PID03** | 0.00 | 480.56 | 620.00 | 139.43 | 0.00 | 18.63 | 38.83 | 20.20 |
| **PID04** | 0.00 | 15.85 | 562.76 | 546.91 | 0.00 | 1.84 | 36.90 | 35.06 |
| **PID05** | 0.00 | 68.75 | 755.31 | 686.56 | 0.00 | 0.19 | 2.47 | 2.28 |
| **PID06** | 11.54 | 25.67 | 74.23 | 48.56 | 0.00 | 0.05 | 1.12 | 1.07 |
| **PID07** | 0.00 | 5.49 | 299.91 | 294.42 | 0.00 | 0.21 | 4.81 | 4.61 |
| **PID08** | 10.31 | -6.68 | 25.55 | 32.23 | 0.00 | 0.27 | 3.72 | 3.44 |
| **PID09** | 47.72 | 82.88 | 729.73 | 646.85 | 0.00 | 1.07 | 48.26 | 47.19 |
| **PID10** | 0.00 | 19.57 | 399.54 | 379.97 | 0.00 | 0.11 | 1.64 | 1.54 |
| **PID11** | 0.00 | 566.17 | 795.34 | 229.16 | 0.00 | 0.82 | 10.94 | 10.12 |
| **PID12** | 0.00 | 2.09 | 106.01 | 103.93 | 0.00 | 0.87 | 30.49 | 29.62 |
| **PID13** | 0.00 | 279.06 | 764.92 | 485.86 | 0.00 | 1.86 | 25.48 | 23.61 |
| **PID14** | 0.00 | 12.32 | 215.79 | 203.47 | 0.00 | 0.04 | 2.79 | 2.75 |
| **PID15** | 0.00 | **27.92** | 901.82 | 873.90 | 0.00 | 0.46 | 17.38 | 16.92 |
| **PID16** | 0.00 | **23.09** | 425.11 | 402.02 | 0.00 | 0.41 | 29.18 | 28.77 |
| **PID17** | 0.00 | **24.03** | 312.83 | 288.80 | 0.00 | 0.24 | 8.98 | 8.74 |